Exploring the Structural and Functional Aspects of Sialic acid Mimetics

A Thesis
Submitted in partial fulfillment of the requirements
of the degree of
Doctor of Philosophy

By
Rohan Dattatray Yadav
ID: 20113102

Indian Institute of Science Education and Research, Pune

Dedicated to

My Family and Teachers

CERTIFICATE

This is to certify that the work incorporated in this thesis entitled **"Exploring the Structural and Functional Aspects of Sialic acid Mimetics"** submitted by Rohan Dattatray Yadav carried out by candidate at Indian Institute of Science Education and Research(IISER), Pune, under my supervision. The work presented here or any part of it has not been included in any other thesis submitted previously for the award of any degree or diploma from any other University or institution.

19th October, 2016

Dr. Raghavendra V. Kikkeri
(Research Supervisor)
Associate Professor, IISER, Pune
Pune 411008, India.

Declaration

I hereby declare that the thesis entitled**"Exploring the Structural and Functional Aspects of Sialic acid Mimetics"** submitted for Doctor of Philosophy in Chemistry at Indian Institute of Science Education and Research(IISER), Pune, has not been submitted by me to any other University or Institution. This work presented here was carried out at the, Indian Institute of Science Education and Research, Pune, India under the supervision of Dr. Raghavendra V. Kikkeri.

19th October, 2016

Rohan Dattatray Yadav
ID- 20113102
(Senior Research Fellow)
Department of Chemistry, IISER
Pune- 411008, India.

Acknowledgments

The past six years has become one of the most important and memorable chapters in my life. This. In many ways, is the beginning, not the end, of my journey. Looking back , there are so many people that deserve my heartfelt gratitude. First, let me start by expressing my heartfelt sincere profound thanks to my supervisor Dr. Raghavendra V. Kikkeri in bringing me in field of glycobiology and pursuing good knowledge of interdisciplinary research. As a first Ph.D student it gives me a great pleasure to express my deep sense of gratitude to my research supervisor for all his advice, guidance, support and encouragement in chemistry and its relevance in biological systems. His energy and tireless enthusiasm and passion for science have been an inspiration for me in the past six years and will always be in me years to come. I cannot think of a better advisor who can give me such freedom to pursue science and foster me to become independent thinker.

I thank our Director, Prof. K. N. Ganesh for giving excellent research platform, financial support and facilities that I have been privileged with during my research here Indian Institute of Science Education and Research, Pune. Besides I gained many novel ideas and enthuse regarding how to utilize and develop the science. Also special vote of thanks to Dr. R. G. Bhat and Dr. H. V. Thulasiram for valuable suggestion during research advisory committee(RAC) meeting. I am also thankful for UGC-CSIR, India for my 5 year research fellowship. I would like to acknowledge Dr. M. Jeganmohan and Dr.

A. Natu for their support and cooperation during my research tenure. I am thankful to all the chemistry faculties IISER-Pune for their support. Also my work wouldn't be possible without help from our collaborators Prof. Ajit Varki and Dr. Vered P. Karavani.I also thank to all administrative staff of our department.

The research become interesting and productive due to wonderful lab mates was around with me. I am graceful to have hardworking lab mates Krishna, Siva, Madhuri, Chethan, Balamurugan and they made friendly environment for research work. My special thanks to Dr.Raghavendra, Dr. Preeti and Geetanjali for mentoring in biological experiments. I would also give vote of thanks to Suraj, Prashant, Phani, Catherine, Chinmay, Sandhya, Akhil for sharing and active participation in group tour and joyful moments.

I am greatful to Shriram, Sakharam, Balsaheb, Shrikant, Sachin and Mahadev for being my roommates and sharing many life experience and thoughts. I enjoyed with them an adventurous treckking across the Sahyadri mountain range on weekends and they made it memorable.

I had greate time with Dinesh, Ravi and I really learnt and enjoyed their company in many memorable moments.

I thankful to Nagesh, Nilesh, Trimbak, Sharad, Vinayak, Balu, Maroti, Narshimha, Sopan, Prabhakar and all my IISER friends.

This thesis remains incomplete without mentioning blessings and love of my family. There is no better words to express my heartfelt gratitude for their unconditional love, gracious understanding and life time support.

Finally, I pray to almighty Lord ‘Ganesha’ whose blessings made me able to complete the research work and submit this thesis for Ph.D degree.

Rohan Dattatray Yadav

Contents

Chapter 2: Sialic acid Mimics

Chapter 4:Head-to-Head Comparison of Sialylated-quantum dots Toxicity, Biodistribution and Sequestration in Zebrafish and Mouse Model

Abbreviations

6'SLA = sialyllactose

Ac = acetyl

Ac_2O = Acetic anhydride

AcCl= Acetyl chloride

ACN = Acetonitrile

AFM = Atomic force microscopy

AMP = Adenosine monophosphate

APC = Antigen presenting cells

aq. = aqueous

Aβ = Beta amyloid

B-ALL = B-cell acute lymphoblastic leukemia

BCR = B-cell receptor

Bn = Benzyl

BnBr = Benzyl bromide

BPC = Biphenyl carboxylate

BSA = Bovine serum albumine

Bu = Butyl

CD = Cluster of differentiation

CHO = Chinese hamster ovary

CPS = Capsular polysaccharide

CRD= Carbohydrate recognition domain

C-set = Constant set

Da = Dalton

DC = Dendritic cells

DCM = Dichloromethane

DFO = Des-ferrioxamine

DIPEA = Diisopropylethylamine

DLS = Dynamic light scattering

DMAP = *N*,*N*-dimethylaminopyridine

DMB = 4,5-Methylenedioxy-1,2-phenylenediamine hydrochloride

DMF = *N*,*N*'-Dimethylformamide

DMSO = Dimethyl sulfoxide

DPPH = 2,2-Diphenyl-1-(2,4,6 trinitrophenyl)hydrazyl

E.coli = Escherichia coli

EDC = 1-Ethyl-3-(3-Dimethylaminopropyl)carbodiimide

ELISA = Enzyme linked immunosorbent assay

Endo-N = Endo neuraminidase

eq. = equivalents

Et = ethyl

et al. = and others (*et alii*)

EtOAc = Ethyl acetate

Fuc = Fucose

Gal = Galactose

Gal = Galactose

GalNAc = *N*-acetylgalactosamine

Glc = Glucose

GlcNAc = *N*-acetylglucosamine

Glu = Glucose

GM1 = Monosialosetetrahexoseganglioside

Hex = Hexane

HRMS = High resolution mass spectroscopy

IC50 50 = Inhibitory concentration

ICP-MS = Induced couple clasmon mass spectrometry

Ig = Immunoglobulin

ITAM = Immunoreceptor tyrosine based activatory motif

ITIM = Immunoreceptor tyrosine based inhibitory motif

KDN = 2-keto-3-deoxynononic acid

KDO = 2-keto-3-deoxyoctolusonic acid

KLH = Keyhole Limpet Hemocyanin

LD = Lethal dose

M.S. = Molecular sieves

MAG = Myelin associated glycoprotein

MALDI = Matrix-assisted laser desorption ionization

Man = Mannose

m-CPBA = meta-chloroperbenzoic acid

Me = methyl

MeOH = Methanol

MHC II = Major histocompatibility factor II

MS = Mass spectroscopy

MsOH = Methanesulfonic acid

MTT = Methylthiazolyldiphenyl-tetrazolium bromide

Mw = Molecular weight

N. meningitidis = Neisseria meningitidis

NCAM = Neural cell adhesion molecule

NDV = new castle disease

Neu5Ac = *N*-acetylneuraminic acid

Neu5Gc = *N*-glycolylneuraminic acid

NHS = N-hydroxysuccinimide

NIS = *N*-iodosuccinimide

NK cells = Natural killer cells

NMR = Nuclear magnetic resonance

NPCC = 4-Nitrophenylchloroformate

PBS = Phosphate buffered saline

Ph = Phenyl

ppm = parts per million

p-TSA = 4-toluenesulfonic acid

Py = Pyridine

QD = Quantum dots

r.t. = room temperature

RBCs = Red blood cells

RNA = Ribonucleic acid

SA = Sialic acid

SCMP/SMP = Schwan cell membrane protein

STn = SialylTn

TBDMS = ter-butyl dimethyl silyl

TCR = T-cell receptor

TEM = Transmission electron microscopy

Tf_2O = Trifluoromethanesulfinic anhydride

TFA = Trifluoroacetic acid

TfOH = Trifluoromethanesulfonic acid, triflic acid

THF = Tetrahydrofuran

Thr = Threonine

TLC = Thin layer chromatography

TMB = Tetramethylbenzilidine

TMSOTf = Trimethylsulfoniumtrifluoromethanesulfonate

TOF= Time of flight

Troc = Trichloroethoxycarbonyl

TsCl = 4-Toluenesulfonylchloride

TTBP = 2,4,6 tri -tert-butylpyrimidine

Ty = Tyrosine

V-set = Variable set

WBCs = White blood cells

Abstract

Sialic acids (Sia) are nine-carbon backbone monosaccharides, typically found at the terminal position of the glycoproteins and glycolipids. Over the decades, sias have been reported in various pathological and physiological processes. The invasion of virus, bacteria also depends on specific sia patterns and aberrant sialylation is the feature of numerous of neurological, immune, cancer and congenital disorder of glycosylation. Despite its widespread medical applications, the structure-function relation of the defined sialic acid sequence is still poorly understood. In my thesis, we describe the three distinct sialic acid modifications that independently generate crucial structural-functional relation of sialic acid glycans.

The first target was to decipher the role of galactose as a penultimate sugar in sialic acid glycans. We have synthesized Neu5Acα(2-6)Gal structural analogs and studies their binding to a series of siglec. The results showed distinct binding patterns with conserved Siglec (hCD22 and mCD22) compared to rapid evolving siglec (Siglec -3 & -10) and constitute a valuable tool for designing Siglec specific molecules for therapeutic applications. Furthermore, these isostructural glycans were conjugated to KLH proteins and immunize the mice. The immune response showed that mannose modification at the penultimate position of the sialic acid glycan induced high titer IgG antibody responses and these IgG antibodies showed efficient cross-reactivity with native glycan. Overall, our results highlight a new potential approach to synthesize antigenic sugars to modulate immune responses.

Next, we have synthesized sialic acid hydroxamate to understand the structural-functional relation of the acidic group. We found that biomimetic analogs possessed three distinct properties: antioxidant nature, metals chelating ability and Sia backbone to target AD. Focusing on cytotoxicity caused by radicals and Aβ-metal complexes, we demonstrated that hydroxamate ligand on sialic acid backbone protects the neural cells more efficiently in comparisons to sialic acid alone.

Finally, we locked the sialic acid in two opposite orientations on micelles to effectively tune sia dependent ligand-receptor interactions in their native context. To obtain sialo-micelles that could serve as the multivalent probe, we conjugated amphiphilic group at C-2 and C-9 position of sia respectively. Upon dissolution of amphiphiles in water, self-assembled highly regular micelles

were obtained. The bioavailability of resultant sialo-micelles with plant and human sialic acid binding protein (SBP) was evaluated by surface plasma resonance (SPR) and in-vitro assays. Sambucusnigra agglutinin (SNA), Limaxflavus agglutinin (LFA),30 P, E-selectin and CD22 (Siglec-2) were selected as sialic acid binding proteins (SBP). Where SNA and LFA binds to all common sialic acid residues,31 human CD22-Fc only recognizes siaα(2-6)-linked sias, while E and P-selectin, which belong to the subgroup of the C-type lectins that mediate leukocyte trafficking, are specific to sialylLewisx and sialylLewisaglycans respectively.

Animal models to test the biodistribution and sequestration of specific biomarkers vary from laboratory to laboratory, resulting variable results. Thus, a head-to-head comparison of the different models at same experimental conditions will undoubtedly assist to identify the better model for the therapeutic purposes. Herein, we performed in vivo head-to-head comparison of (2-6) and (2-3) sialic acid glycan conjugated quantum dots in zebrafish (Daniorerio) and mouse model (intraperitoneal injection) to advocate fish as an ideal living simple system for the preliminary screening of pharmacokinetics of sugar conjugated-QDs. The results suggest that (2-6) sialylated-QDs preferentially has prolonged circulation half-life and uptake by the liver, kidney and spleen, while (2-3), sialic acid and galactose conjugated-QDs accumulated in the liver and cleared after several hours in both models. These results suggested that zebrafish is a competitive model for sialic acid-mediated pharmacokinetics studies.

Publications

1 **RohanYadav**,RaghavendraKikkeri; "Carbohydrate functionalized Iron(III) complexes as biomimetic siderophores"*Chem. Commu.* **2012**, 48, 1704.

2 **RohanYadav**,RaghavendraKikkeri; "Exploring the effect of sialic acid orientation on ligand receptor interactions" *Chem. Commun.***2012**, 48, 7265.

3 **RohanYadav**, RaghavendraKikkeri; "Sialic acid hydroxamate a potential antioxidant and inhibitor of a metal induced β-amyloid aggregates" *ChemBioChem.* **2015**, 14, 1648.

4 Preeti M. Chaudhari, R. Murthy, **Rohan Yadav**, Raghavendra Kikkeri; "A rationally designed peptidomimetic biosensor of sialic acid on cell surface" *Chem. Commun.* **2015**, 51, 8112.

5 **RohanYadav,** Shani-Ben Arye, Balamurugan Subramani, Vered Padlar Karvani, Raghavendra Kikkeri; " Screening of Neu5Acα(2-6)gal isomers preferences of Siglec with sialic acid microarray"- *Org. Biomol. Chem.* **2016,-accepted.**

6 **Rohan Yadav,** Balamurugan Subramani, RaghavendraKikkeri; "Harvesting the immunogenicity in sialic acid glycans by altering penultimate sugar of the glycans"- **manuscript submitted.**

7 **RohanYadav**, Chaudhari PM, Balamurugan Subramani, Suraj Toraskar, Harikrishna Bavireddi, R. V. Murthy, Sivakoti Sangabathiuni, , RaghavendraKikkeri; "Imaging and Quantification of α(2- 6)and α(2-3) Linked Sialic Acid Conjugated Quantum dots Biodistribution in Zebrafish and Mouse models."-**manuscript submitted.**

Chapter 1

Introduction

1.0 Sialic acid

Sialic acids (Sia) are unusual 9-carbon backbone sugar, which are α-keto acids in nature. Sias are an integral part of the *N*- and *O*-glycans of eukaryotic glycoproteins and glycolipids. There are more than 50 different types of naturally occurring Sias. The structural diversity of sialic acids are primarily generated by hydroxyl group modification at C-4, C-7, C-8, and C-9 by *O*-acetylation, *O*-methylation, *O*-lactylation, *O*-sulfation and *O*-phosphorylation. The lactonization of the carboxylate at C-1 with hydroxyl group include further structure diversity. Legionaminic acid and pseudaminic acid are two important bacterial sialic acid derivatives. Since these molecules are synthesized *via* the similar biosynthetic pathway of sialic acid, they have been classified under nonlusonic acid sugars. Being the terminal residue, sia encapsulated different underlying glycans and involved in various physiological, pathological and immune responses.[1]

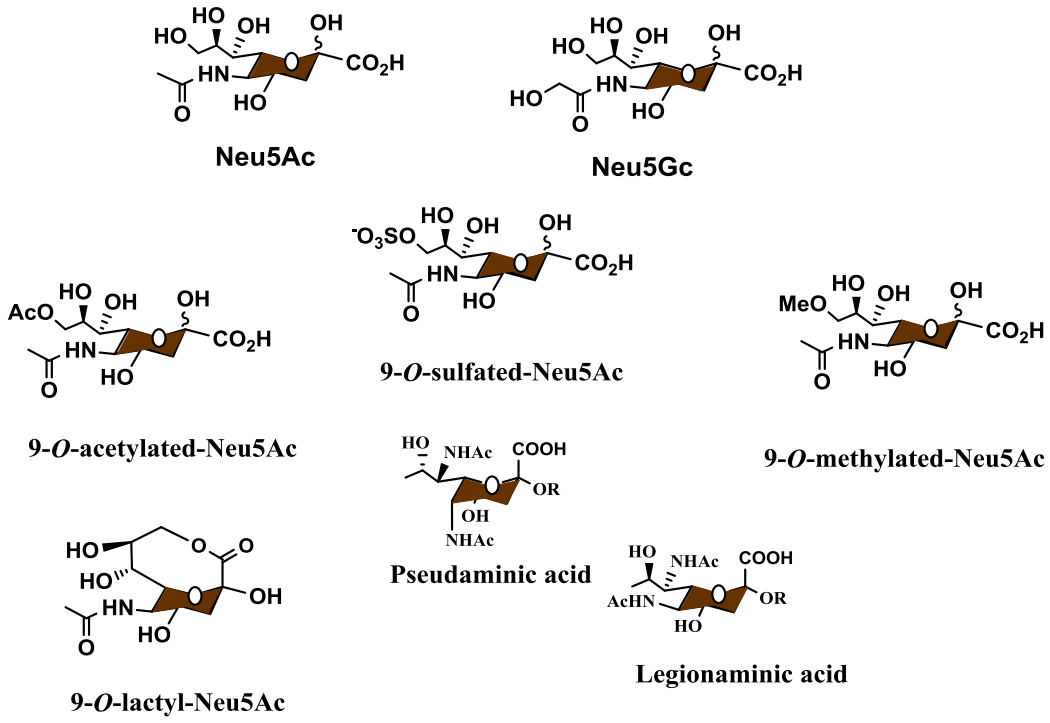

Figure 1. Structural diversity of sialic acid expressed on cell surfaces.

Along with its structural analogs, sialic acid shows diversity with underlying glycans through the linkage isomerism. Some pathogenic species express sialic acid in the form of α(2-6) and α(2-3) linkage and alters the binding or recognition pattern with the host cell and vice a verse.[2] The

lectins of immunoglobulin super family called siglecs have specific selectivity to the sialic acid ligand based on its α(2-3) or α(2-6) linkage system.[3] The human leukocyte, endothelial cells expresses Neu5Acα(2-3) linkage with fucose residue at the C-3 or C-4 position of GlcNAc and forms tetrasaccharide antennae called sialyl lewis^{x} and sialyl lewis^{a}. This sialyl antenna plays a crucial role in leukocyte rolling, adhesion and extravasation at the inflammatory site to recruit the RBCs and WBCs.[4] It is believed that the process of gametogenesis initiated by recognition of sialyl lewis^{X} antennae on receptor cells.[5] Multivalent display of sialic acid α(2-6) and α(2-3) glycans on the cancerous cell is the determinant of antigen for the metastasized tumor and efforts have been made to explore its synthetic and clinical utility as a potential vaccine candidate.[6] Moreover, the sialic acid linkage diversity extends to its homopolymeric forms such as α(2-8) and α(2-9) polysialic acid. This polymeric form of usually expressed on brain cells and function for neural plasticity and maintaining homeostasis of metal ions in the brain.[7]

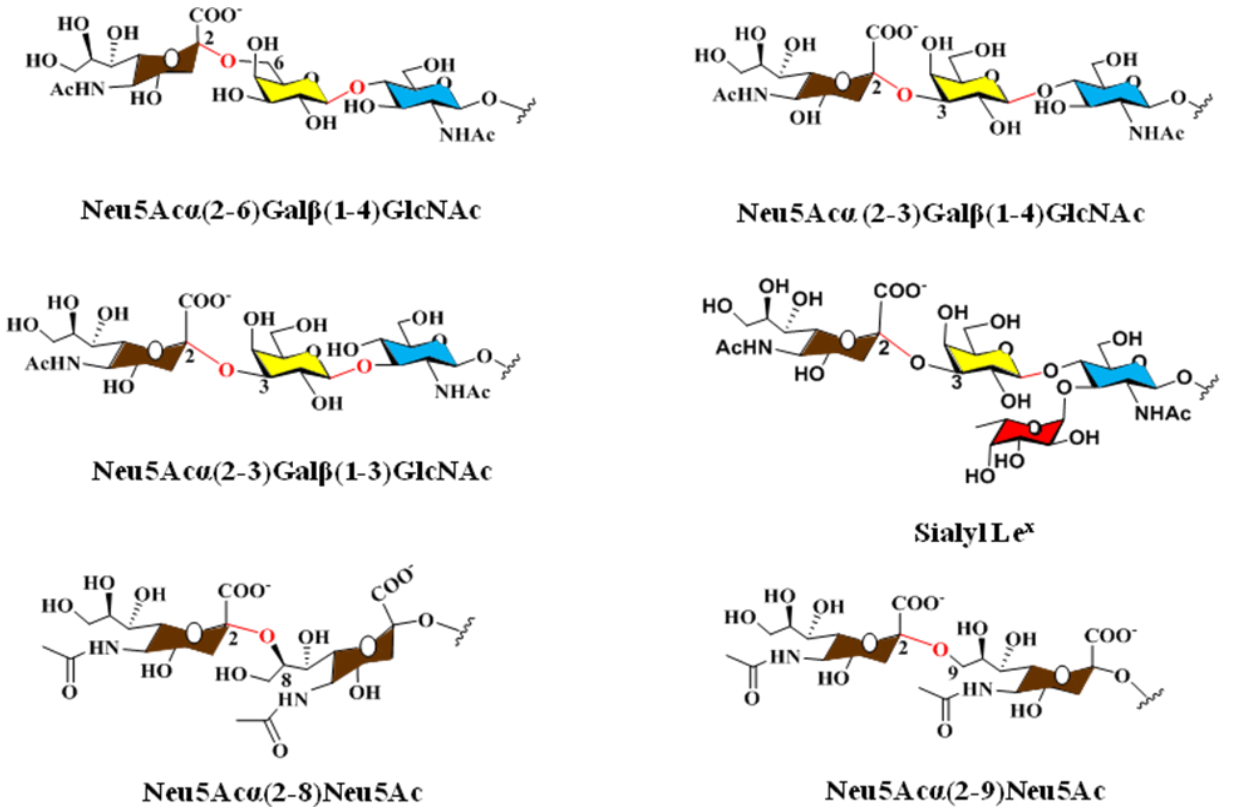

Figure 2. Structural diversity of sialic acid with underlying glycans.

1.2. Sialic acid Recognizing Protein

1.2.1 Lectins

Lectins are carbohydrate binding proteins. Lectins are relatively resistance to both heat and digestive enzymes. Lectins are classified by their structural, carbohydrate recognition pattern and its expression on a type of cells. Evolutionarily conserved carbohydrate sequence mainly classify lectins into selectins and its subtypes C-type, P-type, I-type, etc.[17] There are nearly 100 lectins in nature recognizes sialic acids as a ligand in its native and unnatural form. It has grouped and subgrouprd into various categories like vertebrate pathogen lectins, vertebrate endogenous lectins, and lectins from other sources (plants, protostomes, etc.).[8]

1.2.2 Hemagglutinins

Viral sialic acid binding lectins are usually capable of agglutinating red blood cells (RBC). Hence they are conventionally called hemagglutinins rather than lectins. Viruses utilize sialic acid glycans to recognize the host cells and infection. Newcastle disease virus (NDV, an avian pathogen), hemagglutinins of influenza viruses (A, B, and C), Sendai virus (a rodent pathogen), mouse hepatitis virus and polyoma virus and some others have been shown to recognize sialic acid glycans as initial point of recognition.[9] Recently, several of these hemagglutinins (from influenza A, C, NDV, and polyomaviruses) has crystallized and their 3D structure has been resolved by X-ray crystallography.[10]

One of the most familiar and extensively studied molecules of this kind is the influenza A virus hemagglutinin. Influenza virus is a segmented single-stranded RNA virus from Orthomyxoviridae family cause infection to mammals and birds. Trimeric viral haemagglutinin protein binds specific sialic acid glycan to adhere host cells. Influenza viruses show near essential dependence on the host cell surface sialic acids for infection. Sialic acid binding preferences of influenza A hemagglutinins isolated from different host species vary with the type of sialic acids expressed on the host cell and with the difference in the sialic acid linkage (α(2−3)/α(2−6)). For example, Human influenza virus binds Neu5Acα(2−6)Gal, while avian influenza preferentially binds Neu5Acα(2−3)Gal linkage on host cell surface. Studies have shown that the natural reservoir of influenza viruses is in various species of wild waterfowl. Through a series of cross-species infections involving domestic animals (ducks and pigs) and adaptations to the new types of sialic acids encountered in the new hosts, and/or reassortment of

genomic fragments from human and bird influenza viruses in pigs, which are susceptible to both types of viruses, influenza viruses adapt to infect humans and cause seasonal epidemics.

Also, the influenza C virus hemagglutinin-esterase is notable for being specific for 9-*O*-acetylated sialic acid glycans and enzymatically activates to destroy the 9-*O*-acetyl ester. This protein has recognized as a useful probe for studying 9-*O*-acetylated sialic acids. Mouse hepatitis virus also has a hemagglutinin-esterase, which is specific to sialic acids substituted by *O*-acetyl group at the C-4 position (Neu4,5Ac2).[11] Another famous example of receptor−recognition proteins are the hemagglutinin−neuraminidases of parainfluenza viruses and NDV.[12] In the case of influenza A virus which carry distinct hemagglutinin and neuraminidase proteins, the balance between these two functions appears to be essential for efficient viral replication, which involves several cycles of host cell attachment internalization, amplification, and assembly and detachment from the host cell. Differential glycan expression in reovirus which binds sialic acid glycans found to be more virulent as it targets the central nervous system in mice model. The adenovirus that recognizes the specific sialic acid pattern on host cell causes serves damage to the upper respiratory track in the human system.

1.2.3. Adhesins

Bacterial pathogens interact with host cells *via* specific sialic acid glycans. The bacterial lectins are typically called adhesins.[13] The water soluble bacterial lectins are typically called toxins. Although many toxins have high specificity toward sialic acid glycans, some are not as specific as with the Pasteurella hemolytic adhesion, or sulfated sugars, as with the *E. coli* heat-stable enterotoxin b.[14]

Bacterial adhesins are often articulated in a strain-specific way and can influence the range of tissues the strain can infect or colonize. There are some pathogenic and non-pathogenic sialidases exploit sialic acid as a source of carbon and energy. Apart from it pathogenic bacteria expose this enzyme to host cell surfaces and interferes the immune functions. Such examples include *Helicobacter pylori*, which involved in the etiological agent of peptic ulcers in humans and *E. coli* K99 causes lethal dysentery among piglets and calves. *H. pylori* express two different adhesins (in an environment-dependent manner) which can recognize sialic acid glycans. Adhesins of this bacteria firmly attach to the endothelial cell lining of stomach and duodenum. The bacterial adhesions to endothelial cells occur *via* sialyl Lewis^x residue on cell surface.

Despite detailed analyses, structural aspect of these adhesins and their exact role in the establishment of infection is not yet investigated. The adhesins expressed by *E. coli* K99 strain shows high selectivity toward Neu5Gcα(2−3)Galβ(1-4)Glc structure on glycolipids, which is expressed in the gastrointestinal tract of piglets.[14]

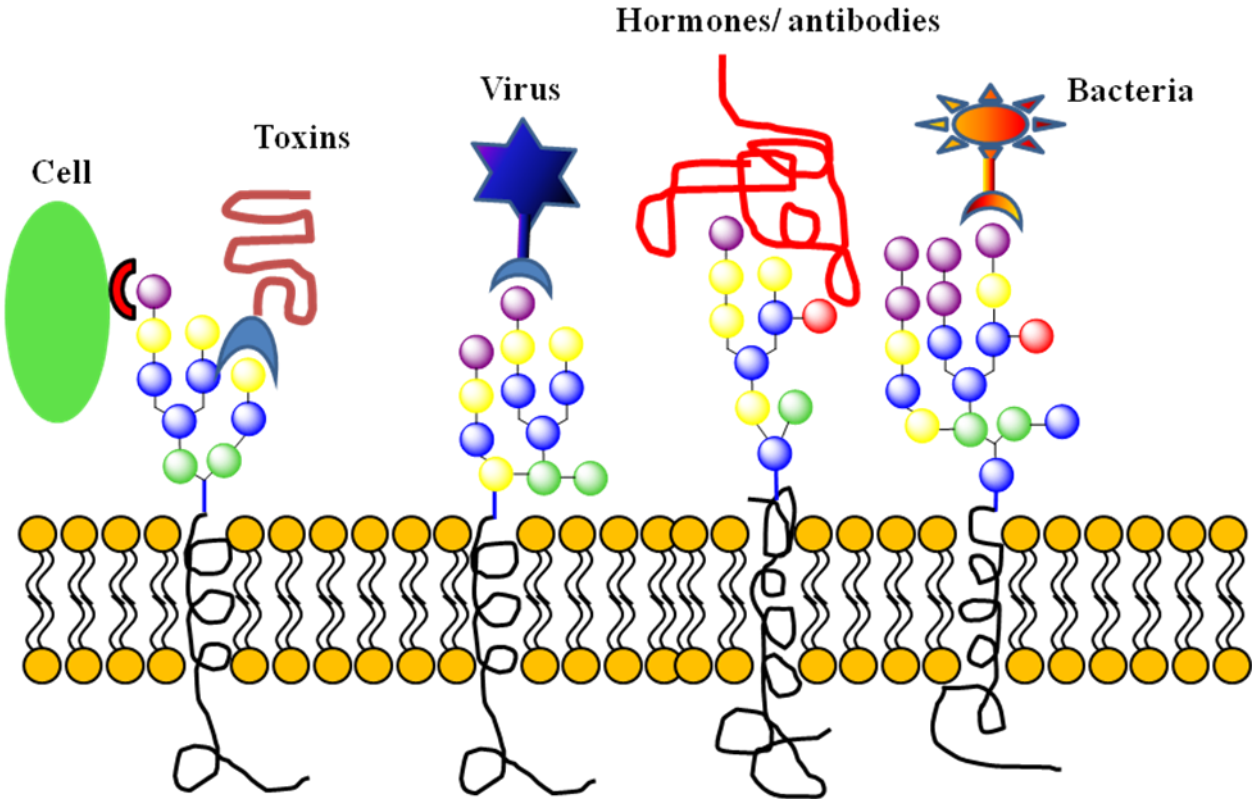

Figure 3. Interaction of Cell Surface Glycans with Different Biological Species.

Cholera toxin from *Vibrio cholera* represents a classic example of soluble sialic acid-binding lectins.[14, 15] It is composed of an A subunit and five B subunits. The B subunits show specific binding to a sialylated glycolipid (ganglioside GM1), delivering the A subunit to the cytosol. This, in turn, causes overactivation of an intracellular signaling pathway (adenylate cyclase, producing cyclic AMP) in gastrointestinal epithelial cells, causing severe diarrhea and electrolyte imbalance.[15] Other examples of sialic acid-dependent toxins are from *Clostridium tetani* and *Clostridium botulinum*, causing tetanus and botulism,[15] respectively.

Neisseria meningitides bacterial pathogen causes bacterial meningitis and sepsis. Capsular polysaccharide (CPS) coating on bacteria is the most conserved component in the form of α(2-8)

and α(2-9) homopolysaccharides unit and less frequently its 8-*O*-acetyl derivative.[16] The CPS on bacterial lining found to be more potent to induce immunogenicity. The synthetic mimic of CPS proven to induce the T-cell dependent immune response and finally approved as a vaccine candidate against the infection in children and adults.[16]

1.2.4 Selectins and Siglecs

Selectins are a family of C-type lectins (calcium requirement for carbohydrate recognition) which recognize specific carbohydrate sequence containing sialyl Lewis ^{x} (Le^{x}) and sialyl Lewis^{a} (Le^{a}), with or without sulfation at adjacent residues.[18] E-selectin is expressed on activated endothelial cells, while L-and P-selectin expressed on leukocytes and activated platelets or endothelial cells and all these are involved in leukocyte rolling, e.g., initiation of leucocyte localization at the inflammation site (E- and P-selectin) and adhesions of leukocyte to lymph nodes (L-selectin). P-selectin has also involved in tumor metastasis.[19] Although the sialic acid-dependent recognition by selectins is established, they interact with a limited range of preferred glycoprotein ligands *in vivo*. For example, P-selectin selectively interacts with P-selectin glycoprotein ligand-1 (PSGL-1), which expresses not only sialyl Le^{x} but also binds to three sulfated tyrosine residues in vicinity to the sugar binding site which enhances the binding.

Selectins also bind to anionic oligosaccharide sugars , such as heparan sulfate,[20] perhaps the biological significance of such binding is not clear. The similarities between the mice deficient in fucosyltransferase (FucT VII), which catalyzes the synthesis of sialyl Le^{x} and sialyl Le^{a} revealed that the selectin interactions with nonsialylated ligands are not prominent under laboratory conditions. However, exogenously injected heparin does affect tumor metastasis in a P-selectin-dependent mechanism.[21]

Selectin orthologs have been identified in putative insect (Drosophila), which shares a similar overall carbohydrate domain structure with selectins (C-type lectin domain + multiple “sushi” repeats).[22]

I-type lectins represent carbohydrate binding proteins though immunoglobulin super family domains (I-type CRDs). Siglec family are well characterized class of I-type lectins.[3] Siglecs are type I transmembrane proteins with a single *N*-terminal V-set immunoglobulin-like domain functions for sialic acid-recognizing domain. This domain is exposed from the cell surface by a string of C-set immunoglobulin-like domains with inconstant numbers depending on siglec

family.[3] An uncommon inter-domain disulfide bond, characteristic of siglecs, attaches the V-set domain to the adjacent C-set domain. Siglecs bind wide range of sialic acid ligand with precise glycoside linkage and some bind very restricted sets of sialic acid ligands.[3] In some cases differences in ligand selectivity have been observed by structural studies of the ligand binding site. All siglecs exhibits conserved arginine residue which makes an essential electrostatic interaction to sialic acid. In addition, a small number of siglec-like proteins which lack this conserved arginine have been discovered, including human siglec.[12] Further, two hydrophobic aromatic residues in the protein also contribute to ligand binding. In some siglecs (including siglec 7) residues in the loop between beta-strands, C and C' are involved in fine-tuning binding specificity.[23]

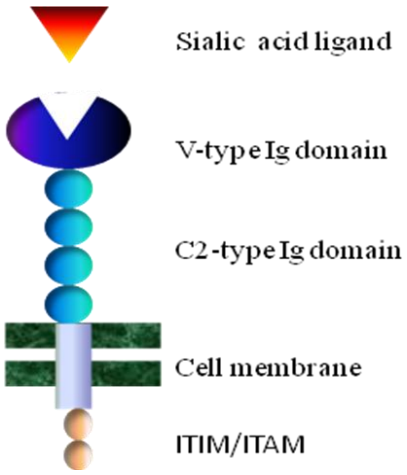

Figure 4. Structure of Siglecs.

In humans, 11 different form of siglec (Siglecs-1−11) and one Siglec-like molecule (Siglec-L1) have been identified and shown to be expressed on specific cell types, such as macrophages (sialoadhesin/Siglec-1), B-cells (CD22/Siglec-2), myeloid precursors/monocytes (CD33/Siglec-3), and oligodendroglia and Schwann cells (myelin-associated glycoprotein/Siglec-4). Many Siglecs (Siglecs-1, -3, -5, -7,−10) are expressed on the cells play crucial role in innate immune responses, such as monocytes, macrophages, NK cells and granulocytes. The number of Siglec genes appears to be different between species, e.g., mice have only eight Siglec genes.[3]

Biological functions of some of the Siglecs have elucidated through gene interruption Siglec-2/CD22 is involved in the regulation of B-cell signaling and Siglec-4a/MAG in the maintenance of myelin sheath structure. X-ray crystallography of the first Ig-like domain of Siglec-1 in

complex with its sialic acid ligand (Neu5Acα2−3Galβ1−4Glc) showed that the side chains of three amino acid residues highly conserved among Siglecs are in direct contact with sialic acid. This data shown the importance of these residues in ligand recognition predicted by the preceding site-directed mutagenesis studies.[3]

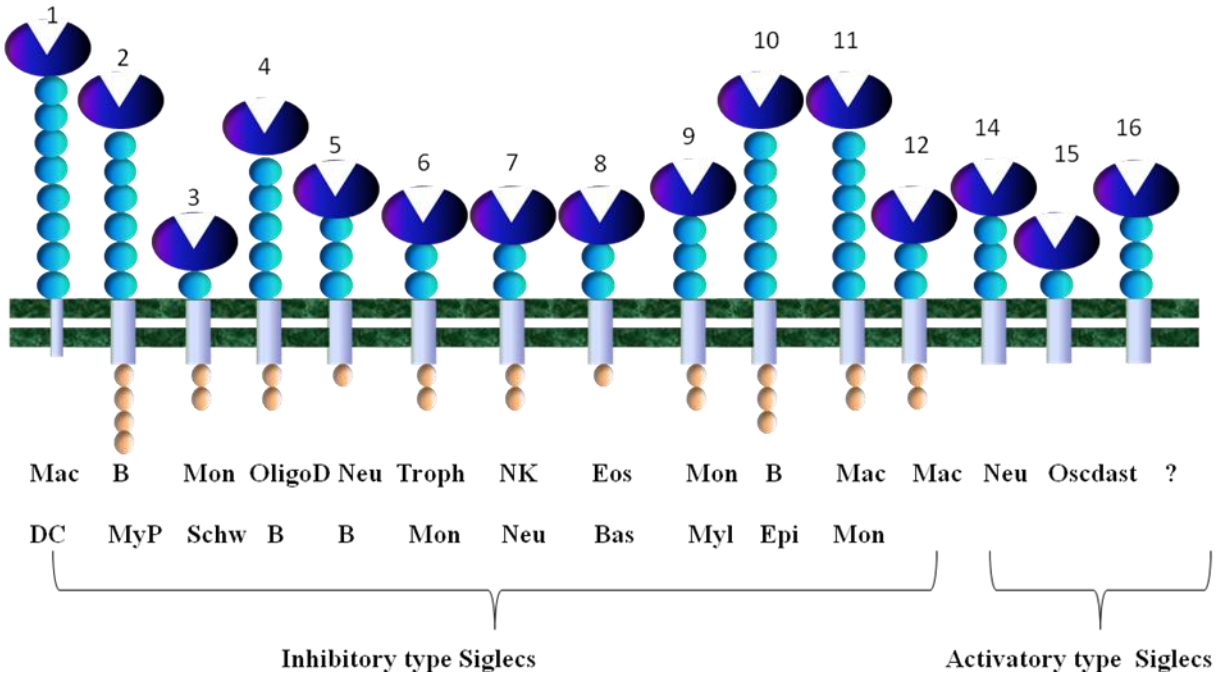

Figure 5. Specificity of Siglecs on Hematopoietic lineage (Immune cells). Abbreviations; Mac-macrophage; B-B-cells, Mon-monocytes, OligoD-oligodendrocytes, Neu-neutrophils, Troph-trophoblast, NK-natural killer cells, Eos-eosinophils, MyP-myeloid precursor, DC-dendritic cells, Bas-basophils, Schw-schwann cells.

There are more Siglec pseudogenes than there are functional Siglec genes in the human genome, suggesting that numerous gene duplications and subsequent loss of specific function due to inactivating mutations have taken place. This fact may have some relevance to the ongoing evolutionary arms race between vertebrate hosts and pathogens. A alleged Siglec-4a/MAG ortholog Schwann cell membrane protein (SMP or SCMP, Siglec-4b) in birds (quail and chicken) is reported.[24] There are no identifiable Siglec orthologs in the invertebrate genomes currently available for evaluation. Thus, it is possible that the sialic acid-binding features of Siglecs evolved after the emergence of prominent expression of sialic acids in deuterostomes

1.3 Specific recognition of Sialic acid by endogenous and exogenous receptors

The diverse and complex sialic acids structures are related to the different specificities of endogenous sialic acid-binding lectins. For example, mSiglec-2/CD22 prefers Neu5Gc to Neu5Ac, while m or hSiglec-1/sialoadhesins prefer Neu5Ac.[25] Similarly, IL-4(interlukin-4) interacts selectively with Neu5Ac, 1,7-lactone compared to other Neu5Ac derivatives. Also, alteration of sialic acid "mask" the sialic acid residue to block the endogenous lectins binding site, as reported for 9-*O*-acetylation which blocks recognition by Siglec-2 and lactoniation of Neu (Neu1,5-lactam) prevents recognition by L-selectin.[26]

The complexity of sialic acids in echinoderms can be explained by requirement of specific recognition during fertilization.[27] These animals release gametes (sperms and eggs) into open-water environments where they interact in a species-selective manner to avoid infertile hybrids. One way to prevent cross-species hybridization is harmonized release of gametes within a defined time period different from that of other species ("time-sharing"). However, this may work even more productively if these sperm and eggs have a species-specific receptor-ligand interactions. On the other hand, sialic acid modifications may drive speciation of echinoderms: gametes from an individual that acquired a new sialic acid modification allow to interact with only a fraction of gametes from the same species with relaxed recognition specificity and progeny of such mating could over generations develop into a subspecies and results in new species. In this process of development, sialic acid−gamete lectin compatibility may work as a reproductive obstacle. In accordance with these hypotheses, gametes of different species of sea urchins reportedly express glycosphingolipids unique to each species.[27]

Numerous pathogens recognize host sialic acids due to their high rate of replication (allowing rapid evolution) and the survival and propagation of only the efficient infectious units. Hence, pathogens inclined to evolve lectins with relatively strict specificity for sialic acid types and linkages. In contrast, it is suggested that endogenous lectins requires to tolerate a certain degree of structural variation of ligands.[28] This may allow escape of pathogens by changing modifications and linkages of sialic acids on surfaces exposed to the pathogens, all the while maintaining normal internal functions. Even a reduction in rate of infection (partial immunity) could benefit the host by decresing the severity of disease and limits the spreading. Also, pathogens, by virtue of their shorter generation time, they can diversify much faster than more complex hosts with longer generation times. As many pathogens develop different binding specificities, the hosts counter with various further modifications, thus driving structural

diversification of the sialic acids. Of course, inhibition of one pathogen by a particular type of sialic acid modification may actually make the host more susceptible to another (for example, 9-*O*-acetylation of Neu5Ac prevents recognition by influenza A virus, but this modification is the preferred ligand for influenza C virus). Since evolution does not occur in a goal-oriented way, host organisms are possibly forced to differentiate themselves by a shotgun approach involving a certain amount of "waste", which might make up some part of the diversity in sialic acids in a given cell type of a given species.

It is difficult to track the evolutionary variations of sialic acids in a multicellular host species in relation to multiple pathogens with well-defined sialic acid binding specificity. However, some circumstantial evidence supports the idea. For example, the viral infection is exaggerated by the type of sialic acid expressed on host cell surface, e.g., the case of influenza A virus as described above. The prominent location of sialic acid 9-*O*-acetylation on mucosal surfaces and changes in response to infection realed that sialic acid acetylation could originated as a counter measure against pathogens. In support, this changes is also the fact that such modified sialic acids resistant to various microbial sialidases. On the other hand, many endogenous sialic acid-binding lectins are related with the immune system and they are relatively tolerant of sialic acid structural variations.[30] This explanations support the hypothesis discussed above that endogenous receptors with relaxed recognition specificity are more tolerant to sialic acid modification, making it feasible to escape pathogens by modifying sialic acids without compromising endogenous function. Of course, if the binding selectivity of a particular endogenous lectin is too specific and not permits to modifications, such a lectin gene might get inactivated and/or replaced by a new lectin with more relaxed specificity. Some of the numerous Siglec pseudogenes in the human genome signify the results of such selection events.

Although the general direction of evolution of sialic acids inclined toward diversification, the same driving force may cause loss of variety if the situation permits it. For example, if a host can get rid of a particular type of sialic acid and reduce liability to certain types of pathogens without affecting endogenous lectin recognition, then individuals with the genetic mutation causing such loss could better fitness (survival/reproductive success) and the mutation will be positively selected and fixed in the whole species. Since the hosts can now generate antibodies against Sialyl Lewis^{X}, they may even shield themselves from pathogens conveyed from other species carrying same sialic acid moieties. The loss of Neu5Gc expression in humans [31] and the sporadic

presence of anti-Neu5Gc antibody in human blood may be related to a zoonotic Neu5Gc-binding pathogen which might be threatened human survival in the past.

Applying the same perception, the rather radically diverse "sialic acids" repertoire in bacteria (Neu5Ac, KDN, Legionaminic acid, Pseudaminic acid) could be explained by their evolutionary race against bacteriophages, the viruses that infect bacteria. It is known that the host range of bacteriophage is determined by the polysaccharides expressed by the host bacteria, and phage NM8, which infects and lyses a soil bacteria (Sino) rhizobium meliloti M11S strain, is shown to utilize the bacterial sialic acid containing lipopolysaccharides as its attachment site.[32] Rhizobia are known to express various sialic acids (Neu5Ac, KDN, and pseudaminic acid derivatives) as well as KDO on their extracellular polysaccharides.[33] Hence, the diversity of sialic acids in bacteria represent an escape mechanism from bacteriophage infections.

Alternative linkages (α(2−8) or α(2−9)) and sporadic *O*-acetylation of Neu5Ac found in polysaccharides produced by some pathogenic bacteria, such as *E. coli* K1 and N. meningitidis group C to counter the bacteriophage threat while avoiding detection by the host's immune system, which should easily detect unusual sugars such as legionaminic acid and pseudaminic acid. Indeed, Endo-N, an enzyme expressed by bacteriophage phi 92 (a lytic phage of *E. coli* K92 strain) which catalyzes hydrolysis of α(2−8) linked poly(Neu5Ac) on the bacterial cell surface, is unable to hydrolyze α(2−9) linked poly(Neu5Ac). There are also examples of bacteriophage evasion by bacteria involving acetylation sialic acid of surface polysaccharides.

1.4 Sialic acid structural and biological functions

1.4.1 Physiological Function

Sialic acid and its negative charge and hydrophilicity contribute biophysical features to several biological systems. Negative charge on human erythrocytes and other cell types exerts repulsive force to prevent unwanted interactions in blood circulation.[34] The endothelial lining of glomerulus with sialic acid coated podocytes prevents the filtration of the blood component into the urine.[35] Sialic acid relates to the half-life of glycoprotein in blood circulation.[36] The cleavage of the sialic acid susceptible the penultimate sugar to recognized by liver asialoglycan receptors and eventually cleared out from the system.[37] It has been shown that many glycans influence the process of fertilization not only in sperm-egg contact but also with various fluids and surface of female reproductive track before reaching to ovum.[38] The sialic acid expression are regulated by

the set of gene in nuclear machinery. The over expression of associated gene dysregulate the sialidase function and results into accumulation of sialic acid in lysosomes and extracellular space of the cell matrix and disease called as Salla Disease.[39] Sialic acid isolated from brain of gray matter named neuraminic acid and found tobe most abundant in rest other part of the body of animal. Peripheral and cortex part of the brain occupied by highly dense and complex structure of ganglioside. This ganglioside is sialylated and its composition varies from animal to human brain. During the developmental stage of brain this ganglioside matures and form a complex structure. The growth rate and density is higher during the brain development. Homopolymer of polysialic acid attached to neural cell adhesion molecule and has crucial impact on many neuronal functions. Polysialic acid acts as modulator of cell interaction in brain which has effectively proven by steric hindrance model. According to this model polysialic acid not only it affects carrier protein also it increases the intracellular space and abrogate adhesive binding of the other cell surface molecules like cadherines and integrins.[40]

In series of in vitro studies its shown that NCAM control the cell signaling. Endo N-mediated removal of polysialic acid from cell surface alter the initiate NCAM interaction which influence cell-cell interaction and therefor leads to the reduction in cell proliferation and parallel activation of the extracellular signal-regulating kinase. This activated kinase promoted survival and neuronal differentiation which enhance formation of neurite like process. This demonstrate that polysia-free-NCAM acts as ligand for heterophilic molecule partner. Receptor activation and downstream signaling kinase pathway activation believed to be initiated by fibroblast growth factor and cis and trans interaction of NCAM.[41]

1.4.2 Immunological role sialic acid

Sialic acid involved in regulation of alternative pathway of complement activation. The mechanism involves major serum protein factor H which recognize sialic acid as self gets recruited to native cell surface and thus down regulate the constant tick over of complement pathway on all cell surface. Details of this mechanism have elucidated, including accelerated dissociation of complement protein complex.[42] Thus sias and underlying glycans may act as self-associated molecular patterns(SAMP) for recognition by factor H.[43] Also it is reported that besides sias, its O-acetylation pattern on red blood erythrocytes in mice restricts the control to regulate complement activation pathway.[44]

1.4.3 Sialic acid as biological mask

First discovered vertebrate glycan binding protein was asialo-glycan receptor on hepatocytes hence called Ashwell receptor.[45] As name suggest that binding occur when removes sialic acid from glycoprotein and exposes underlying beta-linked galactose residue. Since, additional galactose binding receptor in macrophage have been discovered. On the other hand when bacterial sialidase enter into the blood circulation there can be extensive desialylation of cell and protein and this receptor becomes relevant. The removal of sias could generate the eat me signals and allow macrophage to recognize and eliminate or dying apoptotic cells. Therefore it has been extensively studied to find role of galactose binding receptor involved in such phenomenon from soluble galactins.

1.4.4 Antibody against intrinsic sialic acid

Sialic acid is intrinsic to host immune cells which recognized by the IgM of immune cells and cleared out before coming out from bone marrow. Hence it is not surprising that the least probability of finding the antibody against sialic acid. Indeed it might be one of the advantage to the pathogen bearing sias to circulate into the blood stream. Therefore natural sias considered as host immunosuppressive for host organism but exception are found.[46]

1.4.5 Sialic acid as Xenu autoantigen

The mammalian cellular machinery unable to synthesize the Neu5Gc from its natural precursor Neu5Ac because the phenotype fixed is the loss of function mutation of cytidine monophosphate -N-acetylneuraminic acid hydroxylase(CMAH) gene which remains intact with our closet evolutionary relative chimpanzees. Therefore dietary intake of Neu5Gc from red meat will be taken up and expressed on cell surface which results in the generation of antibody against Neu5Ac and increases risk of the inflammation associated disease like carcinomas, cardiovascular disease and macular degeneration cancer in the mammals.[47]

1.4.6 Sialic acid and cancer

Mucin is high molecular weight heavily glycosylated type1 transmembrane glycoprotein composed of cytoplasmic signaling peptide, transmembrane domain and ectodomain which consist of tandem repeating units of 20 amino acids. Each tandem repeat unit has five active sites of glycosylation and type and pattern depends on the site and physiological state of the tissue.[48] Tumor-associated muc1 abbarently glycosylated due to altered expression of sialyltransferase and lack of core galactosyl transferase produces truncated carbohydrate antigen like T, STn.

Humoral and immune response against muc1 antigen have observed in cancer patients. The presence of circulating antibodies against muc1 have diagnosed which correlates with favorable disease outcome of cancer.[48] Also, its has shown that sialyl Tn antigens have poor immunogenicity as they induce moderate T-cell independent immune response and weak T-cell mediated immune response.[48] Perhaps sialic acid α(2-6/3)GalNAc mucin glycopeptides are considered as the antigen of metastasized tumor. Thus sialic acid terminal sugar and underlying glycan and its mimics of structural analogues are immunogenic therefore many research group have put their efforts to induce a T cell mediated immune response in the form of IgG antibody against the TACAS. Some research group has used conjugation of carrier protein to TACAS to improve its immunogenicity.[49] Another group developed structural mimics of sialyl Tn analogs where they discovered the possibility of improvement in immunogenicity by modifying heteroatom of glycosydic linkage,[49] truncated antigen and lactone structures.[49] Few of them applied clustered antigen strategy and natural antigen modification strategy. Some of them have shown the modification with carrier proteins are crucial to implement for vaccine candidate against the cancer as it could induce better T-cell mediated immune response against tumor-associated carbohydrate antigen(TACA).[49] Therefore sialic acid is crucial cell surface component of metastasized tumor for the development of vaccine candidate.

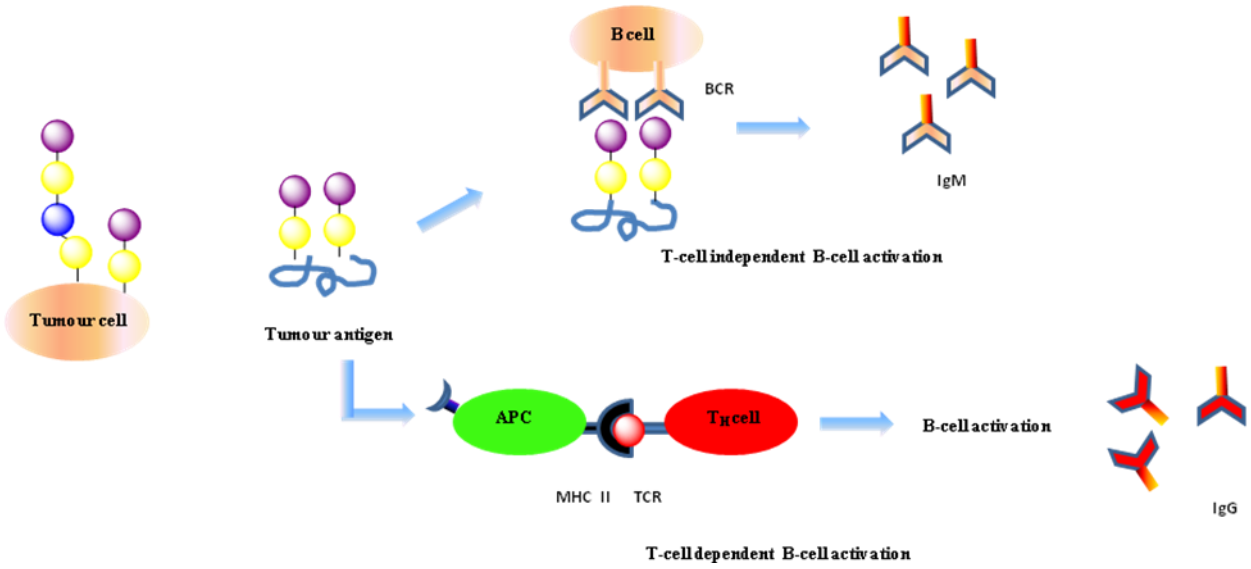

Figure 6. Immunology of glycoconjugates.

1.4.7 Role of Siglec-sialic acid complex in immunity

Siglecs are endocytic receptors and they are constitutively cycle between cell surface and intracellular endosomes or are induced to undergo endocytosis upon ligation of antibody or multivalent ligands.[50] Mechanism of endocytosis varies some are being clathrin-dependent and some are independent. Cytoplasmic Ty-based motif tail is the regulator of endocytic pathway of siglecs, however, sialoadhesin does not have regulatory motif yet undergo endocytosis and carry ligand bearing cargo in the cell.[50] Siglecs are expressed on specific cell type resulting in partial and complex overlapping expression pattern in innate and adaptive immune system.[50] Each siglecs has the preference for the specific sialylated structure that is expressed on mammalian cells which have revealed by the variety of method including glycan microarray analysis.[51] It is interesting that siglecs help immune cell to distinguish between self and nonself by use of sialic acid as ligand recognition. This ligand binding affects the immune modulatory function of siglecs for example, cis interaction with ligand is important for the signaling as it is been proved by B cell knock-in mutation of the sialic acid binding site of CD22 and Siglecs-G. This studies suggest that cis binding ligand sequester CD22 from association with BCR but promote association of Siglec-G exerting opposite effect on setting for B cell threshold signaling. Siglecs on dendritic cells and macrophage can modulate Toll-like receptor cytokine response by overexpression or ligation of antisiglec antibody or host-derived glycan.[52]

1.4.8 Sialic acid in therapeutic applications

Restricted expression pattern of siglecs makes this family targets for developing therapeutic for the treatment of wide range of disease. For example, high expression of certain siglecs on various lymphomas and leukemias has made them as a potential targeting candidate. Several additional features of siglecs suited for targeting the diseases.[53] It is known that most of the siglecs rapidly undergoes endocytosed after engaging with the antibody or its sialic acid ligand and again recycles to the cell surface, therefore, this feature of the siglecs can be used to deliver the cargo to the specific cell type. Moreover cellular signaling property of siglecs have been explored to alter the cell fate.[53]

1.4.9 Targeting siglecs using glycan ligands

Antibody-based siglecs therapy approach is unfavorable for its therapeutic applications because the auxiliary function of antibody (e.g binding to complement and Fc receptor) can cause serious side effect and development of the antidrug antibody against therapeutic antibodies produce their

long term use.[54] Therefore glycan-based siglecs targeting approach has proven as efficient therapeutic applications. Some of the novel features like absence of auxiliary function, lower immunogenicity than protein and dissociate at mild physiological condition makes this approach unique and significant for specific cell targeting.[55] Sialic acid glycan acts as ligand in ligand-based siglecs targeting strategy. Therefore it is not surprising that more efforts has been involved in molecular modeling, development of synthetic methods and innovative glycoconjugate protocol for the best potent ligand and its better engagement with the siglecs. Each siglecs express distinct preference with type of sialic acid, its glycosidic linkage with penultimate sugar and underlying glycans.

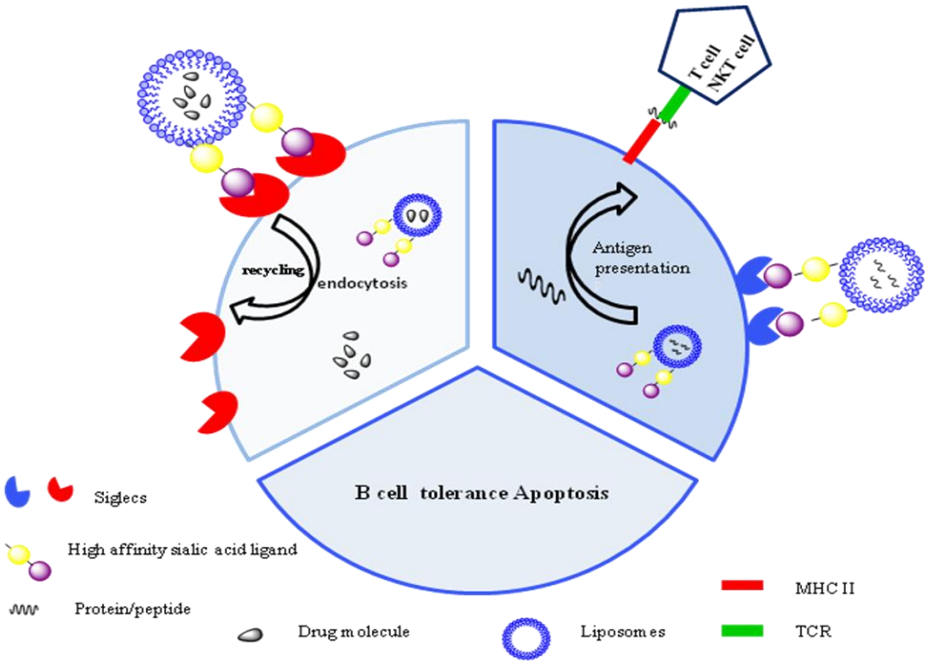

Figure 7. Glycan ligand based approaches with therapeutic potential.

Recently, the crystal structure of siglec-1 complexed with sialyl α(2-3) lactose suggested that C-9 modified sialic acid could enhance the affinity. The hydrophobic biphenyl substituent at C-9 position accommodate to the binding pocket adjacent to sialic acid with 13-fold increase in affinity with siglec-1.[56] Different ligand designed strategies have emerged with respect to choice of underlying structure at C-2 position of sialic acid. For example first generation high-affinity CD22 ligand combined preferred specificity for glycan sequence Neu5Acα(2-6)Galβ(1-4)GlcNAc with C-9 modification. Chemoenzymatically synthesized 9-BPC Neu5Acα(2-6)Galβ(1-4)GlcNAc demonstrated 16-fold increase in affinity against CD22 compared with methyl BPC Neu5Ac.[57] Also hydrophobic substitution by benzyl group over methyl at C-2

position results gain in affinity against siglec-1 and siglec-4. In recent years various approaches have been employed to develop high affinity Siglecs ligand like modification at C-5, C-4 and C-2 position.[57] Crystal structure of ligand-binding domain of various Siglecs have been solved and library of ligands have been screened to achieve the best molecular fitting ligand for particular Siglecs. Moreover homology model has constructed for several Siglecs to interpret binding affinity by molecular modeling and docking study. It has been hypothesized that hydrophobic modification at C-4 position may enhance the binding affinity with siglecs-2. Further synthetic library of modified sialic acid have evaluated to identify potential Siglecs ligand by using inhibition assay, surface plasmon resonance, isothermal titration calorimetry. Simultaneously this approach used for development of Siglec inhibitors. Recent development in high-throughput rapid strategy to synthesize sialoside library and its rapid screening. Glycan library of Neu5Acα(2-6)Galβ(1-4)GlcNAc and Neu5Acα(2-3)Galβ(1-4)GlcNAc with C-9 or C-5 of sialic acid was synthesized *via* copper catalyzed azide-alkyne cycloaddition reaction.[58] For high throughput screening resulting library of sialoside was printed as microarray on the glass slide and studied with recombinant Siglecs to identify high affinity ligand. With this recent advancement large number of the sialoside library have been screened for different Siglecs. After identifying the high affinity ligand, it has been employed for delivering the cargo to the specific cell type .For example the displaying high-affinity CD22 ligand conjugation on nanoparticle results in rapid endocytosis of cargo *via* CD22. Once in endosome, CD22-glycan ligand interactions are weakened by P^H acidification allowing nanoparticles bearing CD22 ligand to be dropped off while CD22 returns to the cell surface to pick up more cargos. This technique has employed and encapsulated the doxorubicin in sialic acid ligand liposomes and effectively deliver to the human lymphoma B cells. Furthermore a soluble high affinity dimeric sialic acid CD22 ligand has effectively targeted B-ALL in vitro.[59] Interestingly by making use of ligand-Siglec complex interaction specific antigen has been efficiently processed by antigen presenting cells (APC) like macrophage and dendritic cells to activate CD4+ T helper cells and NKT cells respectively.[60]

1.4.10. Modulating cellular signaling

Inhibitory type Siglecs contain ITIM motifs which activate the cascade responsible for the inhibition of immune cell activation. Hence recruitment of this inhibitory siglecs like CD22, Siglec-10 within appropriate context has potential to dampen the immunity where it is necessary

to control unwanted immune cell activation like autoimmune disease.[60] Since Siglecs are immunomodulator they are mainly driven by particular proximity to an activatory receptor. Therefore to understand the specificity of the inhibitory action of siglecs *in vivo* model has been studied. The model studies the ability of CD22 and Siglecs-10 to inhibit B cell receptor and induction of antigen-specific B-cell tolerance by studying the activation profile of SHP pathway and subsequent calcium flux measurement across the cell membrane. Also similarly liposomal nanoparticle bearing T-dependent (protein) antigen and high-affinity CD22 ligand were employed to test the ability of induction of immunological tolerance towards this type of antigen.[61] It has been shown that even after exposure of strong T-dependent antigen could not produce strong immune response as the engagement of CD22 ligand of B-cell to BCR results in preventing an antibody response to that antigen. Therefore tolerance was shown to be results of apoptosis of B-cell recognizing the antigen, which stemmed from inhibition of basal BCR signaling that is essential in B-cell. Thus concept of inducing immunological tolerance by recruiting CD22 to immunological synapse of the cell recognizing antigen was shown to be useful in preventing unwanted antibody response to biotherapeutics.

1.5 References

1. T. Angata, A.Varki, *Chemical Reviews*., **2002**, 102, 439; (b) A. Varki, R. D. Cummings, J. D. Esko, H. H. Freeze, P. Stanley, C. R. Bertozzi, G. W. Hart, M. E. Etzler, *Essentials of Glycobiology.,* **2009**, 2nd edition, Cold Spring Harbor Press, 199; (c) X. Chen, A. Varki, *ACS Chem. Biol.,* **2010**, 5, 163.
2. I. Ramos, A. Fernandez-Sesma, *Front Microbiol.,* **2012**, 28, 117; b) G. L. Sassaki, S. Elli, T. R. Rudd, E. Macchi, E. A. Yates, A. Naggi, Z. Shriver, R. Raman, R. Sasisekharan, G. Torri, M. Guerrini, *Biochemistry.*,**2013**, 52, 7217; c) E. S. Yoo, *J Microbiol Biotechnol.,* **2011**, 21, 449; d) J. E. Stencel- Baerenwald, K. Reiss, D. M. Reiter, T. Stehle, T. S. Dermody, *Nat Rev Mocrobiol.,* **2014**, 12, 739.
3. A. Varki, T. Angata, *Glycobiology.,* **2005**, 1R-27R; b) P. R. Crocker, A. Varki, *Immunology.,* **2001**, 103, 137.
4. S. A. Hudson, N.V. Bovin, R. L. Schnaar, P. R. Crocker, B. S. Bochner, *J Pharmacol Exp Ther.,* **2009**, 330, 608; b) D. Vestweber, J. E. Blanks, *Physiol Rev.,* **1999**, 79,181; c)

K. G. Bowman, B. N. Cook, C. L. de Graffenried, C. R. Bertozzi, *Biochemistry.*, **2001**, 40, 5382.

5. P. C. Pang, P. C. Chiu, C. L. Lee, L. Y. Chang, M. Paniko, H. R. Morris, S. M. Haslam, K. H. Khoo, G. F. Clark, W. S. Yeung, A. Dell, *Science.*, **2011**, 333, 1761.
6. K. Ohtsubo, J. D. Marth, *Cell.,* **2006**, 126, 855; b) D. H. Dube, C. R. Bertozzi, *Nat Rev Drug Discov.*, **2005**, 4, 477.
7. a) J. Finne, P. H. Makela, *J Biol Chem.*, **1985**, 260, 1265; b) G. Kochlamazashvili, O. Sekovo, S. Grebenyuk, C. Robinson, M. F. Xiao, K. Stummeyer, K. Gerardy, R. Schannar, A. K. Engel, L. Feig, A. Semyanov, V. Suppiramanian, M. Schachner, A. Dityatev, *J Neurosci.*, **2010**, 30, 4171.
8. a) A. G. Murzin, S. E. Brenner, T. Hubbard, C. Chothia,*J Mol Bio.*, **1995**, 247, 536; b) R. Loris, T. Hamelryck, J. Bouchaert, L. Wyns, *Biochim Biophys.Acta.*, **1998**, 138, 9.
9. a) C.M. Nycholat, R. McBridge, D. C. Ekiert, R. Xu, J. Rangarajan, W. Peng, N. Razi, M. Gilbert, W. Wakarchuk, I. A. Wilson, J. C. Paulson, *Angew Chem Int Ed Engl.*, **2012**, 51, 4860; b) L. Sanchez-Felipe, E. Villar, I. Munoz-Barroso, *Glyconj J.*, **2012**, 29, 539; c) M. H. Buch, A. M. Liaci, S. D. O'Hara, R. L. Garcea, U. Neu, T. Stehle, *Plos Pathog.*, **2015**, 11, doi: 10.1371/journal.ppat.1005104; d) C. Winter, C. Schwegmann- Wessels, D. Chavanagh, U. Neumann, G. Herrler, *J Gen Virol.*, **2006**, 87, 1209.
10. a) N. Tzarum, R. P. de Vries, X. Zhu, W. Yu, R. McBride, J. C. Paulson, I. A. Wilson, *Cell Host Microbe.*, **2015**, 11, 369; b) F. Wang, J. Qi, Y. Bi, W. Zhang, M. Wang, J. Liu, J. Yan, Y. Shi, G. F,Gao, *EMBO J.*, **2015**, 34, 1661.
11. M. J. Bakkers, Q. Zeng, L. J. Feitsma, R. J. Hulswit, Z. Li, A. Westerbeke, F. J. van Kuppeyeld, G. J. Boons, M. A. Langereis, E. G. Huizinga, R. J. de Groot, *Proc Natl Acad Sci U S A.*, **2016**, 113, doi: 10.1073/pnas.1519881113.
12. a) A. Baradaran, K. Yusoff, N. Shafee, R. A. Rahim, *J Cancer.*, **2016**, 7, 462; b) K. Fukushima , T. Takahashi, H. Ueyama, M. Takaguchi, S. Ito, K. Oishi, A. Minami, E. Ishitsubo, H. Tokiwa, T. Takimoto, T. Suzuki, *FEBBS Lett.* **2015**, 589, 1278.
13. a) S. S. Pang, S. T. Nguyen, A. J. Perry, C. J. Day, S. Panjikar, J. Tiralongo, J. C. Whisstock, T. Kwok, *J Biol Chem.*, **2014**, 289, 6332; b) N. Roche, J. Angstrom, M. Hurtig, T. Larsson, T. Boren, S. Teneberg, *Infect. Immun.*, **2004**, 72, 1519.
14. F. Lehmann, E. Tiralongo, J. Tiralongo, *Cell Mol Life Sci.*, **2006**, 63, 1331.

15. a) G. H. Thomas, E. F. Boyd, *Microbiology.,* **2011,** 157, 3253; b) W. I. Lencer, T. R. Hirst, R. K. Holmes, *Biochim Biophys Acta.*, **1999**, 1450, 177; c) M. Kitamura, S. Igimi, K. Furukava, *Biochim Biophys Acta.*, **2005**, 1741, 1.

16. a) M. Vossen, D. Mitteregger, C. Steininger, *Vaccine.*, **2016**, 34, 4364; b) K. O. Johswich, J. Zhou, D. K. Law, F. St Michael, S. E. McCaw, F. B. Jamierson, A. D. Cox, R. S. Tsang, S. D. Gray- Owen, *Infect Immun.*, **2012**, 80, 2346; c) E. C. Schulz, D. Schwarzer, M. Frank, K. Stummeyer, M. Muhlenthoff, A. Dickmanns, R. Gerardy-Schahn, R. Ficner, *J Mol Biol.*, **2010**, 39, 341; d) J. Hutter, B. Lepenies, *Methods Mol Biol.*, **2015**, 1331, 1.

17. a) Z. Fujimoto, H. Tateno, J. Hrabayashi, *Methods Mol Biol.*, **2014**, 1200, 579; b) I. R. Nabi, J. Shankar, J. W. Dennis, *J Cell Sci.*, **2015**, 128, 2213; c) I. M. Dambuza, G. D. Brown, *Curr Opin Immunol.*, **2015**, 32, 21.

18. a) N. Sharon, *Trends Biochem Sci*., **1993**, 18, 221; b) D. C. Kilpatrick, Biochim. *Biophys Acta Gen Subj.,* **2002**, 1572, 187.

19. K. Ley, *Trends Mol Med.,* **2003**, 9, 263; b) M. Hirai, H. Minematsu, N. Kondo, K. Oie, K. Iqarashi, N. Yamazaki, *Biochem Biophys Res Commun.,* **2007**, 353, 553.

20. a) Koeniq, K. Noegard-Sumnicht, R. Linhardt, A. Varki, *J Clin Invest.,* **1998**, 101, 877.

21. L. Bortsig, R. Wong, J. Feramisco, D. R. Nadeau, N. M. Varki, A. Varki, *Proc Natl Acad Sci U S A.*, **2001**, 98, 3352.

22. Mei- Ling Chin, M. Mlodzik, *Dev Cell.*, **2013**, 26, 455.

23. H. Attrill, A. Imamura, R. S. Sharma, M. Kiso, P. R. Crocker, D. M. Aalten, *J Biol Chem.,* **2006**, 281, 32774.

24. a) Dulac, M. B. Tropak, P. Cameron-Curry, J. Rossier, D. R. Marshak, J. Roder, N. M. Le. Douarin, *Neuron.,* **1992**, 8, 323.

25. a) Van der, E. C. M. Linden, A. Varki, *J Biol Chem.*, **2000**, 275, 8625.

26. a) Mitsuoka, K. Ohmori, N. Kimura, A. Kanamori, S. Komba, H. Ishida, M. Kiso, R. Kannagi, *Proc Natl Acad Sci U S A.,* **1999**, 96, 1597.

27. a) V. D. Vacquier, *Science.*, **1998**, 281, 1995; b) Y. Nagai, M. Hoshi, *Biochim Biophys Acta.,* **1975**, 388, 146.

28. P. Gagneux, A. Varki, *Glycobiology.,* 1999, 9, 747.

29. L. Van Valen, *Nature.*, **1974**, 252, 298.

30. A. Varki, *FASEBJ.*, **1997**, 11, 248.
31. A. Muchmore, S. Diaz, A. Varki, *Am J Phys Anthrol.*, **1998**, 107, 187.
32. A. Defives, M. Werquin, P. Mary, J. P. Homez, *Curr Microbiol.*, **1996**, 33, 371.
33. L. Reuhs, D. P. Geller, J. S. Kim, J. E. Fox, V. S. Kolli, S. G. Pueppke, *Appl Envion Microbiol.*, **1998**, 64, 4930.
34. H. P. Fernandes, C. L. Cesar, L. Mde. Barjas-Castro, *Rev Bras Hematol Hemoter.*, **2011**, 33, 297.
35. S. E. Quaggin, *J Clin Invest.*, **2007**, 117, 1480.
36. T. S. Raju, J. B. Briggs, S. M. Chamow, M. E. Winkler, A. J. Jones, *Biochemistry.*, **2001**, 40, 8868.
37. P. H. Weigel, J. H. Yik, *Biochim. Biophys. Acta.*, **2002**, 1572, 341
38. K. J. Mengerink, V. D. Vacquier, *Glycobiology.*, **2001**, 11, 37R.
39. R. Biancheri, E. Verbeek, A.Rossi, R. Gaggero, L. Roccatagliata, R. Gatti, O. Van Diggelen, O. Verheijen, G. M. Mancini, *Clin Genet.*, **2002**, 61, 443.
40. C. P. Johnson, I. Fujimoto, U. Rutishauser, D. E. Leckband, *J Bio Chem.*, **2005**, 280, 137.
41. R. L. Schnaar, R.Gerardy-Schahn, H. Hilderbrandt, *Physiaol Rev.*, **2014**, 94, 461.
42. M. K. Pangburn, H. J. Muller-Eberhard, *Proc Natl Acad Sci USA.*, **1978**, 75, 2416.
43. A. Varki, *Glycobiology.*,**2011**, 11, 1121.
44. U. E. Nydegger, D. T. Fearon, K. F. Austen, *Proc Natl Acad Sci USA.*, **1978**, 75, 6078.
45. P. Weiss, G. Ashwell, *Prog Clin Biol Res.*, **1989**, 300, 169.
46. Y. Song, K. Kitajima, Y. Inoue, *Glycobiology.*, **1993**, 3, 31.
47. A. Varki, *Proc Natl Acad Sci USA.*, **2010**, 107, 8939.
48. a) T. Feizi, *Immunol Rev*., **2000**, 173, 79; b) M. R. Kundelka, T. Ju, J. Heimburg-Molinaro, R. D. Cummings, *Adv. Cancer Res.*, **2015**, 126, 53; c) F. M. Tuccillo, A. de Laurentiis, C. Palmieri, G. Fiume, P. Bonelli, A. Bonelli, P. Tassone, I. Scala, F. M. Bounaguro, I. Quinto, *Biomed. Res. Int.*, **2014**, 70.
49. a) R. A. De Silva, Q. Wang, T. Chidley, D. K. Appulage, P. R. Andreana, *J. Am. Chem. Sco.*, **2009**, 131, 9622; b) D. R. Bundle, J. R. Rich, S. Jacques, H. N. Yu, M. Nitz, C. Ling, *Angew. Chem. Int. Ed.*, **2005**, 44, 7725; c) M. Wilstermann, L. O. Kononow, U. Nilson, A. K. Ray, G. Magnusson, *J. Am. Chem. Sco.*, **1995**, 117, 4742; d) L. F. Tietze,

H. Keim, C. O. Janben, C. Tappertzhofen, J. Olschimke, *Chem. Eur.J.*, **2000**, 6, 2801; e) A. Arcangeli, L. Toma, L. Contiero, O. Crociani, L. Legnani, C. Lunghi, E. Nesti, G. Moneti, B. Richichi, C. Nativi, *Bioconjugate Chem.*, **2010**, 21, 1432.

50. a) P. R. Crocker, J. C. Paulson, A. Varki, *Nat Rev Immunol.*, **2007**, 7, 255; b) M. S. Macauley, P. R. Crocker, J. C. Paulson, *Nat Rev Immunol.*, **2014**, 14, 653.
51. a) C. D. Rillahan, E. Schwartz, C. Rademacher, R. McBridge, J. Rangarajan, V. V. Fokin, J. C. Paulson, *ACS Chem Biol.*, **2013**, 8, 1447.
52. J. Jellusova, U. Wellmann, K. Amann, T. H. Winkler, L. Nitschke, *J.Immunol.*,**2010**, 184, 3618.
53. S. Pillai, I. A. Netravali, A. Cariappa, H. Mattoo, *Annu Rev Immunol.*,**2012**, 30, 357.
54. a) O. Haji- Ghassemi, R. J. Blackler, N. Martin Young, S. V. Evans, *Glycobiology.*, **2015**, 25, 920; b) B. E. Collins, O. Blixt, S. Han, B. Duong, H. Li, J. K. Nathan, N. Bovin, J. C. Paulson, *J.Immunol.*, **2006**, 177, 2994.
55. a) S. Kelm, J. Gerlach, R. Brossmer, C. P. Danzer, L. Nitschke, *J Exp Med.*, **2002**, 195, 1207; b) N. R. Zaccai, K. Maenaka, T. Maenaka, P. R. Crocker, R. Brossmer, S. Kelm, E. Y. Jones, *Structure.*, **2003**, 11, 557.
56. S. Kelm, R. Brossmer, R. Isecke, H. J. Gross, K. Strenge, R. Schauer, *Eur J Biochem.*, **1998**, 255, 633.
57. C. D. Rillahan, E. Schwartz, R. McBridge, V. V. Fokin, J. C. Paulson, *Angew Chem Int Ed Engl.*, **2012**, 51, 11014.
58. A. Schweizer, M. Wohner, H. Prescher, R. Brossmer, L. Nitschke, *Eur J Immunol.*, **2012**, 42, 2792.
59. M. F. Bachmann, G. T. Jennings, *Nat Rev Immunol.*, **2010**, 10, 787.
60. B. H. Duong, H. Tian, T. Ota, G. Completo, S. Has, J. L. Vela, M. Ota, M. Kubitz, N. Bovin, J. C. Paulson, D. Nemazee, *J Exp Med.*, **2010**, 207, 173.
61. M. S. Macauley, F. Pfrengle, C. Rademacher, C. M. Nycholat, A. J. Gale, A. von Drygalski, J. C. Paulson, *J Clin Invest.*, **2013**, 123, 3074.

Chapter 2
Sialic acid Mimics

Chapter 2a. Screening of Neu5Acα(2-6)Gal Isomers Preferences of Siglec with Sialic acid Microarray.

2.1.1 Introduction

Sialic acids are the terminal sugars of glycoproteins and glycolipids on cell surfaces that are characterized by a 9-carbon backbone.[1] To date, nearly fifty different forms of Sias have been identified. Among them, *N*-acetylneuraminic acid and its *N*-glycolyl derivatives are the most prominent.[2] Given their structural diversity, Sias act in several biological processes. Sias on the cell surfaces are involved in regulation of cell cycle, autoimmune disorders, and are also involved in pathogens recognition.[3] Sialic acid binding lectins (Siglecs) are major homologues subfamily of I-type lectins, that mediate Sia recognition *via* immunoglobulin (Ig)-like domains.[4] Expression of specific Siglecs modulate immune responses, inflammation, tumorigenesis and apopotosis.[5]

Siglecs are classified into two subgroups, CD33-related subgroups, (Siglec-3, -5, -6, -7 & -10) which appear to be rapidly evolving with complex expansion in different mammalian lineages and the second subgroup include the evolutionarily conserved ones (Siglec-1, -2 and -4).[6] In general, Siglecs bind to common epitopes containing Neu5Acα(2-6)gal and/or Neu5Acα(2-3)gal linkages. Various Siglecs exhibits overlapping actions as a result of similar glycan binding preferences that complicate the assessment of distinct siglec functions. Hence, identifying the distinct Sias glycans recognition patterns is essential for revealing the Siglecs functions. To this end, C-9 and C-4 position of sialic acids was modified with aromatic and sulphate derivatives to increase the Siglec-2 binding affinity.[7] The synthetic glycan microarray analysis of these glycans revealed that biphenyl substitution at C-9 position and sulphate at C-4 position shown 750,000-fold higher affinity to hCD22 compared to the native sialic acid ligands.[8] Similarly, potential modification on sialic acid has been studied to elucidate role of Siglecs in biological system. However, the basic differences between the conservative and evolutional siglec selectivity remains largely unclear and it is unknown what factors are responsible for the specificity. To understand how Siglecs generate specificity for sias glycans, it is essential to construct structural analogs of Neu5Acα(2-6)Gal to modulate the distinct binding patterns.

Here, we have systematically investigated the effect of sialic acid as terminal sugar and galactose/glucose/mannose as penultimate sugar to study the major human Siglecs binding

patterns. Based on the binding affinities, it could be possible to deduce how nature differs with the evolutionary and conserved siglec-ligand selectivity.

2.1.2 Retrosynthesis of Sialosides

A) Disaccharides

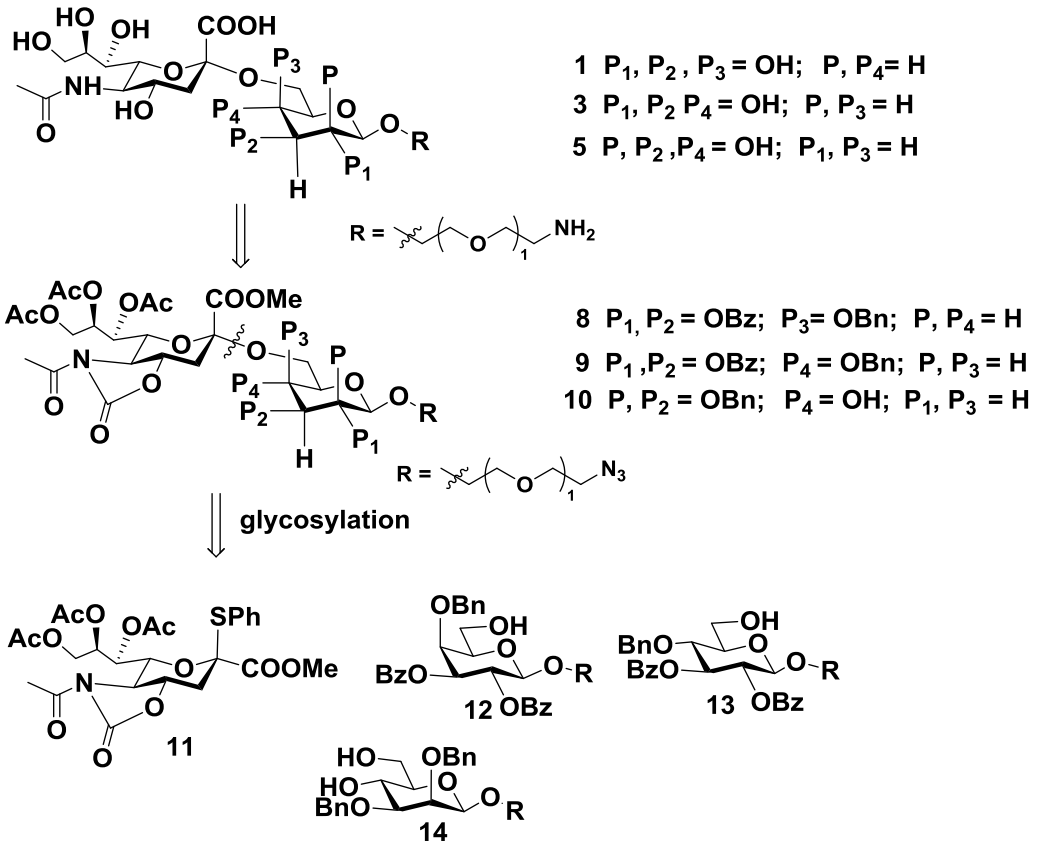

Scheme 1. Retroynthesis of sialic acid disaccharides.

The sialic acid disaccharides (**1**, **3** and **5)** were obtained from fully protected disaccharide **8**, **9** and **10** respectively. The esters, ether and azide functionality on **8-10** was successively removed by use of global deprotection protocol (Scheme 1). The sialic acid donor (**11**) and galactose/mannose/glucose acceptors (**12-14**) were synthesized according to modified literature procedure.[9] The glycosylation of donor and acceptor were carried out by NIS/TfOH at -40^{0}C which gave protected form of disaccharides in moderate to good yield. The 4, 6-benzylidine protection of galactose and glucose thiotoulene pentahydroxy derivatives and its successive C-2,

C-3 benzoylation afforded protected form of galactose and glucose thiotoluene. The stereodirecting benzoyl group at C-2 position was chosen to avail beta configuration which usually found on natural linkage of glycans. The glycosylation of galactose and glucose derivative with linker in presence of NIS/TfOH at -40^{0}C and successive regioselective ring opening by $PhBCl_2/Et_3SiH$ afforded acceptor **12** and **13** with good yield. Simultaneously the regioselective C-4, C-6 bezylidine protection and C-2, C-3 benzylation gave thiophenol mannose derivative which then converted into its sulfoxide in presence of m-CPBA at lover temperature to afford the highly active mannose-sulfoxide thiophenol donor. The mannose donor was glycosylated with linker in presence of Tf_2O/TTBP, at -78^{0}C and the benzylidine ring cleavage by acid catalyst afforded acceptor **14** in moderate yield.

B) Trisaccharides:

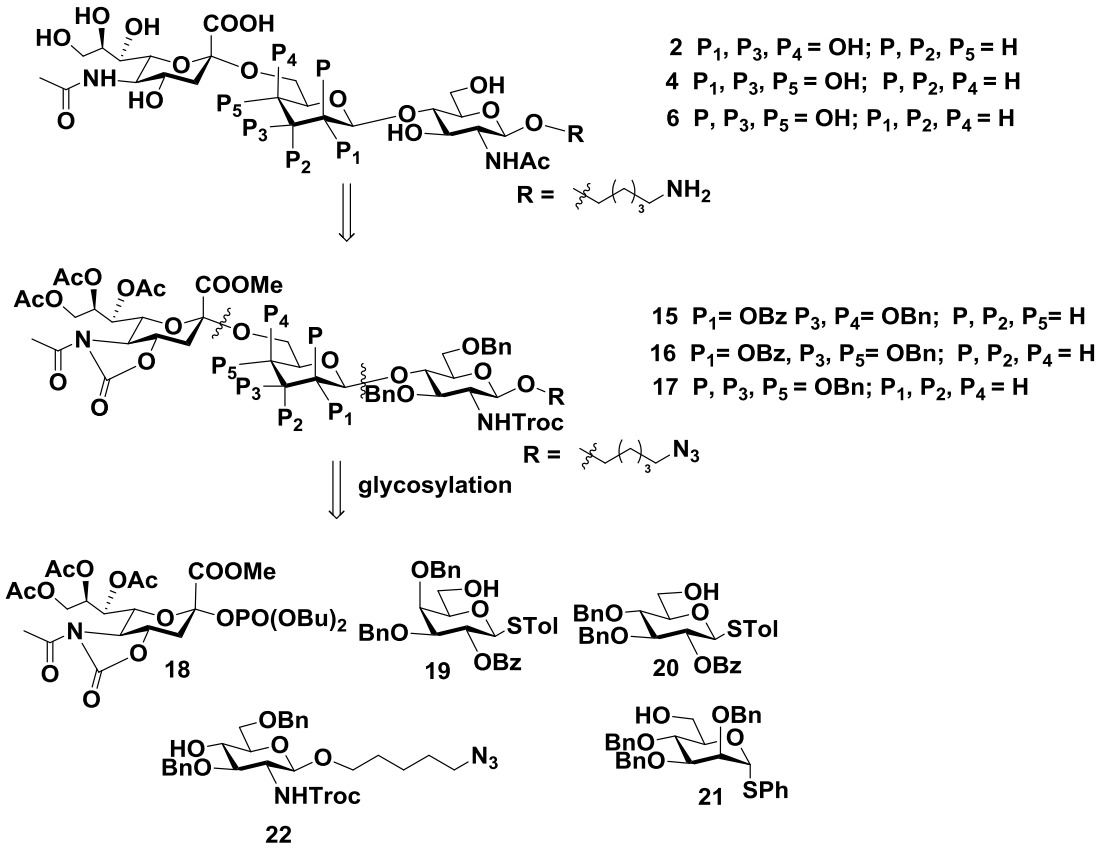

Scheme 2. Retrosynthesis of sialic acid trisaccharides.

2.1.3 Synthesis of Donors and Acceptor

The trisaccharide analogs of Neu5Acα(2-6)Galβ(1-4)GlcNAc were obtained by global deprotection of fully protected trisaccharide **15-17** in moderate yield. Synthetic convergent approach involves sialic acid dibutylphosphate donor (**18**) and C6-OH thiotoulene, thiophenol acceptor of galactose (**19**) glucose (**20**), mannose (**21**) and glucosamine (**22**) at the non-reducing end (Scheme 1). The donor **18** was synthesized from *N*-acetylneuraminic in 7 steps according to literature protocol.[10] Synthesis of acceptors **19** and **20** was achieved in four steps involving C-4, C-6-benzylidine protection then selective C-3 benzylation with nBu_2SnO/BnBr followed by C-2 benzoylation and finally regioselective benzylidine ring opening with $PhBCl_2/Et_3SiH$ afforded C6-OH acceptor in good yield. Similarly mannose C6-OH acceptor (**21**) was synthesized from its pentahydroxy thiophenol derivative by following temporary C6-OH TBDMS protection, then benzylation of remaining hydroxyl-groups and finally removal of temporary silyl protection by p-TSA gave desired compound in good yield. The synthesis of building block **22** was challenging and successfully achieved in 11 steps by following published protocol.[11] Sialic acid donor 18 was glycosylated with acceptors **19-21** in presence of TMSOTf at -78^0C gave expected disaccharides, which subsequently glycosylated with acceptor **22** in presence of NIS/TfOH at -40 to -20^0C yielded fully protected trisaccharide analogs (**15-17**). Finally esters, troc, oxazolidinone protection was removed by global deprotection protocol and later removal of benzyl ether and simultaneous azide to amine reduction was achieved by hydrogenolysis to afford fully deprotected trisaccharide (**2**, **4** and **6**) in moderate yield.

2.1.4 Glycan microarray screening of sialoside library with Siglecs

Next, the synthetic di- and tri-saccharides were printed onto epoxide-functionalized microarray slides at 100 µM in replication of 4 as described in the experimental section. Human (H) and mouse (m) Siglec-Fc chimeras (H-Siglec-2, m-Siglec-2, H-Siglec-3 and -10) were incubated on the slide at three concentrations (5 ng/µl, 10 ng/µl and 20 ng/µl,) in PBS with 1% ovalbumin, followed by the secondary antibody (Cy3-anti-human IgG). Slides were scanned and the binding determined by the fluorescence intensity as described in the experimental section. Initially the sialic acid microarray was analyzed by incubating with control lectins of known binding specificity. As expected, sambucus nigra lectin (SNA), which is specific of Neu5Acα(2-6)gal bound to **1** and **2** and displayed no binding with **3-6**. After confirming the binding affinity with

control lectin, H-Siglec-2 and m-Siglec-2 binding in microarray was established. H-Siglec-2 displayed weak binding with **1** and **2** compared to m-Siglec-2. Interestingly, isomers of compound 1 and 2 did not show any binding. while H-siglec-3 and H-siglec-10 bound to **1** and **2**. Remarkably, the isomers of **1** and **2** displayed better binding to Siglec-3 and -10 compared to the native form. According to the microarray studies, compound **1-6** sialic acid glycans possess two distinct binding patterns. The evolutionarily conserved H-Siglec-2 or m-Siglec-2 displayed selective binding towards **1** and **2**, indicating that the interaction between the penultimate sugar (galactose and specific amino acid sequence in Siglec-2 is conserved, thus generating the specific binding motif. On the other hand, the rapidly evoluving siglec-3 and 10 displayed spatial flexibility, allowing them to bind galactose isomers (mannose and glucose). Overall, identification of these detailed binding preferences provides the basis for understanding and targeting siglec selectively. The mannose isomers of sialic acid glycans are common side products of the *β*-mannosidosis[12] disease and the binding between **5** and **6** with siglec-3 and 10 reveals possible the mechanism of immune responses in human system.

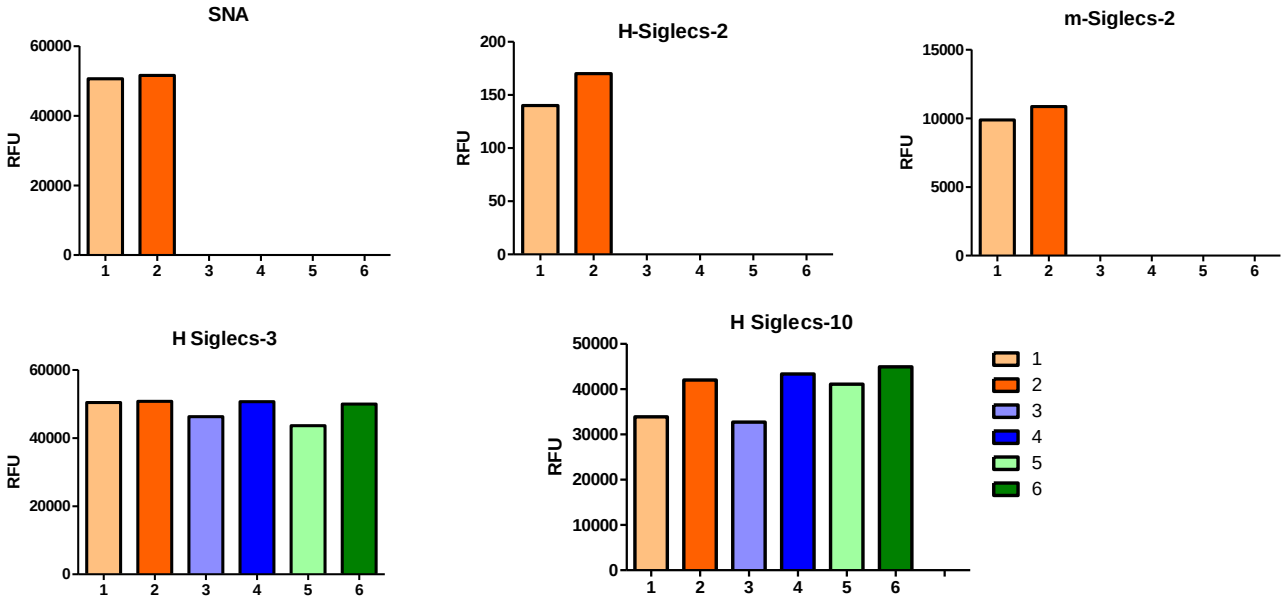

Figure 2. Microarray analysis of sialic acid derivatives (**1-6**) lectin binding (at 20 ng/µl).

2.1.5 Conclusion

We have synthesized a library of sialic acid glycans by modifying the penultimate sugar and expressing them on the glycan microarray to determine siglec binding preferences. Comparison of the siglec binding patterns allows further understanding of the basic differences between the conserved and evolving Siglecs, and constitute a valuable tool for designing siglec specific molecules for therapeutic applications.

Chapter 2b. Harvesting the Immunogenicity in Sialic acid Glycans by Altering the Penultimate Sugar of the Glycans.

2.2.0 Introduction

N- and *O*-glycans represents important class of glycoproteins present on the cell surfaces, involved in several essential cellular functions, including cell growth, migration, and differentiation.[13-18] Often *N*- and *O*-glycans share a common core sugars sequence with complex or hybrid terminal sugar. Among them, Neu5Acα(2-6)Galβ(1-4)GlcNAc (6'SLN) is frequently found at the terminal glycans, serves as a ligand for several proteins, including Siglecs,[19-21] influenza virus hemagglutinin proteins,[22-26] bacterial proteins and cytokines.[27-29] Studies linking specific lectin for sialic acid glycans indicate the existence of many sialic acid forms within the trisaccharides.[18] These molecular sequences with the sialic acid glycans regulate the particular feature of a given species, e.g. the 9-*O*-acetyl 6'SLN exhibited enhanced B-cell receptor activation compared to native form.[30] *N*-glycolyl form of 6'SLN binds to human H3 virus.[31] Moreover, glycoproteins and glycolipids of blood samples composed of Neu5Ac8Me, Neu, Neu4,5Ac2, Neu5,7Ac2, Neu5,9Ac2, Neu5Ac9Lt, Neu5,8Ac29Lt and Neu5Ac8S derivatives.[32-33] However, detail structure and functions of these glycans are yet to decipher due to the lack of appropriate tools. Hence the development of sequence-specific monoclonal antibodies is the ideal strategy for studying diversity. However, these glycans are poor immunogenic to induce antibodies in the mammalian system. To circumvent this, we have adopted the molecular mimicry strategy to generate antigenic sugars, which may ultimately produce IgG immune response against these glycans.

Previously, the molecular mimicry strategy has been extensively used to design sugar scaffolds with superior lectin affinity and antigenicity. Paulson et al. utilized this strategy to develop efficient sialic acid ligands for Siglecs binding.[34] Jennings group reported N-propionyl polysialic acid to produce high titer IgG antibody against polysialic acid ligand.[35] This method was further extended to develop immunogenic tumor-associated carbohydrate antigens (TACAs). For example, Lin et al. incorporated different substitutions at amide group of STn antigen to produces strong immunogenic sugars. Among them fluorinated N-propionyl substitution on STn demonstrated most immunogenic nature.[36-40] Huo et al. reported S-glycosidic linkage in STn scaffold improves the stability and resistance to endogenous glycosidases.[41] Although these

modifications improved the antigenicity of the glycans, they compromised in the structural aspects. Herein, we adopted the molecular mimicry strategy to modulate the immune response of the 6'SLN glycan. The synthetic analogs of 6'SLN glycan were constructed by replacing the penultimate sugar scaffold within the glycan by its isomers to maintain the similar H-bond network and protein binding pocket. Finally, these molecules are conjugated to a carrier protein (KLH) and immunize the mice to investigate suitable modification in 6'SLN to induce antigenicity. We examined the serum IgG antibody titers level at different time intervals and its cross-reactivity. By these results, crucial structural aspects to design antigenic sugar for vaccine candidates were proposed.

2.2.1 Sialoside glycoconjugates

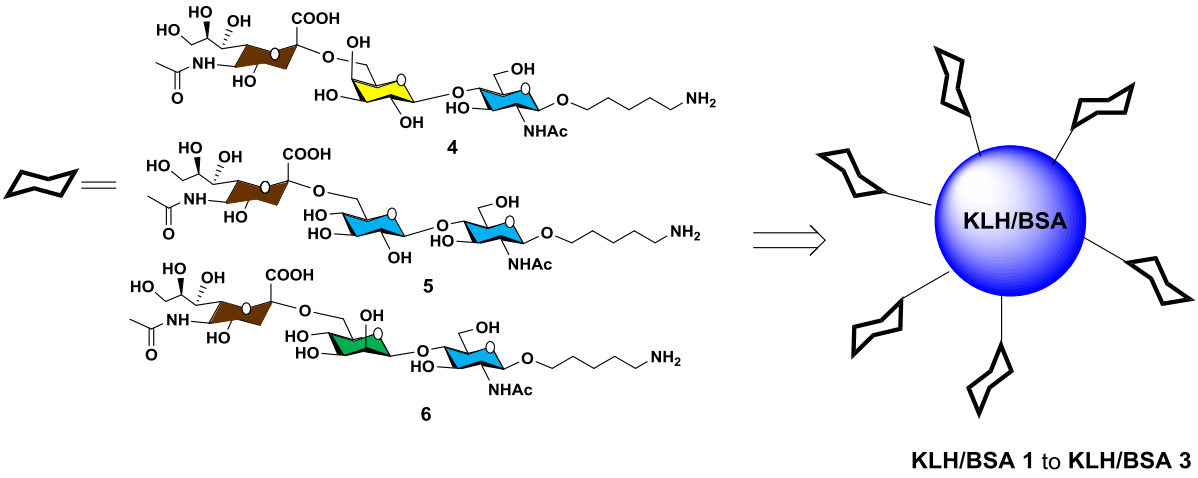

Figure 3. Chemical structures of 6'SLN analogs (**4-6**) and its KLH conjugation.

Generation of KLH/BSA glycoconjugates (KLH/BSA-1 to KLH/BSA-3)

Sialic acid trisaccharide in the form of galactose, glucose and mannose as penultimate sugar derivatives appended with a C-5 amino linker were synthesized. The corresponding KLH/BSA conjugation of these glycans was generated by using cross-reactive coupling reagent dimethyl adipimidate. HCl. In the first step, sialic acid glycans-amino linker (**4-6**) were activated and then cross-linked to KLH/BSA residue in a second step. The resultant mixture was dialyzed afford desired conjugated product in a quantitative yield. The glycoconjugates products were characterized by resorcinol method to quantify the amount of sialic acid per mg of protein.[42] As characterized by resorcinol and Bradford protein assay, the percentage of 1-3 per mg of

KLH/BSA is around 7-13%. These results indicate multivalent display of sialic acid glycans on protein (table. 2 and 3).

2.2.2 Detection and analysis of immune response induced by sialo-glycoconjugates(KLH-1 to KLH-3)

A group of six female C57BL mice of 2–4 weeks old was immunized biweekly intervals with KLH conjugated sialic acid derivatives and KLH as such and phosphate buffer as control. After two weeks of 3rd and 4th immunization, animal sera were withdrawn and pooled with respect to the individual group. ELISA plate analysis of the total antigen-specific antibody or a specific isotype of antibody including IgG, IgG1, IgG2a,IgG2b and IgG3 of the pooled sera indicate the immune response of the molecules.

At first, 96-well plate was coated with **BSA-1** to **BSA-3** and then treated with the sera pooled after 13th and 14th day of 3rd and 4th immunization of five immunized mice. Antibodies affinity by the coating antigens were detected with HRP conjugated goat anti-mouse kappa light chain specific antibody, which would expected to detect about 95% of the total antibody response. The sera obtained after the primary immunization, namely obtained after 2nd, gave low ELISA titers hence data not shown. The IgG antibody titers **BSA-1** to **BSA-3** of mouse immunized with KLH-1 to KLH-3 which induced significant immune response after 3rd and 4th immunization indicating the immunogenicity of modified KLH conjugates (fig. 4A, table 4 and 5). Also the moderate IgM antibody titer of KLH glycoconjugates (fig. 4B, table 4 and 5) shows the weak induction of B-cell mediated (T-cell independent) immune activation. Interestingly it has been observed that modified analogs of sialoside conjugates **KLH-2** and **KLH-3** showed comparative antibody titer (IgG and IgM) for the antigen-specificity. After 4th immunization, the titer values showed substantial increase in the antibodies level between the native and the biomimetic analogs compared to 3rd immunization.(table-4) After 4th immunization pooled serum analysis shows that KLH-3 displayed a remarkable 1.75-fold higher IgG antibody titer compared to native conjugate analog i.e. **KLH-1**. thus indicating the importance of mannose in the immune modulation of sialic acid glycans. Interestingly, glucose analogs **KLH-2** also displayed nearly 1.2-fold increase in the IgG antibody responses compared to native glycoconjugate (**KLH-1**). Similarly, IgM antibody titer of **KLH-2** and **KLH-3** shown around 2.5 fold higher compare to the native conjugates (fig. 4B and table-4).

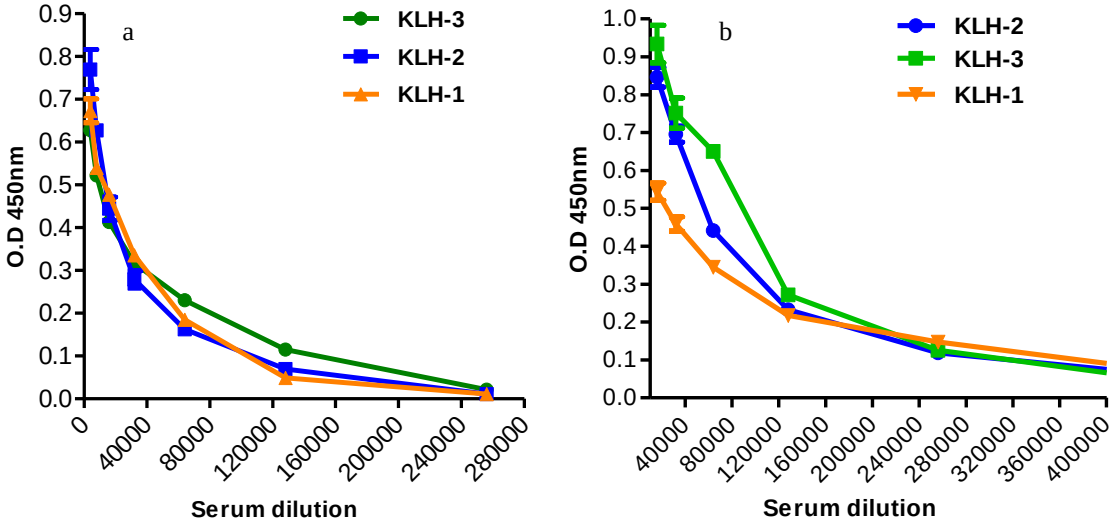

Figure 4A. IgG antibody titers of pooled sera immunized with **KLH-1, KLH-2** and **KLH-3** by ELISA. (a) IgG response from pooled sera obtained from 13 days after 3rd immunization; (b) response from pooled sera obtained from 14 days after 4th immunization. All data points were the mean of three parallel measurement data. Some error bars are smaller than symbol width.

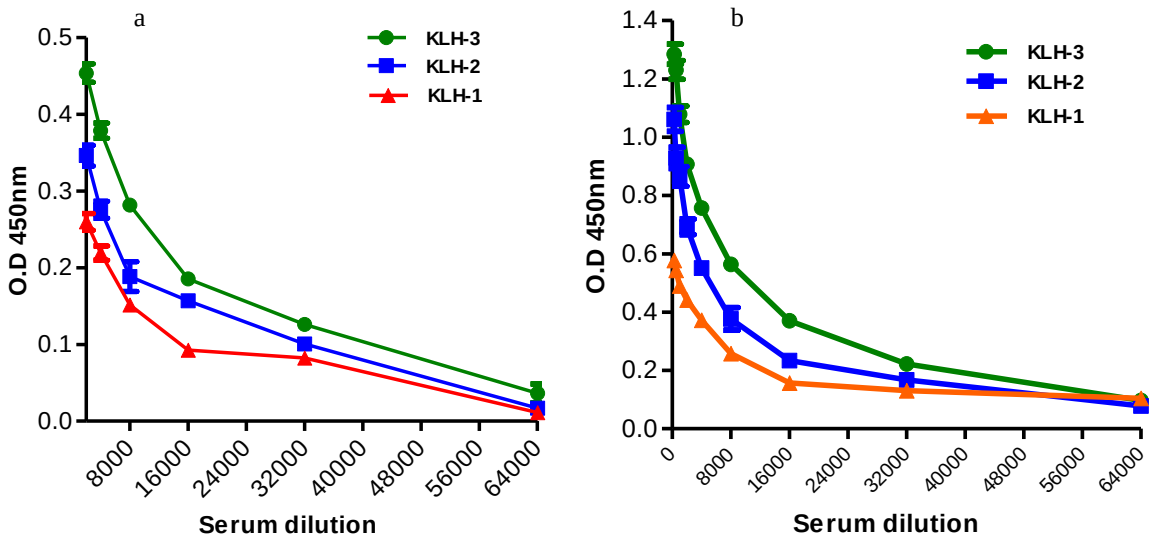

Figure 4B. IgM antibody titers of pooled sera immunized with **KLH-1, KLH-2** and **KLH-3** by ELISA. (a) IgM response from pooled sera obtained from 13 days after 3rd immunization; (b) response from pooled sera obtained from 14 days after 4th immunization. All data points were the mean of three parallel measurement data. Some error bars are smaller than symbol width.

Along with immunogenicity, cross-reactivity of antigen against native analog is also important factor for the improvement of T-cell dependent immune cell activation therefore we performed the cross-reactivity assay of our natural and modified sialoside conjugates. In this

ELISA assay we coated 96 well plates with **BSA-1** as a capture antigen and analysed the pooled serum from group of five mouse immunized with **KLH-1** (table. 6), **KLH-2** (table. 7), and **KLH-3** (table. 8) conjugates. The modified sialic acid conjugates KLH-3 produced higher IgG antibody titer against native 6'SLN (BSA-1) conjugates than that of KLH-2. Also IgM antibody titer produced by KLH-3 against native conjugates is comparatively higher than **KLH-1** and **KLH-2** (fig. 5). Further subtype of IgG, of respective **KLH-3** displayed a Strong immune responses against BSA-1 in IgG subtype compared to **KLH-2** (fig. 6, table. 9 and 10)). Significant titer of IgG1 compared to IgG2 and IgG3 may revealed the induction of Th1/Th-2 cell mediated immune response. Therefore it indicates that mannose modified sialoside conjugate is comparatively efficient potent immunogen to induce high antibody titer than that of glucose analog of sialoside.

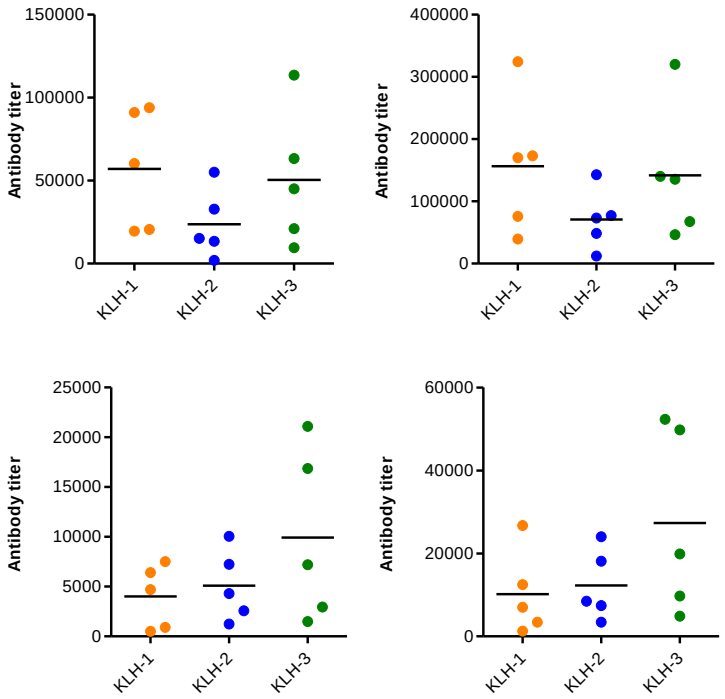

Figure 5. Cross-reactivity assay Serum antibody titer against **BSA-1** of group of five mouse immunized with **KLH-1, KLH-2** and **KLH-3** on 13th and 14th day after 3rd and 4th immunization respectively. (a) IgG response after 3rd immunization; (b) IgG response after 4th immunization; (c) IgM response after 3rd immunization and (d) IgM response after 4th immunization. Each dot represent ELISA result of individual mouse serum was separately detected. Three parallel micropores were arranged for each serum dilution. Titer were defined as highest dilution yielding an optical density of 0.2. Black line indicates median antibody level of group of five mouse.

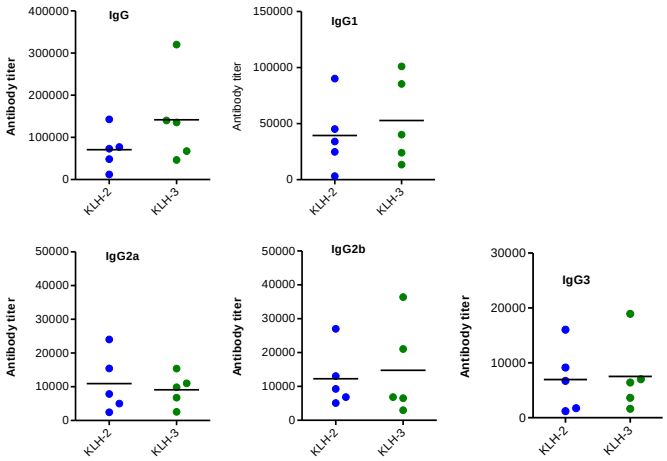

Figure 6. Serum antibody IgG isotypes titer against BSA-1 of group of five mouse immunized with KLH-2 and KLH-3 after 14th day of 4th immunization.

Based on the ELISA data, we can conclude that chemical modifications at the penultimate sugar of antigen could modulate the antigenicity of the glycan. Most importantly, though the 6'SLN antigens induced exclusively IgG antibodies, significant titers of IgG antibodies by **KLH-2** and **KLH-3** indicates a T-cell dependent immune response. The switching of T-cell independent immune response to T-cell dependent immune response by **KLH-3** is important for the production of stable IgG antibodies and vaccines against the specific glycan. The probably reasons for the antigenicity improvement of modified forms of 6'SLN antigen and their capability to stimulate T-cell dependent immune responses are not clear, but we believe that the stability of the molecules toward glycosidase and variable affinity toward siglec may play a critical role to induce T-cell dependent immune responses.

2.2.3 Conclusions

Our work demonstrated the immune responses of the molecular mimicry of 6'SLN. The amount of IgG antibodies generated by **KLH-3** was nearly 2.5- and 1.5-fold higher antibody responses than that of **KLH-2** respectively after 4th immunization. Further, the proportion of antibodies recognizes the native state of 6'SLN was found statistically significant. These results indicated that the incorporation of mannose in the 6'SLN can induce immunogenicity to the sialic acid glycan and IgG antibodies against them can recognize the native form of the glycan. This finding open up a new strategy to induce the immunogenicy to the glycan, which can be extended to

develop IgG antibodies against tumor-associated antigens and may be useful for cancer immunotherapy.

Chapter 2c. Effect of Sialic acid Orientation on Ligand Receptor Interactions.

2.3.0 Introduction

It has been shown that modified sias are more widely distributed than parental Neu5Ac ligand.[43] Motivated by the diverse structural and functional role of sialic acid, we planned to synthesize sialic acid mimics to tune the biological properties. In this case, sialic acid was locked in two opposite orientations on micelles to elucidate sia dependent ligand-receptor interactions in their native context. To obtain sialo-micelles that could serve as multivalent probe, we conjugated amphiphilic group at C-2 and C-9 position of sia respectively. Upon dissolution of amphiphiles in water, self-assembled highly regular micelles were obtained. The bioavailability of resultant sialo-micelles with plant and human sialic acid binding protein (SBP) was evaluated by surface plasma resonance (SPR) and *in-vitro* assay. *Sambucus nigra* agglutinin (SNA), *Limax flavus* agglutinin (LFA), P, E-selectin and CD22 (Siglec-2) were selected as sialic acid binding proteins (SBP), where SNA and LFA binds to all common sialic acid residues,[44] human CD22-Fc recognizes siaα(2-6)-linked sias,[45] and P and E-selectin, which belong to the subgroup of the C-type lectins that mediate leukocyte trafficking, are specific to sialyl Lewis^x and sialyl Lewis^a glycans respectively.[46]

2.3.1 Synthetic of C-2 and C-9 modified sialic acid analogs

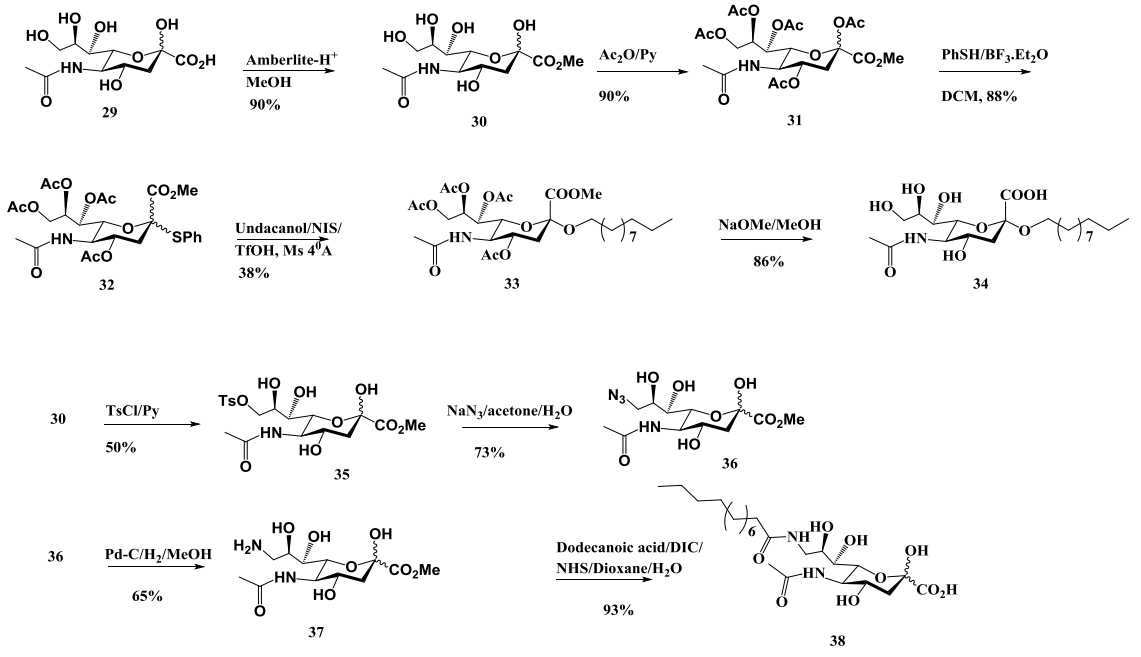

Scheme 3. Synthesis of sialic acid C-2 and C-9 modified derivatives.

The synthesis of compound **33** and **38** are depicted in scheme.3 The synthesis of *O*-sialoside **33** was carried out with *β*-thioglycoside donor **32** which was glycosylated with *n*-undecanol, followed by de-acetylation**.** 9-amidosialic acid **38** was synthesized starting from mono-tosylation of sialic acid 35, followed by azidation, hydrogenation 36 and coupling with dodacanoic acid (scheme 3). The structure of 34 and 38 confirmed by mass spectrometry and NMR spectrometry in MeOD. Both ^{1}H and ^{13}C NMR spectra displayed characteristic signals of aliphatic chains and sialic acid units.

2.3.2 Micelles formation and characterization

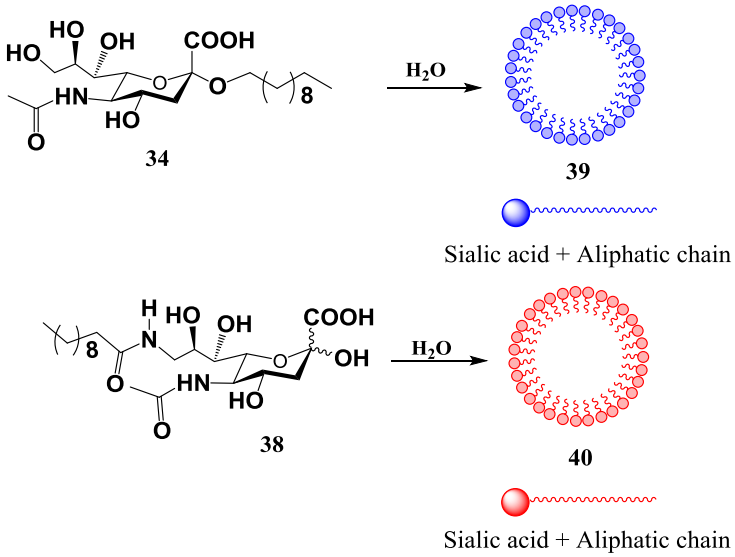

Scheme 4. Micelles formation from **34** and **38**.

Upon dissolution of 10 mg/ml of **34** and **38** in water, the self-assembling behavior of the sialic acid conjugated aliphatic molecules was investigated by means of dynamic light scattering (DLS) and atomic force microscopy (AFM). DLS patterns of **39** and **40** were almost identical and the corresponding hydrodynamic radius (R_H) was from 100-150 nm. Evidence for the formation of circular aggregates was provided by AFM experiments (fig. 7).

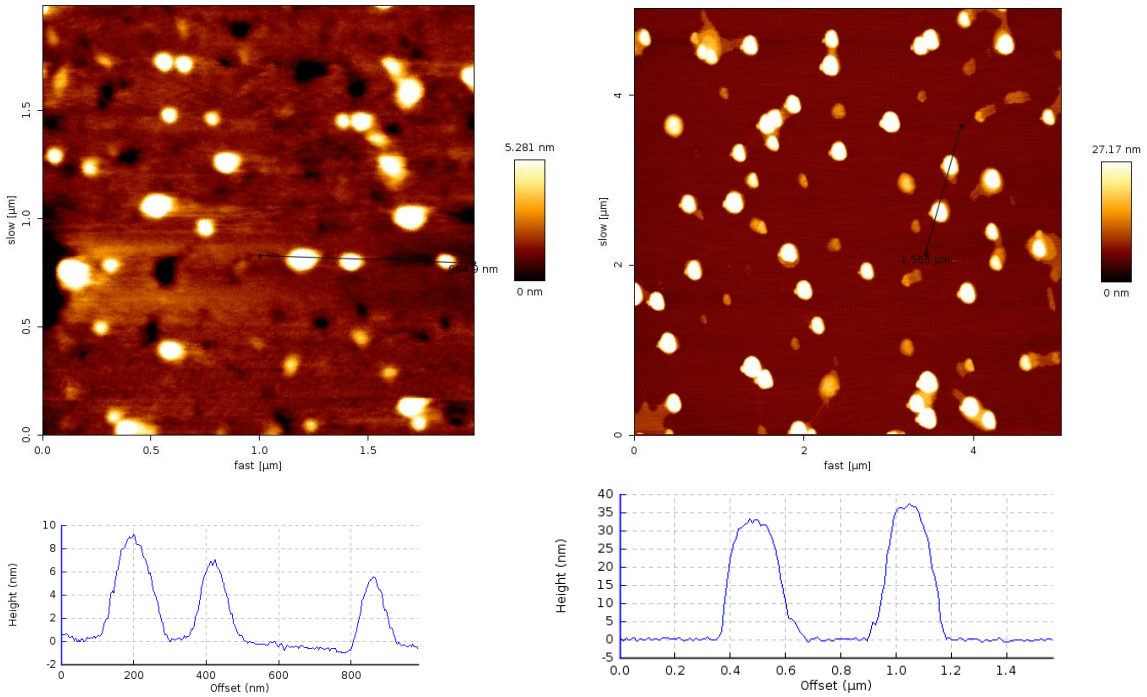

Figure 7. AFM topographical images of (a) **39**; (b) **40** and its corresponding topology. The image scale is in micrometers.

2.3.3 Kinetics and mechanism of sialic acid binding protein

	K_D (µM)	
Lectins	**39**	**40**
Sambucus nigra agglutinin (SNA)	0.146	0.129
Limax flavus agglutinin (LFA)	0.149	0.134
E-selectin	0.32	0.31
P-selectin	0.35	0.36
CD22-Fc	0.43	No binding

Table 1. Equilibrium constant, K_D of **39** and **40**.

After synthesizing sialic acid micelles, the kinetics and mechanism of SBP binding was investigated using surface plasmon resonance(SPR). To understand the influence of sialic acid orientation on lectin binding, the interaction of micelles with sialic acid-specific lectins from plant and animal was investigated. SPR and kinetic analyses were based on a 1:1 interaction model.[47] 25 µg concentrations of SBP was covalently bound to a polycarboxylated CM5 sensor

chip. Of the five SBP, four bind to **40** (fig. 8 and table 1) in a varying extent and no binding has been observed with CD22-Fc. **39** served as a positive control. For SNA lectin interaction at 25°C, there is a marginal decrease in the binding of **40** compared to **39** (0.88-fold decrease in affinity versus **39)**. With the LFA lectin module, there is 0.9 –fold decrease in affinity to compound 40, which also disassociates from LFA much slower than compound **39**. Overall, the degree of plant lectin binding induced by micelle **40** was more or less similar to that of **39**. This indicates that SNA and LFA prefer both orientations of sialic acids. Further, K_D values were 6-fold less than that of the SNA-sialic acid glycan binding constant.[48] This disparity is due to the different sialic acid epitopes of the two assays employed to measure the binding.

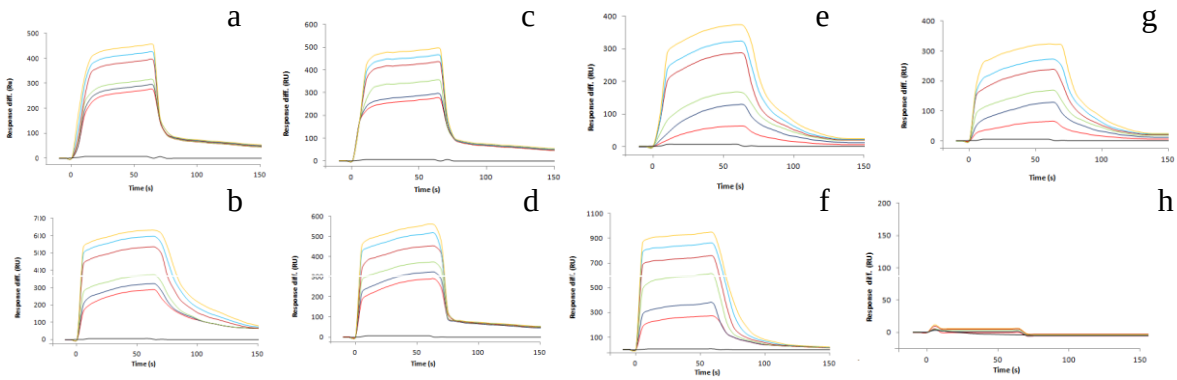

Figure 8. SPR sensorgrams of different sialic acid binding protein (SBP) binding to captured micelles containing two opposite orientations of sialic acid. Sensorgrams a and b show different concentrations of **39** and **40** binding to CM5 surface expressing SNA lectin; Sensorgrams c and d show binding with LFA lectin; Sensorgrams e and f show binding with E-selectin lectin; Sensorgrams g and h show binding with P-selectin lectin; Sensorgrams g and h show binding with CD22-Fc; Concentration of **39** and **40**: 0 µM (black line), 5 µM (red line), 10 µM (dark blue line),20 µM (green line), 30 µM (dark red line) 40 µM (blue line) and 50 µM (orange line) respectively.

For E and P-selectin-micelle interactions, K_D for 40 was almost similar to **39**. This may be due to the α-hydroxycarboxylic acid residue of 40 which coordinates with calcium ion in a manner akin to sialyl LewisX. To confirm this hypothesis, we soaked compound **40** with Ca^{2+} ion. Interestingly, DLS measurements showed aggregates of size ~1000-1500 nm (fig. 14) which was further supported by AFM imaging (fig. 9). Taken together, lectin binding assays indicate that sialic acid orientation has little impact and **40** may be a small potential mimic of sialyl $Lewis^X$ ligand.

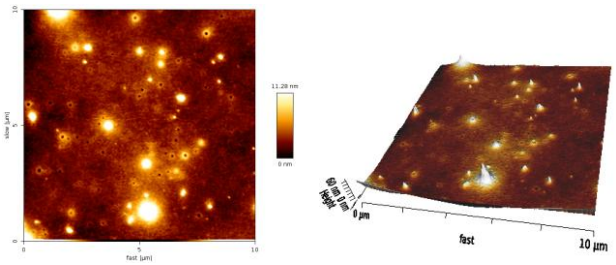

Figure 9. AFM topographical images of (a) compound **40** with 200 mM of $CaCl_2$ solution; (b) topology. The image scale is in micrometers.

2.3.4 Flow cytometry assay

With the CD22-Fc (siglec-2) module there was a significant difference between **39** and **40**. Data derived from SPR assay demonstrate no binding activity with **40**, whereas binding of **39** displays a K_D value of 0.43 µM. The binding curves obtained for interaction between **40** and CD22-Fc was comparable to results obtained using only buffer as a negative control. These observations were consistent with Kelm and Oetke et al, who reported the requirement of hydroxyl group of C-9 for sialic acid recognition by CD22.[49] To further support our assessment by SPR, CD22 transfected CHO cell line was used to study sialic acid orientation dependent lectin recognition and binding. Fluorescently labeled sialic acid micelles were prepared by mixing 5 mg of fluorescein dye with equal amount of ligand **34** and **38** in water, followed by 10K cutoff microcon filtration to obtain fluorescein hosted sialic acid micelles.(fig. 10) The sialic acid-CD22 interactions on the cell surfaces were then measured by flow cytometry. As shown in fig. 11, compound **42** did not bind effectively to CD22-transfected CHO-cells, indicating the requirement for native sialic acid orientation for the recognition (fig. 11). On the other hand, CHO-K1 cell line served as negative control and showed no major uptake of either **41** or **42**.These findings indicate that compound **42** is a potential sialic acid moiety for fine-tuning sialic acid based ligand-receptor interaction in mammalian SBP.

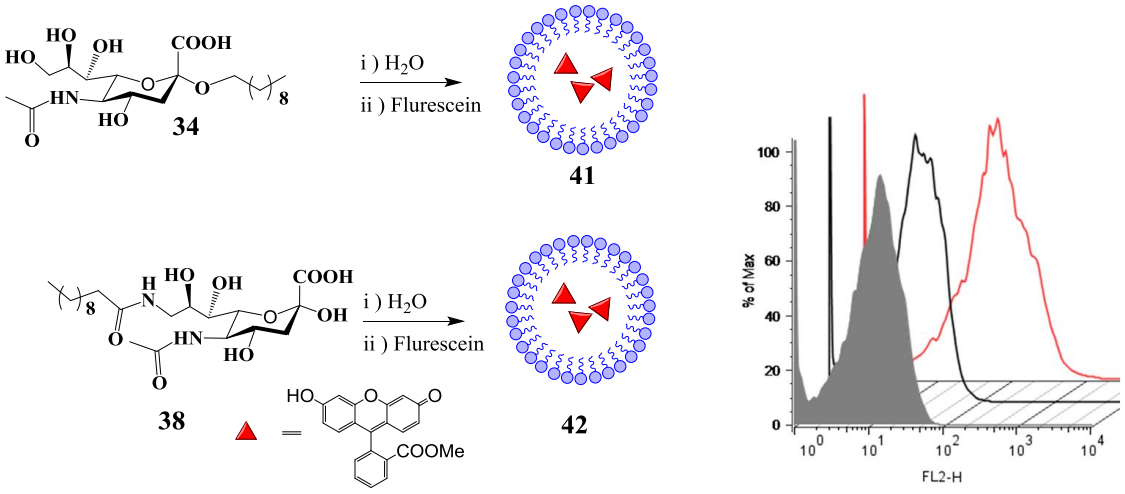

Figure 10. i) Synthesis of sialic acid micelles: (a) water/fluorescein; ii) Flow cytometry graph of CHO-CD22 with **41** and **42**: CHO-CD22 cells were left untreated (tinted area), incubated with 50 µM of compound comp 41 (red line area,positive control), compound 42 (black line area).

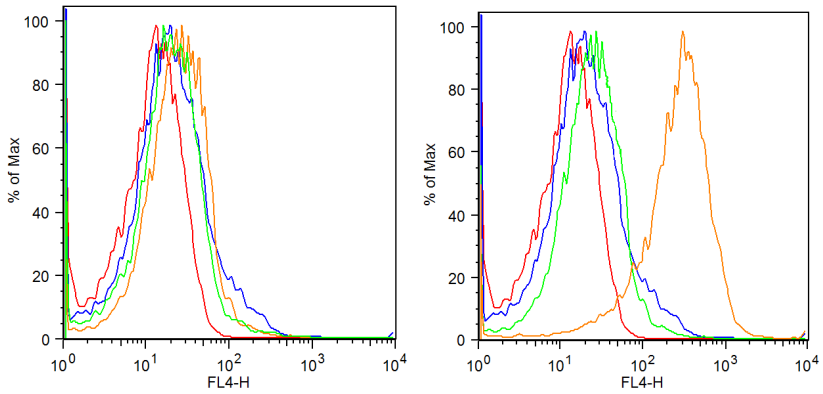

Figure 11. Flow cytometry graph of CHO-CD22 with **41** and **42**: CHO-K1 and CHO-CD22 cells were left untreated (red area), incubated with 50 µM of compound comp **41** (saffron line area, positive control), compound 42 (blue area,50 µM) and (green, 100 µM).

2.3.5 Conclusison

Motivated by results of orientation dependent sialic acid-protein interactions. We investigated the role of C-9 sialic acid derivatives and siglec interactions, more specifically CD22 lectin. We have shown that structural rearrangement of sialic acid moiety around a multivalent system could modulate the ligand-receptor interactions. Surface plasmon resonance (SPR) and *in-vitro* binding assays show that out of five potential sialic acid binding plant and human lectins (SBP), only CD22 (Siglec-2) abolishes binding with amphiphile at C-9 position of sialic acid under biophysical conditions, while *O*-sialoside was used as positive control. These differences in the

relative binding affinity of two human lectins provide a novel lead in the development of inhibitors and biomarkers for specific human SBP. Such studies are currently being considered. Furthermore, stereo-specificity of carboxylic acid residue of sialic acids also influence Ca^{2+} mediated carbohydrate-carbohydrate interactions. Extension of this approach might be a great value in sialic acid related biophysical properties.

2.4 Materials and Methods.

2.4.1 General information. All chemicals were reagent grade and used as supplied except where noted. Analytical thin layer chromatography (TLC) was performed on Merck silica gel 60 F254 plates (0.25 mmol). Compounds were visualized by UV irradiation or dipping the plate in CAM/ninhydrin solution followed by heating. Column chromatography was carried out using force flow of the indicated solvent on FlukaKieselgel 60 (230–400 mesh). ^{1}H and ^{13}C NMR spectra were recorded on Jeol 400 MHz, with cryo probe using residual solvents signals as an internal reference ($CDCl_3$ δ_H, 7.26 ppm, δ_C 77.3 ppm and CD_3OD δ_H 3.31 ppm, δ_C 49.0 ppm). The chemical shifts (δ) are reported in ppm and coupling constants (*J*) in Hz. UV-visible measurements were performed with Evolution 300 UV-visible spectrophotometer (Thermo Fisher Scientific, USA). Fluorescence spectra were recorded in FluoroMax-4 spectrofluorimeter (Horiba Scientific, U.S.A.).

2.4.2 Glycan microarray details

2.4.2.1 Sialoglycan microarray fabrication. Arrays were printed on Epoxide-derivatized Corning slides as described for Array 1 in Ref. {Padler-Karavani et al., 2012, J BiolChem} with some modifications. Arrays were fabricated with NanoPrint LM 60Microarray Printer (Arrayit, CA) on epoxide-derivatized slides (Corning) with 16 sub-array blocks on each slide. Glycoconjugates were distributed into one 384-well source plates using 4 replicate wells per sample and 8 µl per well. Each glycoconjugate was prepared at 100 µM in an optimized print buffer (300 mM phosphate buffer, pH 8.4). The arrays were printed with four 946MP3 pins (5 µm tip, 0.25 µl sample channel, ~100µm spot diameter; Arrayit, CA) with spot to spot spacing of 225 µm. The humidity level in the arraying chamber was maintained at about 66% during printing. Printed slides were left on arrayer deck over-night, allowing humidity to drop to ambient levels (40-45%). Next, slides were packed, vacuum-sealed and stored in a desiccant chamber at room temperature(RT) until used.

2.4.2.2 Microarray binding assay. Slides were developed {23520510} and analyzed {Padler-Karavani et al., 2012, J BiolChem} as previously described. Slides were rehydrated with dH2O and incubated for 30 min in a staining dish with 50°C pre-warmed 0.05 M ethanolamine in 0.1 M Tris, pH 9.0 to block the remaining reactive epoxy groups on the slide surface, then washed with 50°C pre-warmed dH2O. Slides were centrifuged at 200×g for 3 min then fitted with ProPlate™ Multi-Array 16-well slide module (Invitrogen) to divide into the sub-arrays (blocks). Slides were washed with PBST(PBS pH 7.4, 0.1% Tween-20), aspirated and blocked with 200 µl/sub-array of blocking buffer (PBS pH 7.4, 1% ovalbumin;PBS/OVA) for 1 hour at RT with gentle shaking. Next, the blocking solution was aspirated and 200 µl/ block of primary detectionwas added (Siglec-human IgGFc chimeras; R&D). Primary detections were incubated with gentle shaking for 2 hours at RT. Slides were washed three times with PBST then with PBS for 5 min/wash with shaking. Bound antibodies were detected by incubating with secondary detection diluted in PBS, 200 µl/block at RT for 1 hour: Cy3-anti–human-IgG (Jackson;0.4µg/ml). Slides were washed three times with PBST then with PBS 5 min/wash followed by removal from ProPlate™ Multi-Array slide module and immediately dipping slide in a staining dish with dH_2O for 10 min with shaking, then centrifuged at 200×g for 5 min. Dry slides were vacuum-sealed and stored in dark until scanning.

2.4.2.3 Array slide processing. Processed slides were scanned and analyzed as described {Padler-Karavani et al., 2011, Cancer Res, 71, 3352-63; Padler-Karavani et al., 2012, J BiolChem} at 10 µm resolution with a Genepix 4000B microarray scanner (Molecular Devices) using 350 gain. Image analysis was carried out with Genepix Pro 6.0 analysis software (Molecular Devices). Spots were defined as circular features with a variable radius as determined by the Genepix scanning software. Local background subtraction was performed. Data was analyzed by Excel using pivot tables.

2.5 Immune Study Details

2.5.1 General procedure for glycoconjugates synthesis.

Dimethyladipimidate(16mg) and compound 5,6,7,8 (5mg) was incubated for 20 min at 4^0C in triethanolamine buffer(pH 8.5, 0.2M). The KLH or BSA (5mg) dissolved in buffer was added and incubated for another 1-2h at same temperature. Quenched reaction mixture by 100mM glacial acetic acid and then The KLH-glyconjugates were purified by dialysis (membrane cutoff

10Kd). The solution of glycoconjugates then lyophilized to get white floppy solid of comp (**1-4**) and stored at -20^{0}C until further use.

2.5.2 Glycoconjugates: protein content and conc. of sugar determination.

The epitope ratios of the glycoconjugates (carbohydrate-KLH/BSA) were determined by estimating protein content by Brardford Protein Assay and Sialic acid content using the resorcinol method described by Svennerholm. The glyco-conjugate (100 μL) was mixed well with the resorcinol reagent (100 μL) and heated in a boiling water bath for 30 min, then cooled on ice for 10 min. Then organic solvent mixture was added (1-butanol acetate and 1-butanol, 85:15 v/v, 250 μL) to it. The mixture was kept standing still for 15 min after it was shaken vigorously to allow the organic layer to separate well from the inorganic layer. The absorbance at 580 nm of organic layer was determined by an UV-vis spectrometer, using organic solvent as a control.

Glycoconjugates	KLH/BSA (mg/ml)	Sialic acid (μg/ml)
KLH-1	1.67	188
KLH-2	1.95	154
KLH-3	1.84	162
BSA-1	2.10	248
BSA-2	2.31	204
BSA-3	1.92	307

Table 2. Concentration of protein and sialic acid.

2.5.3 Loading of glycoconjugates: The carbohydrate loading of each conjugates was calculated according to equation shown below.

Loading of conjugates (%)

$$\frac{\text{content of trisaccharide in sample (mg)}}{\text{content of trisaccharide (mg)+ content of KLH (mg)}} \times 100$$

Loading yield to KLH conjugation (%)

$$\frac{\text{Conc of trisaccharide in sample (mg)}}{\text{total amount of trisaccharide (mg) employed for reaction}} \times 100$$

Glycoconjugates	KLH/BSA conjugates loading %	Loading yield to KLH/BSA %
KLH-1	11.2	3.76
KLH-2	7.8	3.08
KLH-3	8.8	1.76
BSA-1	10.59	4.96
BSA-2	8.12	4.08
BSA-3	13.82	6.14

Table 3. Sialic acid loading on KLH/BSA.

2.5.4 Immunization of mice and serological assay

Pathogen-free C57BL mice aged 6–8 weeks were obtained from Reliance Life Science Biotech. Groups of six mice were immunized four times at 2-week intervals with **KLH** and **KLH-1** to **KLH-3** glycoconjugates (each containing 2 μg of carbohydrate in PBS). The compounds were administered through tail vain. Mice were bled prior to the initial immunization, 13 days after the second and the third immunizations, and 28 days after the fourth immunization. Blood was clotted to obtain sera, which were stored at -80^{0}C.

The total antigen-specific antibody titers of the pooled sera were assessed by means of ELISA. ELISA plate was coated with 100 μL of **KLH**, **KLH-1** to **KLH-3**（including 0.02 μg glycoconjugates）overnight at 4^{0}C (0.1 M bicarbonate buffer, pH = 9.5). After three washing with PBST (0.05% Tween20 in PBS), microwells were blocked with 5% BSA. After the plate was washed, serially diluted sera were added to microwells (100 μL /well) and incubated for 1 h at 37^{0}C. The plate was washed and incubated with 1:5000 or 1:2000 dilution of horse radish peroxidase-conjugated goat anti-mouse IgG or IgM or for 1 h at 37^{0}C. The plate was washed and developed with Tetramethylbenzilidine (TMB) substrate in the dark for 15 min, then

terminated with 50µL of 2 M H_2SO_4, and O.D was read at 450 nm. The antibody titer was defined as the highest dilution showing an absorbance of 0.3, after subtracting background.

2.5.5 Antibody Titer Analysis

Mouce	**BSA-1**		**BSA-2**		**BSA-3**	
	IIIrd	**IVth**	**IIIrd**	**IVth**	**IIIrd**	**IVth**
1	7443	30282	54215	119656	141285	361998
2	52638	126863	91127	286239	50973	237695
3	79289	239592	59342	208016	127216	199267
4	30299	63901	25165	55279	40774	86543
5	114562	322014	43304	98197	32010	50676

Table 4. IgG antibody titer of pooled sera of mice immunized with **KLH-1, KLH-2** and **KLH-3** after 3rd and 4th immunization. In the analysis , there were five mice per group (n = 5). The and IgG titer of individual mouse serum was separately detected three parallel wells were arranged in plates for each serum diluted concentration . The titer represented the average of two detections. The data of titers dealt with logarithmic function to base 10. Value of $p < 0.05$ was considered to be statistically significant and was identified by *. The results indicated that IgG level for conjugates of 2 and 3 increases after 3rd and 4th immunization.

2.5.6 Average IgG and IgM antibody titer against BSA-1 to BSA-3 of pooled srea of mice immunized with KLH-1, KLH-2 and KLH-3 after 3rd and 4th immunization.

Glycoconjugates	IgG		IgM	
	IIIrd	**IVth**	**IIIrd**	**IVth**
BSA-1	40846	126530	4412	12250
BSA-2	54630	153477	8514	21500
BSA-3	78449	187255	15510	37250

Table 5. Average antibody titer of KLH conjugates after respective immunization.

2.5.7 Antibody titer tgainst BSA-1 (cross reactivity analysis)

Mouse	**KLH-1**			
	IgG		IgM	
	IIIrd	**IVth**	**IIIrd**	**IVth**
1	60302	170082	912	3440
2	93912	324543	4689	7010
3	20576	39592	510	1250
4	19562	75901	7502	12450
5	91013	173145	6401	26748

Table 6. IgG Antibody titer against **BSA-1** of individual mouse immunized with **KLH-1**, after 3rd and 4th week of immunization.

Mouse	**KLH- 2**			
	IgG		IgM	
	IIIrd	**IVth**	**IIIrd**	**IVth**
1	15210	77300	2571	7412
2	1935	12045	10056	24014
3	13404	48560	7241	18145
4	55120	142678	1247	3420
5	32810	73140	4302	8475

Table 7. IgG Antibody titer against **BSA-1** of individual mouse immunized with **KLH-2**, after 3rd and 4th week of immunization.

Mouse	KLH-3			
	IgG		IgM	
	IIIrd	**IVth**	**IIIrd**	**IVth**
1	45010	135400	2958	9742
2	9578	46540	16870	49751
3	113540	320145	1480	4874
4	63274	140230	21087	52307
5	21041	67482	7201	19870

Table 8. IgG Antibody titer against **BSA-1** of individual mouse immunized with **KLH-3**, after 3rd and 4th week of immunization.

Mouse	KLH- 2				
	IgG	**IgG1**	**IgG2a**	**IgG2b**	**IgG3**
1	77300	45140	15420	6870	9142
2	12045	3210	2450	5103	1742
3	48560	24802	7850	13048	1205
4	142678	90140	24015	9254	16048
5	73140	34015	5014	27012	6710

Table 9. Serum antibody titer of IgG isotypes against **BSA-1** mice immunized with modified conjugates **KLH-2** after 4th immunization.

Mouce	KLH- 3				
	IgG	**IgG1**	**IgG2a**	**IgG2b**	**IgG3**
1	135400	101080	9845	21045	3645
2	46540	13450	6789	6540	18942
3	320145	24012	2548	2974	1640
4	140230	85472	11021	36402	6420
5	67482	40125	15402	6874	7021

Table 10. Serum antibody titer of IgG isotypes against **BSA-1** mice immunized with modified conjugates **KLH-3** after 4th immunization.

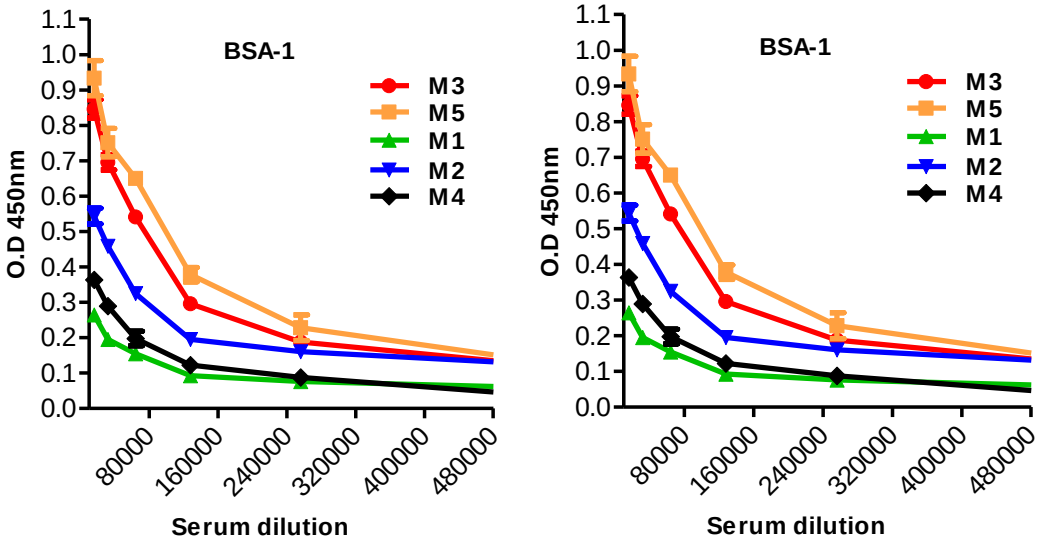

Figure12. IgG antibody titers of pooled sera of five mice immunized with **BSA-1** by ELISA. (a) IgG response from pooled sera obtained from 13 days after 3rd immunization; (b) response from pooled sera obtained from 14 days after 4th immunization. All data points were the mean of three parallel measurement data. Some error bars are smaller than symbol width.

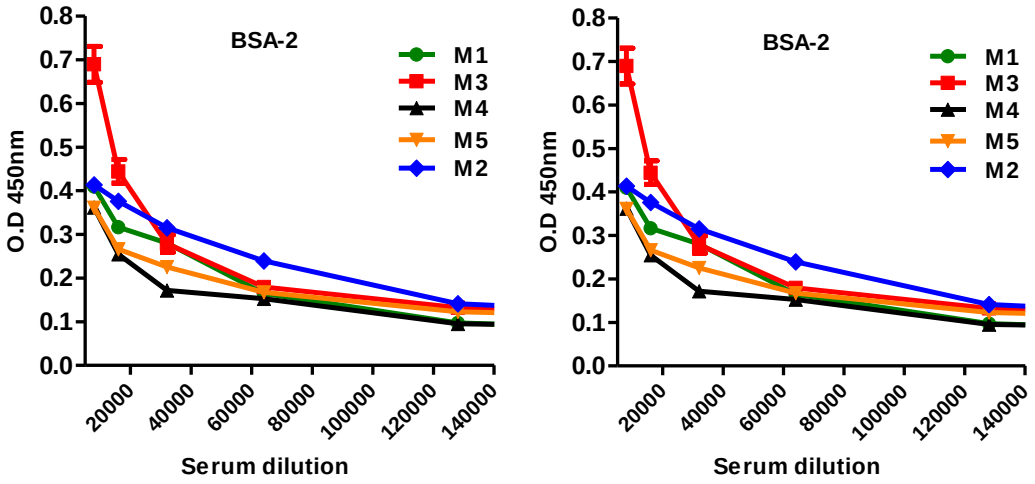

Figure 13. IgG antibody titers of pooled sera of five mice immunized with **KLH-2** by ELISA. (a) IgG response from pooled sera obtained from 13 days after 3rd immunization; (b) response from pooled sera obtained from 14 days after 4th immunization. All data points were the mean of three parallel measurement data. Some error bars are smaller than symbol width.

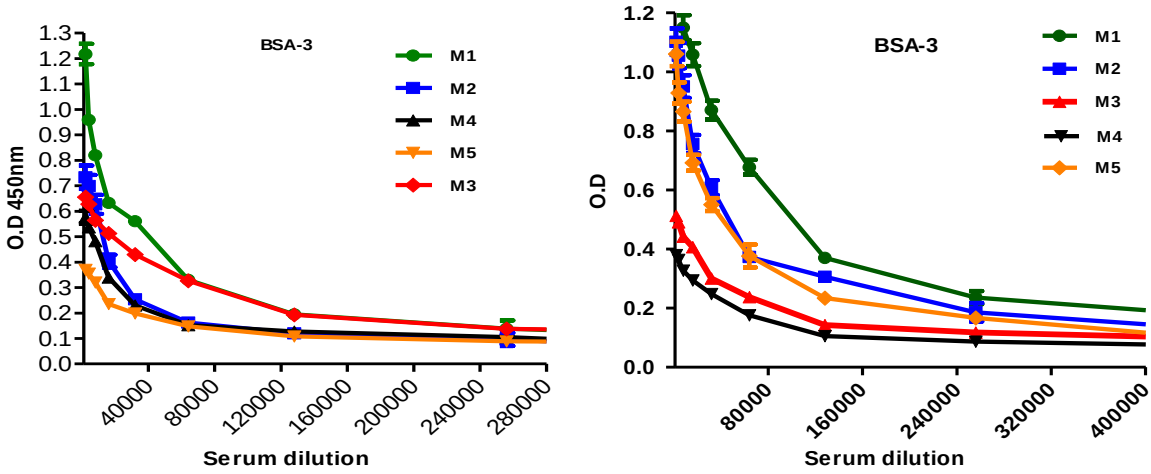

Figure 14. IgG antibody titers of pooled sera of five mice immunized with **KLH-3** by ELISA. (a) IgG response from pooled sera obtained from 13 days after 3rd immunization; (b) response from pooled sera obtained from 14 days after 4th immunization; All data points were the mean of three parallel measurement data. Some error bars are smaller than symbol width.

2.6.1 Fluorescent hosted micelles: 5 mg of amphiphiles **34** or **38** and 3 mg of fluorescein methylester were dissolved in 1 mL of milli-Q water and sonicated for 30 mins at RT. The fluorescein hosted micelles were purified by filtering with a microcon centrifugal filter device

with a cutoff range of 100 KD. Then filtrate was dissolved in 1 mL of milli-Q water and used as such for further experiment. The concentration of sialic acid was established by DMB-HPLC method. The concentration of fluorescein was determined by the O.D of the fluorescein.

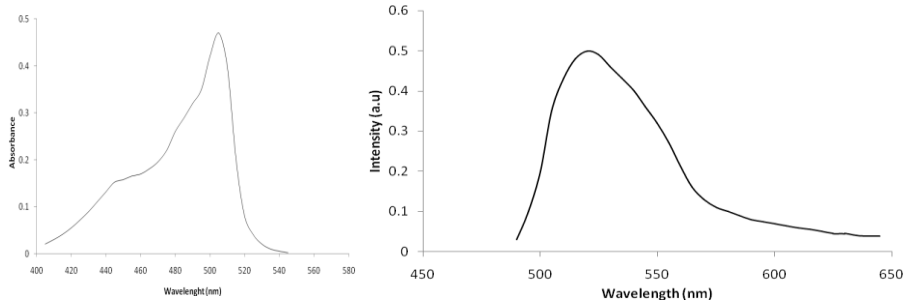

Figure 15. UV-visible and fluorescent spectra of the fluorescein hosted sialic acid micelles.

2.6.2 Dynamic light scattering (DLS). The size of the micelles was assessed using DLS measurements. The experiments were performed using Malvern Zetasizer Nano ZS-90 apparatus utilizing 633 nm red laser. The samples were kept at 25^{O}C. All samples were systematically studied at 90 degree. The solutions were put in ordinary 10 mm in diameter glass cells. The minimum sample volume required for an experiment was 1 mL.

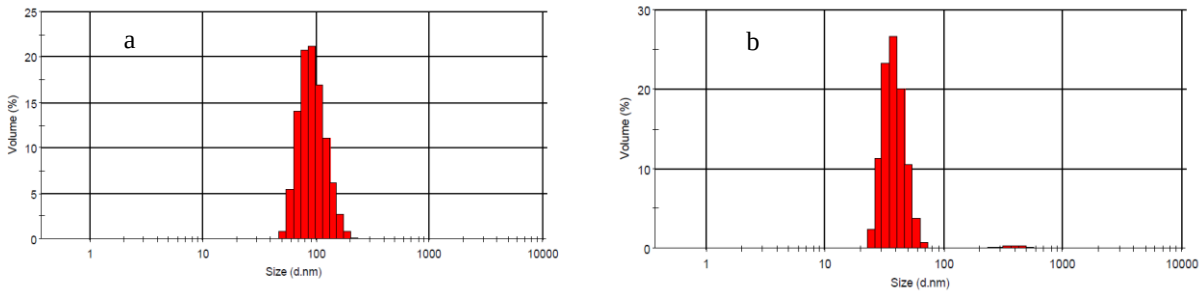

Figure 16. DLS of compound (a) **39** and (b) **40**.

2.6.3 Calcium mediated carbohydrate-carbohydrate interactions.

As shown in the figure 4a-4d, after each addition of calcium chloride (0, 100, 200, 300 mM) to **40**, a large aggregates of size 5000-9000 nm was observed. This is due to specific carbohydrate-carbohydrate interaction between sialic acid moiety of **40**. Similar experiment with **39**, didn't show any aggregation with calcium chloride (data not shown). Taken together, our data suggests that spatial orientation finely tunes sialic acid mediated carbohydrate-carbohydrate interactions.

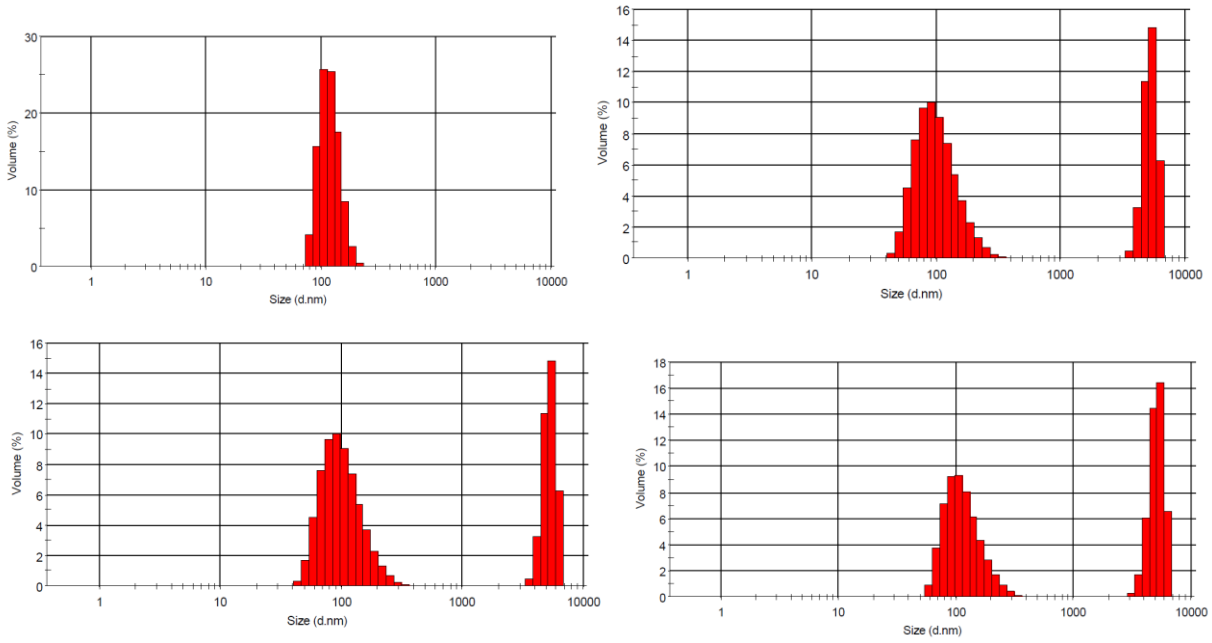

Figure 17. DLS of compound **40** in presence of different concentration of calcium chloride solution (a) no $CaCl_2$; (b) 100 mM; (c) 200 mM and (d) 300 mM respectively.

2.6.4 Surface plasmon resonance (SPR). Binding kinetics were determined by SPR using a BIACORE 300 biosensor instrument (GE Biosystems). *Sambucus Nigra* agglutinin (SNA) and *Limax flavus* agglutinin (LFS) was purchased from Vector lab and E- and P-selectin were purchased from Calbiochem (EMD Biosciences, Darmstadt, Germany). CD22-Fc was gifted by Prof. Ajit varki. The CM5 chip and different running buffer (table 1) were obtained from GE Healthcare Life Science (India). Neu5Acα(2-6)gal, neuraminic acid and lactose were as an inhibitor. All SPR experiments were performed using Biacore 3000 (Australian biobest biotechnology service, Australia). For the preparation of lectin/protein-coated surfaces, CM5 chip was activated with EDC and NHS followed by injecting 25 $\mu g \cdot mL^{-1}$ of lectin at a flow rate of 10 $\mu l \cdot min^{-1}$for 10 mins. The unreacted carboxylic active ester were neutralized with 1 M ethanolamine for 10 mins. As a control, cell was treated with EDC/NHS as described above.[1] This followed by injecting **39** and **40** (5, 10, 20, 30, 40 and 50 μM) for 60 s at 10 $\mu L \cdot min^{-1}$, followed by regeneration using respective inhibitor at 30 $\mu L \cdot min^{-1}$ for 300 s. The equilibrium dissociation constant (K_D) was determined globally by fittin to the kinetic simultaneous K_a/K_d model, assuming Langmuir (1:1) binding, using BIAevaluation software (BIAcore). The surfaces

were strictly regenerated with multiple pulses of 2 M NaCl, 1.5 M glycine-HCl, pH 2.0 followed by an extensive wash procedure using running buffer.

Lectin	Specificity	Inhibitor used	Running buffer
Sambucus nigra agglutinin (SNA)	Sialic acid	200 mM neuraminic acid	10 mM HEPES, pH 7.5, 10 mM NaCl, 10 mM $CaCl_2$, 0.005% surfactant P20
Limax flavus agglutinin (LFA)	Sialic acid	200 mM neuraminic acid	PBS, 10 mM $CaCl_2$ and 0.005% surfactant P20
E - selectin	Sialyl lewisX	200 mM Neu5Acα(2-6)gal	10 mM HEPES, pH 7.5, 10 mM NaCl, 10 mM $CaCl_2$, 0.005% surfactant P20
P - selectin	Sialyl lewisA	200 mM Neu5Acα(2-6)gal	10 mM HEPES, pH 7.5, 1 mM NaCl, 1mM $CaCl_2$, 0.005% surfactant P20
CD22-Fc	Neu5Ac/Gcα(2-6)gal	200 mM Neu5Acα(2-6)gal	10 mM HEPES, pH 7.5, 10 mM NaCl, 0.005% surfactant P20

Table 11. Different sialic acid binding proteins and its specificities.

Lectins	**39**			**40**		
	K_a	K_d	K_D (µM)	K_a	K_d	K_D (µM)
Sambucus nigra agglutinin (SNA)	(0.42 ± 0.05) X 10^5	(0.6 ± 0.01) X 10^{-2}	0.146	(0.35 ± 0.05) X 10^5	(0.45 ± 0.01) X 10^{-2}	0.129
Limax flavus agglutinin (LFA)	(0.37 ± 0.02) X 10^5	(0.55 ± 0.03) X 10^{-2}	0.149	(1.12 ± 0.03) X 10^4	(0.15 ± 0.07) X 10^{-2}	0.134
E-selectin	(0.44 ± 0.15) X 10^4	(0.14 ± 0.03) X 10^{-2}	0.32	(0.39 ± 0.15) X 10^4	(0.12 ± 0.03) X 10^{-2}	0.31
P-selectin	(0.56 ± 0.1) X 10^4	(0.19 ± 0.03) X 10^{-2}	0.35	(1.2 ± 0.1) X 10^4	(0.43 ± 0.03) X 10^{-2}	0.36
CD22-Fc	(0.73 ± 0.13) X 10^4	(0.31 ± 0.07) X 10^{-2}	0.43	-	-	-

Table. 12 Kinetic parameters for the different SBM interaction with compound **39** and **40.**

2.6.5 Fluorescence-activated cell sorting assay.

CHO cells stably transfected with full-length human CD22 cDNA were cultured in MEM supplemented with 10% fetal calf serum and L-glutamine. Cells were incubated with a solution

of fluorescein labelled compound **39** and **40** (50 µM in PBS, pH 7.4). After 1 h incubation at 4^0C, cells were washed with phosphate buffered saline (PBS). The cells were then collected with PBS containing 1% FCS by shearing force. Binding of micelles and CD22 protein on CHO cells were measured by flow cytometry using a FACSCantoTM II flow cytometer (Becton Dickinson and Co., Mountain View. CA). Cells were gated on living cells and fluorescence channel FL-2 was used to detect CHO cells that had micelles on it. All data were analyzed with the FlowJo software.

2.7 Synthetic procedures of sialosides

A) Synthesis of disaccharide library

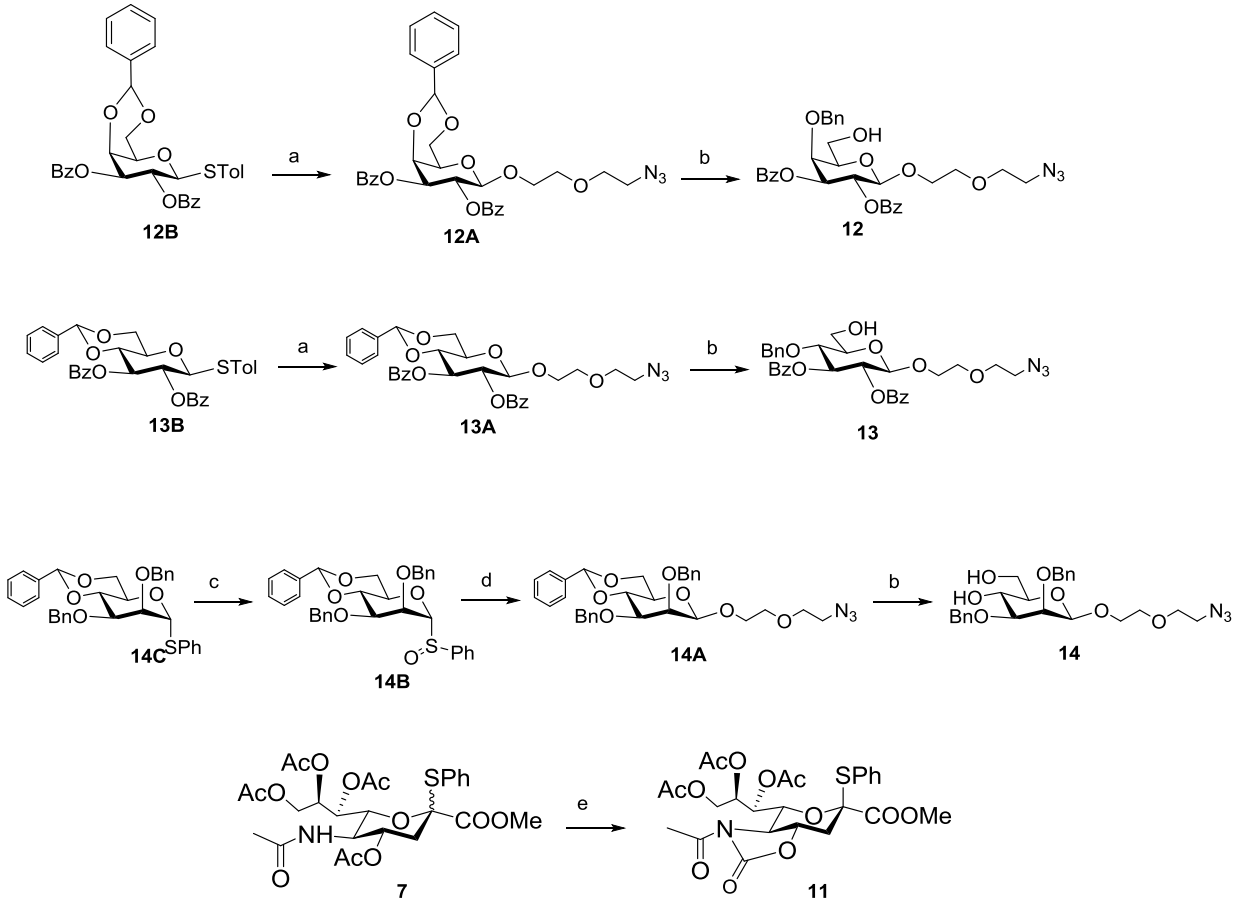

Scheme 5. ***Reagents and conditions:*** (a) 2-azidoethoxyethanol, NIS/TfOH, -40^0C, DCM; (b) $PhBCl_2$, Et_3SiH, -78^0C, DCM; (c) mCPBA,-78^0C, DCM; (d) 2-azidoethoxyethanol, Tf_2O, TTBP, -78^0C, DCM; (e) (i) MsOH, MeOH; ii) NPCC, $NaHCO_3$, CH_3CN:H_2O(2:1); (iii) AC_2O/Pyridine; (iv) AcCl, DIPEA, DCM.

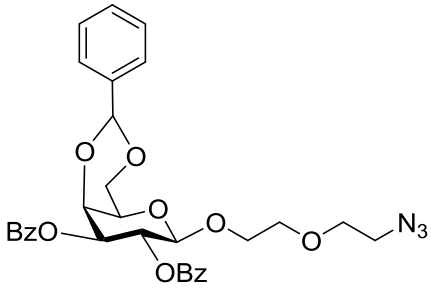

Synthetic procedure for comp 12A: A solution of **12B** (500 mg, 1.08 mmol, 1.0 equiv), 2-Azidoethoxyethanol (1.28 mmol, 1.2 equiv), and activated 4Å powdered molecular sieves (1.5 gm) in anhydrous dichloromethane (5 ml) was stirred for 2h at room temperature under an argon atmosphere, and then cooled to -40^{0}C followed by addition of NIS (290 mg, 1.28 mmol, 1.2 equiv) and TfOH (9.58 μl, 0.108 mmol, 0.1 equiv). The reaction mixture was stirred at -40^{0}C for 0.5 h to 3 h until the disappearance of the donor on TLC, then quenched with triethylamine (81 µl, 0.81 mmol, 0.75 equiv) and warmed to room temperature. The mixture was diluted with dichloromethane, filtered through Celite, washed with 20% aqueous $Na_2S_2O_3$ solution, dried over Na_2SO_4, and concentrated under reduced pressure. The residue was purified by column chromatography on silica gel eluting with Ethylacetate/Hex (1:1) system to afford the compound **12A** (450mg, 70%). ^{1}H-NMR (400 MHz, $CDCl_3$) δ 8.04–7.92 (m, 4H), 7.55–7.43 (m, 4H), 7.43–7.29 (m, 7H), 5.86 (dd, *J* = 10.4, 8.0 Hz, 1H), 5.54 (s, 1H), 5.37 (dd, *J* = 10.4, 3.6 Hz, 1H), 4.86 (d, *J* = 8.0 Hz, 1H), 4.58 (dd, *J* = 3.6, 1.6 Hz, 1H), 4.39 (dd, *J* = 12.4, 1.2 Hz, 1H), 4.13 (dd, *J* = 11.3, 1.6 Hz, 1H), 4.04 (dt, *J* = 11.3, 3.6 Hz, 1H), 3.79 (ddd, *J* = 11.3, 7.4, 3.6 Hz, 1H), 3.68 (s, 1H), 3.60 (dt, *J* = 7.4, 3.6 Hz, 2H), 3.45 (t, *J* = 5.1 Hz, 2H), 3.04 (m, 2H). ^{13}C-NMR (400 MHz, $CDCl_3$) δ 165.68, 165.27, 136.82, 133.37, 133.19, 130.08, 130.04, 129.99, 129.90, 129.87, 129.46, 129.40, 129.12, 128.57, 128.49, 128.40, 128.44, 128.38, 128.28, 126.20, 101.95, 101.57, 78.90, 72.56, 72.07, 70.44, 70.18, 69.81, 68.72, 66.68, 50.60. Maldi-ToF m/z calc'd for $C_{31}H_{31}N_3O_9Na$ ($M+Na^+$): 612.1958; found: 612.1951.

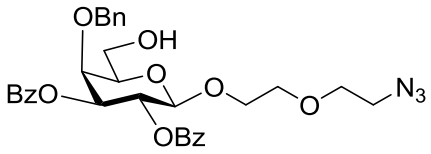

Synthetic procedure for comp 12: A solution of compound **12A** (300 mg, 0.509 mmol) and activated 4Å powdered molecular sieves 1.5 g were stirred 1h at room temperature. The mixture was cooled to -78^{0}C and then to the stirred solution Et_3SiH (259 µl, 1.62 mmol) and $PhBCl_2$ (147 µl, 1.38 mmol) were added successively. After being stirred for 1 h at -78^{0}C, Et_3N (1 ml) and MeOH (1 ml) were added successively, and the mixture was diluted with $CHCl_3$ and washed with aqueous $NaHCO_3$, dried over $MgSO_4$, filtered and concentrated. The crude product was purified by silica gel column Hexane:Ethylacetate (1:1) to afford comp **12** (260 mg, 86%). **^{1}H NMR** (400 MHz,$CDCl_3$) δ 8.00–7.94 (m, 4H), 7.54–7.47 (m, 2H), 7.36 (dd, *J* = 10.7, 4.8 Hz, 4H), 7.28 – 7.21 (m, 5H), 5.84 (dd, *J* = 10.5, 7.9 Hz, 1H), 5.34 (dd, *J* = 10.4, 3.0 Hz, 1H), 4.78 (dd, *J* = 9.8, 4.4 Hz, 2H), 4.48 (d, *J* = 11.7 Hz, 1H), 4.13 (d, *J* = 2.5 Hz, 1H), 3.99 (ddd, *J* = 11.4, 4.5, 3.3 Hz, 1H), 3.86 (dd, *J* = 11.2, 6.9 Hz, 1H), 3.81 – 3.69 (m, 2H), 3.64 – 3.53 (m, 3H), 3.46 (t, *J* = 5.1 Hz, 2H), 3.14 – 2.99 (m, 2H), 1.76 (bs, 1H). **^{13}C NMR** (101 MHz, $CDCl_3$)δ 166.11, 165.43, 137.30, 133.60, 133.24, 129.98, 129.98, 129.78, 129.78, 129.02, 128.62, 128.61, 128.60, 128.59, 128.44, 128.23, 127.95, 101.65, , 75.03, 74.81, 74.78, 73.32, 70.56, 70.15, 69.35, 61.79, 50.64, . Maldi-ToF m/z calc'd for $C_{31}H_{33}N_3O_9Na$ ($M+Na^+$): 614.2114; found: 614.2120.

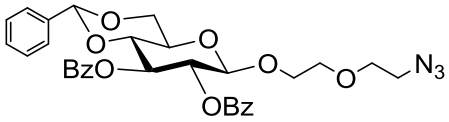

Synthetic procedure for comp 13A: Compound was synthesized from **13B** by following synthetic procedure explained for 12A. **13A** (420 mg, 65%). **^{1}H-NMR** (400 MHz, $CDCl_3$) δ 7.99–7.91 (m, 4H), 7.55–7.27 (m, 11H), 5.78 (t, *J* = 9.6 Hz, 1H), 5.53 (s, 1H), 5.47 (dd, *J* = 9.6, 7.9 Hz, 1H), 4.89 (d, *J* = 7.9 Hz, 1H), 4.42 (dd, *J* = 10.5, 4.9 Hz, 1H), 3.99 (ddd, *J* = 11.3, 4.9, 3.5 Hz, 1H), 3.92 (t, *J* = 8.4 Hz, 1H), 3.90–3.85 (m, 1H), 3.79–3.73 (m, 1H), 3.69 (td, *J* = 9.6, 4.9 Hz, 1H), 3.62–3.52 (m, 2H), 3.48–3.39 (m, 2H), 3.12–3.00 (m, 2H). **^{13}C-NMR** (400 MHz, $CDCl_3$) δ 165.68, 165.27, 136.82, 133.37, 133.19, 130.08, 129.99, 129.90, 129.87, 129.54, 129.46, 129.40, 129.22, 129.12, 128.57, 128.49, 128.38, 128.32, 128.28, 126.20, 101.95, 101.57,

78.90, 72.56, 72.07, 70.44, 70.18, 69.81, 68.72, 66.68, 50.60. Maldi-ToF m/z calc'd for $C_{31}H_{31}N_3O_9Na$ ($M+Na^+$): 612.1958; found: 612.1955.

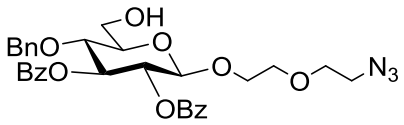

Synthetic procedure of comp 13: Compound synthesized from **13A** by same procedure explained for 12 to give **13** (240 mg, 80%). **^{1}H-NMR** (400 MHz, $CDCl_3$) δ 7.96–7.89 (m, 4H), 7.53–7.45 (m, 2H), 7.39–7.32 (m, 4H), 7.18–7.11 (m, 5H), 5.73 (t, *J* = 9.6 Hz, 1H), 5.33 (dd, *J* = 9.6, 8.0 Hz, 1H), 4.80 (d, *J* = 8.0 Hz, 1H), 4.59 (s, 2H), 4.01–3.90 (m, 3H), 3.81 (dd, *J* = 11.2, 3.9 Hz, 1H), 3.74 (ddd, *J* = 11.2, 4.8, 3.2 Hz, 1H), 3.63–3.54 (m, 3H), 3.45 (m, 2H), 3.08 (m, 2H), 2.01(bs, 1H). **^{13}C NMR** (400 MHz, $CDCl_3$) δ 165.78, 165.38, 137.22, 133.30, 133.28, 129.85, 129.84, 129.82, 129.47, 129.44, 128.47, 128.40, 128.38, 128.37, 128.35, 128.34, 128.32, 128.30,128.28, 128.07, 101.31, 77.33, 75.55, 74.96, 74.91, 72.20, 70.46, 70.19, 69.69, 61.59, 50.61. Maldi-ToF m/z calc'd for $C_{31}H_{33}N_3O_9Na$ ($M+Na^+$): 614.2114; found: 614.2120.

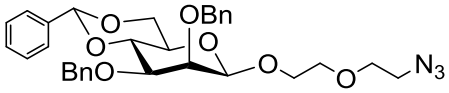

Synthesis of compound 14A: To a stirred solution of sulfoxide **14B** (500 mg, 0.900 mmol, 1eq) and TTBP (468 mg, 2.1 eq) in CH_2Cl_2(10 ml) at -78^{0}C was added Tf_2O (151 µl, 1eq) and, 5 min later, the solution of the glycosyl acceptor (78 mg, 1.2 eq) in CH_2Cl_2 (2 ml) drop wise were added. The reaction mixture was stirred at -78 ^{0}C for 2 h and then allowed to warm to 0 ^{0}C over 2 h and maintained there for a further 0.5 h before quenching with saturated aqueous $NaHCO_3$, washing with brine, drying, concentrating, and purified by chromatography on silicagel Hexane:Ethylacetate to give compound **14A** (320 mg, 64%); **^{1}H-NMR** (400 MHz, $CDCl_3$) δ 7.51–7.44 (m, 2H), 7.40–7.25 (m, 13H), 5.61 (s, 1H), 4.96 (d, *J* = 12.2 Hz, 1H), 4.87 (d, *J* = 12.2 Hz, 1H), 4.66 (d, *J* = 12.5 Hz, 1H), 4.57 (d, *J* = 12.5 Hz, 1H), 4.54 (s, 1H), 4.29 (dd, *J* = 10.4, 4.9 Hz, 1H), 4.19 (t, *J* = 9.6 Hz, 1H), 4.05–3.99 (m, 1H), 3.98 (d, *J* = 3.0 Hz, 1H), 3.92 (t, *J* = 10.3 Hz, 1H), 3.74–3.62 (m, 5H), 3.58 (dd, *J* = 9.6, 3.1 Hz, 1H), 3.33 (dt, *J* = 9.6, 5.4 Hz, 3H). **^{13}C-NMR** (400 MHz,$CDCl_3$) δ 138.56, 138.39, 137.64, 134.56, 129.84, 129.09, 128.93, 128.72,

128.63, 128.42, 128.38, 128.27, 128.18, 128.05, 127.86, 127.65, 127.60, 126.14, 102.09, 101.50, 81.48, 78.67, 74.92, 73.29, 71.09, 70.69, 70.30, 69.19, 67.50, 63.10, 50.82. Maldi-ToF m/z calc'd for $C_{31}H_{35}N_3O_7Na$ ($M+Na^+$): 584.2372; found: 584.2380.

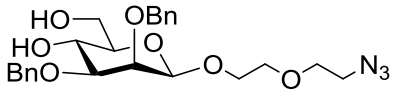

Synthesis of compound 14: A solution of compound **14A** (350 mg 534 mmol) was dissolved in dichloromethane (7 ml) and stirred for 1h at room temperature. The mixture was cooled to 0^0C and then catalytic amount of *p*-TsOH were added to it. Allowed this reaction to stir at RT till complete disappearance of starting material on TLC. Then quenched the mixture by TEA and diluted with DCM followed by extraction with sat.$NaHCO_3$. The organic layer were concentrated and purified by silica gel column chromatography (DCM:MeOH) to afford colourless syrup (250 mg. 85%) **^{1}H NMR** (400 MHz, $CDCl_3$) δ 7.49–7.41 (m, 2H), 7.36–7.24 (m, 8H), 4.96 (d, *J* = 12.3 Hz, 1H), 4.80 (d, *J* = 12.3 Hz, 1H), 4.56 (s, 1H), 4.51 (d, *J* = 11.8 Hz, 1H), 4.33 (d, *J* = 11.8 Hz, 1H), 4.10–4.03 (m, 1H), 4.02–3.98 (m, 1H), 3.97–3.91 (m, 1H), 3.89–3.80 (m, 1H), 3.78–3.67 (m, 5H), 3.39 (ddd, *J* = 9.6, 5.5, 4.4 Hz, 2H), 3.37–3.29 (m, 2H), 2.75 (d, *J* = 3.8 Hz, 1H), 2.55 (s, 1H), 2.03 (s, 1H). **^{13}C NMR** (400 MHz, $CDCl_3$) δ 138.52, 137.66, 128.56, 128.54, 128.36, 128.34, 128.20, 128.18, 127.92, 127.79, 127.77, 127.56, 101.97, 81.41, 75.94, 74.26, 73.41, 71.10, 70.66, 70.20, 69.08, 67.37, 62.91, 50.74. Maldi-ToF m/z calc'd for $C_{26}H_{28}O_5S$ ($M+Na^+$): 496.2059; found: 496.2061.

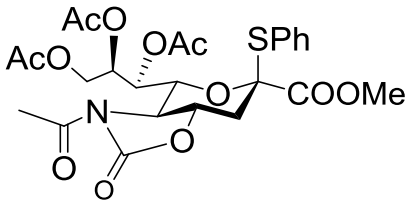

Synthesis of compound 11: A stirred solution of **7** (5.00 g, 8.57 mmol, 1.00 equiv) in methanol (80 ml) was treated with methanesulfonic acid (1.68 ml, 25.7 mmol, 3.0 equiv) at room temperature, and then refluxed under Ar for 24 h. After being cooled to room temperature, the reaction mixture was quenched with excess triethylamine, and then concentrated. The concentrate and $NaHCO_3$ (3.60 g, 42.8 mmol, 5.0 equiv) were dissolved in CH_3CN (30 ml) and H_2O (60 ml) and cooled to 0^0C. To the vigorously stirred mixture was added 4-

nitrophenylchloroformate (4.32 g, 21.4 mmol, 2.5 equiv) in CH_3CN (30 ml) slowly through a dropping funnel, after which stirring was continued for 3 h at 0°C. The resulting mixture was extracted with ethylacetate and the combined extracts were washed with brine, and then dried over Na_2SO_4 and concentrated. The residue was purified by silica gel column chromatography, eluting withEtOAc then EtOAc/MeOH from 10/1 to 5/1 to give the title residue as white foam. A solution of residue (2.67 gm) in pyridine (20 ml) was treated with Ac_2O (24 ml) and stirred at room temperature overnight, then concentrated under reduced pressure. The residue was dissolved in anhydrous CH_2Cl_2, treated with EtN(*i*-Pr)$_2$ (11.6 ml, 66.8 mmol, 10 equiv), and cooled to 0°C before acetyl chloride (3.87 ml, 53.4 mmol, 8 equiv) was added dropwise, then the mixture stirred at 0°C for 1 h. After warming to room temperature, the resulting solution was poured into saturated aqueous $NaHCO_3$ solution, the organic layer was separated, the aqueous layer was extracted twice with CH_2Cl_2, and the combined organic phase was washed with brine, dried over Na_2SO_4, and concentrated.The residue was purified by column chromatography on silica gel eluting with EtOAc/Hex (1:1) to give donor **1** as a yellowish solid (2.8 g, 82%),which can be further purified by recrystalization from EtOAc/Et_2O/Hex to afford white needle crystals. **^{1}H-NMR** (400 MHz, $CDCl_3$) δ 7.55–7.32 (m, 5H), 5.57 (t, *J* = 2.3 Hz, 1H), 5.01 (dt, *J* = 8.2, 2.3 Hz, 1H), 4.90 (dd, *J* = 9.1, 2.5 Hz, 1H), 4.80 (ddd, *J* = 12.8, 11.4, 2.5 Hz, 1H), 4.38 (dd, *J* = 12.1, 2.5 Hz, 1H), 3.91 (dd, *J* = 12.1, 8.3 Hz, 1H), 3.77 (dd, *J* = 11.3, 9.2 Hz, 1H), 3.64 (s, 3H), 2.92 (dd, *J* = 13.0, 3.7 Hz, 1H), 2.54 (s, 3H), 2.35 (t, *J* = 13.0 Hz, 1H), 2.16 (s, 3H), 2.10 (s, 3H), 1.97 (s, 3H). **^{13}C-NMR** (400 MHz, $CDCl_3$) δ 172.46, 171.24, 170.38, 169.72, 167.80, 153.58, 136.77, 136.70, 130.20, 129.23, 129.20, 128.18, 88.35, 75.72, 75.11, 73.85, 72.69, 62.92, 59.67, 52.79, 36.05, 24.76, 21.17, 20.82, 20.73. Maldi-ToF m/z calc'd for $C_{25}H_{29}NO_{12}SNa$ ($M+Na^+$): 590.1308; found: 590.1307.

Glycosylation of donor and acceptor

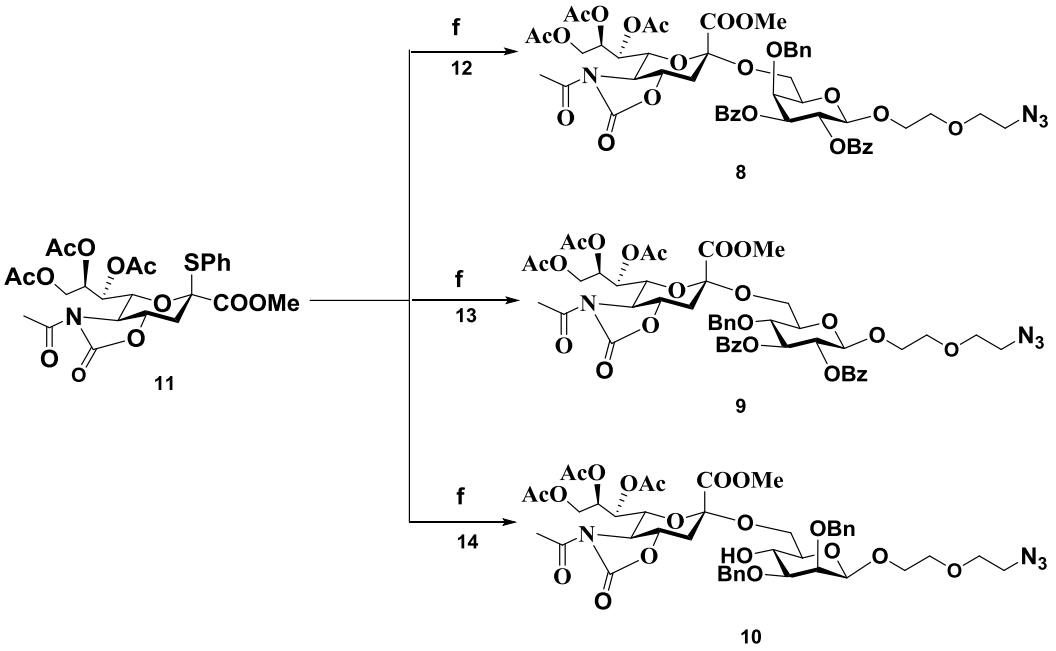

Scheme 6. ***Reagents and Conditions***: (f) NIS/TfOH, -40^{0}C, DCM.

General procedure for glycosylation.A solution of donor **11** (200 mg, 0.11 mmol, 1.0 equiv), acceptor (1.2 equiv), and activated 4 Å powdered molecular sieves (216 mg, 2.0 g/mmol) in anhydrous dichloromethane (2 ml) was stirred overnight under an argon atmosphere, and then cooled to -40^{0}C followed by addition of NIS (172 mg, 0.26 mmol, 2.4 equiv) and TfOH (9.5 *µl*, 0.11 mmol, 1.0 equiv). The reaction mixture was stirred at -40^{0}C for 20 min to 2 h until the disappearance of the donor on TLC, then quenched with triethylamine (22.6 µl, 0.16 mmol, 1.5 equiv) and warmed to room temperature. The mixture was diluted with dichloromethane, filtered through Celite, washed with 20% aqueous $Na_2S_2O_3$ solution, dried over Na_2SO_4, and concentrated under reduced pressure. The residue was purified by column chromatography on silica gel eluting with THF/Hex system to afford the sialic acid disachharide.

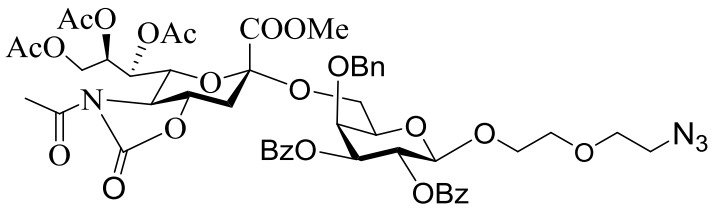

Compound 8: According to general procedure, donor **11** (200 mg) and acceptor **12** (250 mg , 1.2eq) to afford **8** (270 mg , 73%). **^{1}H-NMR** (400 MHz, $CDCl_3$) δ 7.52–7.46 (m, 3H), 7.39–7.31 (m, 6H), 7.30–7.25 (m, 3H), 7.18-7.15 (m, 3H), 5.81 (dd, *J* = 10.5, 8.0 Hz, 1H), 5.58 (dd, *J* = 8.0, 1.6 Hz, 1H), 5.43 (td, *J* = 7.1, 3.1 Hz, 1H), 5.35 (dd, *J* = 10.5, 3.1 Hz, 1H), 4.83 (d, *J* = 8.0 Hz, 1H), 4.70–4.60 (m, 3H), 4.41 (dd, *J* = 12.3, 3.0 Hz, 1H), 4.22 (d, *J* = 3.0 Hz, 1H), 4.06 (dd, *J* = 12.3, 7.0 Hz, 1H), 4.03–3.97 (m, 2H), 3.96-3.85 (m, 3H), 3.81–3.74 (m, 2H), 3.71(s, 3H), 3.58 (m, 2H), 3.47 (t, *J* = 5.1Hz, 2H), 3.08–2.96 (m, 2H), 2.85 (dd, *J* = 12.1, 3.5 Hz, 1H), 2.49 (s, 3H), 2.19 (s, 3H), 2.13 (s, 3H), 2.05 (t, *J* = 12.1 Hz, 1H), 2.00 (s, 3H). **^{13}C-NMR** (400 MHz, $CDCl_3$) δ 172.03, 170.79, 170.14, 170.09, 168.39, 165.67, 165.36, 153.74, 137.44, 133.25, 133.20, 129.98, 129.98, 129.82, 129.78, 129.72, 129.47, 129.02, 128.62, 128.61, 128.60, 128.59, 128.43, 128.33, 128.23, 127.99, 101.21, 99.47, 75.52, 75.36, 75.13, 74.81, 74.60, 74.45, 71.98, 71.63, 70.34, 70.15, 69.53, 68.54, 64.53, 63.10, 59.19, 53.08, 50.60, 36.76, 24.79, 21.28, 20.88, 20.79. HRMS m/z calc'd for $C_{50}H_{56}N_4O_{21}$ ($M+Na^+$): 1071.3314; found:1071.3311.

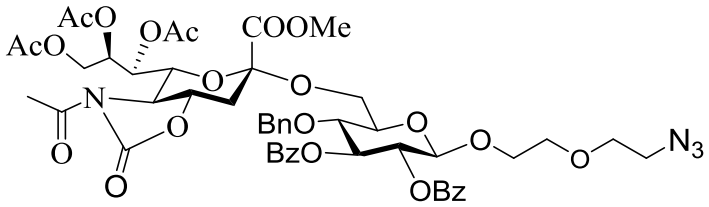

Compound 9: According to general procedure, donor **11**(200 mg) and acceptor **13** (250 mg , 1.2 eq) to afford 9 (255 mg, 69%). **^{1}H-NMR** (400 MHz, $CDCl_3$) δ 7.51-7.46 (m, 4H), 7.37-7.32 (m 5H), 7.15 – 7.08 (m, 6H), 5.69–5.60 (m, 2H), 5.48 (ddd, *J* = 9.0, 6.3, 3.0 Hz, 1H), 5.35-5.28 (m, 2H), 4.72 (dd, *J* = 9.4, 3.9 Hz, 2H), 4.66 (dd, *J* = 9.4, 1.6 Hz, 1H), 4.54 (d, *J* = 10.8 Hz, 1H), 4.35 (dd, *J* = 12.3, 2.9 Hz, 1H), 4.22 (dd, *J* = 11.4, 4.4 Hz, 1H), 4.05 (dd, *J* = 12.3, 6.4 Hz, 1H), 4.02-3.94(m, 2H), 3.90 (dd, *J* = 12.3, 6.6 Hz, 1H), 3.74 (s, 3H), 3.73 – 3.64 (m, 3H), 3.57 (m, 2H), 3.45-3.43 (m, 2H), 3.07-3.04 (m, 2H), 3.01 (dd, *J* = 12.0, 3.4 Hz, 1H), 2.49 (s, 3H), 2.13 (s, 3H), 2.03 (s, 3H), 2.03 (t, *J* = 12.5 Hz, 1H), 1.90 (s, 3H). **^{13}C-NMR** (400 MHz, $CDCl_3$) δ 172.03, 170.79, 170.14, 170.09, 168.39, 165.67, 165.36, 153.74, 137.44, 133.25, 133.20, 129.85, 129.84, 129.82, 129.47, 129.44, 129.47, 129.44, 128.47, 128.43, 128.40, 128.38, 128.37, 128.33, 128.30, 127.99, 101.21, 99.47, 75.52, 75.36, 75.13, 74.81, 74.60, 74.45, 71.98, 71.63, 70.34, 70.15,

69.53, 68.54, 64.53, 63.10, 59.19, 53.08, 50.60, 36.76, 24.79, 21.28, 20.88, 20.79. HRMS m/z calc'd for $C_{50}H_{56}N_4O_{21}$ (M+Na): 1071.3314; found:1071.3322.

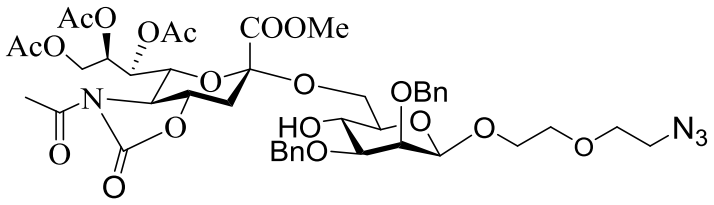

Compound 10: According to general procedure, donor **11** (200 mg) and acceptor **14** (238 mg ,1.2eq) to afford **10** (230 mg , 64%). **^{1}H NMR** (400 MHz, $CDCl_3$) δ 7.45–7.20 (m, 10H), 5.61 (dd, *J* = 8.2, 1.2 Hz, 1H), 5.46–5.32 (m, 1H), 5.05 (dd, *J* = 10.5, 3.1 Hz, 1H), 5.00 (s, 1H), 4.93 (d, *J* = 12.3 Hz, 1H), 4.78 (d, *J* = 12.3 Hz, 1H), 4.58 (d, *J* = 9.3 Hz, 1H), 4.51 (d, *J* = 11.3 Hz, 1H), 4.42 (d, *J* = 11.3 Hz, 1H), 4.34 (dd, *J* = 12.3, 3.2 Hz, 1H), 4.14 (dd, *J* = 9.2, 4.5 Hz, 1H), 4.10 – 4.01 (m, 4H), 3.98-3.90 (m, 3H), 3.78 (s, 3H), 3.76–3.52 (m, 4H), 3.39–3.23 (m, 4H), 3.03 (s, 1H), 2.88 (dd, *J* = 12.3, 3.6 Hz, 1H), 2.48 (s, 3H), 2.25 (s, 3H), 2.11 (s, 3H), 2.05 (t, dd, *J* = 12.4 Hz, 1H) , 2.02 (s, 3H). **^{13}C NMR** (400 MHz, $CDCl_3$) δ 172.12, 170.76, 170.16, 169.81, 168.99, 151.45, 139.06, 138.05, 129.42, 128.39, 128.33, 128.29, 128.25, 128.09, 127.70, 127.43, 126.82, 125.52, 102.08, 98.69, 80.76, 75.61, 75.51, 75.01, 73.99, 73.71, 71.58, 70.46, 69.11, 68.97, 66.42, 64.35, 62.78, 61.41, 59.05, 54.26, 53.00, 50.74, 36.48, 24.70, 21.19, 20.89, 20.85. HRMS m/z calc'd for $C_{43}H_{54}N_4O_{19}$ (M+Na): 953.3279; found: 953.3292.

Global deprotection of comp 8, 9, 10

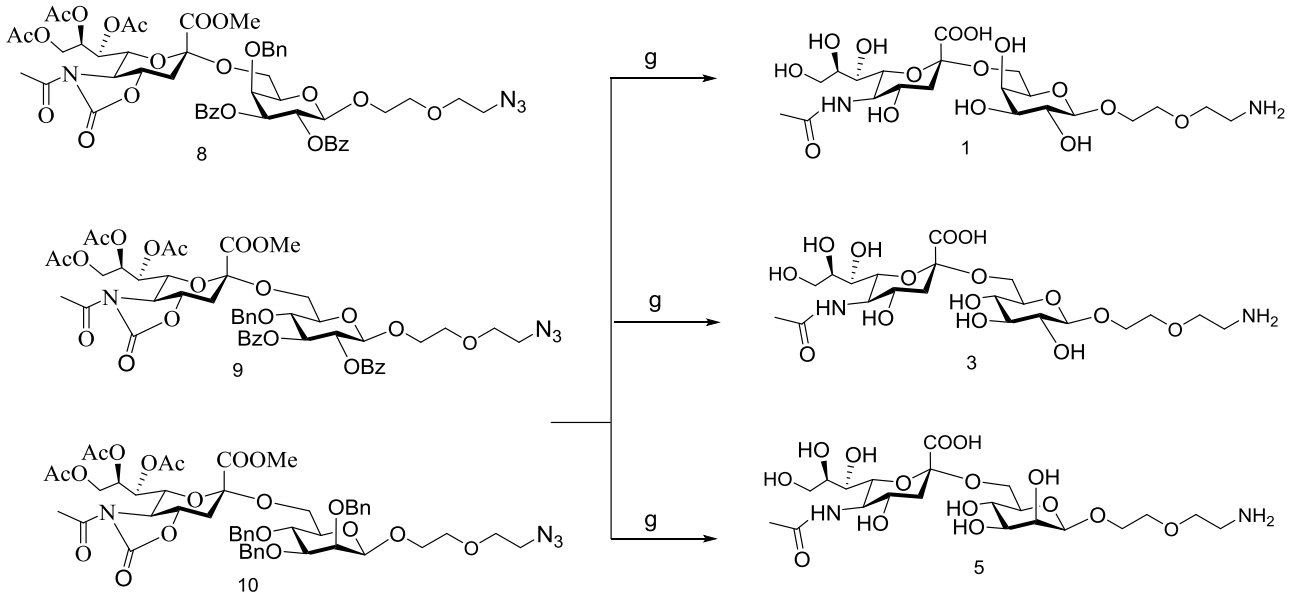

Scheme 7. ***Reagents and Conditions*** g) i) LiOH, EtOH:H_2O(3:1), 80^0C,12h; ii) $NaHCO_3$, Ac_2O, H_2O, rt; iii) H_2/$Pd(OH)_2$, MeOH:H_2(1:1), 12h.

LiOH (30 eq) was added to a stirred solution of protected oligosaccharide(1 eq) in ethanol water (3:1) 5 ml at room temperature. After stirring at 80^0C for 12h, the reaction mixture cooled to room temperature and carefully neutralized by IR-120H^+ resin to pH-7, diluted with methanol, filtered and concentrated. Crude residue was dissolved in water and $NaHCO_3$ (15 eq) were added to it. Cooled the reaction mixture to 0^0C and Acetic-anhydride (10 eq) was added. The reaction were monitored by TLC(ethylacetate:methanol:water 7:2:1), after 3h, LiOH(10 eq) were added and stirred for another 5-6h at room temperature, then reaction mixture carefully neutralized by IR-120H^+resin to pH-7,diluted concentrated andpurified by reverse-phase column chromatography(Bond Elu-C18).The $Pd(OH)_2$(1 mmole) was added to the above residue in methanol water(1:1) 4ml. The reaction mixture was hydrogenalysed under H_2 atmosphere for 12h, filtered and concentrated. The residue was purified by reverse phase column chromatography(Bond Elu-C18) to give deprotected Sialic acid analogues.

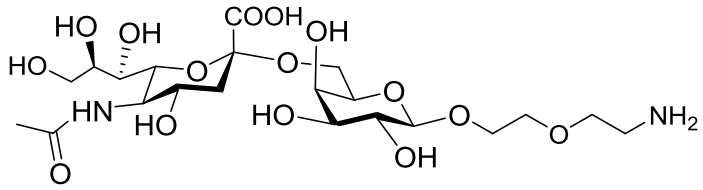

Compound 1: Synthesized from **8** by following general deprotection protocol to yield 36 mg (36%). **^{1}H-NMR** (400 MHz, D_2O) δ 4.33 (d, *J* = 7.7 Hz, 1H), 3.97 (dd, *J* = 11.8, 7.1 Hz, 1H), 3.83 (t, *J* = 8.7 Hz, 2H), 3.76 (dd, *J* = 11.5, 8.7 Hz, 4H), 3.72–3.64 (m, 5H), 3.63–3.45 (m, 7H), 3.42 (dd, *J* = 16.3, 8.3 Hz, 1H), 3.28 (t, *J* = 5.0 Hz, 1H), 3.15–3.10 (m, 1H), 2.63 (dd, J = 12.5, 3.6 Hz, 1H), 1.93 (s, 3H), 1.58 (t, *J* = 12.0 Hz, 1H). **^{13}C-NMR** (400 MHz, D_2O) δ 175.02, 173.42, 103.01, 100.41, 73.44, 72.59, 72.46, 71.72, 71.42, 70.74, 68.59, 68.22, 68.17, 63.44, 62.60, 60.77, 60.37, 51.84, 40.15, 39.74, 22.03. HRMS m/z calc'd for $C_{21}H_{38}N_2O_{15}$ (M+H): 559.2350; found: 559.2352.

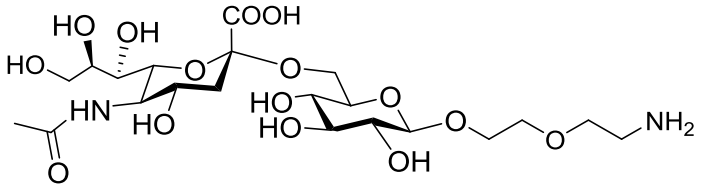

Compound 3: Synthesized from **9** by following general deprotection protocol to yield 20 mg (20%). **^{1}H-NMR** (400 MHz, MeOD) δ 4.34 (d, *J* = 7.8 Hz, 1H), 4.06 (dd, *J* = 10.4, 3.5 Hz, 1H), 3.95 (t, *J* = 9.5 Hz, 1H), 3.93–3.88 (m, 1H), 3.88–3.60 (m, 10 H), 3.58–3.48 (m, 2H), 3.38 (dd, *J* = 16.2, 6.8 Hz, 2H), 3.27–3.11 (m, 4H), 2.76 (dd, J = 12.0, 3.7 Hz, 1H), 2.04 (s, 3H),1.66 (t, *J* = 12.0 Hz, 1H). **^{13}C-NMR** (400 MHz, D_2O) δ 174.90, 173.86, 102.37, 99.79, 75.92, 75.03, 72.92, 71.84, 69.60, 69.18, 68.77, 68.31, 68.12, 67.57, 66.38, 62.67, 61.02, 51.75, 39.73, 39.15, 22.17. HRMS m/z calc'd for $C_{21}H_{38}N_2O_{15}$ (M+H): 559.2350; found: 559.2352.

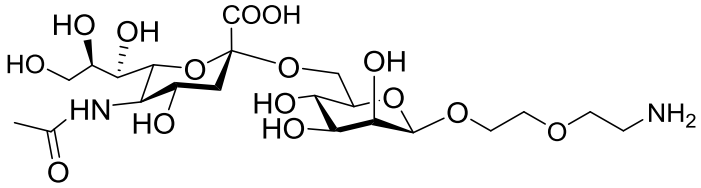

Compound 5: Synthesized from **10** by following general deprotection protocol to yield 27 mg (25%). **^{1}H-NMR** (400 MHz, MeOD) δ 4.57 (d, *J* = 0.8 Hz, 1H), 4.11–4.02 (m, 2H), 3.94–3.81 (m, 6H), 3.81–3.59 (m, 10H), 3.55-3.45 (m, 4H), 2.85 (dd, *J* = 12.4, 4.3 Hz, 1H), 2.03 (s, 3H), 1.66 (t, *J* = 12.4 Hz, 1H). **^{13}C-NMR** (400 MHz, D_2O) δ 175.11, 173.80, 102.52, 99.35, 75.92, 75.03, 72.92, 71.84, 69.60, 69.18, 68.77, 68.31, 68.12, 67.57, 66.38, 62.67, 61.02, 51.75, 39.73, 39.15, 21.84. HRMS m/z calc'd for $C_{21}H_{38}N_2O_{15}$ (M+H): 559.2350;found: 557.2352.

Synthesis of trisaccharide library of compounds:

Synthesis of donor and acceptors

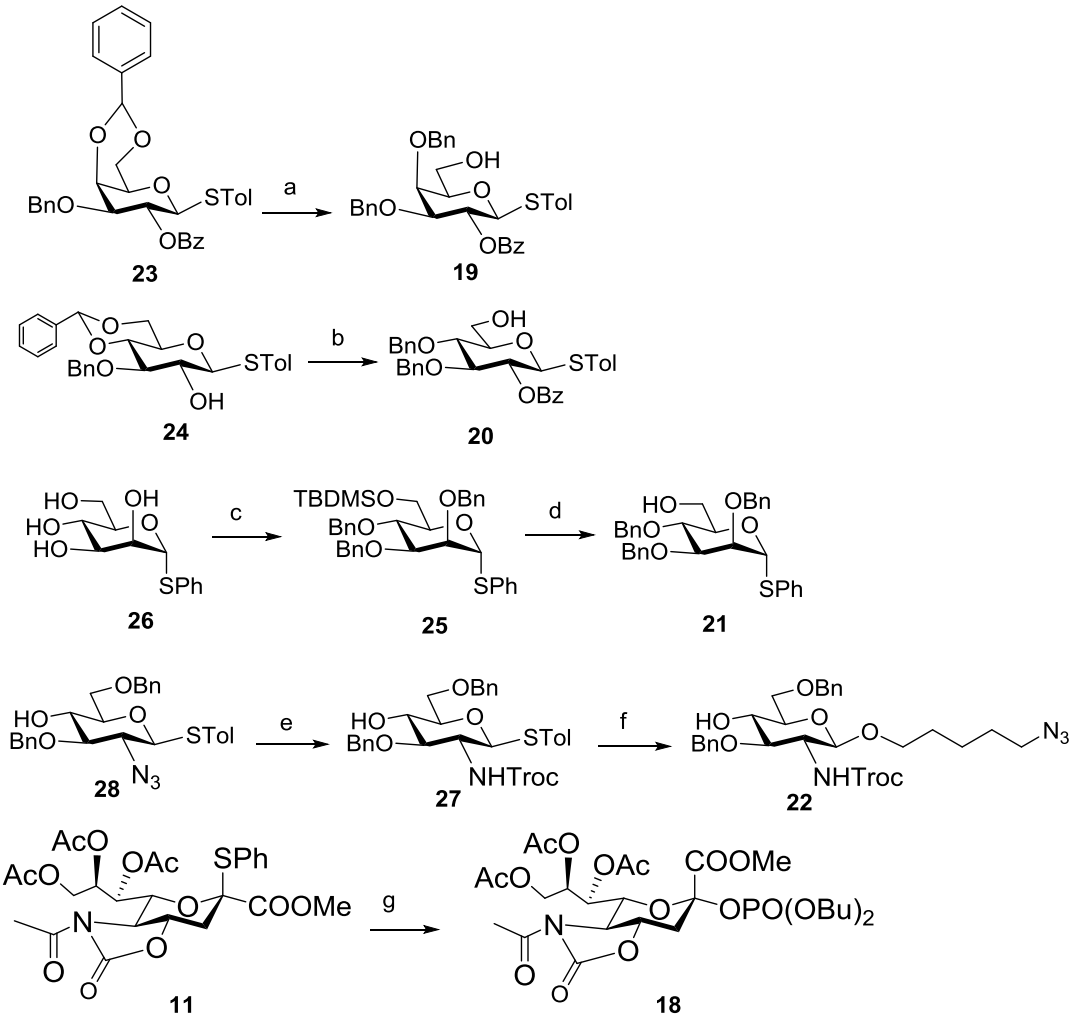

Scheme 8. ***Reagents and conditions:*** a) $PhBCl_2$, Et_3SiH, -78^{0}C, DCM; b) i) BzCl/Py; ii) $PhBCl_2$, Et_3SiH, -80^{0}C, DCM; c) i) TBDMSCl, Imidazole, DMF; ii) BnBr, NaH, DMF; d) p-TSA, MeOH:DCM; e) i) 1,3-dithiopropane, DCM, 35^{0}C; ii) TrocCl, $NaHCO_3$, THF; f) 5-Azidopentanol, NIS/TfOH, -40^{0}C, DCM; g) Dibutylphosphate, NIS/TfOH, DCM:ACN, -20^{0}C.

Synthetic procedure:

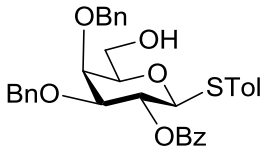

Compound 19: A solution of compound **23** (600 mg, 1.08 mmol) and activated 4Å powdered molecular sieves 1.1 g in dichloromethane were stirred 1h at room temperature. The mixture was cooled to -78^{0}C and then to the stirred solution Et_3SiH (552 µl, 3.46 mmol) and $PhBCl_2$ (265 µl,

2.05 mmol) were added successively. After being stirred for 1 h at -78^{0}C, Et_3N (1 ml) and MeOH (1 ml) were added successively, and the mixture was diluted with $CHCl_3$ and washed with aqueous $NaHCO_3$, dried over $MgSO_4$, filtered and concentrated. The crude product was purified by silica gel column Hexane:Ethylacetate (2:1) to afford white solid (545 mg, 91%).**^{1}H- NMR** (400 MHz, $CDCl_3$) δ 8.06 (d, *J* = 7.6 Hz, 2H), 7.63 (t, *J* = 7.4 Hz, 1H), 7.49 (t, *J* = 7.6 Hz, 2H), 7.42 – 7.31 (m, 7H), 7.27–7.14 (m, 5H), 7.06 (d, *J* = 7.8 Hz, 2H), 5.70 (t, *J* = 9.7 Hz, 1H), 5.02 (d, *J* = 11.8 Hz, 1H), 4.74 (d, *J* = 9.7 Hz, 1H), 4.67 (t, *J* = 10.8 Hz, 2H), 4.57 (d, *J* = 12.2 Hz, 1H), 3.94 (s, 1H), 3.93–3.85 (m, 1H), 3.72 (dd, *J* = 9.0, 2.2 Hz, 1H), 3.59 (dd, *J* = 9.0, 5.2 Hz, 1H), 3.56–3.50 (m, 1H), 2.31 (s, 3H), 1.67 (dd, *J* = 8.5, 3.7 Hz, 1H). **^{13}C-NMR** (400 MHz, $CDCl_3$) δ 165.28, 138.11, 137.85, 137.43, 133.08, 132.71, 132.69, 130.08, 129.90, 129.88, 129.58, 129.51, 128.47, 128.44, 128.45, 128.41, 128.40, 128.39, 128.37, 128.35, 127.92, 127.86, 127.84, 127.79, 127.77, 87.25, 81.32, 78.99, 77.23 74.07, 72.18, 70.54, 62.20, 21.14; HRMS m/z calc'd for $C_{34}H_{34}O_6SNa$ ($M+Na^+$). 593.1973; found: 593.1971.

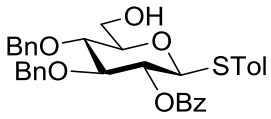

Compound 20: To solution of compound **24** (700 mg, 1.5 mmol) in dry pyridine (10 ml) benzoyl chloride (440ml, 3.7mmol) were added dropwise. Allowed the reaction mixture to stir for 12h at room temperature. After completion quenched the reaction by methanol 2ml and diluted with DCM. Extracted with dilute HCl (5%), dried over Na_2SO_4 and concentrated. Crude residue was purified through silica gel column to afford the white solid. This white solid (575mg, 1.03mmol) dissolved in dry dichloromethane (10ml) containing 4Å M.S. and stirred at room temperature for 1h. Reaction mixture was cooled to -78^{0}C and then Et_3SiH (533 µl, 3.32 mmol) and $PhBCl_2$ (253 µl, 1.95 mmol) were added successively. After being stirred for 1 h at -78^{0}C, Et_3N (1 ml) and MeOH (1 ml) were added successively, and the mixture was diluted with $CHCl_3$ and washed with aqueous $NaHCO_3$, dried over $MgSO_4$, filtered and concentrated. The crude product was purified by silica gel column Hexane:Ethylacetate (1:1) to afford white solid(530mg, 88%).**^{1}H-NMR** (400 MHz, $CDCl_3$) δ 8.08 (dd, *J* = 8.3, 1.3 Hz, 2H), 7.65 – 7.60 (m, 1H), 7.49 (dd, *J* = 8.2, 4.7 Hz, 2H), 7.40–7.29 (m, 7H), 7.18–7.09 (m, 7H), 5.26 (dd, *J* = 9.9, 9.2 Hz, 1H), 4.87 (d, *J* = 11.0 Hz, 1H), 4.77 (dd, *J* = 10.5, 6.1 Hz, 2H), 4.68 (d, *J* = 11.0 Hz, 2H), 3.94 (ddd, *J* = 12.0, 6.0, 2.6 Hz, 1H), 3.88 (t, *J* = 9.0 Hz, 1H), 3.79–3.73 (m, 1H), 3.73–3.67 (m,

1H), 3.51 (ddd, *J* = 9.7, 4.7, 2.6 Hz, 1H), 2.35 (s, 3H), 1.99 (t, *J* = 6.8 Hz, 1H). **^{13}C-NMR** (400 MHz, $CDCl_3$) δ 165.20, 138.44, 137.75, 137.60, 133.32, 133.31, 133.25, 129.88, 129.86, 129.85, 129.75, 129.73, 128.54, 128.52, 128.50, 128.45, 128.30, 128.28, 128.12, 128.10, 128.08, 128.05, 128.03, 127.70, 127.72, 86.34, 84.06, 79.56, 77.51, 75.34, 75.19, 72.55, 62.07, 21.16. HRMS m/z calc'd for $C_{34}H_{34}O_6SNa$ (M+Na). 593.1971; found: 593.1973.

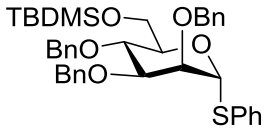

Compound 25 The solution of compound **26** (1.2gm, 4.41 mmol) in dry DMF (10 ml) cooled to -20^{0}C and then imidazole (0.6 gm, 8.82 mmol) were added to it. After 10 minutes TBDMSCl (0.79 gm, 5.29 mmol) were added portion wise and allowed the reaction mixture to stir for 2h. After completion of reaction, evaporated the solvent and then diluted with DCM and extracted with 1N HCl. The organic layer dried over sodium sulphate. This crude residue was purified by flash silica gel column chromatography in DCM:MeOH (9:1) to afford as colorless syrup (0.7 gm, 40%). This syrup was dissolved in dry THF (10 ml) followed by addition of tetrabutylammonium iodide(2 gm, 5.44 mmol). Cooled this reaction mixture to 0^{0}C and then sodium hydride(60%, 450 mg) was added. After 5 minutes benzyl bromide (1.0 ml, 9 mmol) was added dropwise and allowed the reaction mixture to stir for 12h at room temperature. After completion, reaction was quenched with methanol and diluted with ether. The organic layer was extracted with NaHCO3, brine and dried over Na_2SO_4, concentrated. Purification by silica gel column chromatography (Ethylacetate:Hexane) afforded compound **25** as oily syrup (0.9 gm, 76%).**^{1}H-NMR** (400 MHz, $CDCl_3$) δ 7.36 (m, 20H), 5.59 (d, *J* = 1.5 Hz, 1H), 4.98 (d, *J* = 10.9 Hz, 1H), 4.74–4.62 (m, 5H) 4.13 (ddd, *J* = 9.6, 4.8, 1.7 Hz, 1H), 4.05 (d, , *J* = 9.3 Hz, 1H), 4.01(dd, *J* = 3.1, 1.6 Hz, 1H) 3.97-3.87 (m, 3H), 0.92 (s, 9H), 0.09 (s, 3H), 0.08 (s, 3H). **^{13}C-NMR** (400 MHz, $CDCl_3$) δ 138.67, 138.28, 138.02, 134.80, 131.50, 131.48, 128.92, 128.90, 128.43, 128.41, 128.39, 128.37, 128.33, 128.31, 128.03, 128.01, 127.87, 127.86, 127.84, 127.82, 127.69, 127.64, 127.64, 127.24, 85.61, 80.16, 76.54, 75.21, 74.91, 74.23, 72.15, 71.79, 62.70, 25.97, 25.97, 25.97, 18.38, -5.12, -5.30. HRMS m/z calc'd for $C_{39}H_{48}O_5SSiNa$ ($M+Na^+$). 679.2889; found: 679.2891.

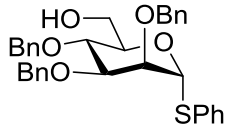

Compound 21 Compound **25** (0.750 gm, 1.14 mmol) was dissolved in dry methanol and dichloromethane mixture(10 ml). To it catalytic amount of *p*-TSOH (110 mg) were added and stirred this reaction mixture for 2h at room temperature. Quenched the reaction mixture with triethylamine and extracted with sat. $NaHCO_3$, brine and dried the organic layer over Na_2SO_4, concentrated. Purification of mixture by silica-gel column chromatography (Ethylacetate:Hexane) yielded compound **21** as colourless syrup (550 mg, 85%). **^{1}H-NMR** (400 MHz, $CDCl_3$) δ 7.41-7.25 (m, 20H), 5.50 (d, *J* = 1.6 Hz, 1H), 4.95 (d, *J* = 10.9 Hz, 1H), 4.67-4.59 (m, 2H), 4.64 (d, *J* = 5.1 Hz, 1H), 4.61 (d, *J* = 11.7 Hz, 1H), 4.15-4.09 (m, 1H), 4.04 (t, *J* = 9.4 Hz, 1H), 3.99 (dd, *J* = 2.9, 1.8 Hz, 1H), 3.88 (dd, *J* = 9.2, 3.1 Hz, 1H), 3.83 (dd, *J* = 8.9, 2.9 Hz, 1H), 3.79 (dd, *J* = 8.7, 4.4 Hz, 1H), 1.75 (bs, 1H). **^{13}C NMR** (400 MHz, $CDCl_3$) δ 138.31, 138.12, 137.84, 133.94, 131.87, 131.85, 129.13, 129.12, 128.48, 128.47, 128.46, 128.45, 128.09, 128.07, 127.95, 127.93, 127.86, 127.85, 127.83, 127.81, 127.80, 127.78, 127.67, 127.65, 86.06, 80.12, 76.43, 75.32, 74.79, 73.25, 72.38, 72.26, 62.24. HRMS m/z calc'd for $C_{33}H_{34}O_5S$ ($M+Na^+$). 565.2024; found: 565.2025.

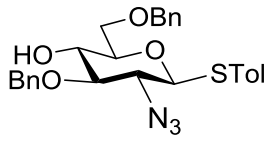

Compound 28 was synthesized by following synthetic reported protocol (C. H. Wang, K. Tony, K. Mong, C. Y. Huang, *J. Org. Chem*., **2003**, 68, 2135-2142**)**. **^{1}H-NMR** (400 MHz, $CDCl_3$) δ 7.50-7.40 (m, 2H), 7.39-7.21 (m, 11H), 7.07 (d, *J* = 7.9 Hz, 1H), 4.88 (d, *J* = 11.0 Hz, 1H), 4.81 (d, *J* = 11.0 Hz, 1H), 4.59 (d, *J* = 11.8 Hz, 1H), 4.54 (d, *J* = 11.8 Hz, 1H), 4.36 (d, *J* = 9.9 Hz, 1H), 3.78 (dd, *J* = 10.4, 4.9 Hz, 1H), 3.73 (dd, *J* = 10.4, 4.4 Hz, 1H), 3.60 (t, *J* = 9.0 Hz, 1H), 3.43 (dt, *J* = 9.4, 4.4 Hz, 1H), 3.35 (t, *J* = 9.0 Hz, 1H), 3.30-3.23 (m, 1H), 2.72 (s, 1H), 2.32 (s, 3H). **^{13}C NMR** (400 MHz, $CDCl_3$) δ 138.86, 137.92, 137.79, 134.30, 129.87, 128..80, 128.72,

128.66, 128.57, 128.40, 128.34, 128.30, 128.22, 127.93, 127.95, 127.78, 127.80, 127.11, 86.25, 84.69, 78.04, 75.58, 73.83, 72.03, 70.39, 64.42, 21.26. HRMS m/z calc'd for $C_{27}H_{29}N_3O_4S(M+Na^+)$. 514.1776; found: 514.1769.

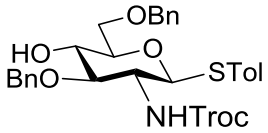

Compound 27. To compound **28** (2.5 gm, 5.09 mmol) in MeOH:DCM (1:1) was added 1,3 dithiopropane (2.5 ml, 25.45 mmol) and TEA (2.45 ml, 25.45 mmol) under Ar atmosphere. Reaction mixture was stirred at 35^0C for 18h. Then coevaporated with toluene, concentrated and purified by flash column chromatography (Ethylacetate:Hexane) to afford oily syrup. This syrup was dissolved in THF and $NaHCO_3$ (0.818 gm, 10.18 mmol) was added to it. Cooled the reaction mixture to 4^0C and Troc-chloride (1 ml, 7.63 mmol) added dropwise. Stirred this reaction mixture at room temperature under argon for 6h. Filtered the reaction mixture and filtrate was concentrated. The residue was dissolved in DCM and washed with water, brine and the organic layer was dried over Na_2SO_4 and concentrated. The residue was purified on silica gel column chromatography (Ethylacetate:Hexane) to afford compound **27** as white solid (2.4 gm, 76%). **^{1}H-NMR** (400 MHz, $CDCl_3$) δ 7.42-7.24 (m, 12H), 7.04 (d, *J* = 7.9 Hz, 2H), 5.14 (d, *J* = 8.1 Hz, 1H), 4.88 (d, *J* = 10.2 Hz, 1H), 4.75 (m, 4H), 4.58 (d, *J* = 11.8 Hz, 1H), 4.53 (d, *J* = 11.8 Hz, 1H), 3.77 (dd, *J* = 4.7, 3.0 Hz, 2H), 3.67 (t, *J* = 9.3, 10.2 Hz, 2H), 3.45-3.55 (m, 1H), 3.35 (dd, *J* = 9.1, 4.2 Hz, 1H), 2.81 (s, 1H), 2.29 (s, 3H). **^{13}C-NMR** (400 MHz, $CDCl_3$) δ 153.91, 138.31, 138.08, 137.80, 133.30, 133.28, 129.81, 129.79, 128.68, 128.66, 128.56, 126.54, 128.26, 128.24, 128.11, 127.95, 127.93, 127.85, 127.83, 95.57, 86.18, 81.91, 77.99, 74.83, 74.55, 73.83, 73.00, 70.64, 56.15, 21.22. HRMS m/z calc'd for $C_{30}H_{32}NCl_3O_6SNa$ $(M+Na^+)$; 662.0913 found: 662.0910.

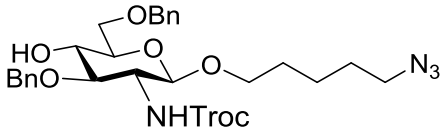

Compound 22 A solution of **27** (2.3 gm, 3.59 mmol, 1.0 equiv), 5-azidopentanol (4.31 mmol, 1.2 equiv), and activated 4Å powdered molecular sieves (1.5 gm) in anhydrous dichloromethane (12 ml) was stirred for 2h at room temperature under an argon atmosphere, and then cooled to -40^{0}C followed by addition of NIS (0.96 gm, 4.31 mmol, 1.2 equiv) and TfOH (32 μl, 0.359 mmol, 0.1 equiv). The reaction mixture was stirred at -40^{0}C for 0.5 h to 3 h until the disappearance of the donor on TLC, then quenched with triethylamine (270µl, 2.69 mmol, 0.75 equiv) and warmed to room temperature. The mixture was diluted with dichloromethane, filtered through Celite, washed with 20% aqueous $Na_2S_2O_3$ solution, dried over Na_2SO_4, and concentrated under reduced pressure. The residue was purified by column chromatography on silica gel eluting with Ethylacetate/Hexane (1:1) system to afford the compound **22** (2.1 gm, 91%). **^{1}H-NMR** (400 MHz, $CDCl_3$) δ 7.44-7.33 (m, 10H), 5.15 (s, 1H), 4.85-4.70 (m, 3H), 4.72 (d, *J* = 11.7 Hz, 2H), 4.64 (d, *J* = 12.0 Hz, 1H), 4.58 (d, *J* = 12.0 Hz, 1H), 3.91-3.84 (m, 2H), 3.83-3.75 (m, 2H), 3.72 (t, *J* = 8.3 Hz, 1H), 3.55-3.43 (m, 2H), 3.27 (t, *J* = 6.8 Hz, 3H), 2.83 (s, 1H), 1.66-1.57 (m, 4H), 1.43 (m, 2H). **^{13}C-NMR** (400 MHz, $CDCl_3$) δ 153.96, 138.19, 137.59, 128.58, 128.56, 128.51, 128.49, 128.16, 128.18, 127.97, 127.92, 127.80, 127.78, 100.29, 95.53, 80.24, 77.23, 74.44, 73.77, 73.50, 73.49, 70.65, 69.50, 57.54, 51.31, 29.04, 28.56, 23.19. HRMS m/z calc'd for $C_{28}H_{35}N_4Cl_3O_7S$ Na ($M+Na^+$); 667.1468; found: 667.1467.

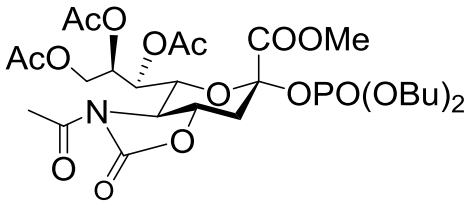

Compound 18A Solution of **11** (3 gm, 4.62 mmol, 1.0 equiv), dibutylphosphate (6.94 mmol, 1.5 equiv), and activated 4Å powdered molecular sieves (2.2 gm) in anhydrous dichloromethane (20 ml) and acetonitrile (10 ml) was stirred for 2h at room temperature under an argon atmosphere, and then cooled to -20^{0}C followed by addition of NIS (2 gm, 9.28 mmol, 2 equiv) and TfOH (200 μl, 2.31 mmol, 0.5 equiv). The reaction mixture was stirred at -20^{0}C for 12 h until the disappearance of the donor on TLC, then quenched with triethylamine (81µl, 0.81 mmol, 0.75 equiv) and warmed to room temperature. The mixture was diluted with dichloromethane, filtered through celite, washed with 20% aqueous $Na_2S_2O_3$ solution, dried over Na_2SO_4, and

concentrated under reduced pressure. The residue was purified by column chromatography on silica gel eluting with Ethylacetate/Hexane (1:1) system to afford the compound **18** (2 gm, 67%). **α-isomer ^{1}H-NMR** (400 MHz, $CDCl_3$) δ 5.69 (dd, *J* = 7.5, 1.5 Hz, 1H), 5.33 (ddd, *J* = 7.5, 6.2, 2.8 Hz, 1H), 4.77 (dd, *J* = 9.5, 1.5 Hz, 1H), 4.42 (dd, *J* = 12.3, 2.8 Hz, 1H), 4.26-4.05 (m, 6H), 3.91-3.83 (m, 4H), 3.02 (dd, *J* = 12.2, 4.0 Hz, 1H), 2.74 (t, *J* = 12.7 Hz, 1H), 2.51 (s, 3H), 2.16 (s, 3H), 2.12 (s, 3H), 2.05 (s, 3H), 1.74-1.64 (m, 4H), 1.43 (dq, *J* = 14.7, 7.4 Hz, 4H), 0.95 (t, *J* = 7.4 Hz, 6H). **^{13}C-NMR** (400 MHz, $CDCl_3$) δ 171.84, 170.62, 169.99, 169.89, 167.30, 167.23, 153.52, 98.22, 98.15, 74.19, 71.48, 69.81, 68.16, 68.10, 68.05, 67.99, 62.51, 58.32, 53.46, 35.91, 35.87, 32.14, 32.10, 32.07, 24.63, 20.96, 20.79, 20.74, 18.63, 18.60, 13.56. HRMS m/z calc'd for $C_{27}H_{42}NO_{16}P$ (M+Na) 690.2139; found: 690.2134.

Glycosylation of Donor and Acceptors:

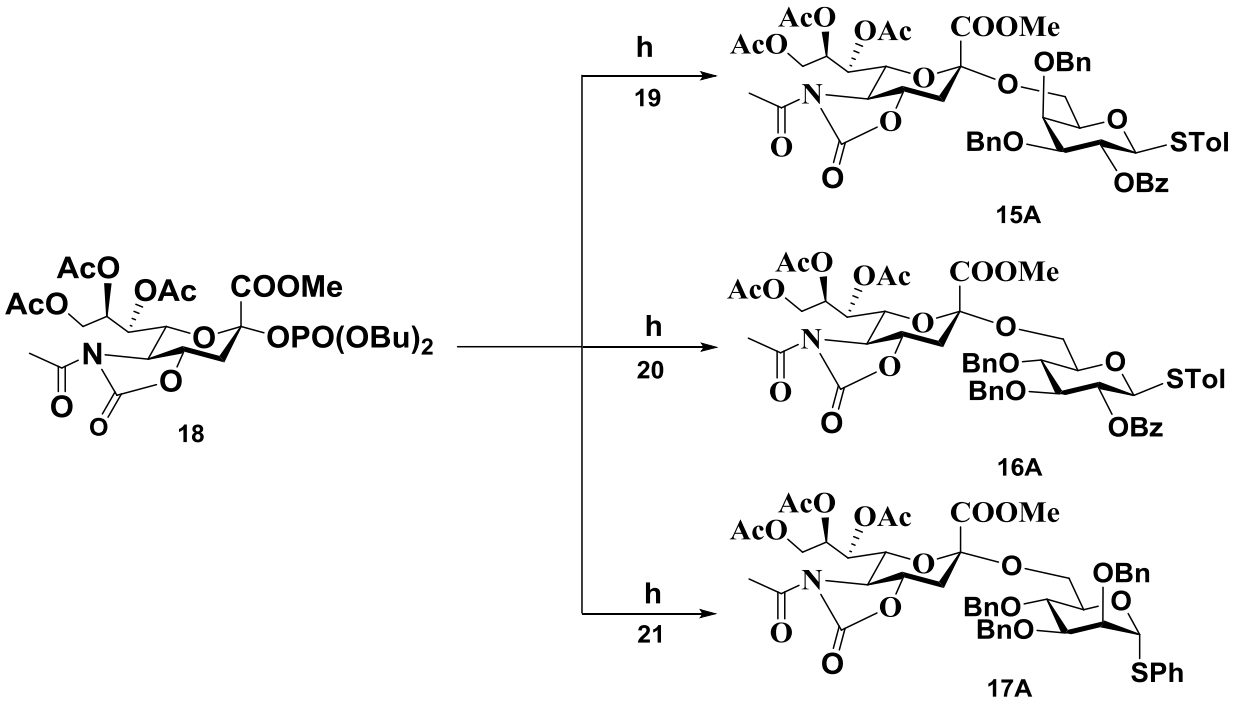

Scheme 9. ***Reagents and condition:*** h) TMSOTf, M.S 4Å, DCM, -78^{0}C.

General procedure of glycosylation The mixture of donor **18** (0.899 mmol, 1eq), acceptor(0.674 mmol, 0.75 eq) and activated 4Å powdered molecular sieves (1.5 gm) in anhydrous dichloromethane(10 ml) and was stirred for 3h at room temperature under an argon atmosphere, and then cooled to -78^{0}C followed by addition of TMSOTf (165 μl, 0.899 mmol, 1

equiv). The reaction mixture was stirred at -78^{0}C for 1-3 h until the disappearance of the donor on TLC, then quenched with triethylamine warmed to room temperature. The mixture was diluted with dichloromethane, filtered through Celite, washed brine solution, dried over Na_2SO_4, and concentrated under reduced pressure. The residue was purified by column chromatography on silica gel eluting with Ethylacetate/Hexane (1:1) system to afford the sialic acid disaccharide analogues.

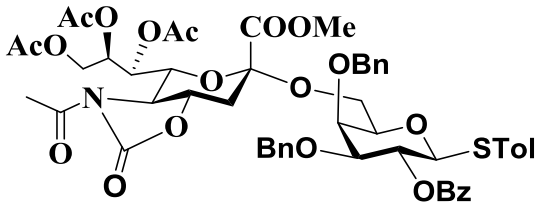

Compound 15A According to general procedure donor **18** and acceptor **19** to yield as white solid (700 mg, 75%). **^{1}H-NMR** (400 MHz, $CDCl_3$) δ 8.05 (d, *J* = 7.6 Hz, 2H), 7.61 (t, *J* = 7.4 Hz, 1H), 7.48 (t, *J* = 7.6 Hz, 2H), 7.41 (d, *J* = 7.9 Hz, 2H), 7.33 (dt, *J* = 7.8, 3.6 Hz, 5H), 7.24 – 7.14 (m, 5H), 7.03 (d, *J* = 7.8 Hz, 2H), 5.66 (t, *J* = 9.7 Hz, 1H), 5.60 (d, *J* = 7.0 Hz, 1H), 5.46 (ddd, *J* = 8.7, 6.7, 3.1, Hz, 1H), 5.02 (d, *J* = 11.3 Hz, 1H), 4.77 (d, *J* = 11.3 Hz, 1H), 4.71 (*J* = 9.4 Hz, 1H), 4.66 (d, *J* = 11.3 Hz, 1H), 4.62 (d, *J* = 9.4 Hz, 1H), 4.54 (d, *J* = 12.2 Hz, 1H), 4.42 (dd, *J* = 12.2, 2.3 Hz, 1H), 4.13-4.04 (m, 2H), 4.04-3.98 (m, 2H), 3.79-3.71(m, 3H), 3.69 (s, 3H), 3.66-6.59 (m, 1H), 2.90 (dd, *J* = 12.0, 3.3 Hz, 1H), 2.52 (s, 3H), 2.31 (s, 3H), 2.15(s, 3H), 2.09 (t, *J* = 12.5 Hz, 1H), 2.09 (s, 3H), 2.03 (s, 3H). **^{13}C-NMR** (400 MHz, $CDCl_3$) δ 172.04, 170.79, 170.17, 169.99, 168.28, 165.21, 153.68, 138.61, 137.99, 137.60, 133.01, 132.64, 130.17, 129.89, 129.87, 129.69, 129.44, 129.42, 128.33, 128.32, 128.29, 128.27, 128.16, 128.14, 127.66, 127.64, 127.62, 127.55, 127.58, 127.53, 127.35, 99.21, 86.85, 81.23, 76.85, 75.86, 74.93, 74.07, 72.65, 72.02, 71.95, 70.41, 69.51, 63.85, 62.95, 59.11, 53.13, 36.43, 24.73, 21.15, 21.11, 20.87, 20.77. HRMS m/z calc'd for $C_{53}H_{57}NO_{18}S$ (M+Na) 1050.3193; found: 1050.3191.

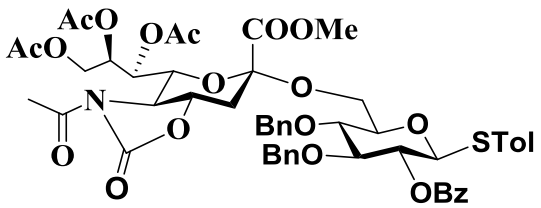

Compound 16A According to general procedure donor **18** and acceptor **20** gave as white solid(765 mg, 83%). **^{1}H-NMR** (400 MHz, $CDCl_3$) δ 8.04 (t, *J* = 6.3 Hz, 2H), 7.60 (t, *J* = 7.4 Hz, 1H), 7.47 (t, *J* = 7.7 Hz, 2H), 7.40 (t, *J* = 7.2 Hz, 2H), 7.38-7.30 (m, 5H), 7.17-7.06 (m, 7H), 5.65 (dd, *J* = 8.6, 1.4 Hz, 1H), 5.51 (ddd, *J* = 8.8, 6.3, 2.8 Hz, 1H), 5.22 (dd, *J* = 9.9, 9.2 Hz, 1H), 4.80 (d, *J* = 10.5 Hz, 1H), 4.78 (d, *J* = 10.5 Hz, 1H), 4.73-4.65 (m, 3H), 4.64-4.60 (m, 1H), 4.38 (dd, *J* = 12.4, 2.8 Hz, 1H), 4.24 (dd, *J* = 11.0, 4.5 Hz, 1H), 4.08-4.00 (m, 2H), 3.82 (m, 4H), 3.77 (m, 1H), 3.71 (t, *J* = 10.2 Hz, 2H), 3.58 (dd, *J* = 8.6, 3.4 Hz, 1H), 3.01 (dd, *J* = 12.0, 3.4 Hz, 1H), 2.52 (s, 3H), 2.35 (s, 3H), 2.17 (s, 3H), 2.13 (t, *J* = 12.3 Hz, 1H), 2.07 (s, 3H), 1.87 (s, 3H). **^{13}C-NMR** (400 MHz, $CDCl_3$) δ 171.86, 170.65, 170.05, 170.03, 168.37, 165.16, 153.66, 138.11, 138.01, 137.70, 133.16, 132.90, 132.88, 129.92, 129.85, 129.83, 129.48, 129.46, 129.44, 129.31, 128.46, 128.43, 128.41, 128.24, 128.22, 128.20, 128.18, 127.99, 127.96, 127.95, 127.63, 99.31, 86.34, 84.05, 78.01, 77.27, 75.31, 75.24, 75.11, 75.00, 72.24, 71.54, 68.61, 64.53, 62.92, 59.18, 53.09, 36.68, 24.70, 21.20, 21.16, 20.80, 20.62. HRMS m/z calc'd for $C_{53}H_{57}NO_{18}S$ (M+Na) 1050.3193; found: 1050.3195.

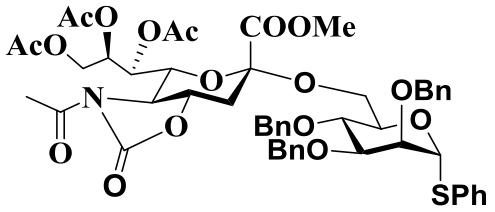

Compound 17A: According to general procedure donor **18** and acceptor **21** to afford as white solid(830 mg, 90%) **^{1}H NMR** (400 MHz, $CDCl_3$) δ 7.49 (dd, *J* = 6.4, 3.0 Hz, 2H), 7.33 (m, 18H), 5.62 (dd, *J* = 8.3, 1.5 Hz, 1H), 5.55 (d, *J* = 1Hz, 1H), 5.47 (ddd, *J* = 8.5, 6.0, 2.9 Hz, 1H), 4.93 (d, *J* = 10.4 Hz, 1H), 4.78(d, *J* = 10.4 Hz, 1H), 4.70 (dd, *J* = 13.1, 6.9 Hz, 2H), 4.67-4.60 (m, 3H), 4.30 (dt, *J* = 9.1, 6.3 Hz, 2H), 4.21 (dd, *J* = 10.8, 6.6 Hz, 1H), 4.07-3.99 (m, 3H), 3.96 (t, *J* = 9.3 Hz, 1H), 3.88 (dd, *J* = 9.3, 3.0 Hz, 1H), 3.73-3.68 (m, 2H), 3.68 (s, 3H), 2.92 (dd, *J* = 12.0, 3.5 Hz, 1H), 2.51 (s, 3H), 2.14 (t, *J* = 12.6 Hz, 1H), 2.12 (s, 3H), 2.02 (s, 3H), 2.01 (s, 3H). **^{13}C-NMR** (400 MHz, $CDCl_3$) δ 171.85, 170.60, 169.99, 169.82, 168.71, 153.74, 138.63, 138.13, 137.85, 133.95, 132.54, 132.52, 128.92, 128.43, 128.41 128.40, 128.39, 128.37, 128.30, 128.28 128.13, 128.10, 127.90, 127.88, 127.83, 127.81, 127.80, 127.79, 127.72, 127.70, 99.41, 85.73, 80.01, 76.13, 75.34, 75.14, 75.05, 74.77, 72.21, 72.13, 71.93, 71.55, 68.66, 65.43, 62.76, 59.16,

52.90, 36.48, 24.72, 21.12, 20.86, 20.77. HRMS m/z calc'd for $C_{52}H_{57}NO_{17}SNa$ (M+Na). 1022.3244; found: 1022.3245.

Synthesis of trisaccharide from disaccharide:

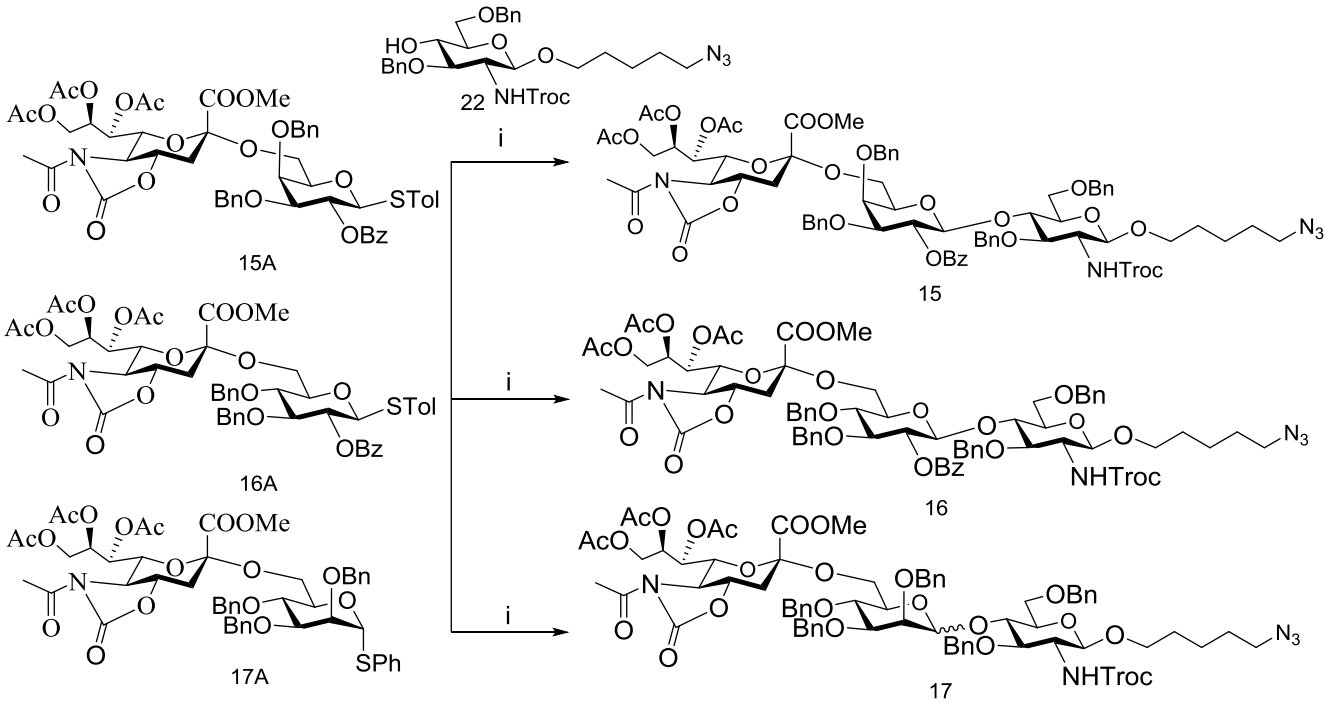

Scheme 10. ***Reagents and condition:*** i) NIS/TfOH, M.S. 4Å, DCM or ACN, -40^{0}C.

General Glycosylation Procedure : A solution of donor **15A/16A/17A** (500 mg, 0.488 mmol, 1.0 equiv), acceptor 22 (0.585 mmol, 1.2 equiv), and activated 4Å powdered molecular sieves(976 mg, 2.0 g/mmol) in anhydrous dichloromethane (10 ml) was stirred overnight under an argon atmosphere, and then cooled to -40^{0}C followed by addition of NIS (109 mg, 0.488 mmol, 1.0 equiv) and TfOH (6.46 μl, 0.048 mmol, 0.1 equiv) dissolved in ether. The reaction mixture was stirred at -40^{0}C for 20 min to 2 h until the disappearance of the donor on TLC and warmed to room temperature. The mixture was diluted with dichloromethane, filtered through celite, washed with sat.$Na_2S_2O_3$ (3:1) 20 ml solution, dried over Na_2SO_4, and concentrated under reduced pressure. The residue was purified by column chromatography on silica gel eluting with Ethylacetate/Hexane system to afford the sialic acid trisachharide.

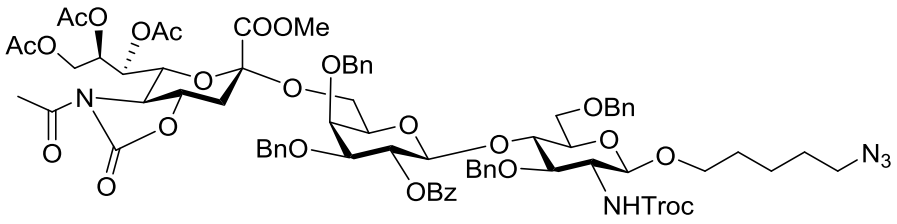

Compound 15 Synthesized from donor **15A** and acceptor **22** by following general glycosylation procedure to afford as white solid (430 mg, 57%). **^{1}H-NMR** (400 MHz, $CDCl_3$) δ 7.99 (d, *J* = 7.7 Hz, 2H), 7.61(t, *J* = 7.4 Hz, 1H), 7.47 (t, *J* = 7.7 Hz, 2H), 7.39 (d, *J* = 7.4 Hz, 2H), 7.37-7.33 (m, 3H), 7.33-7.22 (m, 10H), 7.21-7.14 (m, 5H), 5.70-5.63 (m, 1H), 5.57 (s, 1H), 5.48 (d, *J* = 6.5 Hz, 1H), 5.39 (td, *J* = 6.9, 2.3 Hz, 1H), 5.09 (d, *J* = 11.4 Hz, 1H), 4.97 (d, *J* = 11.1 Hz, 1H), 4.75-4.63 (m, 5H), 4.60 (d, *J* = 12.2 Hz, 1H), 4.52 (d, *J* = 12.2 Hz, 2H), 4.47-4.39 (m, 2H), 4.33 (d, *J* = 12.2 Hz, 2H), 4.05 (dd, *J* = 12.2, 7.2 Hz, 1H), 4.01-3.91 (m, 4H), 3.87 (d, *J* = 6.3 Hz, 2H), 3.76 (m, 2H), 3.68-3.65 (m, 1H), 3.64 (s, 3H), 3.60 (d, *J* = 3.1 Hz 1H), 3.56 (dd, *J* = 10.1, 2.1 Hz, 1H), 3.45 (dd, *J* = 12.9, 7.1 Hz, 1H), 3.34 (m, 3H), 3.24 (t, *J* = 6.9 Hz, 2H), 2.73 (dd, *J* = 12.3, 3.7 Hz, 1H), 2.51 (s, 3H), 2.17 (t, *J* = 12.6, Hz, 1H), 2.13 (s, 3H), 2.03 (s, 3H), 2.02 (s, 3H), 1.62-1.50 (m, 4H), 1.38 (m, 2H). **^{13}C-NMR** (400 MHz, $CDCl_3$) δ 172.19, 170.85, 170.31, 169.85, 168.09, 165.17, 153.98, 153.80, 138.75, 138.44, 138.29, 137.57, 133.20, 133.17, 135.15, 129.87, 129.78, 129.76, 129.77, 128.46, 128.44, 128.42, 128.39, 128.40, 128.37, 128.36, 128.34, 128.32, 128.30, 128.03, 127.75, 127.71, 127.69, 127.68, 127.63, 127.60, 127.52, 127.32, 100.50, 99.75, 99.23, 95.65, 79.82, 77.24 , 76.03, 75.57, 74.91, 74.64, 74.35, 74.26, 74.15, 73.45, 73.30, 72.80, 72.40, 72.16, 71.89, 69.96, 69.34, 68.47, 63.86, 62.97, 58.83, 57.20, 53.12, 51.31, 35.54, 29.00, 28.53, 24.74, 23.15, 21.13, 20.84, 20.73. HRMS m/z calc'd for $C_{74}H_{84}Cl_3N_5O_{25}$ (M+Na). 1570.4418; found: 1570.4411.

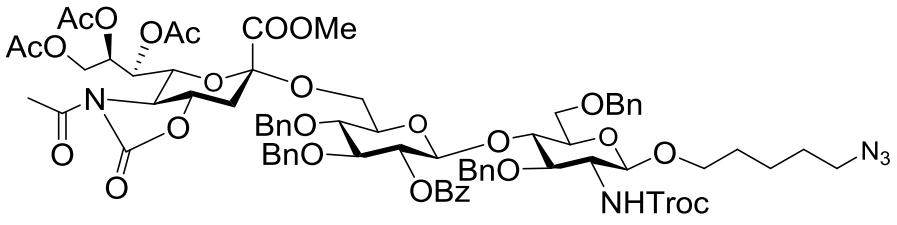

Compound 16 Synthesized from donor **16A** and acceptor **22** by following general glycosylation procedure to afford as white solid (340 mg, 45%). **^{1}H-NMR** (400 MHz, $CDCl_3$) δ 7.93 (d, *J* =

7.4 Hz 2H), 7.59 (t, *J* = 7.4 Hz, 1H), 7.48-7.30 (m, 17H), 7.18-7.05 (m, 5H), 5.59 (dd, *J* = 9.0, 1.4 Hz, 1H), 5.48 (ddd, *J* = 8.9, 6.2, 2.7 Hz, 1H), 5.26 (dd, *J* = 9.4, 8.2 Hz, 1H), 4.98-4.88 (m, 4H), 4.80 (d, *J* = 12.9 Hz, 2H), 4.75 (d, *J* = 10.5 Hz, 1H), 4.71 (d, *J* = 3.4 Hz, 2H), 4.68(s, 2H), 4.66 (d, *J* = 1.4 Hz, 1H), 4.58 (d, *J* = 11.2 Hz, 2H), 4.40 (d, *J* = 12.2 Hz, 2H), 4.33 (dd, *J* = 12.2, 2.7 Hz, 1H), 4.30-4.25 (m, 3H), 4.01 (dd, *J* = 11.5, 6.2 Hz , 2H), 3.95 (dd, *J* = 12.5, 6.2 Hz, 2H), 3.86 (t, *J* = 9.4 Hz, 1H), 3.73(s, 3H), 3.68-3.62 (m, 3H), 3.56-3.47(m, 4H), 3.25 (m, 4H), 2.73 (dd, *J* = 12.0, 3.3 Hz, 1H), 2.49 (s, 3H), 2.18 (s, 3H), 2.07 (s, 3H), 2.07 (t, *J* = 12.3 Hz, 1H), 1.60-1.48 (m, 4H), 1.41-1.26 (m, 2H). **^{13}C-NMR** (400 MHz, $CDCl_3$) δ 171.90, 170.69, 170.00, 169.94, 168.38, 165.03, 154.03, 153.65, 138.92, 138.17, 137.94, 137.84, 133.24, 129.71, 129.63, 128.61, 128.48, 128.31, 128.27, 128.20, 128.15, 128.07, 127.96, 127.71, 127.83, 127.68, 127.58, 127.56, 127.53, 100.93, 99.46, 99.26, 95.70, 82.17, 78.27, 77.23, 75.72, 75.14, 74.95, 74.92, 74.53, 74.45, 74.09, 73.85, 73.65, 73.48, 71.39, 69.18, 68.32, 67.94, 64.37, 63.96, 62.93, 59.11, 57.11, 53.11, 51.30, 36.52, 28.96, 28.51, 24.67, 23.14, 21.18, 20.79, 20.34. HRMS m/z calc'd for $C_{74}H_{84}Cl_3N_5O_{25}$ (M+Na). 1570.4418; found: 1570.4411.

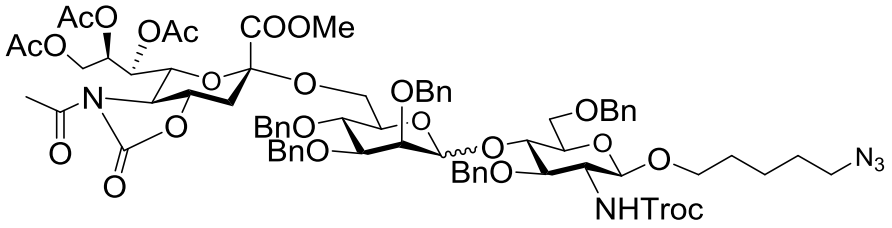

Compound 17 Synthesized from donor **17A** (0.502 mmol)and acceptor **22** (0.603 mmol) by following general glycosylation procedure in DCM:ACN (1:1) solvent to afford as white solid (410 mg, 53%); **α:β(1:3). β-isomer ^{1}H-NMR** (500 MHz, $CDCl_3$) δ 7.47-7.21(m, 25H) 5.65 (dd, *J* = 8.6, 1.4 Hz, 1H), 5.50 (ddd, *J* = 10.5, 5.3, 2.4 Hz, 1H), 5.35 (m, 1H), 5.24 (d, *J* = 7.0 Hz, 1H), 4.90 (d, *J* = 10.4 Hz, 1H), 4.83-4.87 (m, 1H), 4.76 (d, *J* = 7.8 Hz, 2H), 4.73 (d, *J* = 3.9 Hz, 1H), 4.70 (d, *J* = 3.2 Hz, 1H), 4.68 (d, *J* = 1.8 Hz, 1H), 4.64 (d, *J* = 2.9 Hz, 1H), 4.61 (s, 1H), 4.58 (t, *J* = 10.6 Hz, 1H), 4.46 (d, *J* = 12.1 Hz, 1H), 4.35 (d, *J* = 12.1 Hz, 1H), 4.31 (dd, *J* = 12.4, 2.9 Hz, 1H), 4.29 (d, *J* = 2.8 Hz, 1H), 4.23 (dt, *J* = 7.5, 2.8 Hz, 1H), 4.04 (dd, *J* = 6.2, 3.6 Hz, 1H), 4.02-3.96 (m, 2H), 3.94 (dd, *J* = 9.3, 4.2 Hz, 2H), 3.91-3.80 (m, 4H), 3.79-3.68 (m, 3H), 3.64 (d, *J* = 9.8 Hz, 1H), 3.61 (s, 3H), 3.58 (d, *J* = 9.8, 1H), 3.55-3.49 (m, 1H), 3.45-3.38 (m, 1H), 3.30 (t, *J* = 6.9 Hz, 2H), 2.93 (dd, *J* = 7.3, 1.8 Hz, 1H), 2.88 (dd, *J* = 12.0, 3.5 Hz, 1H),

2.54 (s, 3H), 2.15 (s, 3H), 2.07 (t, *J* = 12.5 Hz, 1H), 2.05 (s, 3H), 1.98 (s, 3H), 1.69-1.59 (m, 4H) 1.45-1.41 (m, 2H). **^{13}C-NMR** (400 MHz, $CDCl_3$) δ 171.65, 170.43, 169.78, 169.55, 168.44, 153.74, 153.53, 138.41, 138.19, 138.13, 137.96, 137.59, 137.43, 133.77, 132.36, 131.69, 128.76, 128.74, 128.72, 128.70, 128.66, 128.64, 128.60, 128.59, 128.32, 128.16, 127.97, 127.80, 127.72, 127.60, 127.54, 127.46, 127.38, 127.25, 127.13, 127.08, 126.85, 101.46, 99.65, 99.20, 95.30, 85.55, 80.74, 79.35, 75.66, 75.07, 74.92, 74.75, 74.52, 74.38, 74.16, 73.60, 73.09, 72.18, 71.99, 71.27, 69.54, 69.26, 68.31, 65.41, 65.24, 62.52, 58.93, 57.63, 52.66, 51.14, 36.34, 29.18, 28.87, 24.53, 23.23, 22.52, 20.95, 20.58. HRMS m/z calc'd for $C_{74}H_{86}Cl_3N_5O_{24}$ (M+Na). 1556.4626; found: 1556.4624.

Global Deprotection of Sialoside:

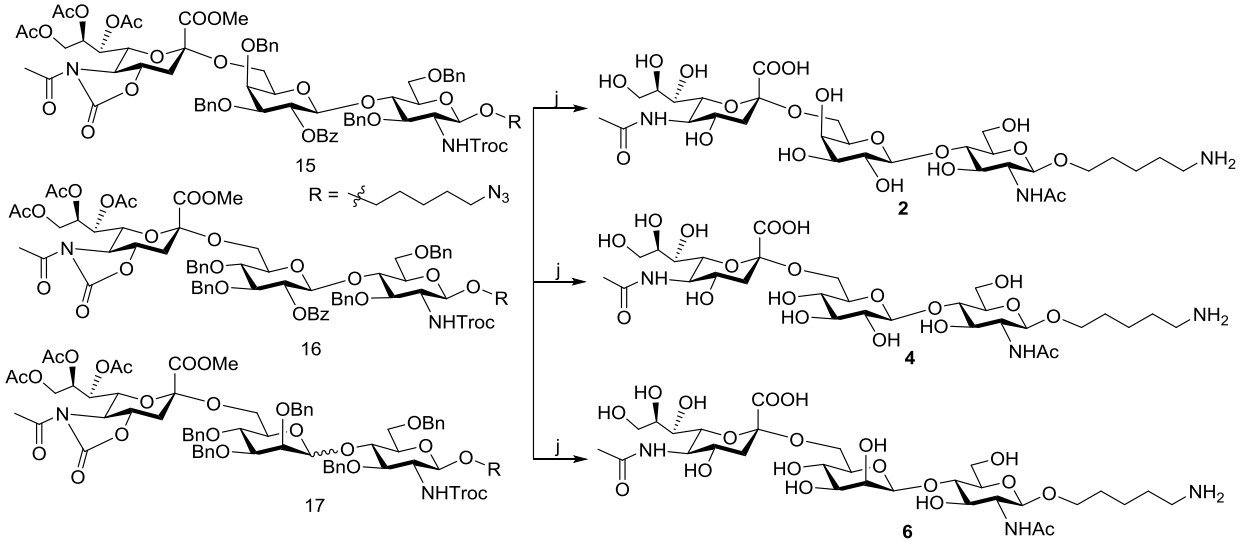

Scheme 11. ***Reagents and Conditions:*** j) i) LiOH, EtOH:H_2O (3:1), 80^0C, 12h; (ii) $NaHCO_3$, Ac_2O, H_2O, rt; (iii) H_2/Pd $(OH)_2$, MeOH:H_2O (1:1).

General Deprotection Procedure: Oligosachharide (1eq) in ethanol water (3:1) 5ml at room temperature. After stirring at 80^0C for 12h, the reaction mixture cooled to room temperature and carefully neutralized by IR-120H^+ resin to pH-7,diluted with methanol, filtered and concentrated. Crude residue was dissolved in water and $NaHCO_3$ (15 eq) were added to it. Cooled the reaction mixture to 0^0C and Acetic-anhydride (10 eq) was added. The reaction were monitored by TLC (ethylacetate:methanol:water7:2:1), after 3h, LiOH (10 eq) were added and stirred for another 5-6h at room temperature, then reaction mixture carefully neutralized by IR-120H^+resin to pH-7, diluted concentrated and purified by reverse-phase column chromatography (Bond Elu-C18). The $Pd(OH)_2$ (1 mmole) was added to the above residue in methanol water (1:1) 4ml. The reaction mixture was hydrogenalysed under H_2 atmosphere for 12h, filtered and concentrated.

The residue was purified by reverse phase column chromatography (Bond Elu-C18) to give deprotected sialic acid analogues.

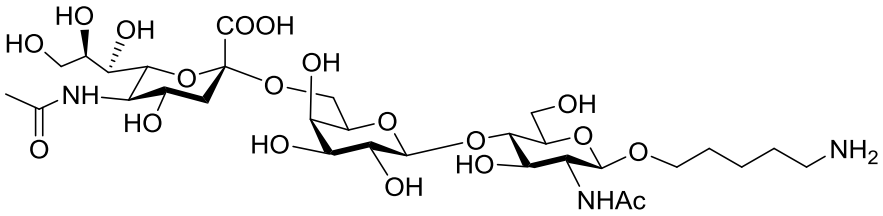

Compound 2 Synthesized from **15** by following general deprotection protocol to afford white solid (50 mg, 50%). **^{1}H-NMR** (400 MHz, D_2O) δ 4.47 (d, *J* = 7.3 Hz, 1H), 4.36 (d, *J* = 7.9 Hz, 1H), 3.97-3.87 (m, 3H), 3.86-3.79 (m, 4H), 3.78-3.67 (m, 4H), 3.64 (dd, *J* = 6.3, 3.9 Hz, 3H), 3.61-3.51 (m, 4H), 3.46 (m, 3H), 2.96-2.88 (m, 2H), 2.58 (dd, *J* = 12.4, 4.7 Hz, 1H), 1.97 (s, 3H), 1.94 (s, 3H), 1.66-1.57 (m, 3H), 1.56-1.48 (m, 2H), 1.37-1.29 (m, 2H). **^{13}C-NMR** (400 MHz, D_2O) δ 174.68, 174.42, 173.50, 103.45, 100.91, 100.13, 80.74, 74.46, 73.68, 72.53, 72.43, 72.41, 71.69, 70.71, 68.39, 68.35, 68.21, 63.35, 62.64, 60.36, 54.87, 51.87, 42.57, 40.06, 39.33, 28.04, 26.34, 25.01, 22.27, 22.03. HRMS m/z calc'd for $C_{30}H_{51}N_5O_{19}$(M+H). 760.3351; found: 760.3358.

2

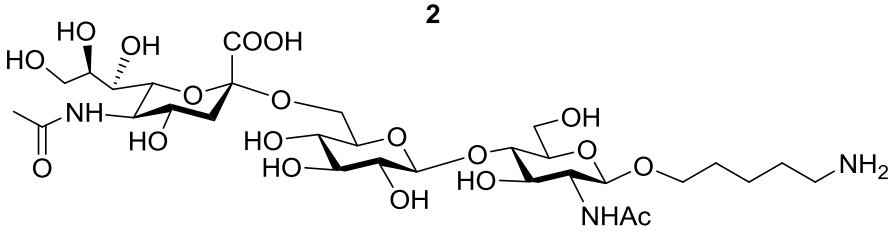

Compound 4 Synthesized from **16** by following general deprotection protocol to afford white solid (40 mg, 35%). **^{1}H-NMR** (400 MHz, D_2O) δ 4.43 (d, *J* = 8.2 Hz, 1H), 4.35 (d, *J* = 8.0 Hz, 1H), 3.92-3.87 (m, 1H), 3.85-3.74 (m, 5H), 3.71 (dd, *J* = 10.0, 3.4 Hz, 1H), 3.67-3.56 (m, 4H), 3.56-3.48 (m, 4H), 3.42 (d, *J* = 9.2 Hz, 2H), 3.39-3.34 (m, 1H), 3.03-2.96 (m, 2H), 2.93 (dd, *J* = 7.8, 5.3 Hz, 2H), 2.69 (dd, *J* = 7.9, 4.8 Hz, 1H), 2.60 (dd, *J* = 12.3, 4.3 Hz, 1H), 1.96 (s, 3H), 1.95 (s, 3H), 1.61-1.50 (m, 4H), 1.49-1.45 (m, 1H), 1.35 -1.21(m, 2H). **^{13}C-NMR** (400 MHz, D_2O) δ 174.94, 174.39, 173.44, 102.96, 100.92, 100.01, 80.69, 75.35, 74.44, 74.24, 72.96, 72.48, 71.68, 70.00, 69.78, 68.32, 68.18, 63.19, 62.59, 60.28, 54.92, 51.85, 42.72, 39.94, 39.04, 28.06,

25.27, 23.04 , 22.24, 22.01. HRMS m/z calc'd for $C_{30}H_{51}N_5O_{19}$(M+H). 760.3351; found: 760.3358.

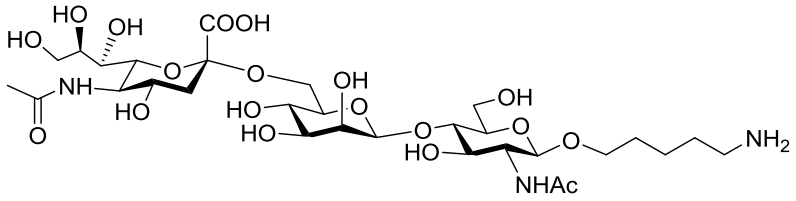

Compoun6 Synthesized from **17** by following general deprotection protocol to afford white solid(35 mg, 30%). **^{1}H-NMR** (400 MHz, D_2O) δ 5.06 (d, *J* = 0.8 Hz, 1H), 4.37 (d, *J* = 8.2 Hz, 1H), 3.90 (m, 1H), 3.82 (dd, *J* = 10.7, 4.4 Hz, 2H), 3.79-3.72 (m, 2H), 3.73 (d , *J* = 2.4 Hz, 1H), 3.70 (d, *J* = 3.5 Hz, 1H), 3.66 (dd, *J* = 7.2, 2.2 Hz, 1H), 3.63 (d, *J* = 3.7 Hz, 2H), 3.59 (d, *J* = 1.6 Hz, 2H), 3.57 (d, *J* = 1.6 Hz, 2H), 3.55 (d, *J* = 4.7 Hz, 2H), 3.53 (d, *J* = 7.6 Hz, 2H), 3.51-3.48 (m, 2H), 3.46 (d, *J* = 9.0 Hz, 2H), 2.88-2.83 2.86 (m, 1H), 2.62 (dd, *J* = 12.5, 4.7 Hz, 1H), 1.91(s, 6H), 1.63-1.50 (m, 4H), 1.50-1.45 (m, 1H), 1.35-1.22 (m, 2H). **^{13}C-NMR** (400 MHz, D_2O) δ 181.55, 175.05, 173.58, 101.70, 100.96, 100.17, 74.64, 74.03, 72.61, 72.34, 71.61, 70.60, 70.20, 69.90, 68.26, 66.61, 66.53, 63.31, 62.62, 60.89, 55.74, 51.89, 51.91, 40.08, 39.36, 27.94, 26.35, 26.32, 22.06, 22.01. HRMS m/z calc'd for $C_{30}H_{51}N_5O_{19}$(M+H). 760.3351; found: 760.3344.

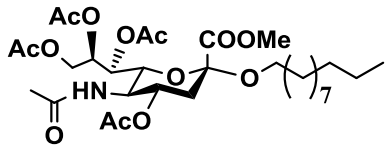

Methyl (undecyl 5-acetamido-4,7,8,9-tetra-*O*-acetyl-3,5-dideoxy-D-*glycero*- -D*galacto*-2-nonulopyranosid)onate(33)

Thiophenyl-sialic acid glycoside (300 mg, 0.51 mmol) and 1-undecanol (177 mg, 1.02 mmol) were dissolved in anhydrous dichloromethane (10.0 mL) under an atomosphere of argon; 4 Å molecular sieves (500 mg) was added. The temperature was cooled to -40 °C and *N*-iodosuccinimide (172 mg, 0.77 mmol) and catalytic amount trifluoromethanesulfonic acid (15 µL, 0.15 mmol)of was added. After stirring for 3 h, the reaction mixture was diluted with DCM (20 mL) and filtered through a pad of celite. After filtration, the organic solution was washed

with a 1:1 mixture of 10% $Na_2S_2O_3$ and sat. $NaHCO_3$, dried and evaporated. The residue was purified by column chromatography on silica gel using DCM : MeOH (95: 5) yield (178 mg , 53.6%) of compound 3 (α/β 3/1) and further purified by a mixture of acetone : CH_2Cl_2 (10 : 90) as eluent to afford sequentially the pure 3 (90.8 mg, yield 28%). R_f = 0.5 (DCM : MeOH, 96: 4); $[\alpha]_D^{r.t}$ = +26.1 (c = 1.0, $CHCl_3$); ^{1}H-NMR (400 MHz, $CDCl_3$): δ 5.38-5.20 (m, 3H), 4.83-4.54 (m 1H), 4.31 (dd, 1H, *J* = 12.4, 2.6 Hz), 4.13-4.01 (m, 3H), 3.87 (dd, 1H, *J* = 9.3, 6.6 Hz), 3.73 (s, 3H), 3.29 (m, 1H), 2.45 (dd, 1H, *J* = 12.8, 4.8 Hz), 2.13 (s, 3H), 2.12 (s, 3H), 2.02 (s, 3H), 2.01 (s, 3H), 1.93 (dd, 1H, *J* = 12.6, 12.6 Hz), 1.86 (s, 3H), 1.46- 1.55 (m, 2H), 1.19-1.34 (m, 16H), 0.86 (t, 3H, *J* = 6.6 Hz). ^{13}C-NMR ($CDCl_3$, 100 MHz): δ 175.0, 174.6, 173.2, 172.1, 169.6, 98.7, 75.1, 72.3, 71.9, 71.5, 70.1 68.8, 67.5, 65.1, 63.4, 52.9, 41.4, 32.1, 29.7, 29.6, 25.9, 23.2 22.7, 14.1. Maldi-ToF m/z calc'd for $C_{31}H_{51}NO_{13}Na$ ($M+Na^+$): 668.3256; found: 668.3411.

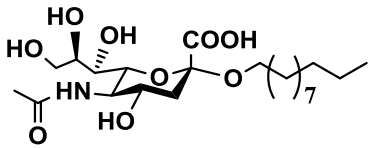

Undecyl 5-acetamido-3,5-dideoxy-D-*glycero*-D-*galacto*-2-nonulopyranosylonic acid (34)

Methyl (undecyl 5-acetamido-4,7,8,9-tetra-*O*-acetyl-3,5-dideoxy-D-*glycero*-_-D*galacto*-2-nonulopyranosid)onate (100.0 mg, 0.12 mmol) was dissolved in methanol (10 mL), and a sodium methoxide (25 mg) was added. The mixture was stirred for 30 minutes and neutralized with amberlite H^+ resin. The residue was finally purified by column chromatography using a gradient of DCM:MeOH (1:1) as eluent to afford the desired 1 as a white solid (75 mg, 93% yield).). $[\alpha]_D^{r.t}$ = +11.9 (c = 1.0, H_2O); ^{1}H-NMR (400 MHz, CD_3OD): δ 3.87-3.83 (m, 2H); 3.79-3.71 (m, 3H); 3.71-3.61(m, 3H); 3.6-3.4 (m, 2H); 2.74 (dd, 1H, *J* = 4.1, 12.0 Hz); 2.02 (s, 3H); 1.48-1.56 (m, 2H); 1.17-1.38 (m, 16H); 0.87 (t, 3H, *J* = 6.3 Hz). ^{13}C NMR (CD_3OD, 100 MHz): 174.6, 98.8, 77.3, 77.1. 75.4, 72.6, 72.2, 71.6, 71.2, 53.3, 40.80, 33.1, 30.1, 29.9, 25.7, 22.6, 13.5. HRMS m/z calc'd for $C_{22}H_{41}NO_9$ $(M-H)^-$: 462.2691; found:462.2698.

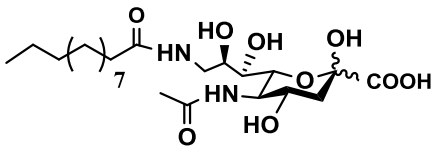

5-Acetamido-9- (dodecanyl) -3,5,9-trideoxy-D-glyceo-D-galacto-2-nonulosonic acid (38).

Dodecanoic acid (300 mg, 1.5 mmol) in N-hydroxysuccinimide (172 mg, 1.7 mmol) and DMAP (183 mg, 1.7 mmol) were dissolved in DCM (10 mL) and stirred at RT. After stirring for 4 h, the reaction mixture was filtered to remove urea and purified by colum chromatography PE : EA (1:1) to yield dodcanoic acid active ester. This was dissolved in dioxane (7 mL) and mixed with 5-Acetamido-9-amino-3,5,9-trideoxy-D-glyceo-D-galacto-2-nonulosonic acid **6** (120 mg, 0.5 mmol) with pH maintained between 8-9 with sodium biocarbohydrate solution. The mixture was stirred at RT for 48 h. The solvent was concentrated and the residue was purified by flash chromatography (DCM:MeOH 1:1) to afford the white solid (85 mg , 38.6%).$[\alpha]_D^{r.t}$ = -2.3 (c = 1.0, H_2O); ^{1}H-NMR (400 MHz, CD_3OD): δ 3.98-3.80 (m, 4H); 3.71 (t, 1H, *J* = 4.0 Hz); 3.56 (dd, 1H, *J* = 4.4 Hz); 3.15(dd, 1H, *J* = 4.0 Hz); 2.18 (t, 2H, *J* = 8.0 Hz); 2.11 (dd, 1H, *J* = 4.0, 2.8 Hz); 1.97 (s, 3H), 1.82 (t, 1H, *J* = 8.8 Hz), 1.59-1.54 (m, 2H), 1.37-1.18 (m, 16H) 0.87 (t, 3H, *J* = 10.0 Hz); ^{13}C NMR (CD_3OD, 100 MHz): 176.6, 174.7, 96.8, 71.3, 71.1. 70.4, 69.6, 53.3, 43.8, 40.4, 36.1, 31.1, 29.8, 29.5, 25.7, 23.7, 22.6, 13.5. HRMS m/z calc'd for $C_{23}H_{42}N_2O_9$ $(M-H)^+$: 488.2890; found:488.2808.

2.8 References

1. (a) A. Varki, R. D. Cummings, J. D. Esko, H. H. Freeze, P. Stanley, C. R. Bertozzi, G. W. Hart, M. E. Etzler, *Essentials of Glycobiology.*, **2009**, 2nd edition, Cold Spring Harbor Press, 199 (b) X. Chen, A. Varki, *ACS Chem. Biol.*, 2010, **5**, 164; (c) D. B. Werz, R. Ranzinger, S. Herget, A. Adibekian, C.-W. von der Lieth, P. H. Seeberger, *ACS Chem. Biol.*, **2007**, 2, 685.
2. (a) T. Aganta, A. Varki, *Chem. Rev.*, **2002**, 102, 439; (b) X. Chen, A. Varki, *ACS Chem. Biol.*, **2010**, 5, 163.
3. (a) K. Furukawa, K. Hamamura, W. Aixinjueluo and K. Furukawa, *Ann. N. Y. Acad. Sci.*, **2006**, 1086, 185; (b) I. Bucior M. M. Burger, *Curr. Opin. Struct. Biol*., **2004**, 14, 631; (c) R. Schauer, *Curr. Opin. Struct. Biol*., **2009**, 19, 507; (d) S. I. Hakomori, Y. Zhang, *Chem. Biol*., 1997, 4, 97; (e) R. D. Astronomo, D. R. Burton, *Nat. Rev. Drug Discovery.*, **2010**, 9, 308; (f) M. M. Fuster, J. D. Esko, *Nat. Rev. Cancer.*, **2005**, 5, 526; (g) R. A. C. Hughes, D. R. Cornblath, *Lancet.*, **2005**, 366, 1653; (h) C. S. Berenson, K. B. Sayles, J. Huang, V. N. Reinhold, M. A. Garlipp H. C. Yohe, *FEMS Immuno., Med.*

Microbiol., **2005**, 45, 171; (i) J. Fantini, D. Hammache, G. Pieroni, N. Yahi, *Glycoconjugate* J., **2000**, 17, 199.

4. H. Cao, P. R. Crocker, *Immunology*., **2011**, 132, 18; b) P. H. Lopez, R. L. Schnaar, *Curr. Opin. Strct. Biol*., **2009**, 19, 549.
5. a) M. S. Macauley, P. R. Crocker, J. C. Paulson, *Nat. Rev. Immunol*., 2014, **14**, 653; b) S. Pillai, I. A. Netravali, A. Cariappa, H. Mattoo, *Annu Rev Immunol*., **2012**, 30, 357.
6. a) A. Varki, T. Angata, *Glycobiology*., **2006**, 1R; b) P. R. Crocker, J. C. Paulson A. Varki, *Nat. Rev. Immunol*., **2007**, 7, 255.
7. a) T. Angata, C. M. Nycholat, M. S. Macauley, *Trends Pharmacol. Sci*., **2015**, *36***,** 645; b) H. Prescher, A. Schweizer, E. Kuhfeldt, L. Nitschke and R. Brossmer, *ACS Chem. Biol*., **2014**, 9, 1444; c) C. D. Rillahan, M. S. Macauley, E. Schwartz, Y. He, R. McBride, B. M. Arlian, J. Rangarajan, V. V. Fokin, J. C. Paulson, *Chem. Sci*., **2014**, 5, 2398.
8. a) O. Blixt, S. Han, L. Liao, Y. Zeng, J. Hoffmann, S. Futakawa, J. C. Paulson, *J. Am. Chem. Soc.*, **2008**, 130, 6680; b) V. Padler-Karavani, X. Song, H. Yu, N. Hurtado-Ziola, S. Huang, S. Muthana, H. A. Chokhawala, J. Cheng, A. Verhagen, M. A. Langereis, R. Kleene, M. Schachner, R. J. de Groot, Y. Lasanajak, H. Matsuda, R. Schwab, X. Chen, D. F. Smith, R. D. Cummings, A. Varki, *J. Biol. Chem*., **2012**, 287, 22593; c) J. Q. Gerlach, M. Kilcoyne, L. Joshi, *Anal. Methods.*, **2014**, 6, 440.
9. a) D. Crich, W. Li, *J. Org. Chem.*, **2007**, 72, 2387; b) C. Wang, Q. Li, H. Wang, L. H. Zhang, X. S. Yi, *Tetrahedron.*, **2006**, 62, 11657; c) M, Sakagami, H. Hamana, *Tetrahedron Lett*., **2000**, 41, 5547; d) S. Serna, J. Etxebarria, N. Ruiz, M. Martin-Lomas, C. Reichardt, *Chem. Eur. J.*, **2010**, 16, 13163.
10. a) H. Y. Liao, C. H. Hsu, S. C. Wang, C. H. Liang, H. Y. Yen, C. Y. Su, C. H. Chen, J. T. Jan, C. T. Ren, C. H. Chen, T. J. Cheng, C. Y. Wu, C. H. Wong, *J. Am. Chem. Soc.*, **2010**, 132, 14849.
11. C. H. Wang, K. Tony, K. Mong, C. Y. Huang, *J. Org. Chem*., **2003**, 68, 2135.
12. J. C. Michalski, A. Klein. *Biochim. Biophys. Acta*., **1999**, 1455, 69.
13. K. Ohtsubo, J. D. Marth, *Cell*., **2006**, 126, 855.
14. K. W. Moremen, M. Tiemeyer, A. V. Nairn, *Nat. Rev. Mol. Cell Biol*., **2012**, 13, 448.
15. R. Schauer, *Cell biology Monographs*., **1982**, 10, Springer-Verlaag, New York.

16. A. Varki, *Glycobiology.*, **1992**, 2, 25.
17. S. Kelm, R. Schauer, *Int. Rev. Cytol*., **1997**, 175, 137.
18. A. Angata, A. Varki, C*hem. Rev*., **2002**, 102, 439.
19. L. D. Powell, A. Varki, *J. Biol. Chem.*,**1994**, 269, 10628.
20. L. D. Powell, R. K. Jain, K. L. Matta, S. Sabesan, A. Varki, *J. Biol. Chem*., **1995**, 270, 7523.
21. V. D. Brinkman, E. C. M. Linden, A. Varki, *J. Biol. Chem*., **2000**, 275, 8625.
22. A. Klein, M. Krishna, N. M. Varki, A. VArki, *Pro. Natl. Acad. Sci. U.S.A.*, **1994**, 91, 7782.
23. R. Vlasak, W. Luytjes, W. Spaan, P. Palese, *Proc. Natl. Acad. Sci. U.S.A.*, **1988**, 85, 4526.
24. B. Schultze, H.-J. Gross, R. Brossmer, H.-D. Klenk, G. Herrler, *Virus Res*., **1990**, 16, 185.
25. N. Kaludov, K. E. Brown, R. W. Walters, J. Zabner, J. A. J. Chiorini, *Virology*., **2001**, 75, 6884.
26. R. Kadirvelraj, O. C. Grant, I. J. Goldstein, H. C. Winter, H. Taneno, E. Fadda, R. J. Wood, *Glycobiology*., **2011**, 21, 973.
27. L. Hazlett, X. Rudner, S. Masinick, M. Ireland, S. Gupta, *Invest. Ophthalmol. Vis. Sci*., **1995**, 36, 634.
28. K. Kawakami, K. Ahmed, Y. Utsunomiya, N. Rikitomi, A. Hori, K. Oishi, T. Nagatake, *Microbiol. Immunol*., **1998**, 42, 697.
29. C. Cebo, T. Dambrouck, E. Maes, C. Laden, G. Strecker, J. C. Michalski, J. P. Zanetta, *J. Biol. Chem*., **2001**, 276, 5685.
30. A. Cariappa, H. Takematsu, H. Liu, S. Diaz, K. Haider, C. Bolila, G. Kalloo, M., Shi, H. N. Connale, N. Varki, A. Varki, S. Pillai, *J. Exp. Med*., **2008**, 206, 125.
31. H. Masuda, T. Suzuki, Y. Sugiyama, G. Horiike, K. Murakami, D. Miyamoto, Ito T. Jwa Hidari KI, H. Kida, M. Kiso, K. Fukunaga, M. Ohuchi, T. Toyoda, A. Ishihama, Y. Kawaoka, Y. Suzuki, *FEBS. Lett*., **1999**, 464, 71.
32. T. Bulai, A. Bratosin D Fau Pons, J. Pons A Fau Montreuil, J. P. Montreuil J Fau Zanetta, J. P. Zanetta, FEBS. Lett., 2003, 534, 185.
33. M. Cohen, N Fau. Hurtado-Ziola, A. Varki, *Blood.*, **2009**, 114, 3668.
34. C. D. Rillahan, M. S. Macauley, E. Schwartz, Y. He, R. McBride, B. M. Arlian, J. Rangarajan, V. V. Fokin, J. C. Paulson, *Chem. Sci*., **2014**, 5, 2398.

35. L. M. Krug, G. Ragupathi, C. Fau Hood, C. George, F. Fau Hong, Shen, R., R Fau. Shen, L. Abrey, H. J. Jennings, M. G. Fau Kris, P. O. Fau Livingston, *Cancer. Immunol. Immunother.*, **2012**, 61, 9.
36. J. Wu, Z. Guo, *Bioconjugate Chem.*, **2006**, 17, 1537.
37. Q. Wang, J. Ekanayaka Sa Fau Wu, J. Wu J Fau Zhang, Guo, Z. Guo, *Bioconjugate Chem.*, **2008**, 19, 2060.
38. Z. Zhou, M. Mondal, G. Fau Liao, Z. Guo, *Org. Biomol. Chem.*, **2014**, 12, 3238.
39. F. Yang, Xj. Fau. Zheng, C.-X. Huo, Y. Wang, Y. Zhang, X.-S. Ye, ACS *Chem. Biol*. **2011**, 6, 252.
40. Q. Wang, Z. Guo, *ACS Med. Chem. Lett.*, **2011**, 2, 373.
41. C.-X. Huo, X.-J. Zheng, A. Xiao, C.-C. Liu, S. Sun, Z. Lv, X.-S. Ye, *Org. Biomol. Chem.*, **2015**, 13, 3677.
42. L. Svennerholm, *Biochim. Biophys. Acta.*, **1957**, 24, 604.
43. (a) N. K. Sauter, J. E. Hanson, G. D. Glick, J. H. Brown, R. L. Crowther, S-J. Park, J. J. Skehel, D. C. Wiley, *Biochemistry.*, **1992**, 31, 9609; (b) S. J. Gamblin, J. J. Skehel, *J. Bio. Chem.*, **2010**, 285, 28403; (c) C. Mitsuoka, K. Ohmori, N. Kimura, A. Kanamori, S. Komba, H. Ishida, M. Kiso, R. Kannagi, *Proc. Natl. Acad. Sci. U. S. A.*, **1999**, 96, 1597; (d) A. Cariappa, H. Takematsu, H. Liu, S. Diaz, K. Haider, C. Boboila, G. Kalloo, M. Connole, H. N. Shi, N. Varki, A. Varki, S. Pillai, *J. Exp. Med.*, **2009**, 206, 125.
44. (a) P. V. Santacroce, A. Basu, *Angew. Chem. Int. Ed.*, **2003**, 42, 95 (b) Y. Nagasaki, K. Yasugi, Y. Yamamoto, A. Harada, K. Kataoka, *Biomacromolecules.*, **2001**, 2, 1067; (c) X. Qu, V. V. Khutoryanskiy, A. Stewart, S. Rahman, B. Papahadjopoulos-Sternberg, C. Dufes, D. McCarthy, C. G. Wilson, R. Lyons, K. C. Carter, A. Schatzlein, I. F. Uchegbu, *Biomacromolecules.*, **2006**, 7, 3452; (d) R. A. Bader, A. L. Silvers, N. Zhang, *Biomacromolecules.*, **2011**, 12, 314.
45. R. L. Miller, J. D. Cannon Jr, *Prog. Clin. Biol. Res.*, **1984**, 157, 31.
46. (a) M. J. Linman, J. D. Taylor, H. Yu, X. Chen, Q. Chen, *Anal. Chem.*, **2008**, 80, 4007; (b) R. Schauer, S. Kelm, G. Reuter, P. Roggentin, L. Shaw, In *Biology of the Sialic Acid*, Edited by A. Rosenberg. New York. **1995**, 7; (c) J. A. Wasylnka, M. L. Simmer, M. M. Moore, *Microbiology.*, 2001, 147, 869; (d) J. M. Wolosin, Y. Wang, *Invest Ophthalmol. Vis. Sci.*, **1995**, 36, 2277.

47. (a) W. C. Chen, G. C. Completo, D. S. Sigal, P. R. Crocker, A. Saven, J. C. Paulson, *Blood.*, **2010**, 115, 4778-4786. (b) N. Razi, A. Varki, *Proc. Natl. Acad. Sci. U S A.*, **1998**, 95, 7469.
48. R. Roy, *J. Carbohydr. Chem*., **2002**, 21, 769; (b) A. Hasegawa, J. Nakamura, M. Kiso, *J. Carbohydr. Chem*., **1986**, 5, 11.
49. K. D. Hardman, C. F Ainswort, *Biochemistry.*, **1972**, *11*, 4910.

2.9 ^{1}HNR and ^{13}CNMR Details

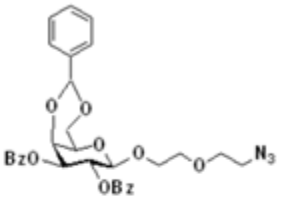
BzO
OBz
O
O
O
O
O
N3

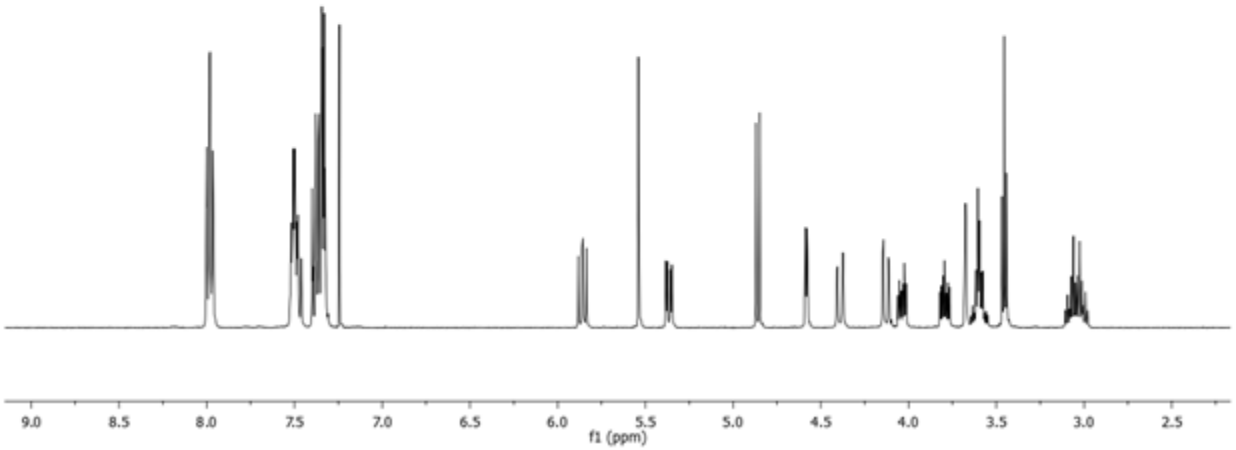
9.0
8.5
8.0
7.5
7.0
6.5
6.0
5.5
5.0
4.5
4.0
3.5
3.0
2.5
f1 (ppm)

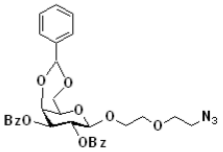
BzO
OBz
O
O
O
O
O
N3

220
210
200
190
180
170
160
150
140
130
120
110
100
90
80
70
60
50
40
30
20
10
0
-10
-20
f1 (ppm)

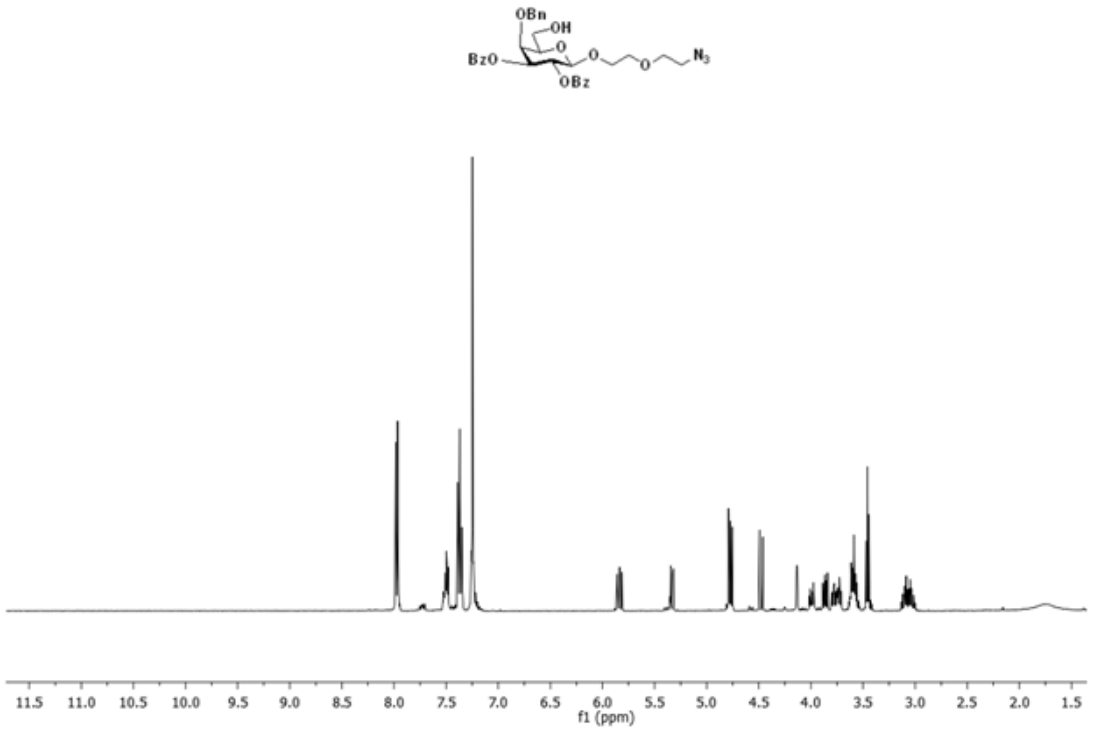
OBn
OH
BzO
OBz
N3
11.5 11.0 10.5 10.0 9.5 9.0 8.5 8.0 7.5 7.0 6.5 6.0 5.5 5.0 4.5 4.0 3.5 3.0 2.5 2.0 1.5
f1 (ppm)

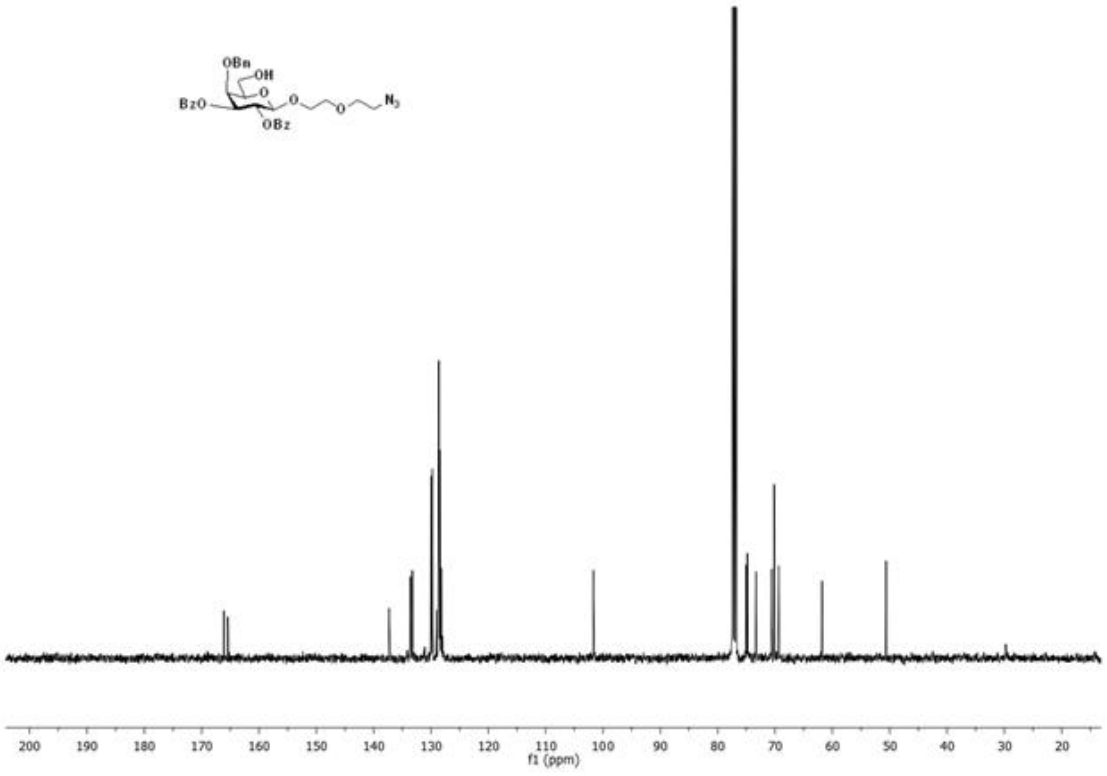
OBn
OH
BzO
OBz
N3
200 190 180 170 160 150 140 130 120 110 100 90 80 70 60 50 40 30 20
f1 (ppm)

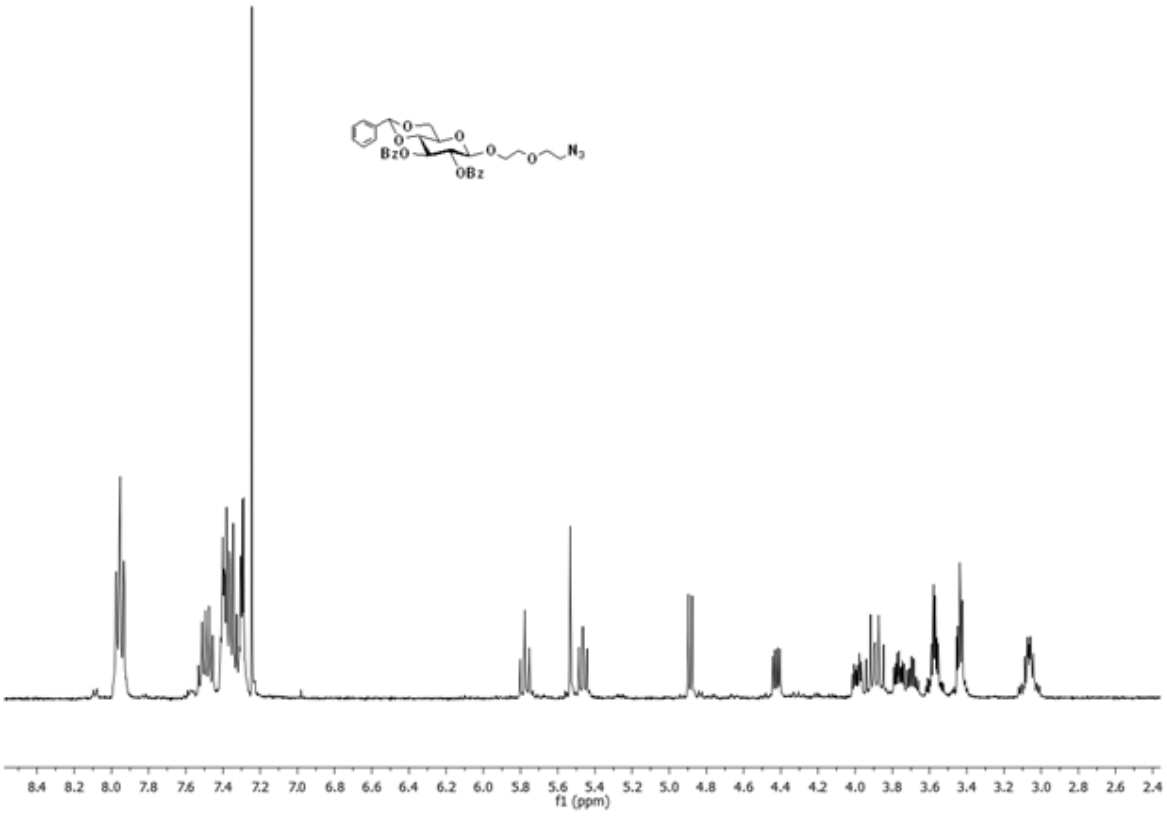
BzO
OBz
N3
8.4 8.2 8.0 7.8 7.6 7.4 7.2 7.0 6.8 6.6 6.4 6.2 6.0 5.8 5.6 5.4 5.2 5.0 4.8 4.6 4.4 4.2 4.0 3.8 3.6 3.4 3.2 3.0 2.8 2.6 2.4
f1 (ppm)

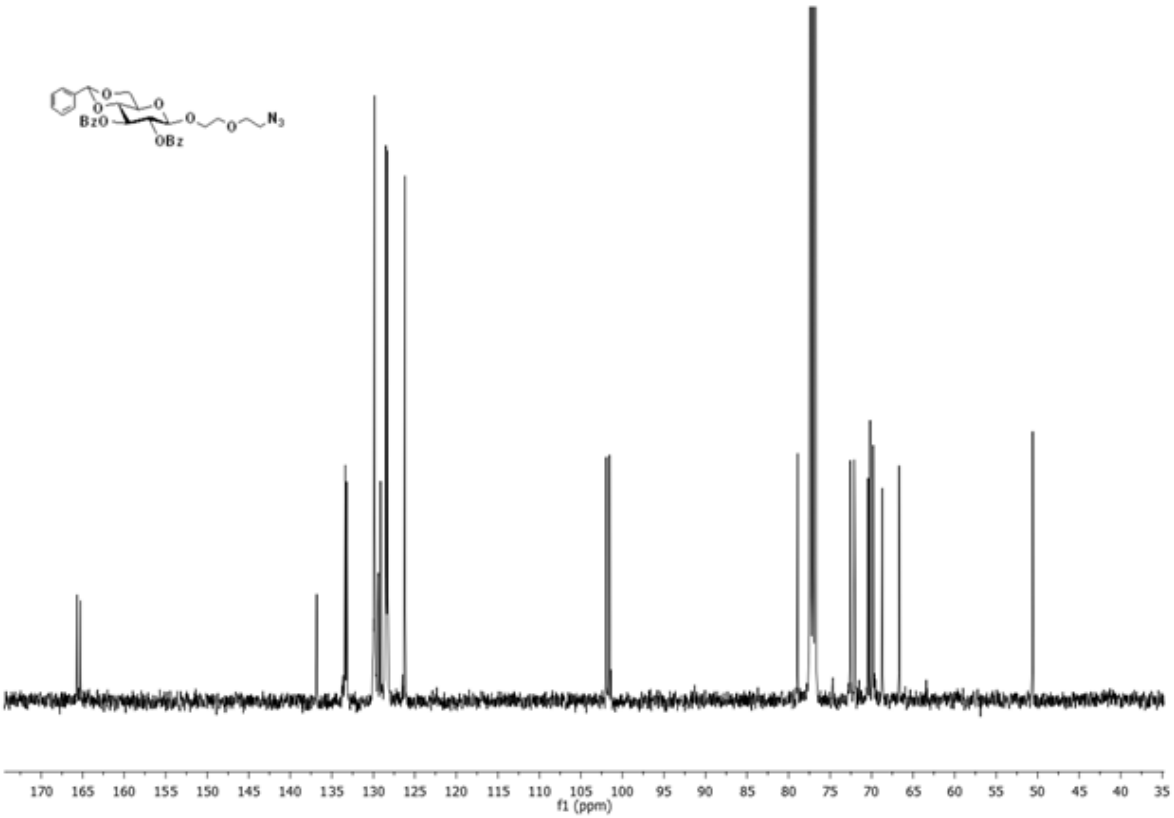
BzO
OBz
N3
170 165 160 155 150 145 140 135 130 125 120 115 110 105 100 95 90 85 80 75 70 65 60 55 50 45 40 35
f1 (ppm)

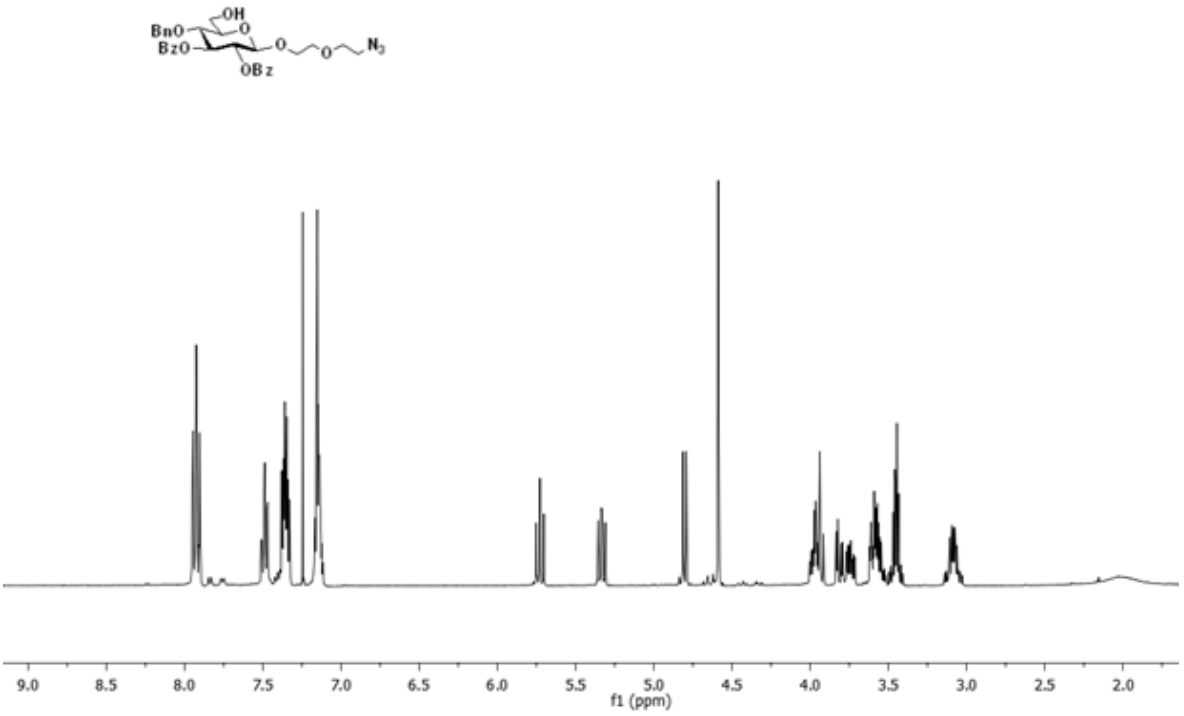
BnO
BzO
OBz
OH
O
O
O
N3
9.0
8.5
8.0
7.5
7.0
6.5
6.0
5.5
5.0
4.5
4.0
3.5
3.0
2.5
2.0
f1 (ppm)

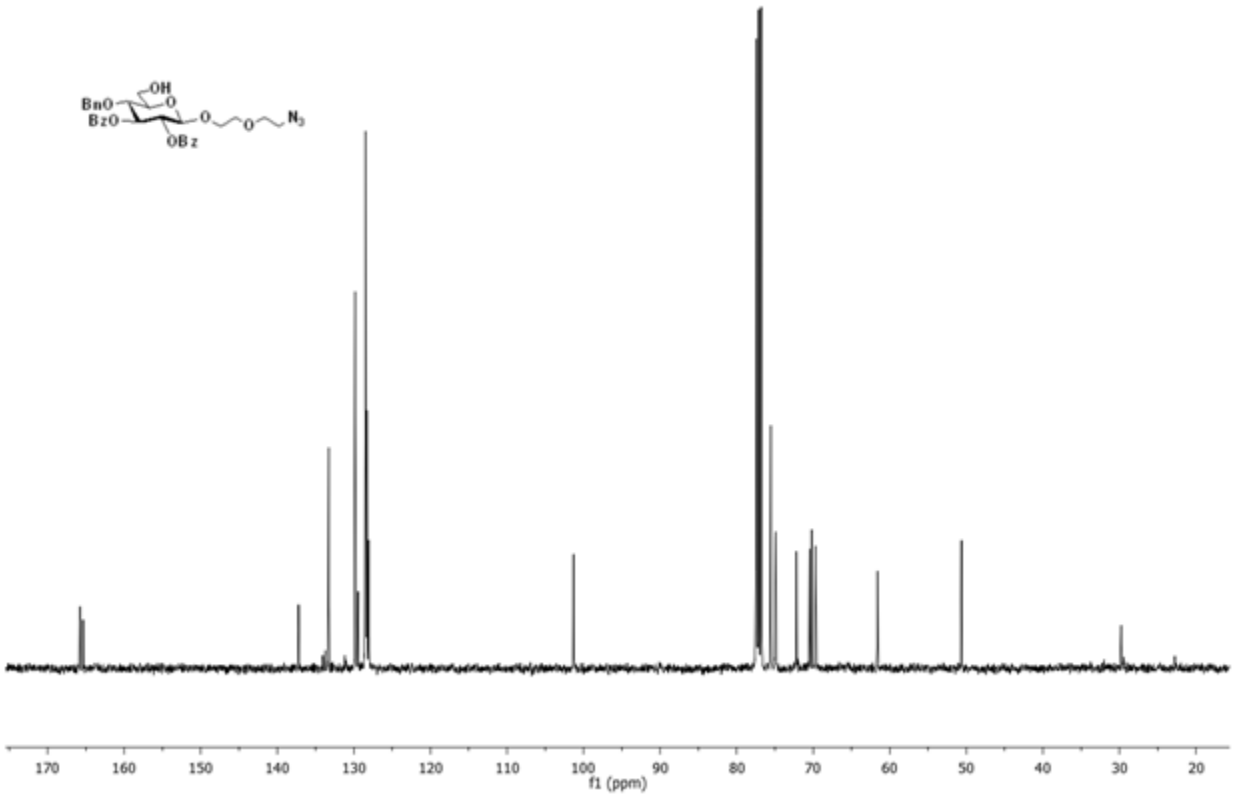
BnO
BzO
OBz
OH
O
O
O
N3
170
160
150
140
130
120
110
100
90
80
70
60
50
40
30
20
f1 (ppm)

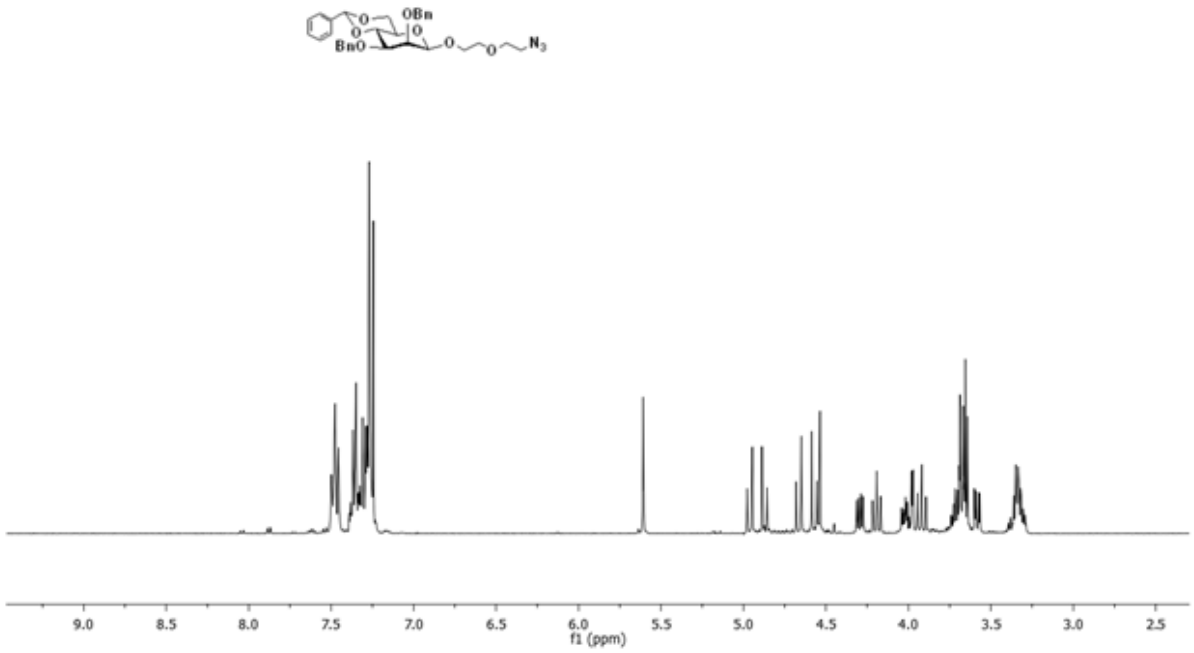
OBn
BnO
O
N3
9.0
8.5
8.0
7.5
7.0
6.5
6.0
5.5
5.0
4.5
4.0
3.5
3.0
2.5
f1 (ppm)

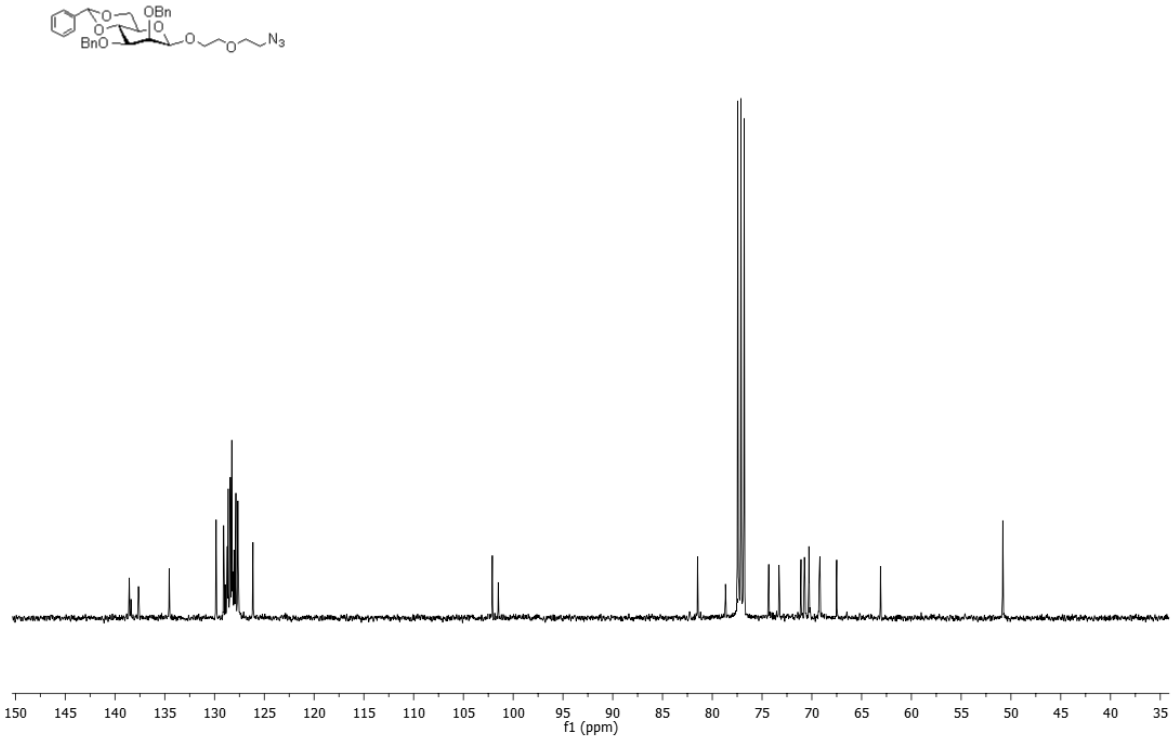
OBn
BnO
O
N3
150
145
140
135
130
125
120
115
110
105
100
95
90
85
80
75
70
65
60
55
50
45
40
35
f1 (ppm)

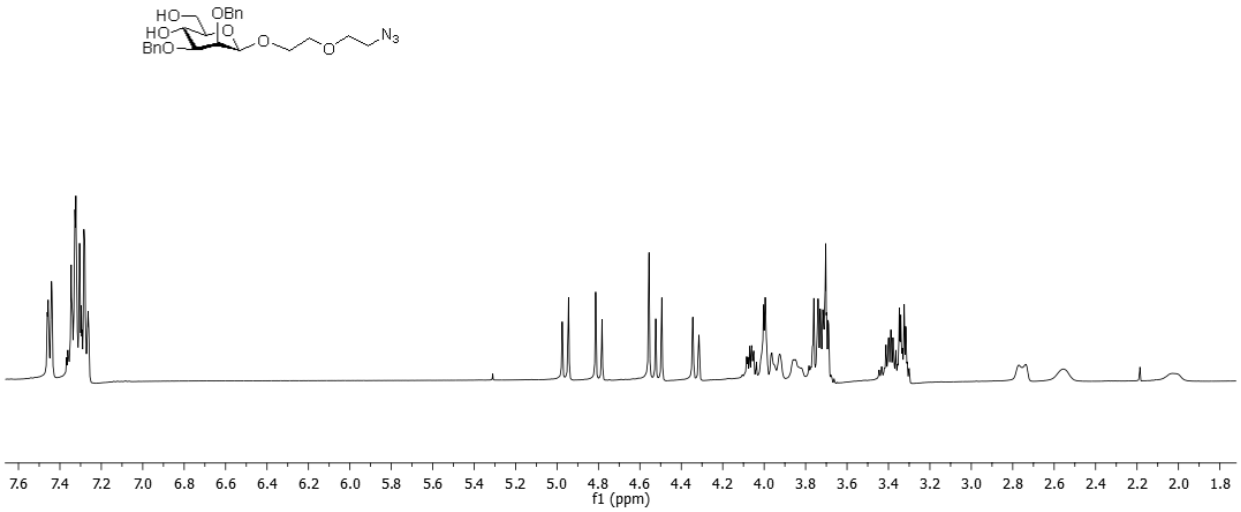
HO
OBn
HO
O
BnO
O
O
N3
7.6 7.4 7.2 7.0 6.8 6.6 6.4 6.2 6.0 5.8 5.6 5.4 5.2 5.0 4.8 4.6 4.4 4.2 4.0 3.8 3.6 3.4 3.2 3.0 2.8 2.6 2.4 2.2 2.0 1.8
f1 (ppm)

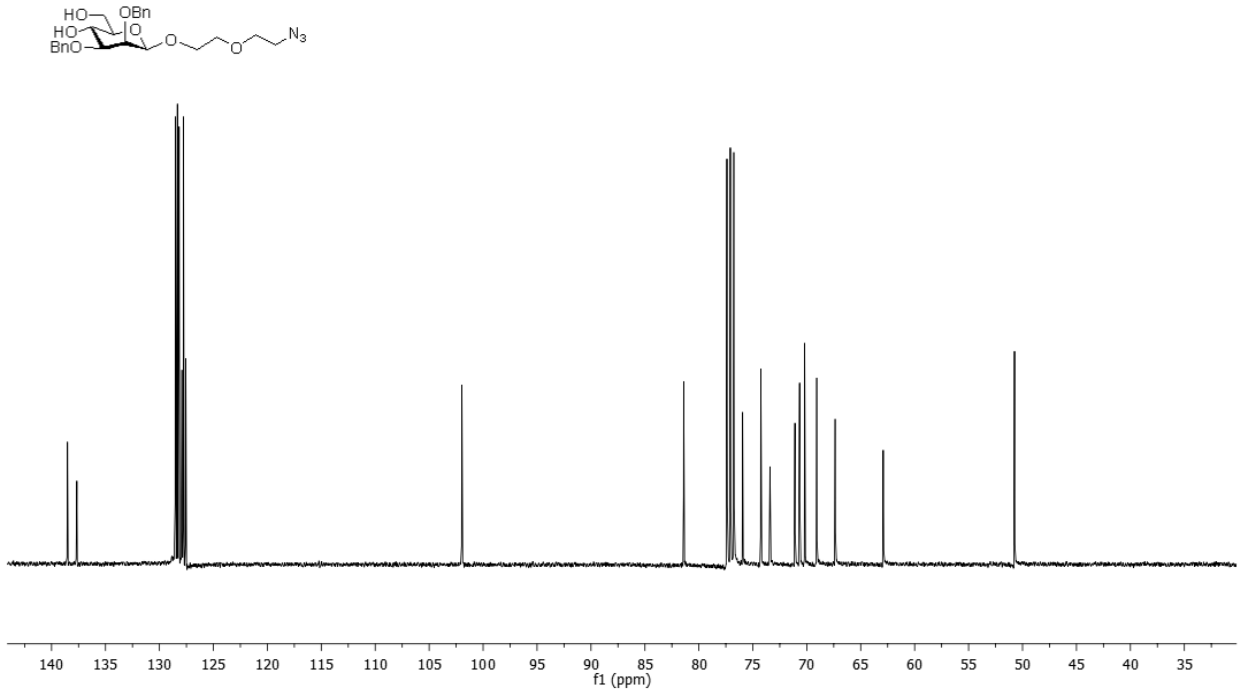
HO
OBn
HO
O
BnO
O
O
N3
140 135 130 125 120 115 110 105 100 95 90 85 80 75 70 65 60 55 50 45 40 35
f1 (ppm)

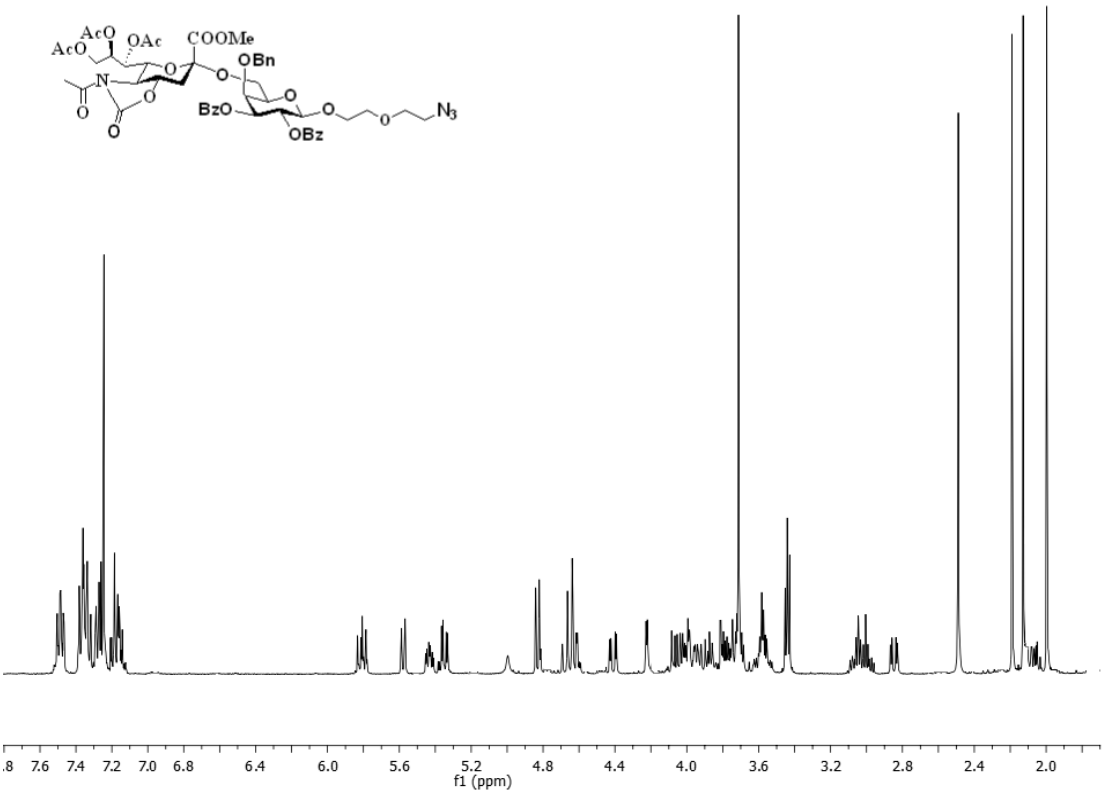
AcO
AcO
OAc
COOMe
OBn
BzO
OBz
N3
f1 (ppm)

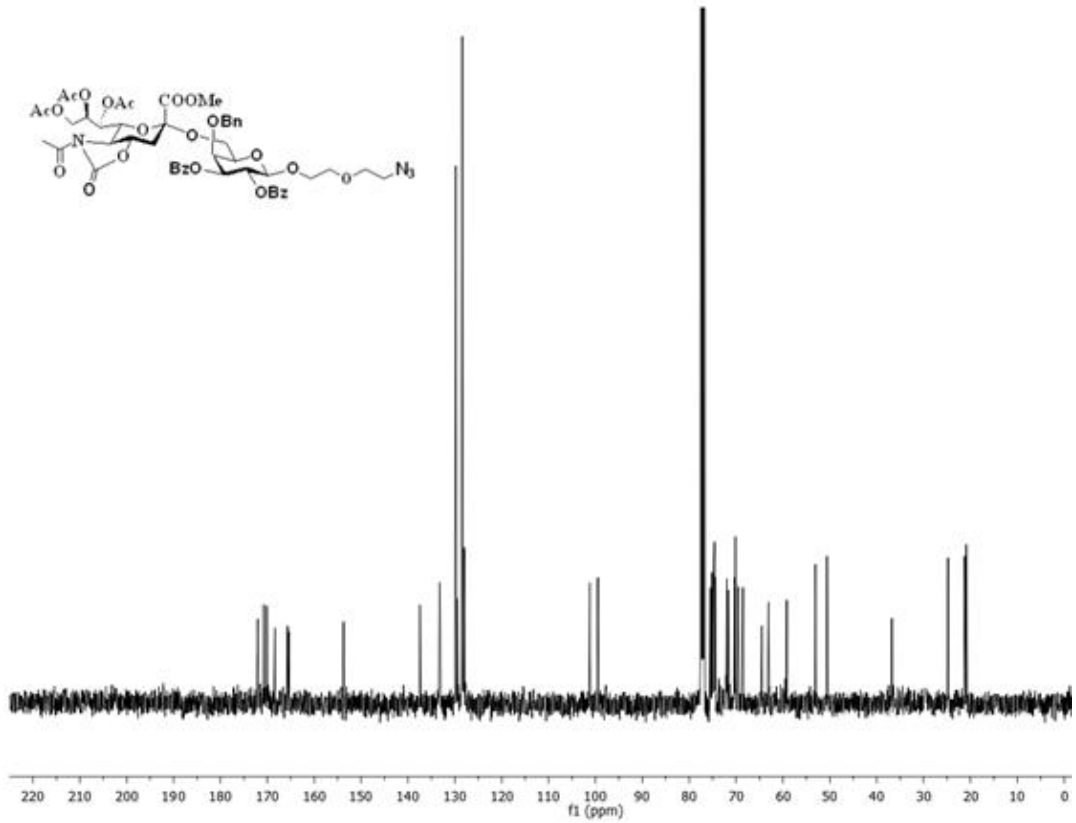
AcO
AcO
OAc
COOMe
OBn
BzO
OBz
N3
f1 (ppm)

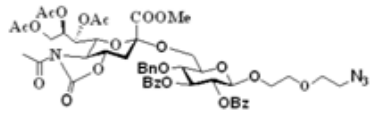
AcO
AcO
OAc
COOMe
N
O
O
O
O
BnO
BzO
O
O
O
N3
OBz

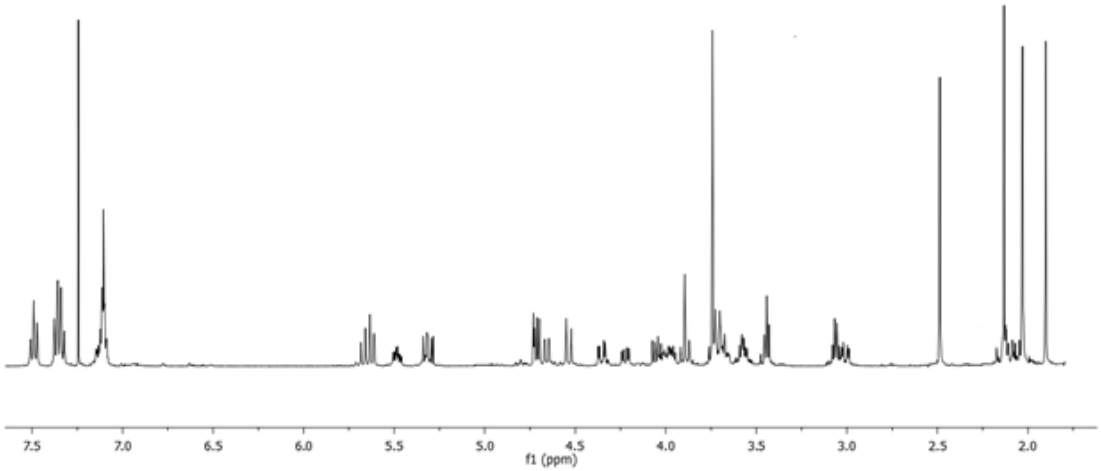
7.5
7.0
6.5
6.0
5.5
5.0
4.5
4.0
3.5
3.0
2.5
2.0
f1 (ppm)

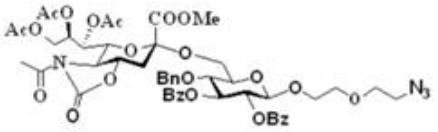
AcO
AcO
OAc
COOMe
N
O
O
O
O
BnO
BzO
O
O
O
N3
OBz

220
210
200
190
180
170
160
150
140
130
120
110
100
90
80
70
60
50
40
30
20
f1 (ppm)

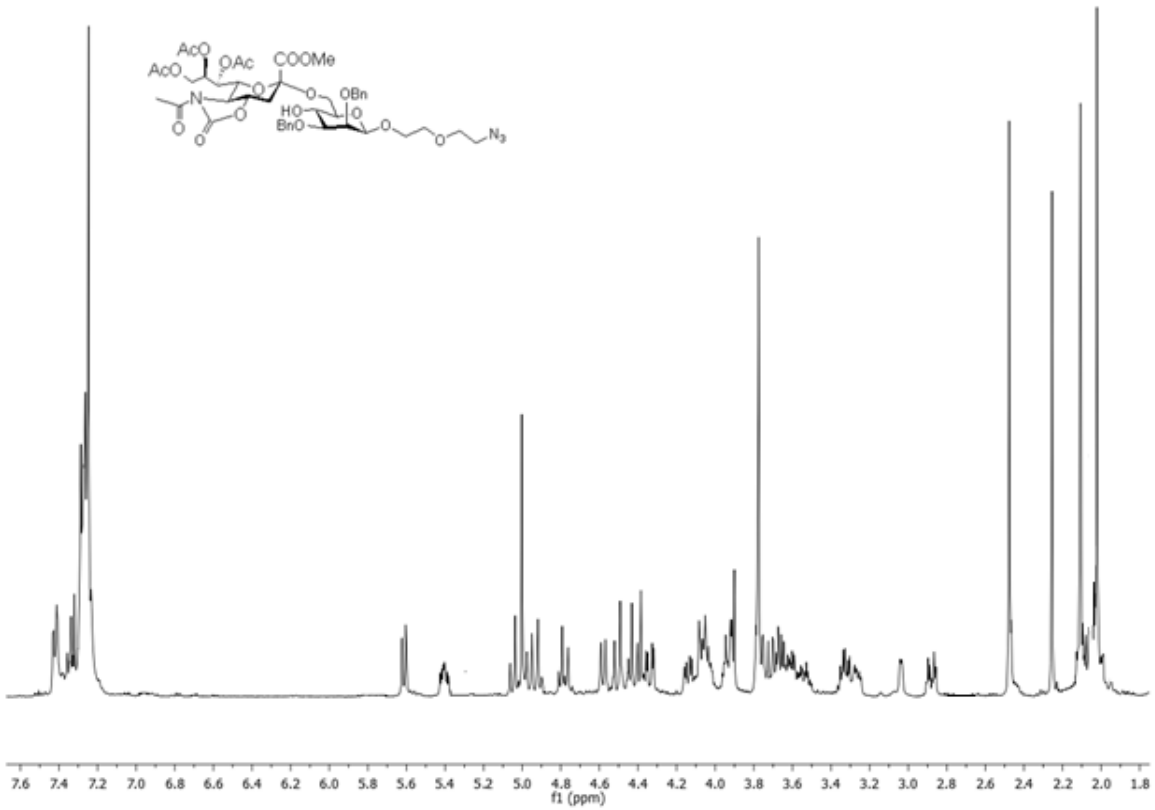
AcO
AcO
OAc
COOMe
OBn
HO
BnO
N3
7.6 7.4 7.2 7.0 6.8 6.6 6.4 6.2 6.0 5.8 5.6 5.4 5.2 5.0 4.8 4.6 4.4 4.2 4.0 3.8 3.6 3.4 3.2 3.0 2.8 2.6 2.4 2.2 2.0 1.8
f1 (ppm)

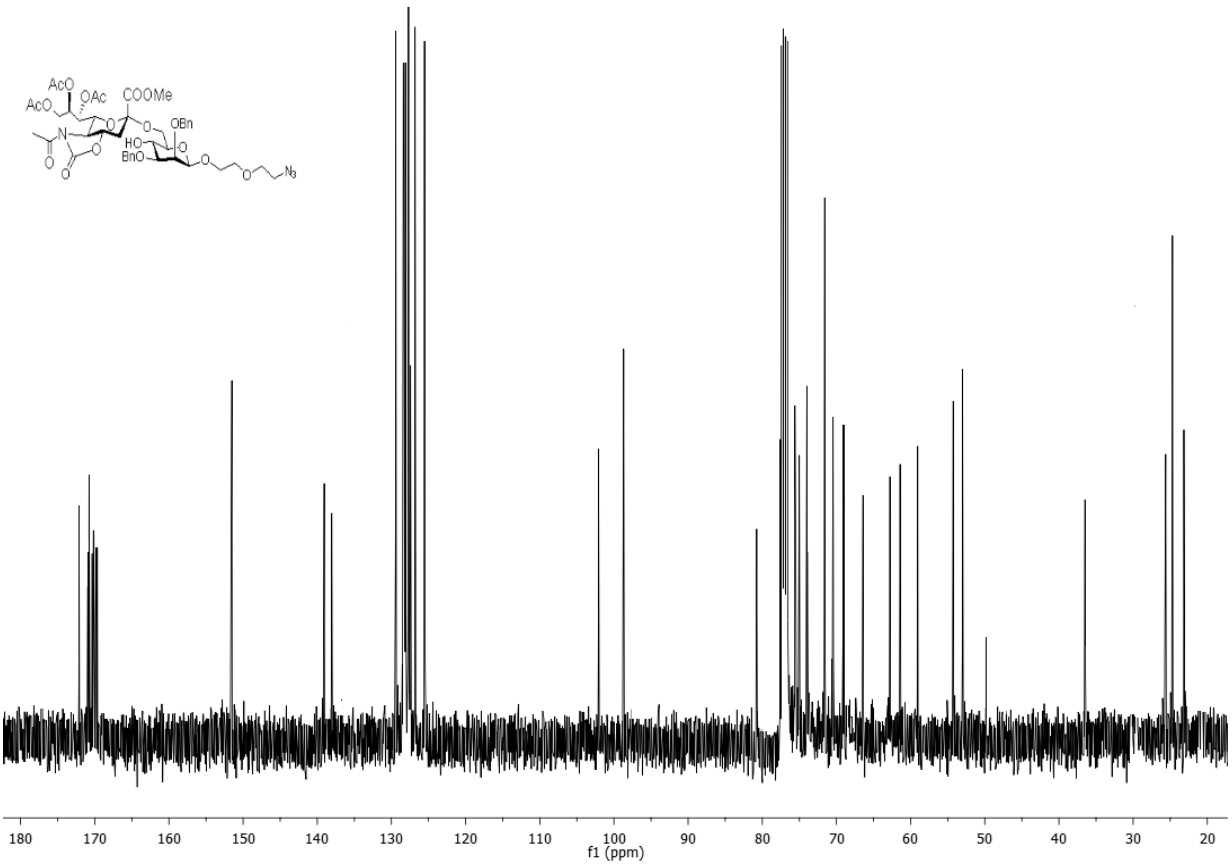
AcO
AcO
OAc
COOMe
OBn
HO
BnO
N3
180 170 160 150 140 130 120 110 100 90 80 70 60 50 40 30 20
f1 (ppm)

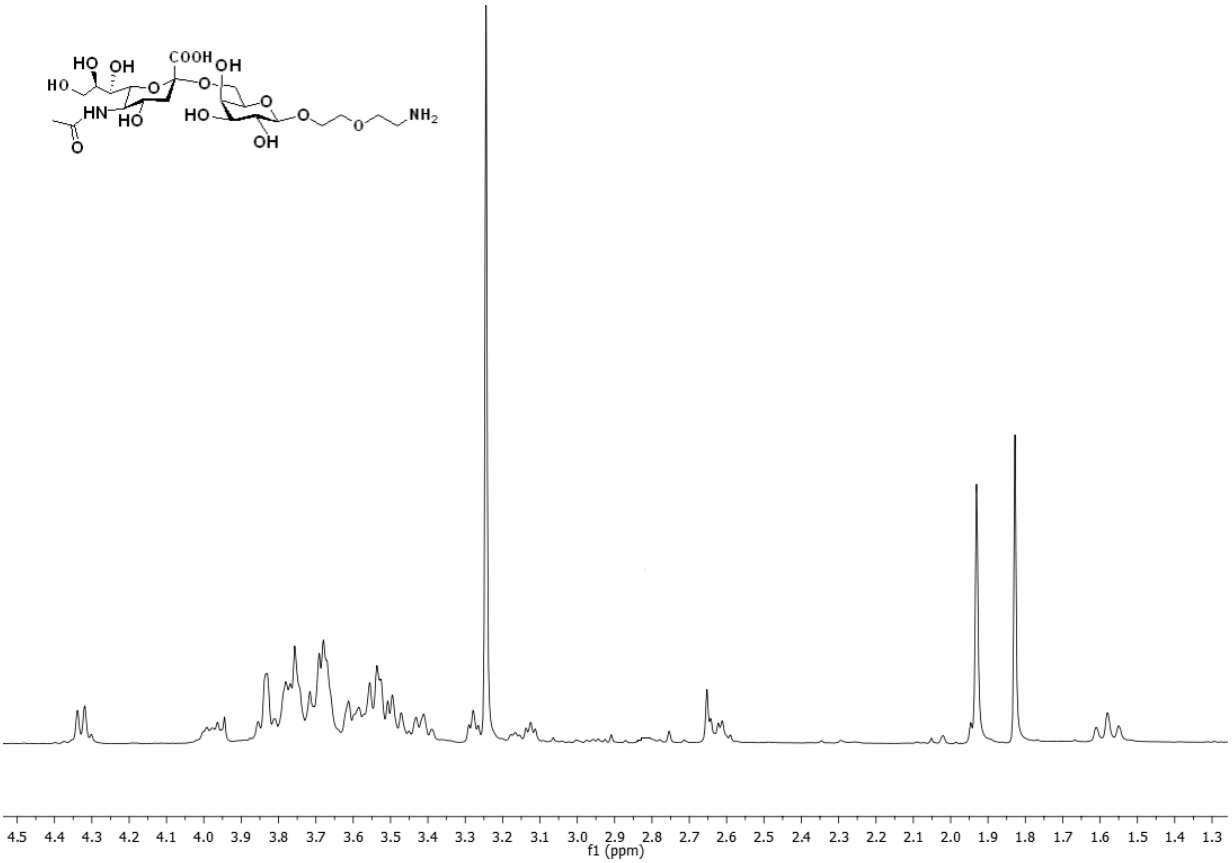
HO
OH
COOH
OH
HO
HN
HO
HO
O
OH
NH2
4.5 4.4 4.3 4.2 4.1 4.0 3.9 3.8 3.7 3.6 3.5 3.4 3.3 3.2 3.1 3.0 2.9 2.8 2.7 2.6 2.5 2.4 2.3 2.2 2.1 2.0 1.9 1.8 1.7 1.6 1.5 1.4 1.3
f1 (ppm)

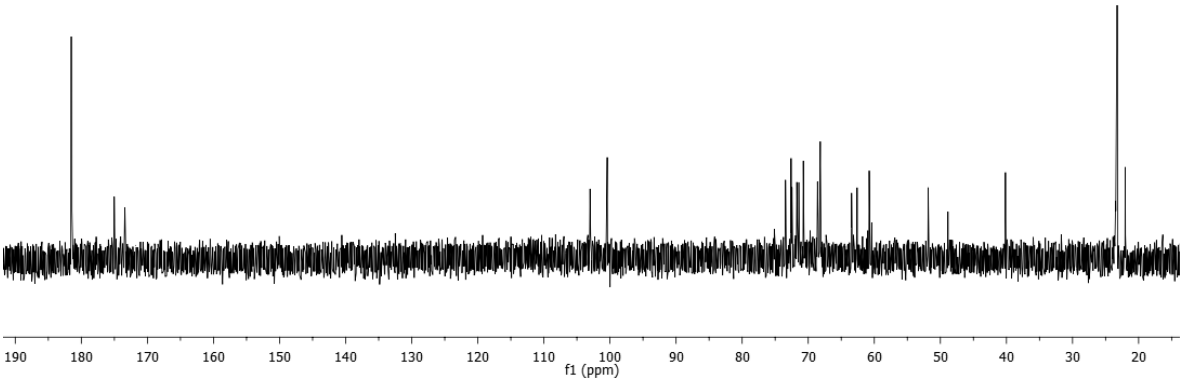
190 180 170 160 150 140 130 120 110 100 90 80 70 60 50 40 30 20
f1 (ppm)

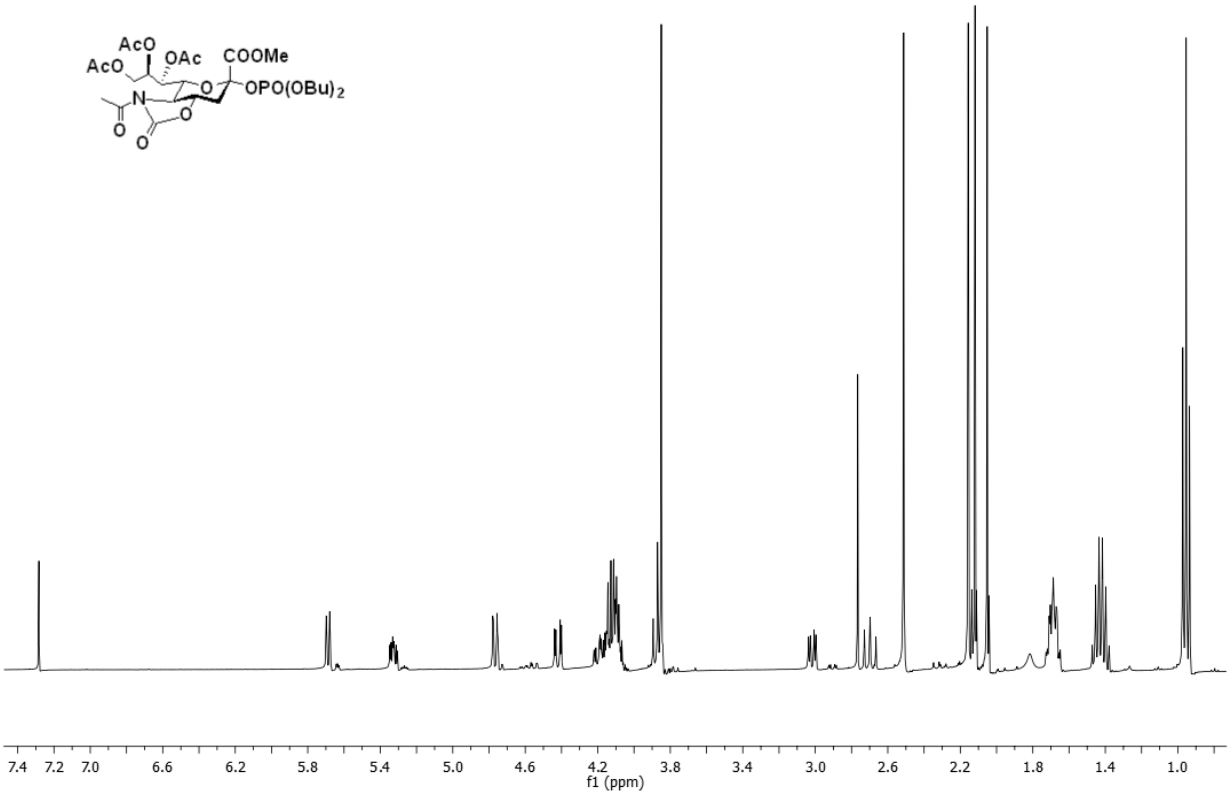
AcO
AcO
OAc
COOMe
OPO(OBu)2
N
O
O
O
7.4 7.2 7.0 6.6 6.2 5.8 5.4 5.0 4.6 4.2 3.8 3.4 3.0 2.6 2.2 1.8 1.4 1.0
f1 (ppm)

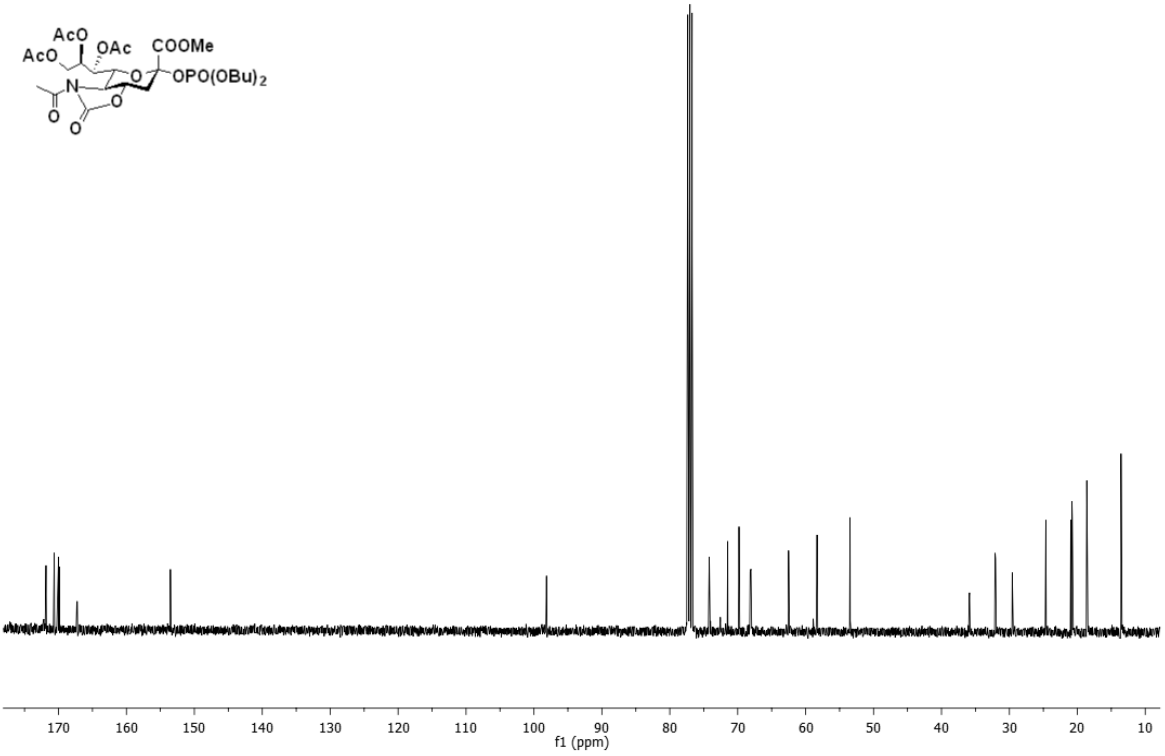
AcO
AcO
OAc
COOMe
OPO(OBu)2
N
O
O
O
170 160 150 140 130 120 110 100 90 80 70 60 50 40 30 20 10
f1 (ppm)

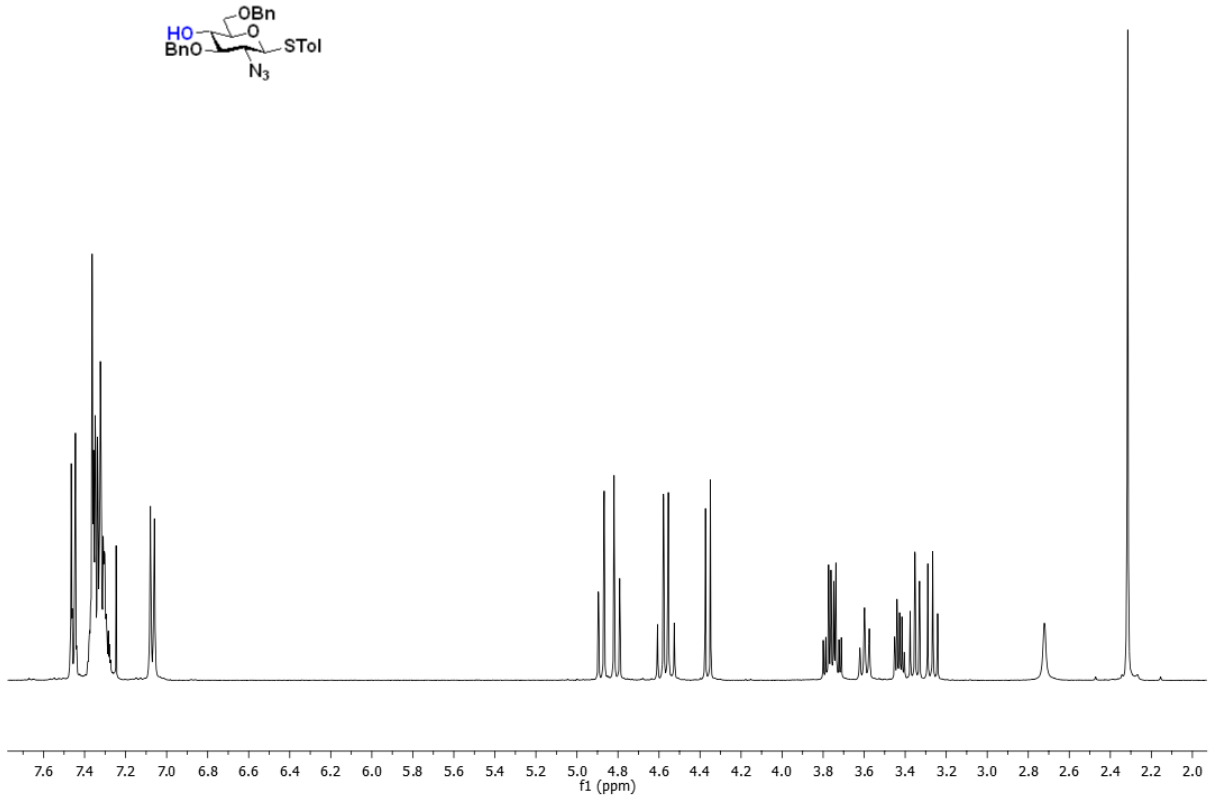
OBn
HO
O
BnO
STol
N3
7.6 7.4 7.2 7.0 6.8 6.6 6.4 6.2 6.0 5.8 5.6 5.4 5.2 5.0 4.8 4.6 4.4 4.2 4.0 3.8 3.6 3.4 3.2 3.0 2.8 2.6 2.4 2.2 2.0
f1 (ppm)

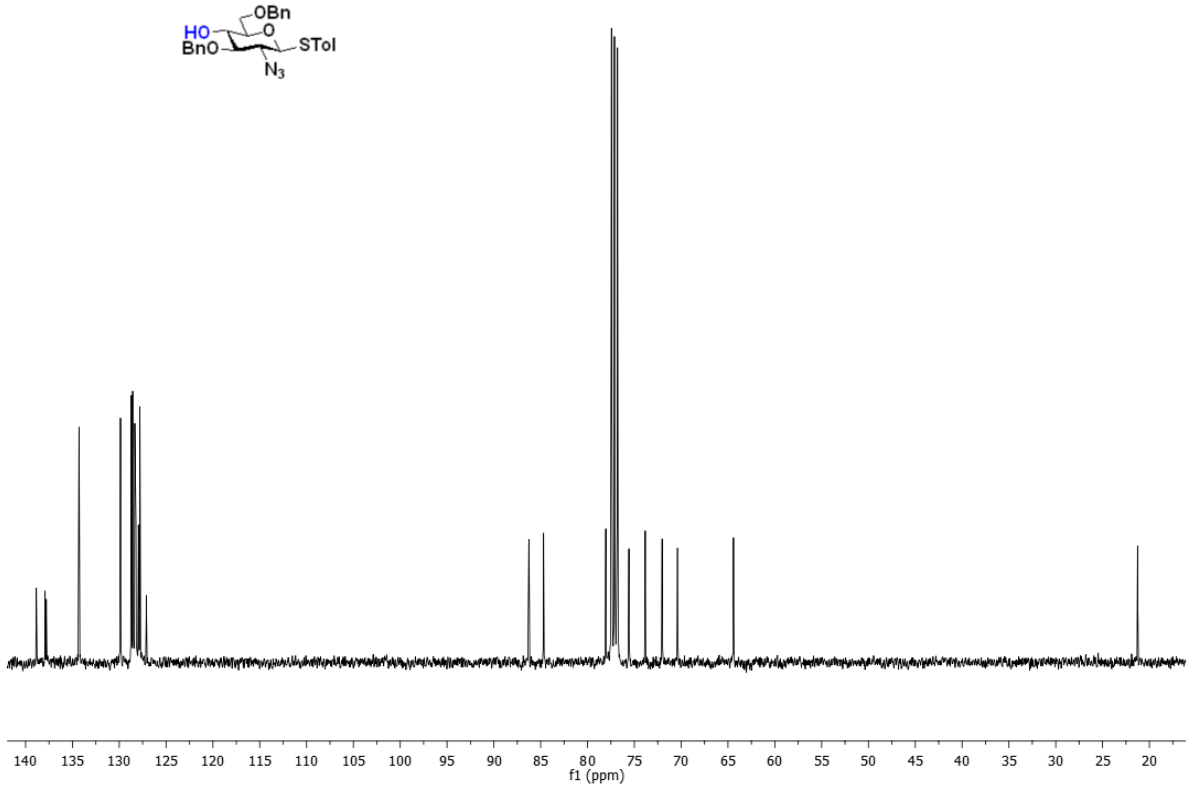
OBn
HO
O
BnO
STol
N3
140 135 130 125 120 115 110 105 100 95 90 85 80 75 70 65 60 55 50 45 40 35 30 25 20
f1 (ppm)

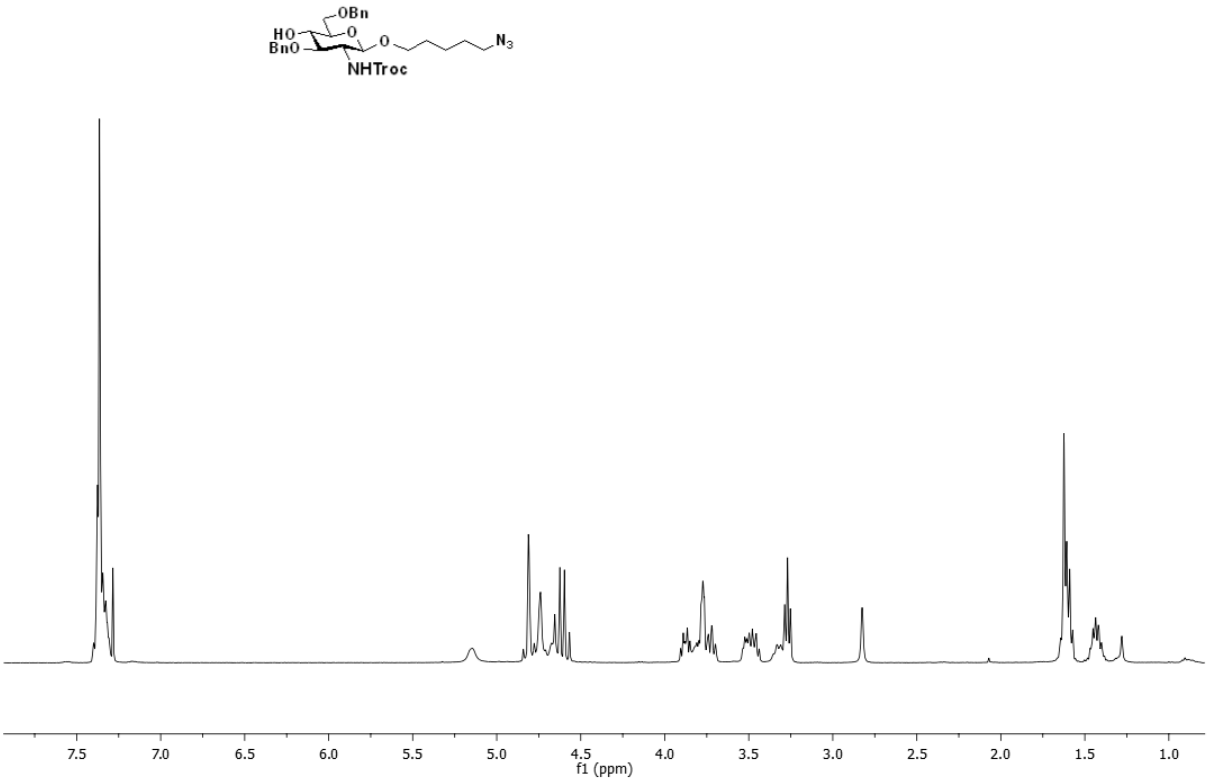
OBn
HO
BnO
O
O
N3
NHTroc
7.5
7.0
6.5
6.0
5.5
5.0
4.5
4.0
3.5
3.0
2.5
2.0
1.5
1.0
f1 (ppm)

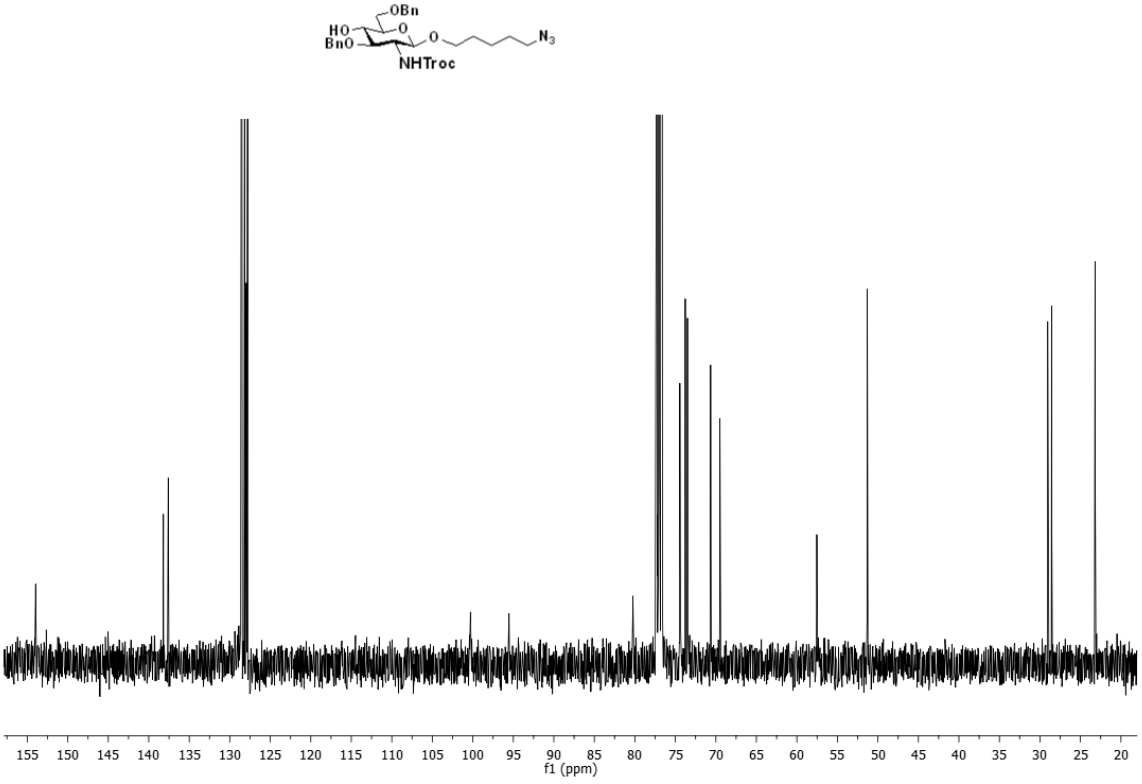
OBn
HO
BnO
O
O
N3
NHTroc
155
150
145
140
135
130
125
120
115
110
105
100
95
90
85
80
75
70
65
60
55
50
45
40
35
30
25
20
f1 (ppm)

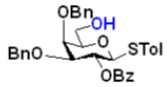
OBn
OH
O
BnO
STol
OBz

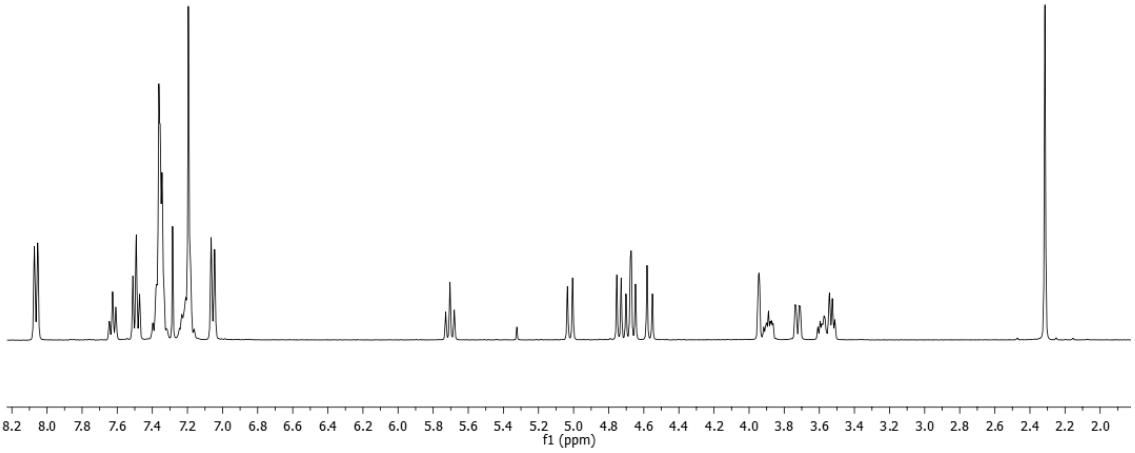
8.2 8.0 7.8 7.6 7.4 7.2 7.0 6.8 6.6 6.4 6.2 6.0 5.8 5.6 5.4 5.2 5.0 4.8 4.6 4.4 4.2 4.0 3.8 3.6 3.4 3.2 3.0 2.8 2.6 2.4 2.2 2.0
f1 (ppm)

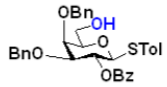
OBn
OH
O
BnO
STol
OBz

210 200 190 180 170 160 150 140 130 120 110 100 90 80 70 60 50 40 30 20 10 0 -10
f1 (ppm)

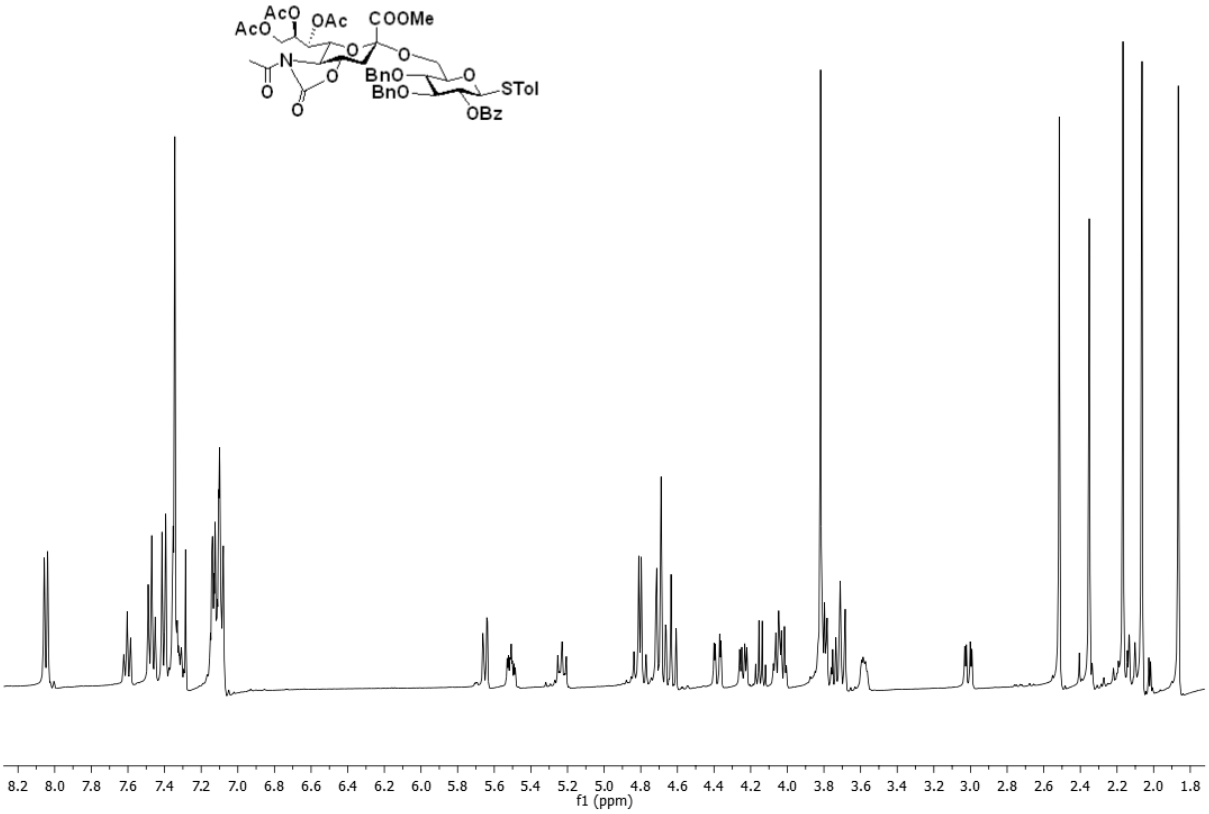
AcO
AcO
OAc
COOMe
O
N
O
O
O
BnO
BnO
O
STol
OBz
8.2 8.0 7.8 7.6 7.4 7.2 7.0 6.8 6.6 6.4 6.2 6.0 5.8 5.6 5.4 5.2 5.0 4.8 4.6 4.4 4.2 4.0 3.8 3.6 3.4 3.2 3.0 2.8 2.6 2.4 2.2 2.0 1.8
f1 (ppm)

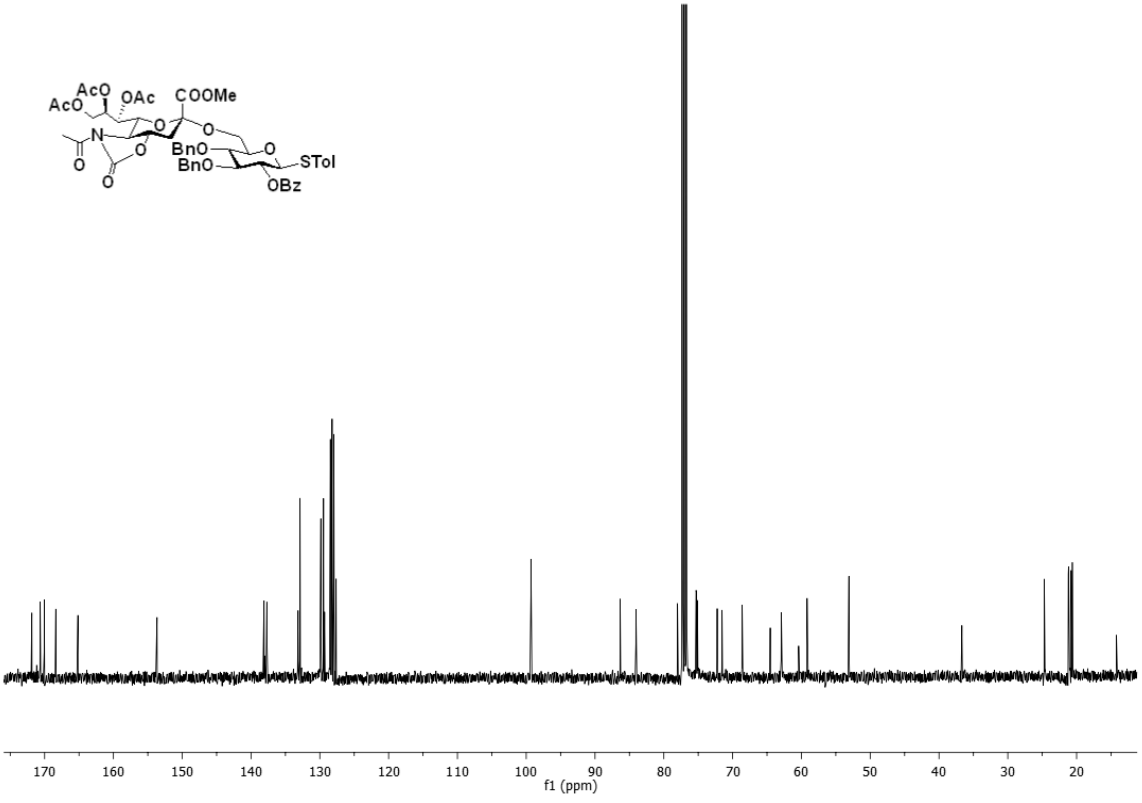
AcO
AcO
OAc
COOMe
O
N
O
O
O
BnO
BnO
O
STol
OBz
170 160 150 140 130 120 110 100 90 80 70 60 50 40 30 20
f1 (ppm)

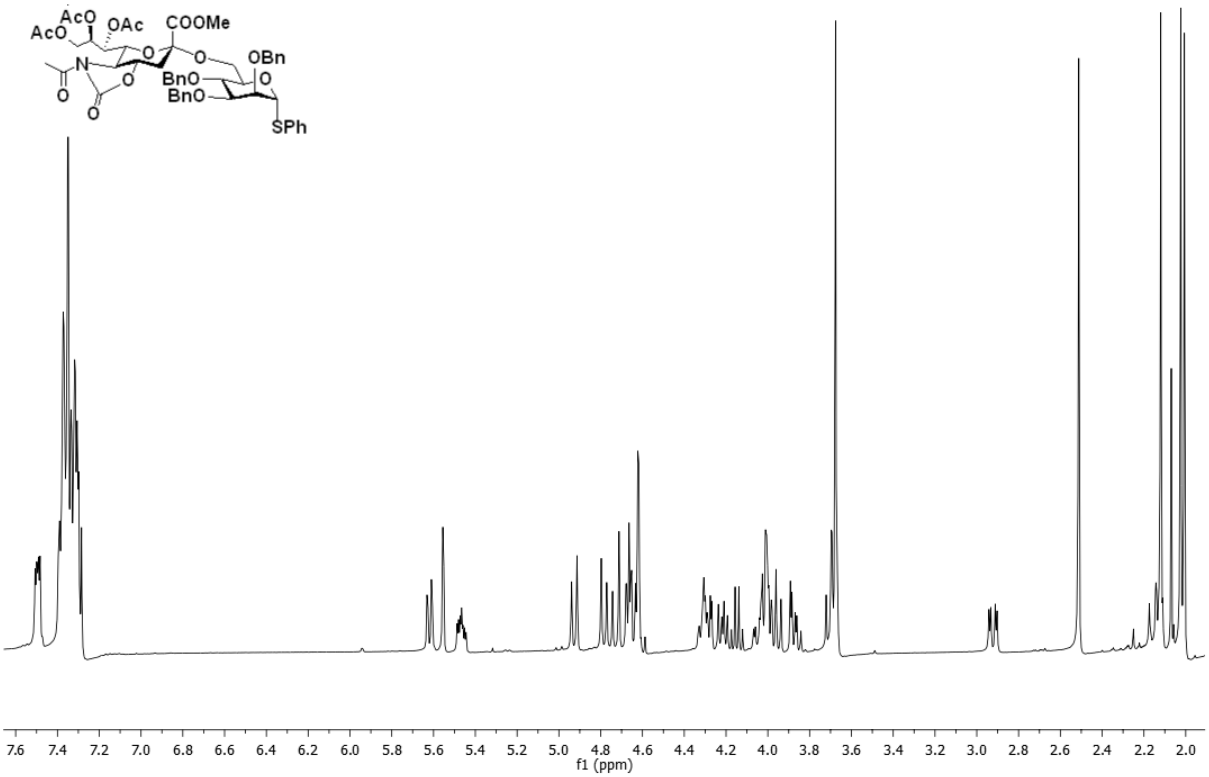
AcO
AcO
OAc
COOMe
OBn
BnO
BnO
SPh
7.6 7.4 7.2 7.0 6.8 6.6 6.4 6.2 6.0 5.8 5.6 5.4 5.2 5.0 4.8 4.6 4.4 4.2 4.0 3.8 3.6 3.4 3.2 3.0 2.8 2.6 2.4 2.2 2.0
f1 (ppm)

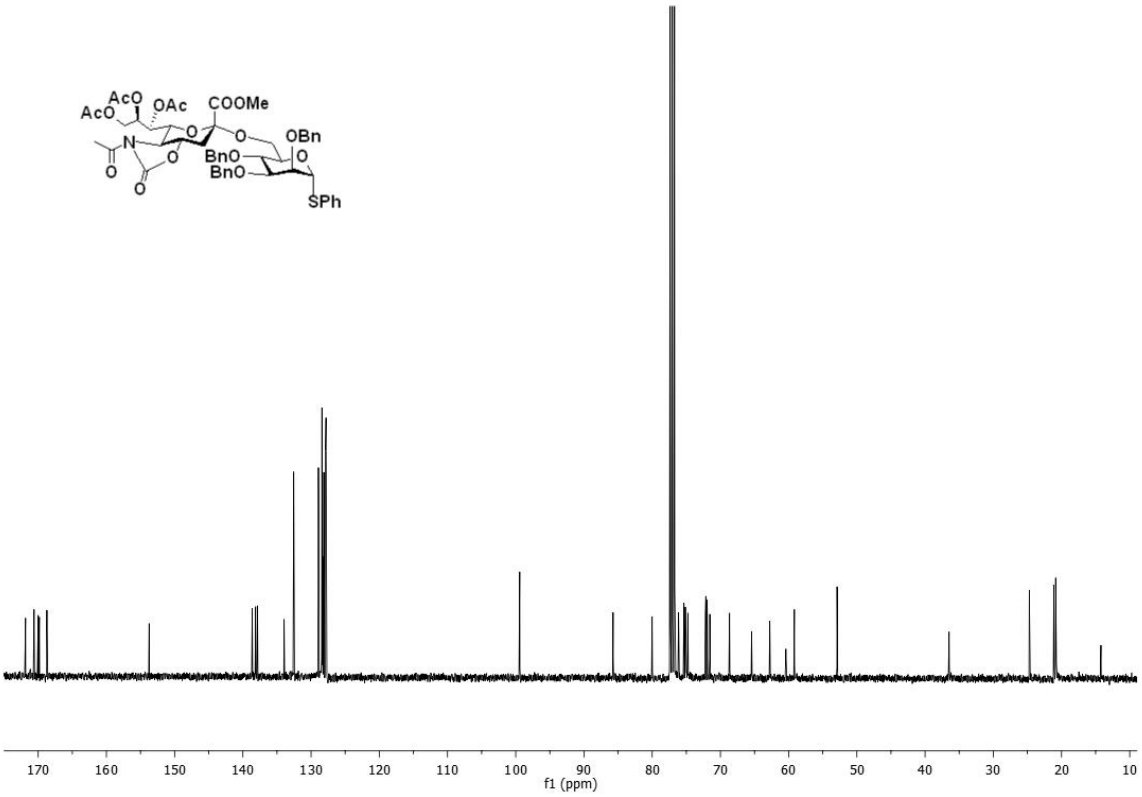
AcO
AcO
OAc
COOMe
OBn
BnO
BnO
SPh
170 160 150 140 130 120 110 100 90 80 70 60 50 40 30 20 10
f1 (ppm)

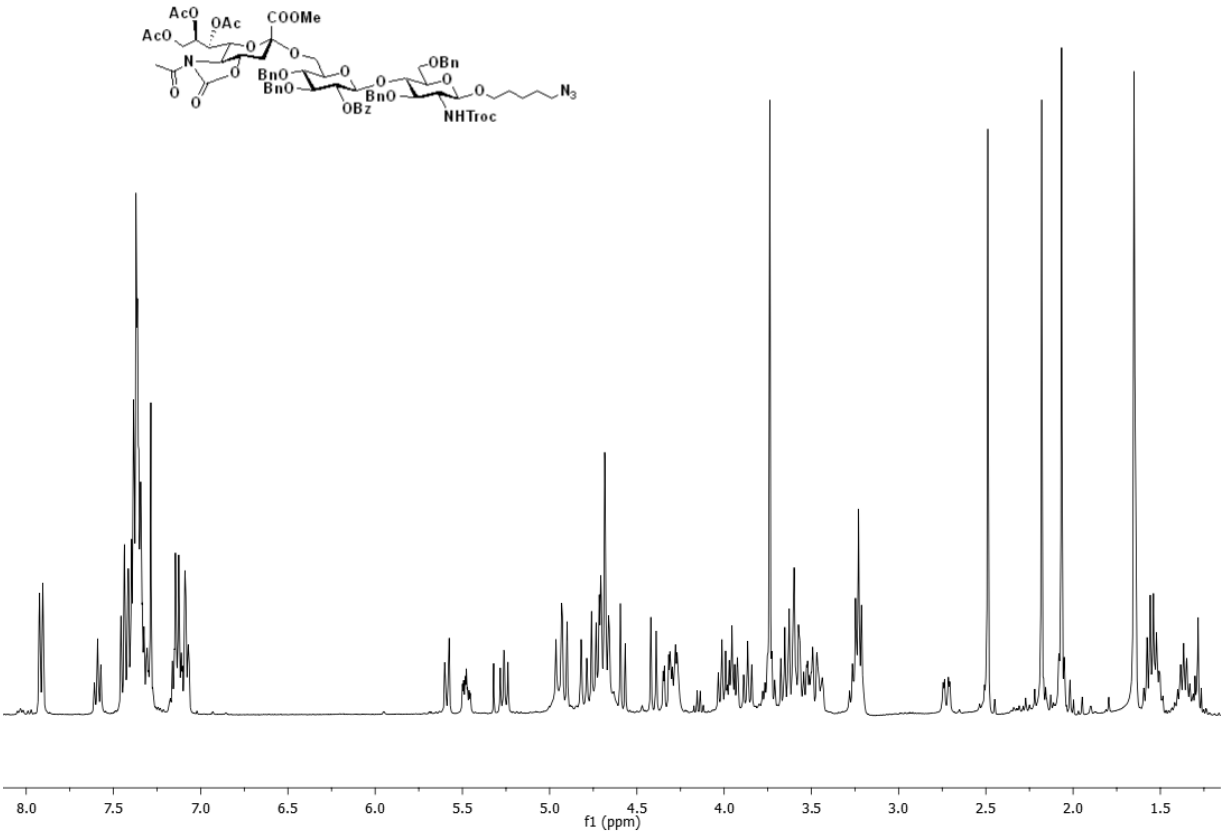
AcO
AcO
OAc
COOMe
OBn
BnO
BnO
OBz
BnO
NHTroc
N3
8.0
7.5
7.0
6.5
6.0
5.5
5.0
4.5
4.0
3.5
3.0
2.5
2.0
1.5
f1 (ppm)

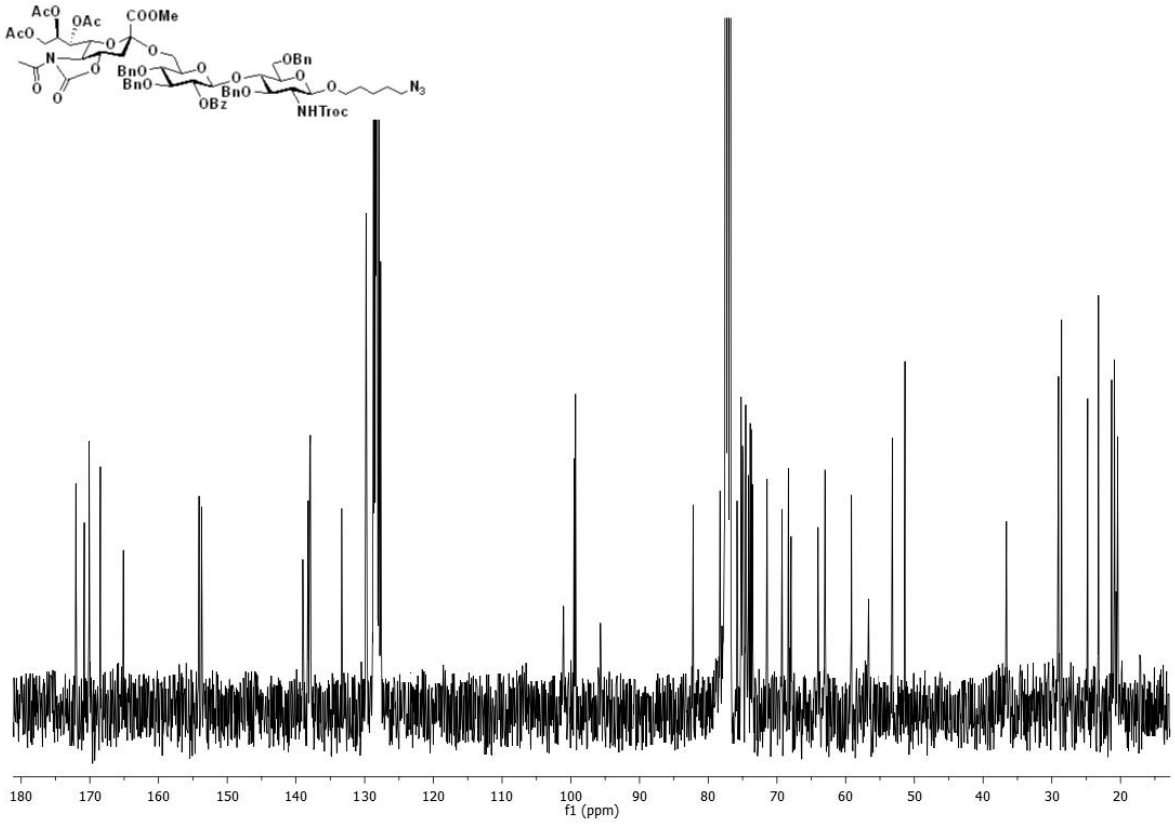
AcO
AcO
OAc
COOMe
OBn
BnO
BnO
OBz
BnO
NHTroc
N3
180
170
160
150
140
130
120
110
100
90
80
70
60
50
40
30
20
f1 (ppm)

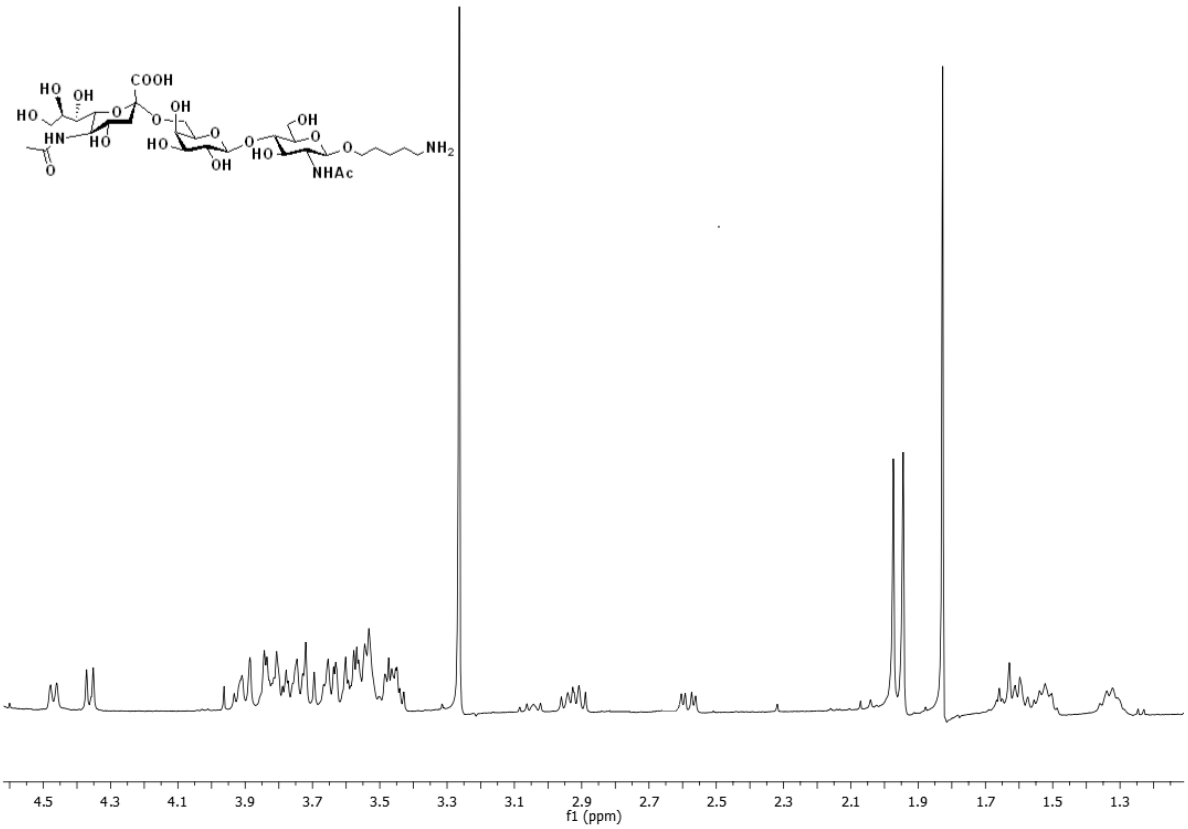
COOH
OH
HO
HN
NHAc
NH2
4.5
4.3
4.1
3.9
3.7
3.5
3.3
3.1
2.9
2.7
2.5
2.3
2.1
1.9
1.7
1.5
1.3
f1 (ppm)

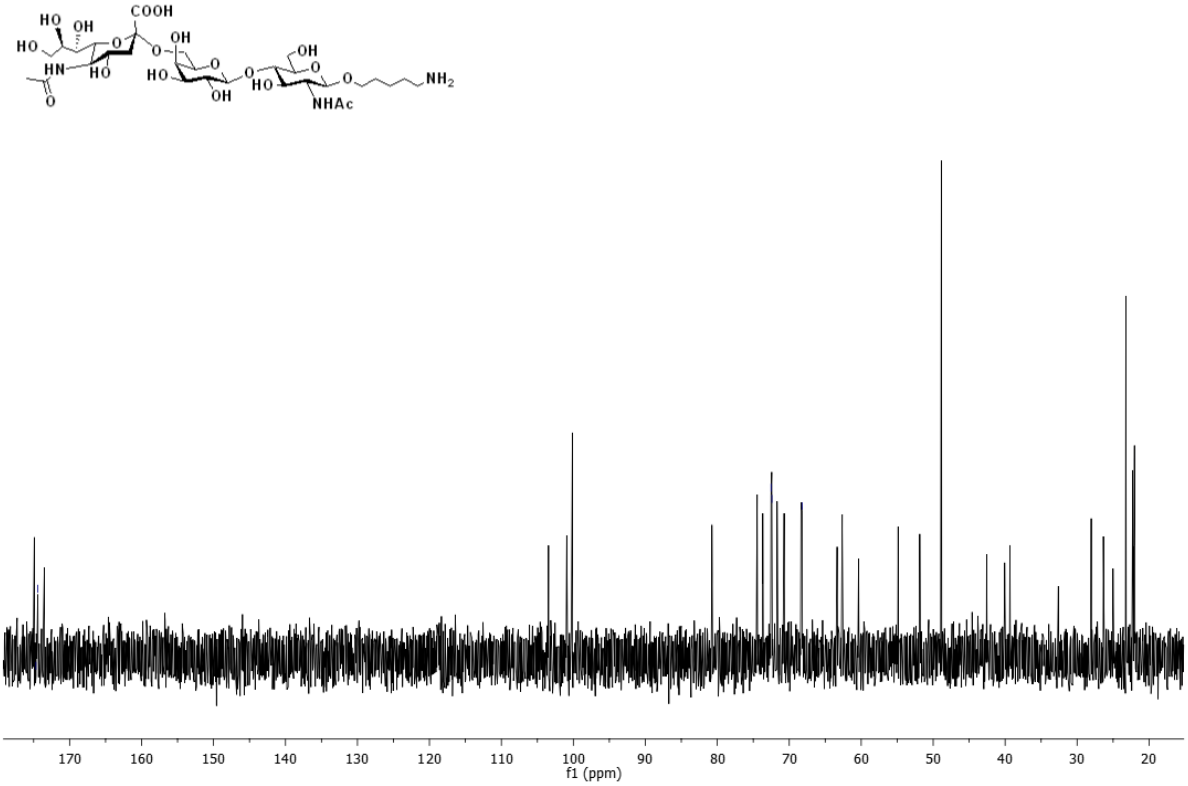
COOH
OH
HO
HN
NHAc
NH2
170
160
150
140
130
120
110
100
90
80
70
60
50
40
30
20
f1 (ppm)

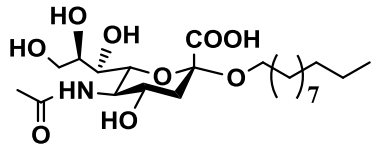
HO
OH
HO
COOH
O
O
7
HN
HO
O

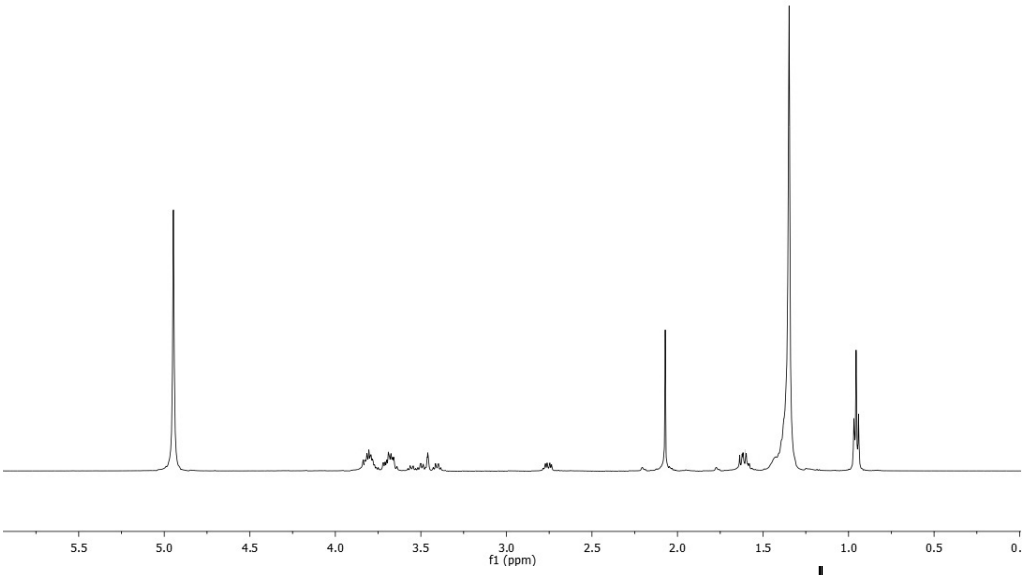
5.5
5.0
4.5
4.0
3.5
3.0
2.5
2.0
1.5
1.0
0.5
f1 (ppm)

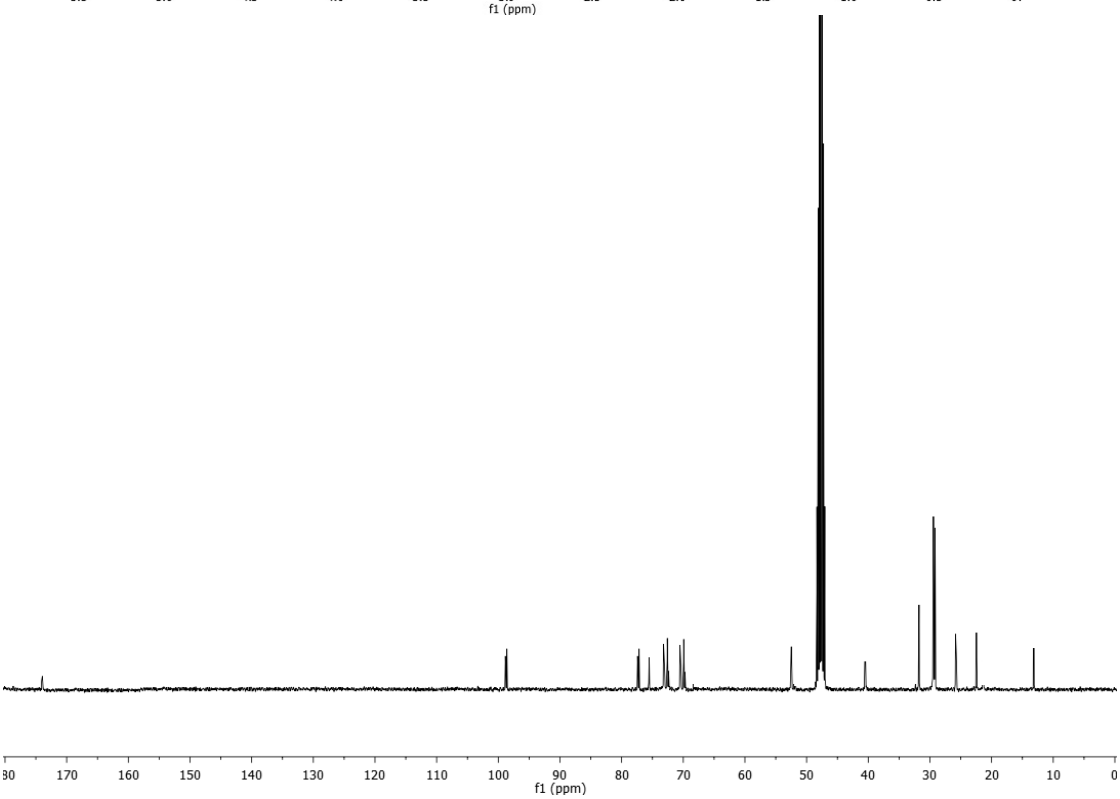
170
160
150
140
130
120
110
100
90
80
70
60
50
40
30
20
10
f1 (ppm)

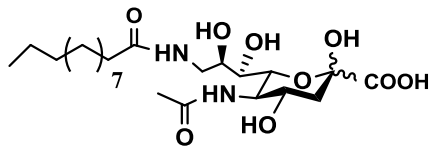
O
HO
OH
OH
HN
7
O
COOH
HN
HO
O

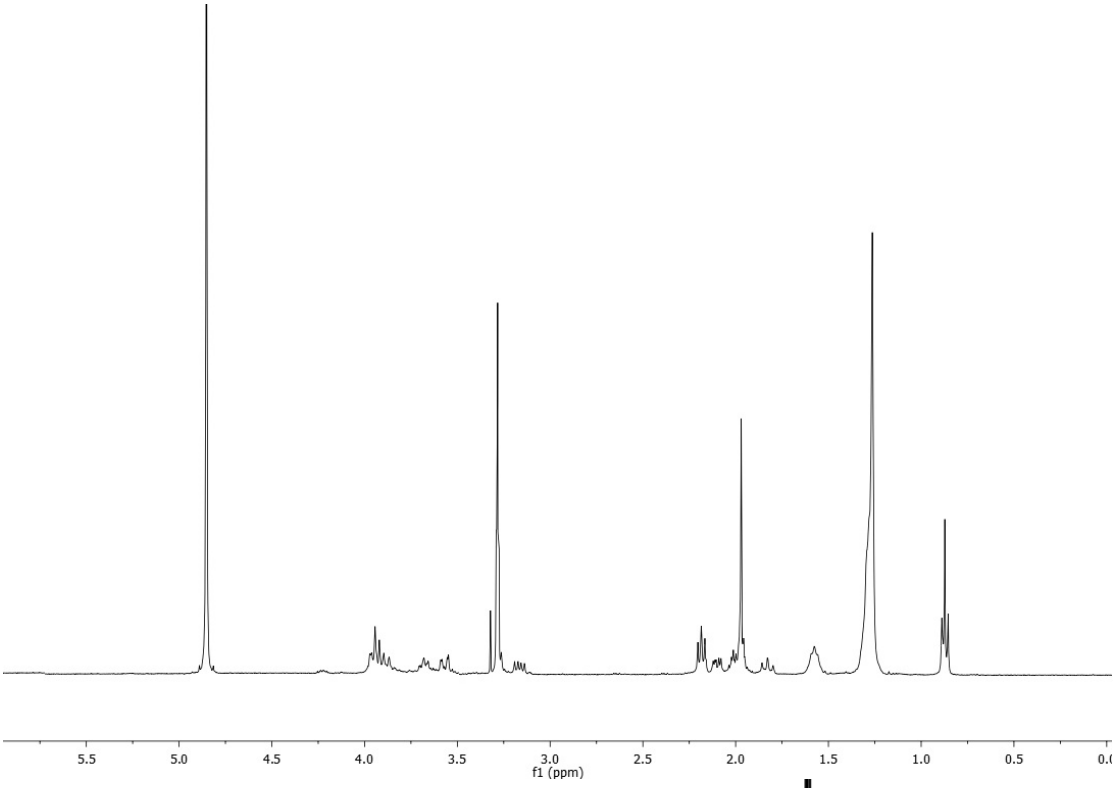
5.5
5.0
4.5
4.0
3.5
3.0
2.5
2.0
1.5
1.0
0.5
f1 (ppm)

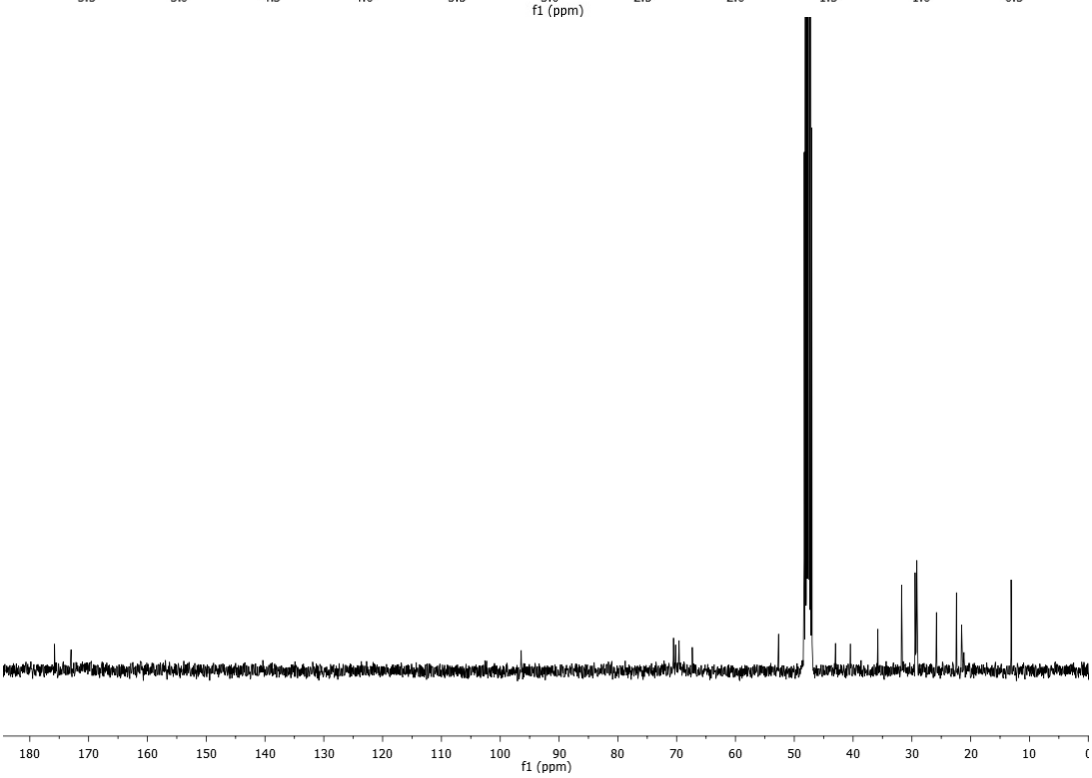
180
170
160
150
140
130
120
110
100
90
80
70
60
50
40
30
20
10
f1 (ppm)

Chapter 3

Sialic Acid Hydroxamate: A potential Antioxidant and Inhibitor of Metal Induced β-Amyloid Aggregates

3.1 Introduction

Alzheimer's disease (AD) is a progressive neurodegenerative disease, which is a growing worldwide health concern among elderly populations. It affects more than 24 million people worldwide and this number is expected to reach over 81 million by 2040.[1-4] It has been established that aggregation of *β*-amyloid (*Aβ*) peptide and elevated levels of transition metals are defining pathological hallmarks of AD.[5-9] During AD, the concentration of metal ions such as Zn(II), Fe(III) and Cu(II) in the regions of cortex and hippocampus have been observed in millimolar levels.[10-13] *Aβ* peptides aggregation *via* cross-linked dimeric species of Tyr10 or forming complex with transition metals leads to the neurotoxicity.[14-17] Moreover, redox active Fe(II/III) and Cu(I/II) can undergo Fenton reaction and there by generating reactive oxygen species (ROS) such as hydrogen peroxide and hydroxyl radicals.[18-19] and these free radicals readily cause oxidative damage to the biological molecules triggering neurodegeneration.

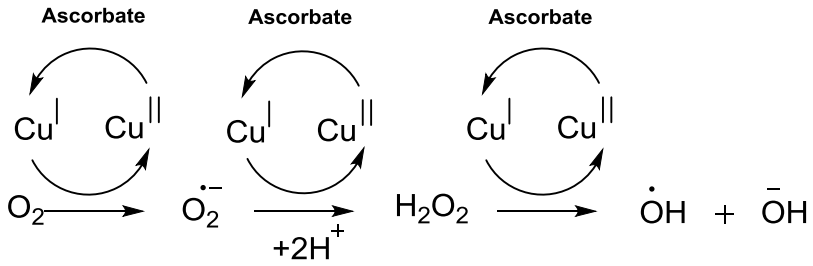

Figure 1. Redox cycling of metal ion and reactive oxygen species generation.

In an effort to control the unevenly distributed metal ions, chelation therapy has been reported to minimize neurotoxicity.[20] To date, several metal chelators such as EDTA (N,N'-1,2-ethanediylbis[N-(carboxymethyl)]glycine), des-ferrioxamine (DFO), clioquinol (CQ, 5-chloro-7-iodo-8-hydroxyquinoline), DF (1,2-dimethyl-3-hydroxy-4(1H)-pyridinone) and an 8-hydroxyquinoline derivative (PBT2) have been used as chelating agents for AD.[21-22] In addition to metal chelators, some bifunctional ligands have also been designed to improve their uptake across the blood-brain barrier (BBB) and simultaneously bind to *Aβ*. For example, EDTA, CQ, or cyclen (cyc, 1,4,7,10-tetraazacyclododecane) chelators were conjugated to ThT, the KLVFF peptide, curcumin, IMPY, and p-I-stilbene (ThT); curcumin; IMPY; p-I-stilbene, a known *Aβ* interaction scaffold to improve the bioavailability.[23-26] Alternatively, metal chelators were glycoconjugated to elevate brain uptake by exploitation of the sugar transport system in the

BBB.[27-30] Sialic acid (Sia) glycans have also been used as a potential *Aβ* recognizing marker.[31-35] Despite well-documented Sia glycans & *Aβ* interactions, therapeutic potentials of sialic acid mimics in AD has not been exploited and/or reported.

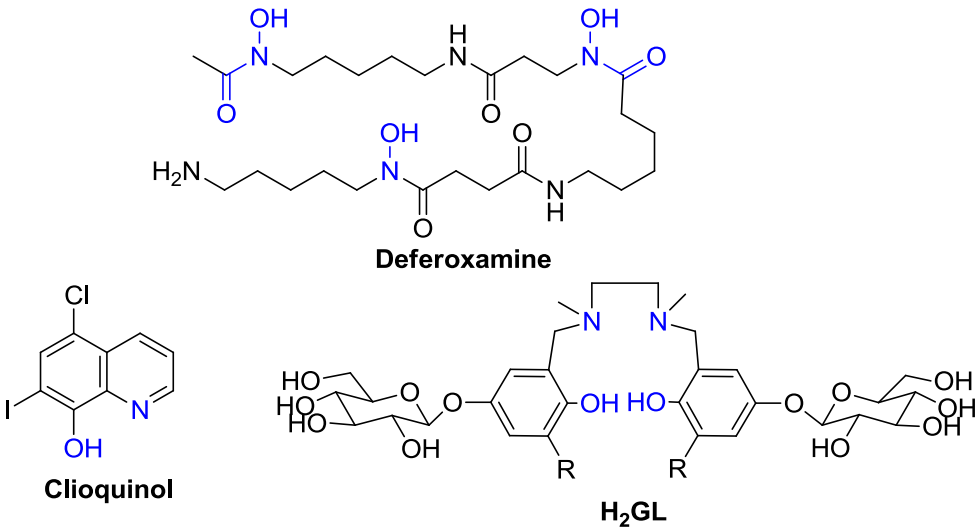

Figure 2. Potential therapeutic molecule to target Alzheimer disease.

Here, we propose to develop Sia mimics, which together with acting as an antioxidant is also capable of chelating metal ions. Moreover, the presence of Sia backbone enhances specific recognition and simultaneously prevents aggregation of *Aβ*.

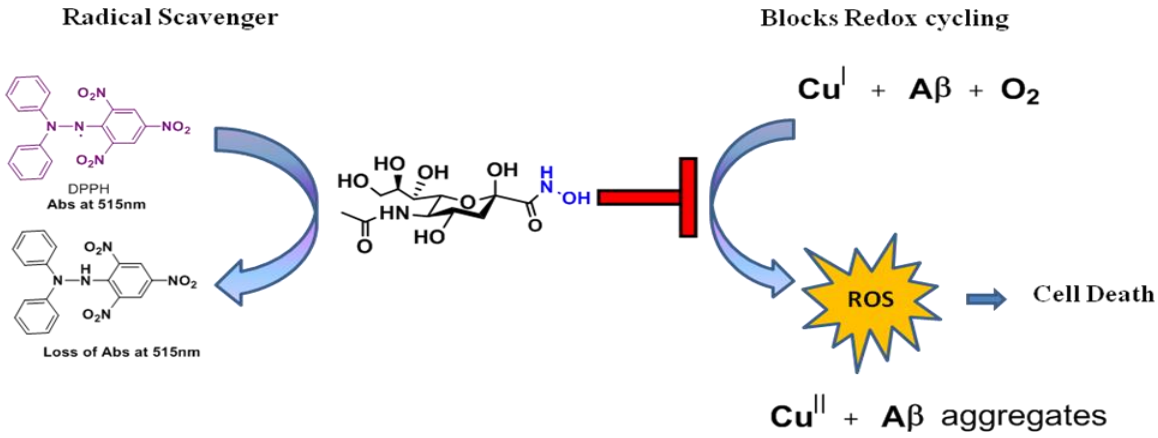

Figure 3. Sialic hydroxamate analogue minimizes the oxidative stress by radical scavenging and metal chelation.

Sias are acidic sugars typically terminating at the outer ends of the cell surface glycan structures. Liu and co-workers have reported that the replacement of carboxylic acid group of glucoronic acid by hydroxamic acid moiety can confer antioxidant properties.[36] Using this approach, galactoronic acid and glucosaminoglycans were synthetically modified into hydroxamate derivatives and have been reported of their antioxidant activity.[37] Moreover, hydroxamate ligands are one of the potential transition metal chelators.[38-40] Hence, we hypothesized that Sia hydroxamate might exert antioxidant properties and metal binding properties for AD treatment. Previously, Sia hydroxamates have been reported as potential scaffolds to validate the significance of the carboxylic acid residue in Sia-lectins binding and enzymatic activities.[41-43] However, to the best of our knowledge, the applications of Sia hydroxamate in AD treatment has not been reported.

Results and Discussion.

3.2 Synthesis of sialic acid hydroxamate analogs

Sia analogs (**43** to **48**) (Scheme 1) were synthesized according to a modified literature procedure.[41-43] The hydroxamic acid moieties were introduced by coupling **29** or **45** with *O*-benzyl hydroxylamine hydrochloride, followed by hydrogenation to obtain **46** and **48**.

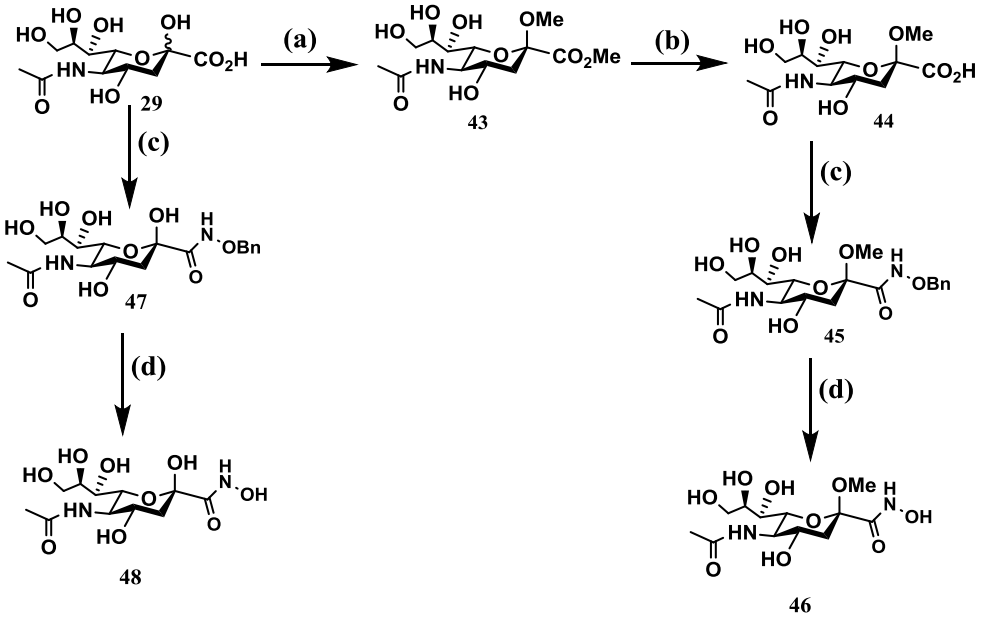

Scheme 1. (a) 50 dowex/MeOH; (b) NaOH/MeOH; (c) EDC/NH_2-OBn.HCl/DMF; (d) H_2/$Pd(OH)_2$-C/MeOH.

3.3 Study of radical scavenging and antioxidant property by DPPH assay

The antioxidant properties of Sia analogs were tested by DPPH assay, and Fenton reaction based cytotoxicity studies. In the DPPH assay the color change from purple to yellow in the presence of the radical scavenger, and their absorption at 517 nm indicated the amount of compound being antioxidant in nature.[44] The radical scavenging assay was performed with various concentrations of **29**, **44**, **46** and **48** were compared with ascorbic acid-*β*-hydroxamate and water as positive and negative controls respectively (fig 4). In this study, we have used the Sia analogs (**29, 44, 46** and **48**) at concentration ranges from 1.0-0.001 mM (fig. 4). Upon addition of Sia analogs, we observed a concentration dependent radical quenching, indicating that the antioxidant potential of Sia hydroxamate in successfully trapping the DPPH free radicals. The IC_{50} of scavenging activity of **46** and **48** was 84 μM and 380 μM respectively, indicating the resonance of the hydroxamic acid moiety of Sia might have contributed to the radical scavenging activities. In contrast, 29 did not exhibit any antioxidant activity.

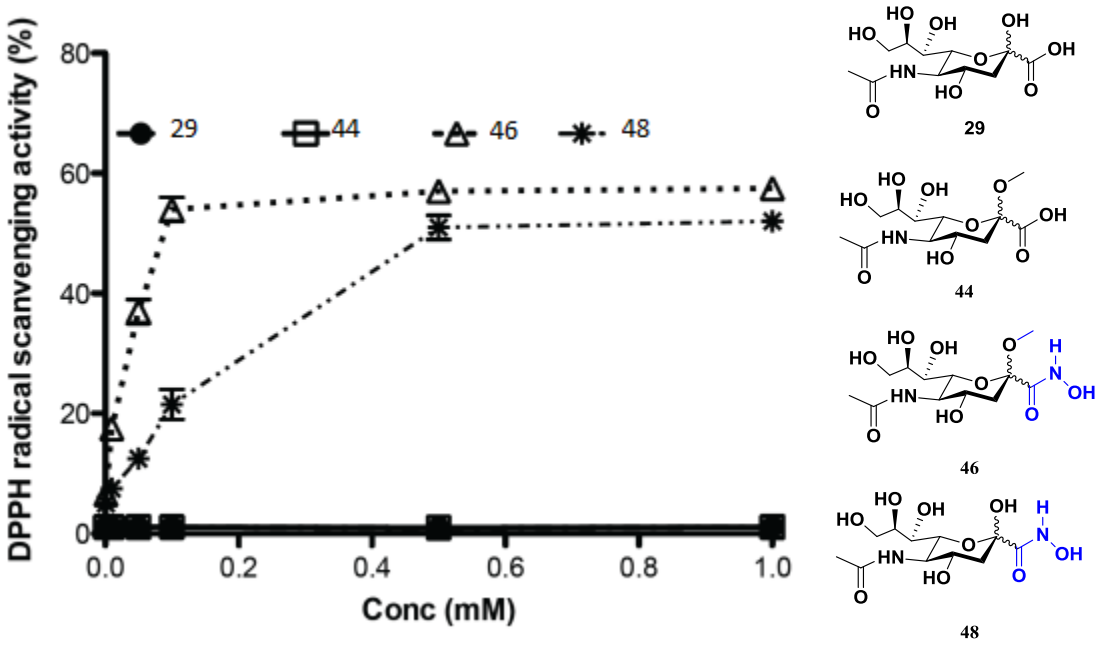

Figure 4. The DPPH scavenging activities of different concentrations of **29, 44, 46** and **48**. Mean values of triplicates were considered. The scavenging activity of DPPH radicals (%) was calculated using the equation: $(A_{517blank} - A_{517sample}) \div (A_{517blank}) \times 100$. The IC_{50} of scavenging activity of aspartic acid β-hydroxamate was 36 μM.

3.4 Study of protective effect of sialic acid analogues MTT assay

To investigate the protective abilities of these sugars, cervix cancer (HeLa) and glioblastoma (LN229) cell lines were chosen as models. These cells were previously used to demonstrate a

remarkable sensitivity to Fenton reaction.[45-46] In the present work, both the cells were seeded in 96-well plates respectively, and after 24 hours of attachment, the cells were incubated with the Sia analogs (**29**, **46** and 4**8**) at different concentrations for another 24 h. A fenton reaction (50 μM $FeSO_4$ and 0.75 mM H_2O_2) was initiated, and after 2 h of incubation, MTT assay was performed to measure the percentage of cells survived. Figure 6 shows the protective effect of Sia analogs on hydroxyl radical induced cell death in HeLa and LN229 cells. As can be seen from the fig 6a, increasing concentrations of Sia hydroxamate analogs exerted a strong protective effect against the hydroxyl free radical induced cell death compared to **29**. The IC_{50} of 48 in HeLa cells was found to be 80 μM compared to **46** having IC_{50} ~ 380 μM. While a similar experiment with LN229 cells showed a strong protection offered by Sia analogs against hydroxy radical induced cell injury (IC_{50} ~ 360 μM and 57 μM for 46 and 48) compared to HeLa cells (fig. 6b). Interestingly these results are comparable to desferrioxamine (DFO) (IC_{50} ~ 98 μM in LN229 and 92 μM in HeLa cell lines), a natural radical scavenger. Overall, these results suggest that **46** and **48** protect cells from oxidative stress, which might trigger neurodegradation.

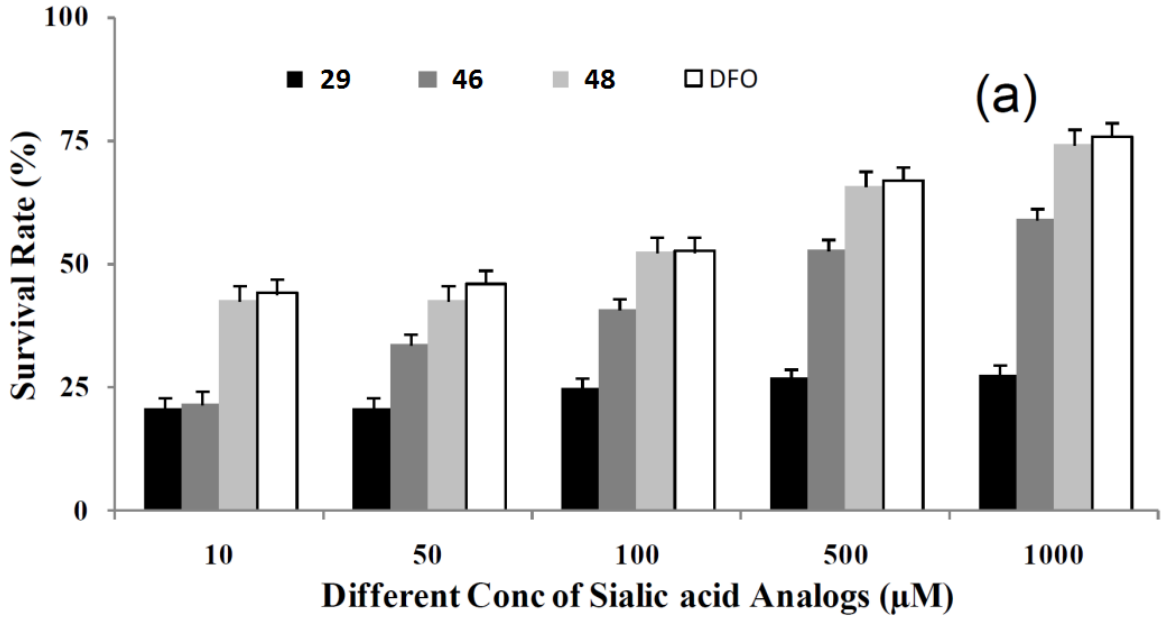

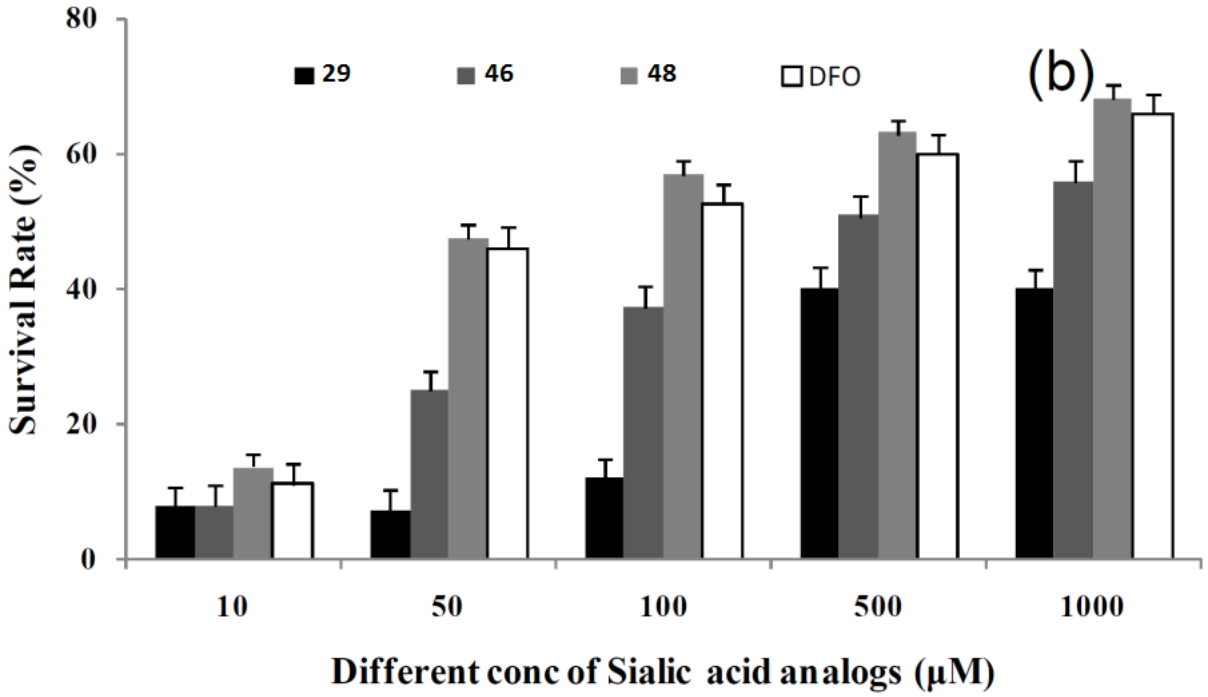

Figure 6. The protective effect of **29**, **46** and **48** as determined by MTT assay. Cells were treated with $FeSO_4$ (50 μM) and H_2O_2 (750 μM) in the presence of different conc of Sia analogs (a) HeLa cells and (b) LN229 cells; cells without and with Fenton reagent were considered as positive (100% protection) and negative (0% protection) controls respectively. Relative survival rates were calculated by $(O.D_{control} - O.D_{sample}) \div (O.D_{control} - O.D_{fenton}) \times 100$. (Note: Sia analogs as such didn't show any toxicity). Data are given as mean ± s.e.m. (n = 10).

3.5 Sedimentation assay

In addition to oxidative stress, it has been suggested that Zn(II) and Cu(II) mediated A*β* aggregation are also involved in neural toxicity and AD. The best way to inhibit the A*β* aggregation is by chelating the Zn(II) and Cu(II) ions. The metal binding properties of Sia-mimics were established by mass spectra. Both **46** and **48** was found to bind to Cu(II) and Zn(II) ions effectively. Moving forward to establish the inhibition of *Aβ* aggregation, we carried out sedimentation assay of A*β*. Freshly prepared *Aβ* (10 μM) was treated with Cu(II) or Zn(II) (10 μM) or no metal (as control) for 24 h and subsequent incubation of Sia-mimics (20 μM) for another 24 h at 37°C. The samples were centrifuged at 12,000 g for 10 mins. The supernatant fractions were removed and collected separately, and the pellets were resuspended in sample buffer containing 0.5 M (Tris/HCl, pH 6.8, 5% glycerol, 0.005% bromophenol blue, 2% SDS and 5% 2-mercaptoethanol). Samples were boiled for 5 min, centrifuged and analyzed by 12% SDS-PAGE (fig. 7b). Similarly, supernatant fractions were also analyzed (fig 7a).

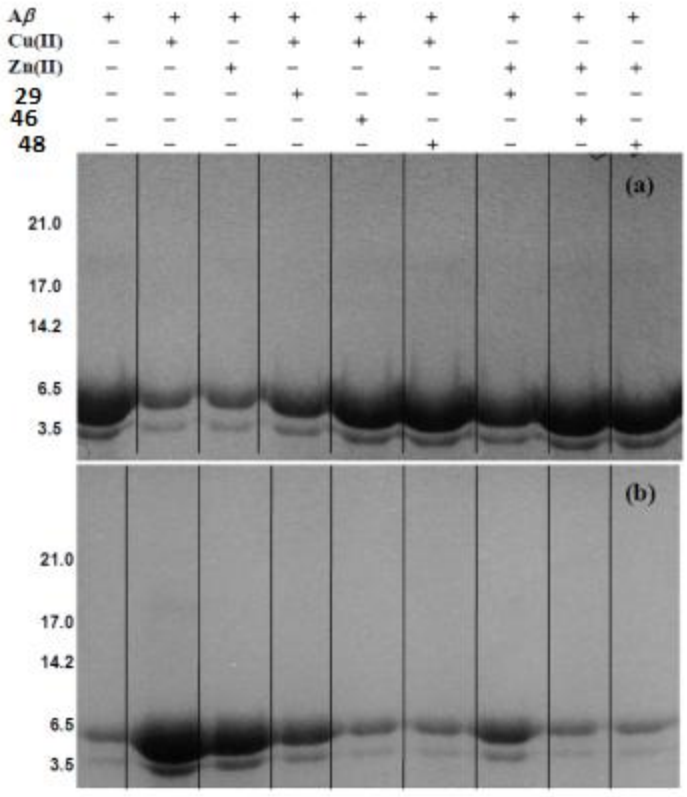

Figure 7. SDS-PAGE of sedimentation assay carried out with Aβ in presence of different compositions of metals and sia-mimics. (a) supernatant (b) precipitate.

As expected, the sharp bands between 3.5-6.5 kDa correspond to Aβ mono and dimeric forms. After 48 h of incubation, most of the Aβ peptides were found in supernatant (fig. 7a). In the presence of metals (Zn(II) and Cu(II)) Aβ band was observed in precipitate, suggesting that the majority of the peptides had been converted to aggregates and during SDS these aggregates regained its native structure (fig. 7b, lane 2 and 3). In the presence of Cu(II) or Zn(II) and **46** or **48**, maximum amount of protein was found in supernatant compared to **29** (fig. 7a lane 4-9), indicating that Siamimics chelated Zn(II) and Cu(II) ions and regenerated Aβ primary structure. These results were further supported by turbidity assay. Briefly, in a 96-well plate, Aβ (25 µM) in 50 mM phosphate buffer (pH 7.4), 25 µM of Cu(II) or Zn(II) or no metal were added and absorbance was measured at 405 nm. To these solutions, **29**, **46** and **48** were added and agitated for 1 min and measured the aggregation at 405 nm. As shown in the figure 8, in the presence of **29**, nearly 35% of the Aβ recovered the primary structure, where as in presence of **46** or **48**

around 75% of the A*β* regained the original structure. Overall, turbidity and sedimentation assays demonstrated the ability of **46** and **48** to modulate the aggregation of A*β*. Finally, scanning electron microscopy (SEM) was used to visualize the morphological features of the A*β* complexes. As expected, addition of **46** and **48** to A*β* -Cu(II) triggered modulation of the A*β*-aggregates.

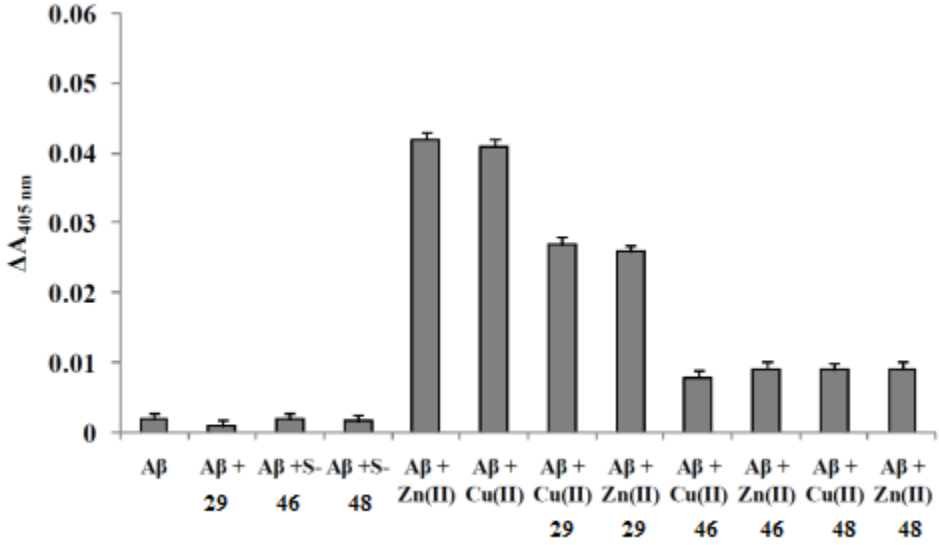

Figure 8. Effect of sia-mimics on metal ions induced A*β* aggregation. Data represent mean ± S.D; n = 3.

3.6 Cell viability assay

We next determined the ability of Sia analogs to attenuate neurotoxicity arising from metal–*Aβ* species in human neuroblastoma SH-SY5Y cells.The cytotoxicity of the metal ions and Sia analogs were measured by incubating the cells with metal ions alone (10 μM), *Aβ*-sia complexes or Sia analogs (50 μM) alone for 24 h. MTT assay of these complexes revealed no toxicity (fig 9). Where as, cells incubated with *Aβ* (10 μM) and with $CuCl_2$ or $ZnCl_2$ (10 μM) for 24 h showed a reduction in the cell survival rate (77(±3) % and 69(±3) %, respectively. The *Aβ*–metal complexes-induced neurotoxicity was rescued by Sia analogs (50 μM), suggesting the ameliorative effects of Sia hydroxamate on *Aβ*-metal complexes-induced cytotoxicity. Based on all the above results, we conclude that the antioxidant, metal chelation and sialic acid backbone of 46 and 48 protects the neuroblastoma cells from toxic *Aβ*-metal complexes. These results are comparable to other *Aβ* metal chelators.[48-50]

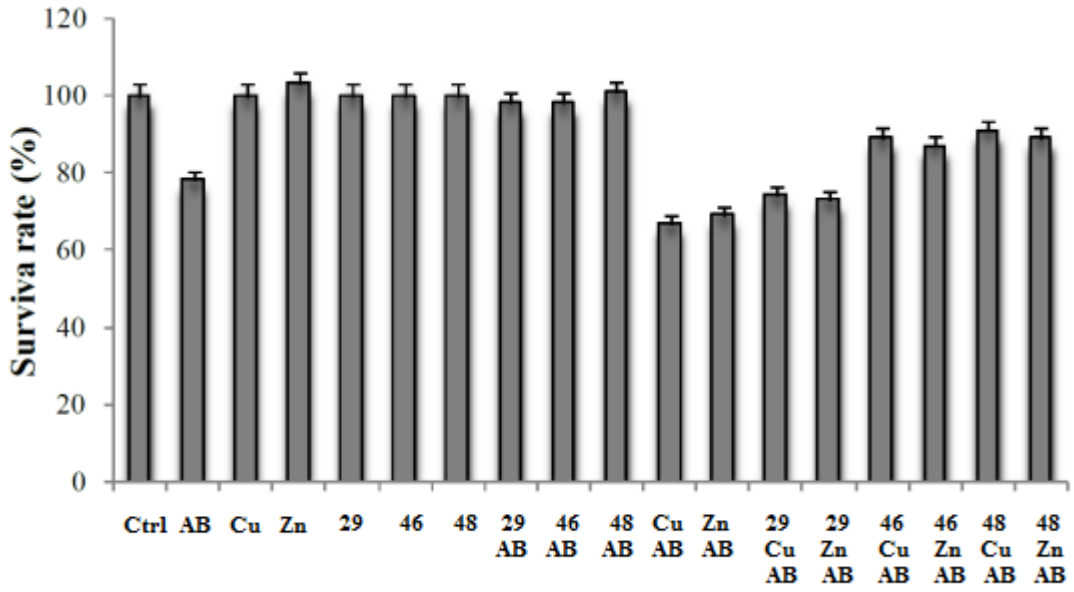

Figure 9. Protective effects of 29, 46 and on SH-SY5Y cells as determined by MTT assay. Cells were treated with *Aβ* (10 μM), $CuCl_2$ or $ZnCl_2$ (10 μM), *Aβ* + metal (1:1) complex (10 μM) and Sia derivatives (50 μM).

3.7 Conclusion

In this investigation, we have shown that Sia hydroxamate possess three important properties: antioxidant nature, metals chelating ability and Sia backbone to target AD. Focusing on cytotoxicity caused by radicals and *Aβ*-metal complexes, we demonstrated that **46** and **48** protects the neural cells more effectively in comparison to **29**. Overall, to the best of our knowledge, the results in this work are the first to demonstrate the reactivity of Sia hydroxamate towards metal-associated *Aβ* species. Moreover, it has been shown that Sias on cell surfaces can be bioengineered with unnatural Sia analogs using its biosynthetic pathways. Current investigations are aimed at bioengineering the neural cell surfaces with Sia hydroxamate to treat A*β* aggregation and metal overloading in brain.

3.8 Materials and Methods

3.8.1 General Information

Sialic acid was purchased from carbasynth Ltd. All other chemicals used were reagent grade and used as supplied except where noted. Analytical thin layer chromatography (TLC) was performed on Merck silica gel 60 F254 plates (0.25 mm). Compounds were visualized by UV irradiation or dipping the plate in CAN solution followed by heating. Column chromatography was carried out using force flow of the indicated solvent on Fluka Kieselgel 60 (230–400 mesh).

^{1}H and ^{13}C NMR spectra were recorded Jeol 400 MHz (or 100 MHz for 13C) using residual solvents signals as an internal reference ($CDCl_3$ δ H, 7.26 ppm, δ c 77.3 ppm and CD_3OH δ H 3.31 ppm, δc 49.0 ppm). The chemical shifts (δ) are reported in *ppm* and coupling constants (*J*) in Hz. DMEM media and 3-(4,5-dimethylthiazol-2-yl)-2,5-diphenyltetrazolium bromide (MTT) were purchased from Invitrogen and sigma-aldrich respectively. HeLa, LN229 and SH-S5SY cells were gifted by Dr. P Shashtri from the National Centre for Cell Science (NCCS), Pune, India. $A\beta_{1\text{-}40}$ peptide was purchased from Sigma Aldrich. SEM measurements were done on the JEOL JSM-5600 LV SEM.

3.8.2 DPPH Assay

Radical scavenger assay was performed using literature produce.[3] Briefly, 0.3 ml of 29 to 48 (0.001, 0.01, 0.05, 0.1, 0.5, 1.0, and 1.2 mM) was added to 0.1 ml of 1 M Tris–HCl buffer (pH 7.9), and mixed for 20 min with 0.6 ml of 100μM DPPH in methanol to give a final concentration of 60 μM. The mixing was carried out under light protection at room temperature. The decrease in absorbance at 517 nm was measured and expressed as A_{517}. Deionised water was used instead of sample solution as the blank. All samples were measured in triplicate and the means were calculated. The scavenging activity of DPPH radicals (%) was calculated using the equation:

$(A_{517blank} - A_{517sample}) \div (A_{517blank})$ X 100.

IC_{50} represents the half-inhibition concentration.

3.8.3 Cell viability assay

Approximately 5000 HeLa and Ln229 cells per well (100 μL) in DMEM were seeded in a 96-well microtitre plate and allowed to attach overnight in a 5% CO_2 incubator at 37 °C. Cells were then treated with **29, 46, 48** and DFO with different concentrations (10, 50, 100, 500 and 1000 μM) and incubated for 24 h in 5% CO_2 at 37 °C. After that, 0.75 mM H_2O_2 and 50 μM $FeSO_4$ solution were added and incubated for 2 h. Media from all the wells were aspirated and 20 μL of MTT reagent from a stock solution of 5 mg mL^{-1} in PBS was added to each well. After incubation for 4 h in the incubator, the purple formazan crystals formed were solubilized using acidified DMSO (62.5 μL conc. HCl in 100 mL isopropanol) and the absorbance was measured at 570 nm.

3.8.4 Amyloid-β (Aβ) peptide experiments

Aβ samples were prepared according to the previously reported literature procedure. Briefly, The *Aβ* peptide was dissolved in 1% NH_4OH (w/v, aq), lyophilized,and stored at –80°C. Concentration of the Ab peptide was quantified by using tyrosinate residue as described in literature.[52]

3.8.5 Sedimentation assay

Sedimentation assay of A*β* was performed as described by Atwood et al.[52] Briefly, 100 μM of A*β* stock solution was prepared in 50 μM phosphate buffer (pH 7.4). From the stock 10 μM of A*β* was treated with 10 μM $ZnCl_2$ or $CuCl_2$ or no metals. After incubation at 37°C for 24 h, sia analogs (20 μM) were added and incubated for another 24 h at 37°C. The resultant sample were centriguated at 12,000 g in microcentrifuge for 10 mins. After centrifugation, the supernatant and pellets were separated. The supernatant was lyophilized and dissolved in sample buffer (100 μl) containing 0.5 M Tris/HCL, pH 6.8, 5% glycerol (v/v), 0.005% bromophenol blue, 2 % SDS and 5% 2-mercaptoethanol. Samples was boiled for 5 mins and analyzed by SDS-PAGE using literature procedure. Similarly, pellets were also dissolved in sample buffer (100 μl) and SDS-PAGE was performed as reported above. Both the gels were socked in fixing solution for 1 h, followed by coomassie blue staining.

3.8.6 Turbidity assay

Turbidity assay of A*β* was measured as described by Huang et al. [53] Briefly, in a 96-well plate, a solution of (100 μl) of 25 μM of Aβ in 50 μM phosphate buffer (pH 7.4) was reacted with $CuCl_2$ or $ZnCl_2$ (25 μM) . The absorbance at 405 nm was monitored at 1 min interval using standard microplate reader. After 10 mins of agitation by orbital shaking, **29** or **46** or **48** (50 μM) was added and agitated for 30 s and absorbance was recorded after every 1 min. The average value of the absorbance was subtracted by the sample buffer (phosphate buffer pH 7.4) and the differences in absorption were recorded. Each value represent an average of n =20 readings.

3.8.7 Cytotoxicity (MTT) assay

As described above, Human neuroblastoma SH-SY5Y cells were cultivated in DMEM and treated with Aβ (10 μM) and $CuCl_2$ or $ZnCl_2$ (10 μM), followed by **29, 46** and **48** (50 μM). Cytotoxicity assay was carried out as mentioned above.

3.8.8 Synthetic procedure and spectroscopic details of sialic acid analogs

General procedure A: To a solution of sialic acid derivative (1eq) in DMF at 0^{o}C was added *O*-benzyl hydroxylamine hydrochloric acid (1.0 eq) and EDC (1.2 eq) . After stirring at 0^{o}C for 1 h and a further 24 h at RT, the mixture was concentrated *in vacuo*. The residue was purified by column chromatography on silica gel.

General procedure B: $Pd(OH)_2/C$ (10% wt) sialic acid derivatives (1 eq) was dissolved in methanol (5 mL) under Ar(g) at room temperature. The resulting reaction mixture was degassed and the flask filled with H_2 gas, after which the reaction was run at room temperature and pressure for 12 hours under a hydrogen atmosphere. The reaction mixture was filtered through Celite and concentrated under reduced pressure. The residue was purified by sephadex G-25 column.

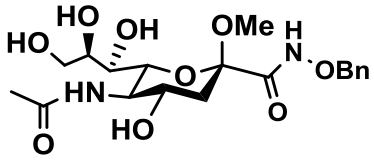

***O*-Benzyl (methyl 5-acetamido-3,5-dideoxy-D-*glycero*-D-*galacto*-2-nonulopyranoside) hydroxamate (45):** General procedure A with **44** (200 mg, 0.62 mmol), *O*-benzyl hydroxylamine HCl (100 mg, 0.63 mmol) and EDC (144 mg, 0.75 mmol), followed by column chromatography on silica gel using DCM : MeOH (5:1) yielded (170 mg , 65%); R_f = 0.7 (DCM : MeOH, 5:1); ^{1}H-NMR (400 MHz, MeOD): δ 7.59 (d, J = 8.1 Hz, 1H), 7.40 – 7.21 (m, 4H), 4.85 – 4.74 (m, 3H), 3.89 – 3.73 (m, 1H), 3.73 – 3.59 (m, 3H), 3.59 – 3.46 (m, 3H), 3.42 (d, J = 9.2 Hz, 1H), 2.76 (s, 3H), 2.06 (dd, J = 13.1, 5.0 Hz, 1H), 1.87 (s, 3H), 1.42 (dd, J = 13.1, 11.3 Hz, 1H); HRMS m/z calc'd for $C_{19}H_{28}N_2O_9$ ($M+1^+$): 429.1795; found: 429.1799.

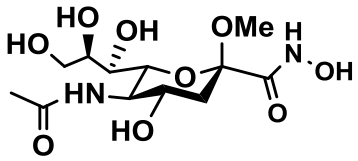

***N*-*Hydroxyl* (methyl 5-acetamido-3,5-dideoxy-D-*glycero*-D-*galacto*-2-nonulopyranosid) amide (46):** General proceudre B with comp **45** (50 mg, 0.12 mmol) and purification by sephadex G-25 column using water yielded (15 mg , 39%); ^{1}H-NMR (400 MHz, MeOD): δ 3.96 – 3.82 (m, 1H), 3.71 – 3.62 (m, 3H), 3.58 – 3.48 (m, 3H), 3.42 (d, J = 9.2 Hz, 1H), 2.84 (s, 3H), 2.23 (dd, J = 13.1, 5.0 Hz, 1H), 1.89 (s, 3H), 1.53 (dd, J = 13.1, 11.3 Hz, 1H). HRMS m/z calc'd for $C_{12}H_{22}N_2O_9$ ($M+1^+$):338.1325; found: 338.1322.

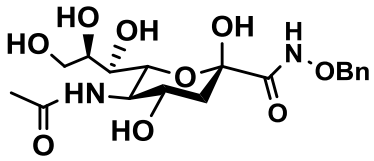

***O*-benzyl (5-acetamido-3,5-dideoxy-D-*glycero*-D-*galacto*-2-nonulopyranoside) hydroxamate (47):** General proceudre A with **29** (100 mg, 0.32 mmol), O-benzyl hydroxylamine hydrochloric acid (50 mg, 0.31 mmol) and EDC (66 mg, 0.33 mmol), followed by column chromatography on silica gel using DCM : MeOH (85: 15) yielded (67 mg , 50.3%); R_f = 0.5 (DCM : MeOH, 80: 10); ^{1}H-NMR (400 MHz, MeOD): δ 7.77 – 7.61 (dd, *J* = 19.2, 7.6 Hz, 1H), 7.48 – 7.23 (m, 4H), 4.10 – 3.98 (m, 1H), 3.83 – 3.73 (m, 3H), 3.73 – 3.64 (m, 3H), 3.64 – 3.55 (m, 2H), 3.55 – 3.43 (m, 1H), 2.24 (dd, *J* = 13.1, 5.0 Hz, 1H), 1.99 (s, 3H), 1.46 (dd, *J* = 13.1, 11.3 Hz, 1H). HRMS m/z calc'd for $C_{18}H_{26}N_2O_6$ ($M+1^+$): 414.1638; found: 414.1646.

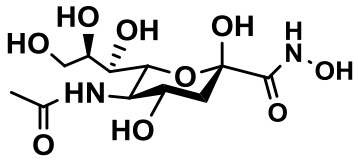

***N*-Hydroxy(5-acetamido-3,5-dideoxy-D-*glycero*-D-*galacto*-2-nonulopyranosid) amide (48):** General proceudre B with comp **47** (50 mg, 0.12 mmol) and purification by sephadex G-25 column using water yielded (17 mg , 43.5%); ^{1}H-NMR (400 MHz, MeOD): δ 4.07 – 3.93 (m, 3H), 3.86 – 3.71 (m, 2H), 3.72 – 3.56 (m, 3H), 3.48 (d, *J* = 9.2 Hz, 1H), 2.31(dd, *J* = 13.1, 5.0 Hz, 1H), 1.99 (s, 3H), 1.52 (dd, *J* = 13.1, 11.3 Hz, 1H). HRMS m/z calc'd for $C_{11}H_{20}N_2O_9$ ($M+1^+$): 325.1169; found: 325.1174.

3.9 References

1. Alzheimer's Disease International Web site: *www.alz.co.uk.media.dementia.html.* **2006**.
2. World Alzheimer's Remport 2010: *The global economic impact of dementia. Lond. Alzheimer's Disease International.* **2010**.
3. K. P. Kepp, *Chem. Rev*., **2012**, 112, 5193.
4. J. T. Pedersen, N. H. H. Heegaard, *Anal. Chem*., **2013**, 85, 4215.
5. R. Roychaudhari, M. Yang, M. M. Hoshi, D. B. Teplow, *J. Biol. Chem*., **2009**, 284, 4749.

6. A. Goate, M. C. Chartier-Harlin, M. Mullan, J. Brown, F. Crawford, L. Fidani, L. Giuffra, A. Haynes, N. Irving, L. James, R. Mant, P. Newton, K. Rooke, P. roques, C. Talbot, M. Pericak-Vance, a,. roses, R. Williamson, M. Rossor, M. Owen, J. Hardy, *Nature*., **1991**, 349, 704.
7. J. Murrell, M. Farlow, B. Ghetti, M. D. Benson, *Science*., **1991**, 254, 97.
8. A. I. Bush, W. H. Pettingell, G. Multhaup, M. D. Paradis, J. P. Vonsattel, J. F. Gusella, K. Beyreuther, C. L. Masters, R. E. Tanzi, *Science*., **1994**, 265, 1464.
9. K. J. Barnham, A. I. Bush, *Curr. Opin. Chem. Biol*., **2008**, 12, 222.
10. G. Danscher, K. B. Jensen, C. J. Frederickson, K. Kemp, A. Andreasen, S. Juhl, M. Stoltenberg, R. J. Ravid, *J. Neuroscience. Methods.*, **1997**, 76, 53.
11. D. L. Samudralwar, C. C. Diprete, B. F. Ni, W. D. Ehmann, W. R. Markesberg, *J. Neurol. Sci*., **1995**, 130, 139.
12. M. A. Deibel, W. D. Ehmann, W. R. Markesbery, *J. Neurol. Sci*., **1996**, 143, 137.
13. M. A. Lovell, J. D. Robertson, W. J. Teesdale, J. L. Campbell, W. R. Markesbery, *J. Neurol. Sci*., **1998**, 158, 47-52.
14. P Faller, C. Hureau, O. Berthoumieu, *Inorg. Chem*., **2013**, 52, 12193.
15. D. Noy, I. Solomonov, O. Sinkevich, T. Adad, K. Kjaer, I. Sagi, *J. Am. Chem. Soc*., **2008**, 130, 1376.
16. Y. Miller, B. Ma, R. Nussinov, *Proc. Natl. Acad. Sci. U. S. A*., **2010**, 107, 9490.
17. V. Tõugu, A. Tiiman and P. Palumaa, *Metallomics.*,**2011**, 3, 250.
18. X. Huang, C. S. Atwood, M. A. Hartshorn, G. Multhaup, L. E. Goldstein, R. C. Scarpa, M. P. Cuajungco, D. N. Gray, J. Lim, R. D. Moir, R. E. Tanzi, A. I. Bush, *Biochemistry*., **1999**, 38, 7609.
19. D. Jiang, L. Men, J. Wang, Y. Zhang, S. Chichenyen, Y. Wang, F. Zhou, *Biochemistry.*, **2007**, 46, 9270.
20. S. Bolognin, D. Drago, L. Messori, P. Zatta, *Med. Res. Rev*., **2009**, 29, 547.
21. R. A. Cherny, C. S. Atwood, M. E. Xilinas, D. N. Gray, W. D. Jones, C. A. McLean, K. J. Barnham, I. Volitakis, F. W. Fraser, Y. -S. Kim, X. Huang, L. E. Goldstein, R. D. Moir, J. T. Lim, K. Beyreuther, H. Zheng, R. E. Tanzi, C. L. Masters, A. I. Bush, *Neuron.*, **2001**, 30, 665.

22. P. A. Adlard, R. A. Cherny, D. I. Finkelstein, E. Gautier, E. Robb, M. Cortes, I. Volitakis, X. Liu, J. P. Smith, K. Perez, K. Laughton, Q. -X. Li, S. A. Charman, J. A. Nicolazzo, S. Wilkins, K. Deleva, T. Lynch, G. Kok, C. W. Ritchie, R. E. Tanzi, R. Cappai, C. L. Masters, K. J. Barnham and A. I. Bush, *Neuron*,. **2008**, 59, 43.
23. C. Hureau, I. Sasaki, E. Gras, P. Faller, *ChemBioChem.*, **2010**, 11, 950.
24. L. R. Perez, K. J. Franz, *Dalton Trans*., **2010**, 39, 2177.
25. L. E. Scott, M. Telpoukhovskaia, C. Rodríguez-Rodríguez, M. Merkel, M. L. Bowen, B. D. G. Page, D. E. Green, T. Storr, F. Thomas, D. D. Allen, P. R. Lockman, B. O. Patrich, M. J. Adam, C. Orvig, *Chem. Sci*., **2011**, 2, 642.
26. A. Dedeoglu, K. Cormier, S. Payton, K. A. Tseitlin, J. N. Kremsky, L. Lai, X. Li, R. D. Moir, R. E. Tanzi, A. I. Bush, N. W. Kowall, J. T. Rogers, X. Huang, *Exp. Gerontol*., **2004**, 39, 1641.
27. T. Storr, M. Merkel, G. X. Song-Zhao, L. E. Scott, D. E. Green, M. L. Bowen, K. H. Thompson, B. O. Patrick, H. J. Schugar, C. Orvig, *J. Am. Chem. Soc.*, **2007**, 129, 7453.
28. H. Schugar, D. E. Green, M. L. Bowen, L. E. Scott, T. Storr, K. Bohmerle, F. Thomas, D. D. Allen, P. R. Lockman, M. Merkel, K. H. Thompson, C. Orvig, *Angew. Chem*. **2007**, 119, 1746-48; *Angew. Chem. Int. Ed.* **2007**, 46, 1716.
29. L. E. Scott, B. D. G. Page, B. O. Patrick, C. Orvig, *Dalton Trans.*, **2008**, 6364.
30. T. Storr, L. E. Scott, M. L. Bowen, D. E. Green, K. H. Thompson, H. J. Schugar, C. Orvig, *Dalton Trans.*, **2009**, 3034.
31. H. Kouyoumdjian, D. C. Zhu, M. H. El-Dakdouki, K. Lorenz, J. Chen, W. Li, X. Huang, *ACS Chem Neurosci*., **2013**, 17, 575.
32. C. B. Cowan, D. A. Patel, T. A. Good, *J. Theor. Biol*., **2009**, 258, 189.
33. C. B. Cowan, G. L. Cote, T. A. Good, *Biomaterials.*, **2008**, 29, 3408.
34. D. Patel, J. Hendry, T. Good, *Biochim. Biophys. Acta*., **2006**, 1760, 1802.
35. D. A. Pate, J. E. Hendry, T. A. Good, *Brain Res*., **2007**, 1161, 95.
36. Y.-H, Liu, W.-L, Lian, C.-C, Lee, Y.-F, Tsai, W.-C, Hou, *Food Chemistry*., **2011**, 129, 423.
37. Y. -H, Liu, W. -J. Huang, Y. -L. Lu, C. -C. Lee, Y. -F. Tsai, W. -C. Wu, *Botonical Studies.*, **2011**, 52, 35.
38. P. Serra, M. Bruczko, J. M. Zapico, A. Puckowska, M. A. Garcia, S. Martin-Santamaria, A. Ramos, B. de Pascual-Teresa, *Curr. Med. Chem*., 2012, 19, 1036.

39. E. Farkas, E. A. Enyedy, H. Csoka, *J. Inorg. Biochem*., **2000**, 79, 205.
40. M. Uttamchandani, J. Wang, J. Li, M. HU, H. Sun. K. Y.-T. Chen, K. Liu, S. Q. Yao. *J. Am. Chem. Soc*., **2007**, 129, 7848.
41. E. L. Kean, S. Roseman, *J. Bio. Chem*., **1966**, 241, 5643.
42. R. N. Knibbs, S. E. Osborne, G. D. Glick, I. J. Goldstein, *J. Bio. Chem*., **1993**, 268, 18524.
43. N. K. Sauter, J. E. Hanson, G. D. Glick, J. H. Brown, R. L. Crowther, S-J. Park, J. J. Skehel, D. C. Wiley, *Biochemistry*., **1992**, 31, 9609.
44. Y. H. Liu, S. Y. Lin, C. C. Lee, W. C. Hou, *Food Chemistry*., **2008**, 109, 159.
45. J. Nakamura, E. R. Purvis, J. A. Swenberg, *Nucleic Acids Res*., **2003**, 31, 1790.
46. N. Berdelle, T. Nikolova, S. Quiros, T. Efferth, B. Kalna, *Mol. Cancer. Ther*., **2011**, 10, 2224.
47. H. Schagger, *Nat. Protocols.*, **2006**, 1, 16.
48. A. S. DeToma, J.-S, Choi, J. J. Braymer, M. H. Lim, *ChemBioChem*., **2011**, 1198.
49. S. Lee, X. Zheng, J. Krishnamoorthy, M. G. Savelieff, H. M. Park. J. R. Brender, J. H. Kim, J. S. Derrick, A. Kochi, H. J. Lee, C. Kim, A. Ramamoorthy, M. T. Bowers, M. H. Lim, *J. Am. Chem. Soc*., **2014**, 136, 299.
50. A. K. Sharma, S. T. Pavlova, J. Kum. D. Finkelstein, N. J. Hawco, N. P. Rath, J. Kum. L. M. Mirica, *J. Am. Chem. Soc*., **2012**, 134, 6625.
51. C. Maierhofer, K. Rohmer, V. Wittmann, *Bioorg. Med. Chem*., **2007**, 15, 7661.
52. C. S. Atwood, R. D. Moir, X. Huang, R. C. Scarpa, N. M. E. Bacarra, D. M. Romano, M. A. Hartshorn, R. E. Tanzi, A. I, Bush, *J. Biol. Chem.*, **1998**, 273, 1464.
53. X. Huang, C. S. Atwood, R. D. Moir, M. A. Hartshorn, J. P. Vonsattel, R. E. Tanzi, A. I. Bush, *J. Biol. Chem.*, **1997**, 272, 26464.

3.9.1 ^{1}HNMR and ^{13}CNMR Details

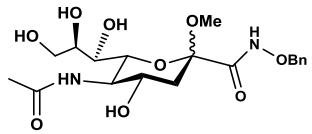

130214-01-RY-247

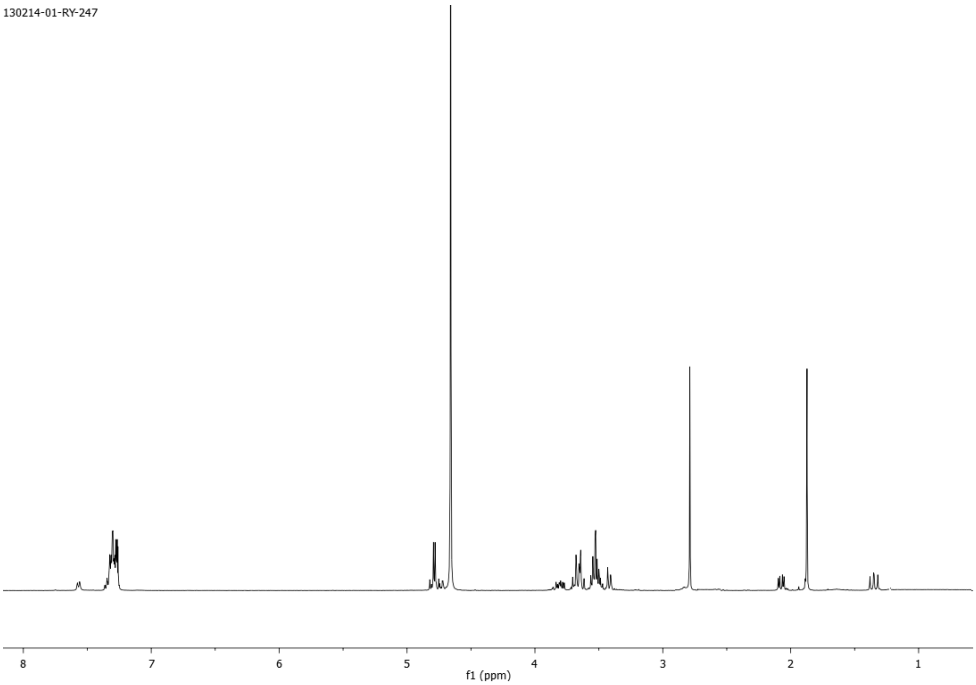

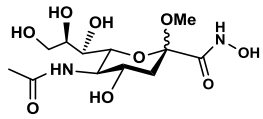

140214-11-RY-247

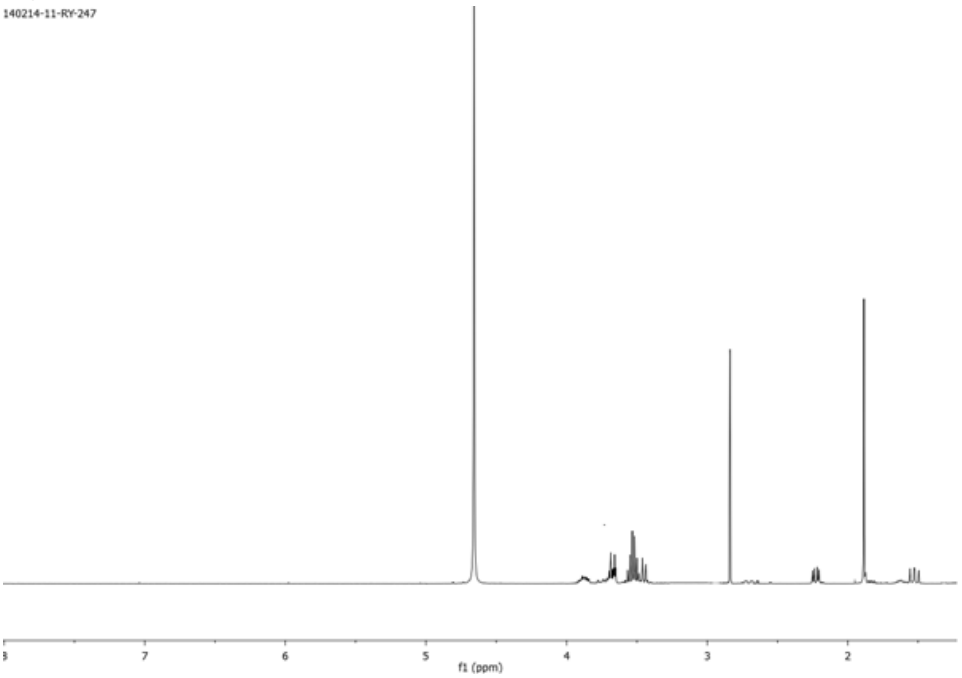

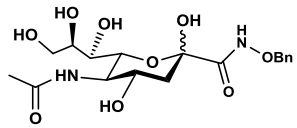

240713-01-RY-K-203

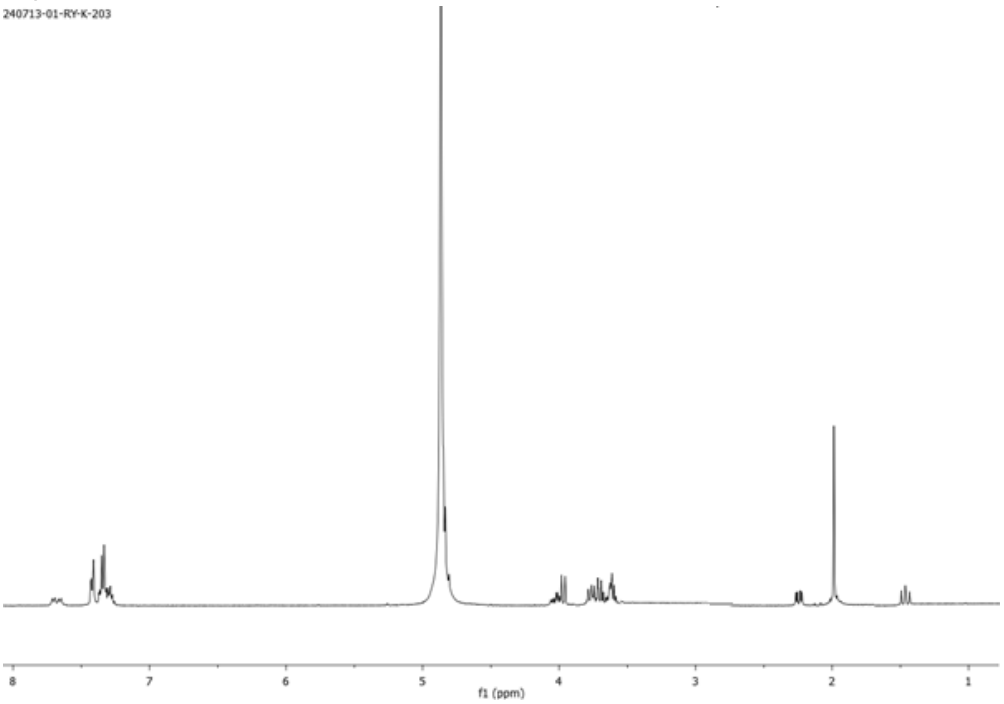

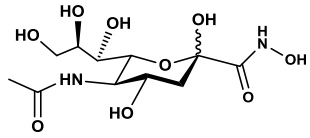

190813-08-RY-K-203F

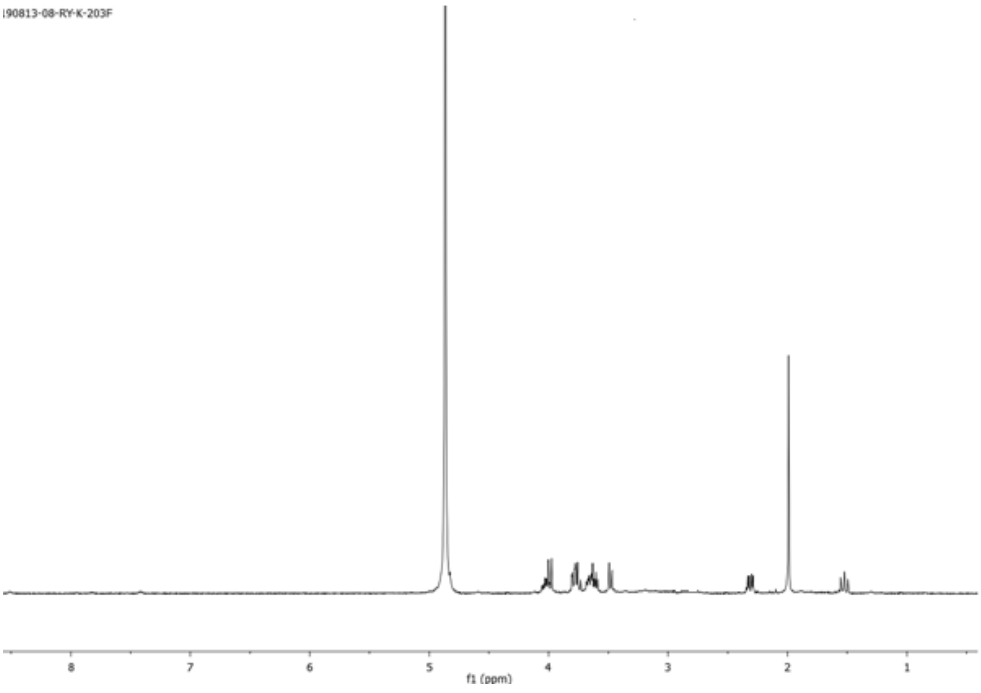

Chapter 4

Head-to-Head Comparison of Sialylated-quantum dots Toxicity, Biodistribution and Sequestration in Zebrafish and Mouse Model

4.10 Introduction

Sialic acids (Sia) are nine-carbon backbone monosaccharides, typically found at the terminal position of the glycoproteins and glycolipids. Over the decades, Sias have been reported in various pathological and physiological processes.[1,2] Hence, the functionalization of Sia on nanocarriers will be undoubtedly assistant to design smart probes for targeting and inhibiting the specific biological events.[3-6] In addition to its targeting ability, Sias are non-immunogenic in nature. Consequently, sialylation of the biomolecules such as proteins, enzymes, nano-carriers mask the active sites of the immune system and prolong their lifetime.[7-8] Recently, Sia residue in the form of *N*-glycan, GM1 and GM3 were conjugated to liposomes, dendrimers, nanoparticles to establish drug delivery system.[9-15] However, the ability to predict clinical significance of these nanoconjugates is based on the in-depth understanding of *in vivo* studies.

To date, mice are the most widely and the most efficient model for preclinical studies.[16] However, owing to large sample consumption, and complex biological system, there is a need for an alternative information rich simple *in vivo* system to reduce the amount of materials consumption and at the same time acquiring useful biological information at inexpensive, before planning the experiment with the complex models. Animals including fish, insects and worms are considered to be the simple model for pre-clinical research and each of these *in vivo* systems have their own merits and demerits. Among them, zebrafish has several advantages as compared to *Caenorhabditis elegans, Drosophila melanogaster* and *Hydra*, which includes quick lifespan from embryo to larva, transparency, ease of maintaining, high level of conservation of the vertebrate genome and also the display cardiovascular, nervous and digestive systems that are similar to the human system.[17-18] Further, as a vertebrate organism, zebrafish presents many organs and cell types similar to that of the mammalian. The zebrafish has been described as "the canonical vertebrate" due to the similarities between mammalian and zebrafish biology.[19] Currently, zebrafish model was used to study the human diseases, including cancer, cardiovascular disorder, neurological diseases, liver diseases, immunological studies and nanoparticle biodistribution.[20-24] Furthermore, the fish model has been extensively used to investigate the pharmacokinetics of nanoparticles and carbon nanorods.[25-28] Hence, deciphering the carbohydrate-mediated bio-distribution and sequestration in zebrafish will give preliminary information to target specific human diseases.

In this study, in order to find a simple, active animal model for glyco-nanotechnology research, we have compared *in vivo* efficacy of sialylated-QDs in zebrafish and mouse model. Although these two models are independently targeted in glycobiology and glyconanotechnology research, the head-to-head comparison at multiple stages will provide a broader profile for pharmacology and clinical research.

4.2 Quantum dots conjugation and physical characterization

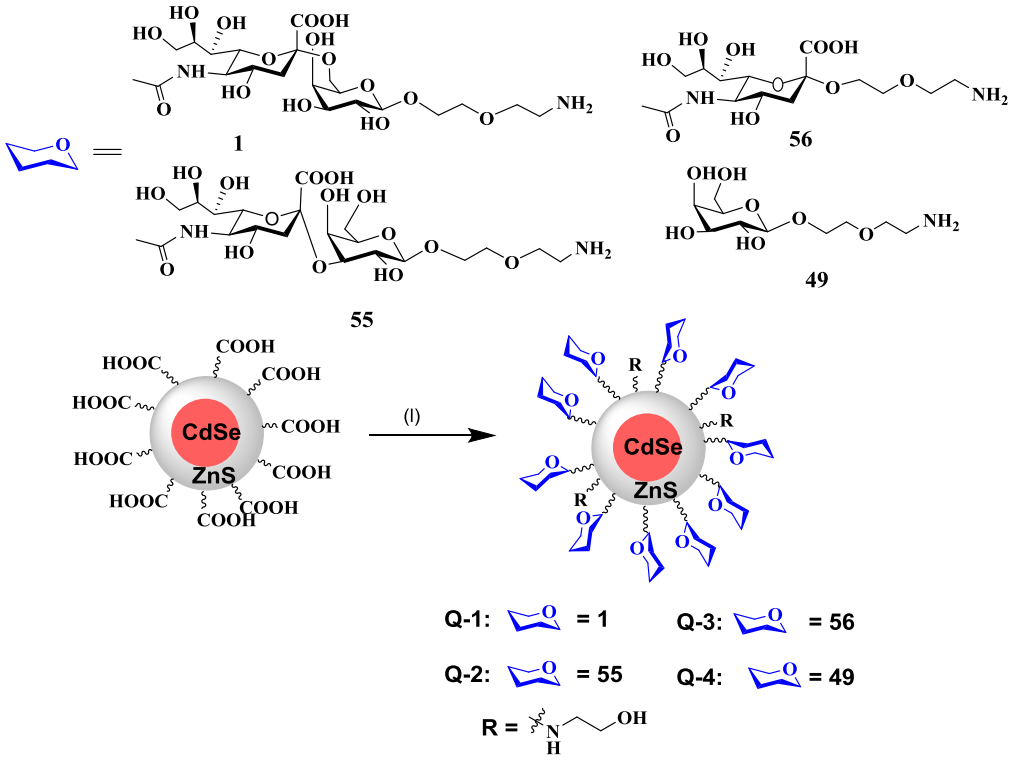

Scheme 1. (a) Synthesis of **Q-1** to **Q-4** nanoparticles. Reagents and Conditions: (l) **1 or 49 or 55** or **56** EDC, *N*-hydroxysuccinimide, ethanolamine, H_2O.

Conjugation: Commercial PEG-COOH conjugated quantum dot was used to the synthesis of glyco-QDs. The sugar functionalization of QDs was carried out by using water soluble coupling reagents and *N*-hydroxysuccinamide, followed by capping the unreacted carboxylic acid terminals by using ethanolamine (Scheme 1).[29,30] The size and shape of the QDs were characterized using TEM (fig. 1). The QDs were well dispersed and shown homogenous size and spherical shape. The diameter of **Q-1** to **Q-4** was around 20-23 nm. After glycan addition, the

surface potential of Q-1 changed from -24.1 mV to -12.5 mV, indicating that negative change of the native QDs was replaced by sialic acid moiety and remaining carboxylic acid groups of the QDs were neutralized with ethanolamine linker. Similarly, **Q-2** and **Q-3** displayed zeta potential of -10.7 and -13.3 mV respectively. While the Q-4 displayed 0.78 mV, due to the non-ionic nature of compound 49. The fluorescence spectra of QDs were recorded to check whether the sugar conjugation altered the fluorescence intensity of the QDs. The quantum yield of all the QDs was slightly increased, indicating that the sugar conjugation stabilizes of CdSe core and enhance the fluorescence intensity. Finally, the number of sialic acid or galactose moieties on each QDs was quantified by resorcinol [31] and phenol-sulfuric acid method. It was observed that each QDs carried around 45-55 sialic acid moieties, demonstrating the multivalent display of sugar on a fluorescent template (table 1).

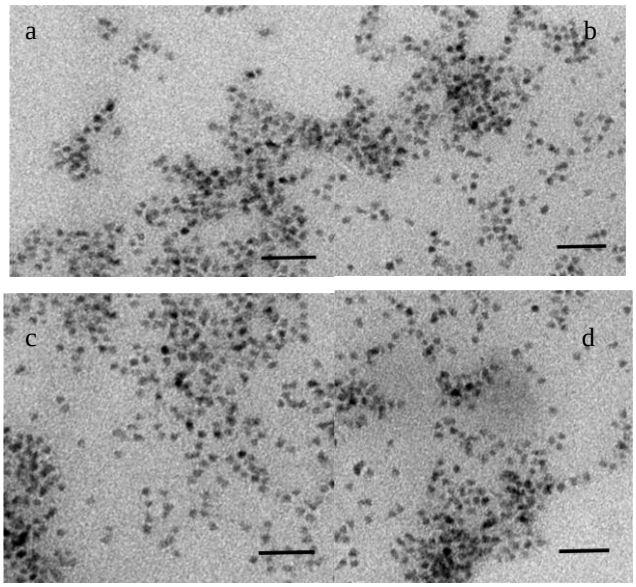

Figure 1. TEM images of carbohydrate conjugated quantum dots: **Q-1** (a); **Q-2** (b); **Q-3** (c); **Q-4** (d). Scale bar = 100 nm.

QDs	Quantum Yield (ϕ)	Number of Sugar unit per QD	Zeta potential (mV)
Q-1	0.37	53 ± 4	-12.5 ± 1.8
Q-2	0.36	47 ± 6	-10.7 ± 1.9
Q-3	0.39	56 ± 3	-13.3 ± 2.4
Q-4	0.44	78 ± 4	+0.78 ± 0.3
QD-COOH	0.32	-	-24.1 ± 3.2

Table 1. Physical characteristics of QDs and plasma clearance.

4.3.0 Mortality Study

After synthesizing and characterizing the glyco-QDs, we first performed the mortality of adult zebrafish and mice after i.p injection of various QDs. (table 2), summarize the LD50 values of the 24h acute toxicity test. As dosage varied from 1 to 20 nmol/kg, a significant difference in the mortality was observed in both animal models. This dosage is similar to that of the concentration used by different research groups to perform *in vivo* experiments with QDs.[32-37] Among the QDs, **Q-1** showed less toxicity compared to other glyco-QDs. It was observed that doses below 5 nmol/kg, no animal death occurred. For **Q-1**, maximum animal death took place at 20 nmol/kg in both animal models. LC50 value was 13.6 nmol/kg and 14.7 nmol/kg in the zebrafish and mice model respectively. While **Q-2** to **Q-4** showed maximum animal death at 15 nmol/kg in both models and the LD50 value were 11.7, 9.6 and 9.3 nmol/kg in the zebrafish model and 11.4, 9.51 and 9.6 nmol/kg in mice model respectively (fig. 2a, 2b and Table 2). Previously, it has been shown that acute toxicity of the QDs in mice and zebrafish varies with the surface functionalization.[38-40] Tang *et al.* tested the acute toxicity of the anionic, cation and non-ionic surfactants on QDs in the mice.[41] The data showed that the mice appeared to be sensitive to cationic and less sensitive to anionic and non-ionic surfactant. Similarly, the Vaughan *et al.* demonstrated that the toxicity of nanoparticles varies with surface functionalization in the zebrafish embryos.[42] Kovrižnych *et al.* showed that the toxicity effect of nanoparticles in zebrafish egg was similar to that of adult fishes.[25] However, the comparative toxicity studies with two animal model have rarely been investigated. Our results clearly demonstrate that surface functionalization of different sialic acid linkage alters the *in vivo* acute toxicity in both the animal models, probably due to the differences in the biodistribution and sequestration level.

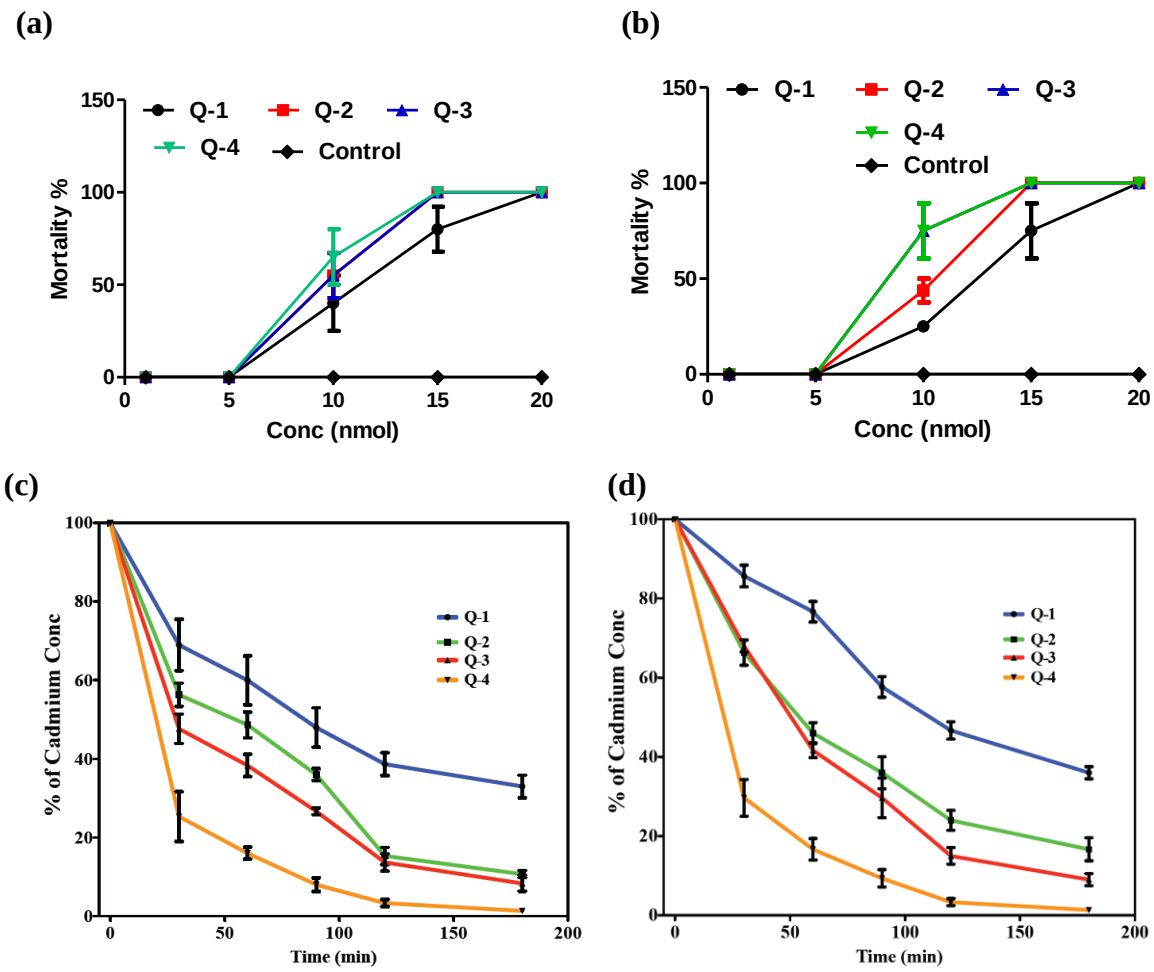

Figure 2. Mortality of (a) zebrafish(*Danio rerio);* (b) mice after 24 h of glyco-QDs i. p injection; blood clearance profile of glyco-QDs (c) zebrafish; (d) mice.

QDs	LD50 (nmol/kg) Mice	LD50 (nmol/kg) Zebrafish	$t_{1/2}$ (mins) Mice	$t_{1/2}$ (mins) Zebrafish
Q-1	13.6	14.2	105 ± 2	82 ± 3
Q-2	11.7	11.4	51 ± 3	52 ± 4
Q-3	9.6	9.7	48 ± 3	31 ± 6
Q-4	9.3	9.5	21 ± 2	23 ± 4

Table 2. LD50 and $t_{1/2}$ of the QDs in animal model.

The above toxicity studies clearly showed the QDs of different sialic acid glycans alter the mortality in both animal model. Next, the half-life of the blood clearance of glyco-QDs elucidates the mechanism of acute toxicity. The concentration of the QDs in blood was quantified by measuring the cadmium concentration by using ICP-MS. We set 7 nmol/kg (weight of the fish or mouse) of QDs as an ideal concentration for head-to-head *in vivo* experiments, as they displayed less toxicity and ideal concentration for the detection of biodistribution of QDs as

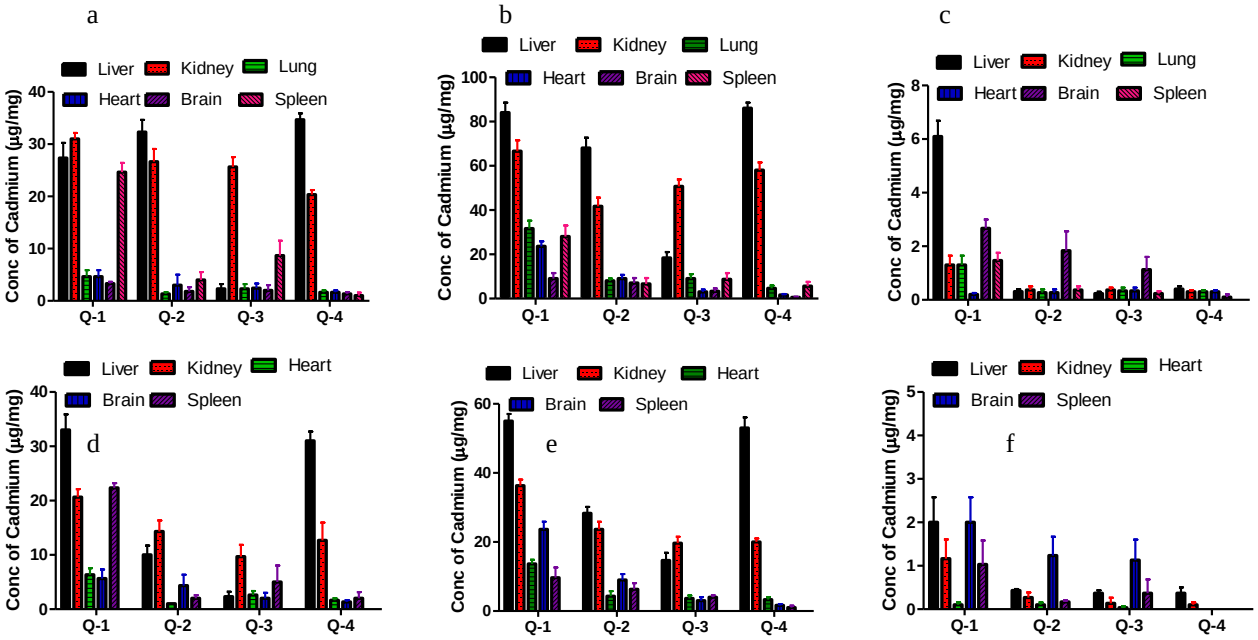

Figure 3. (i) Statistical analysis of ICP-MS biodistribution data of quantum dots at different time intervals. (a) Mouse-1 h; (b) Mouse-3 h; (c) Mouse-24 h; (d) Zebrafish-1 h; (e) Zebrafish-3 h; (f) Zebrafish- 24 h. Results are expressed as mean ±SD (n = 6).

reported in the literature.[38-41] QDs were intraperitoneally injected to respective models and blood was drawn after 0, 30, 60, 90, 120 and 180 mins. Table 2 represents the half-life of glyco-QDs. It could be seen that QDs coated with galactose exhibited a rapid elimination from the bloodstream in both the models, while the sialylated QDs exhibited prolonged circulation in the bloodstream. This result correlates with pharmacokinetic studies of polysialic acid and other sialic acid conjugated therapeutic molecules blood circulation results.[43-47] The half-life ($t_{1/2}$) calculated for **Q-1** was 105 and 82 mins in mouse and zebrafish model respectively (fig 2c, 2d & Table 2). The prolong blood circulation of **Q-1** attributes to the fact that sialic acid moiety on the QDs binds to siglecs receptors to immune cells and increases circulation time and slowly enter in organs.[48] while, **Q-2** and **Q-3** cleared from the bloodstream much faster in both the models.

4.4 Biodistribution and sequestration study

Next, we investigated the biodistribution of QDs in the various organs. QDs were intraperitoneally injected into the zebrafish and mouse model and after 1, 3 and 24 h, fishes and mice were sacrificed and dissected for different organs (liver, kidney, lung, heart, brain and spleen, fig 3). In the mouse model, **Q-4** rapidly cleared from the blood and sequestered in liver and kidney after 1h, due to asialoglycoprotein receptors.[49] ICP-MS analysis after 3h revealed the substantial amount of Q-4 accumulation in the liver compared to other organs. These results are

consistent with previous galactose-QDs results in the mouse model.[37] In case of zebrafish model, similar biodistribution mechanism was observed after 1 h and 3 h respectively, and after 24 h, **Q-4** was completely cleared from most of the organs. Sialylated-QDs have longer blood circulation half-life compared to **Q-4**, found to be sequestered in several organs. Among them, α(2-6) conjugated QDs (**Q-1**) showed significantly broad biodistribution compared to **Q-2** and **Q-3** (fig. 3). The probable reason behind the wide biodistribution is may be due to the stability of comp 1 in the blood stream. In the zebrafish model, similar trend was seen, although it was less pronounced compared to the mouse model. **Q-1** treated zebrafish showed the nearly 1.5-fold maximum QDs sequestration after 3 h compared to that of 1 h. While, in the mice model, nearly 2-fold increase in the **Q-1** sequestration was observed at different organs after 3 h. After 24 h, **Q-1** sequestration was found in liver and traces of QDs were in other organs. In contrast, **Q-2** was readily uptake by the liver and the kidney, compared to other organs and slowly cleared by both the system. While **Q-3** was bio-distributed in the kidney and traces of it was found in other organs. The sequestration of the sialylated-QDs in the spleen is correlated to the binding affinity of QDs with blood components, as spleen is considered to be a reservoir for blood compositions. While the sequestration in liver illustrates the stability of Sia on QDs to form galactose residue which binds to asialoglycoprotein receptor in hepatocyte cells in the liver. The least sequestration of Sialylated-QDs in heart and lungs demonstrated the absence of specific Sia receptors. The slow and steady brain sequestration of **Q-1** and **Q-2** illustrated the potential property of Sias to penetrate the blood-brain barrier (BBB) compared to **Q-3** and **Q-4**.[50-52] Similar our result, more authors referred comp 1 conjugated biomolecules displayed broad biodistribution compared to comp 55 conjugated system in mice model. Tanak *et al.* tested the Gd(III) complexes of α(2-6) and α(2-3) sialylated N-glycans. They found the multivalency and α(2-6) exhibited broad biodistribution.[53] By using sialyl-lewis^X conjugated QDs, Ohyanagi *et al.* showed that α(2-3) sialylated-nanoparticles appeared to be broad biodistribution at initial hours and later sequestered in the liver.[54] Thus, the majority of the mice results seem to be comparable to literature results, and the zebrafish results can be considered a suitable alternative to the mice model.

4.50 Confocal imaging of distributed sialylated quantum dots

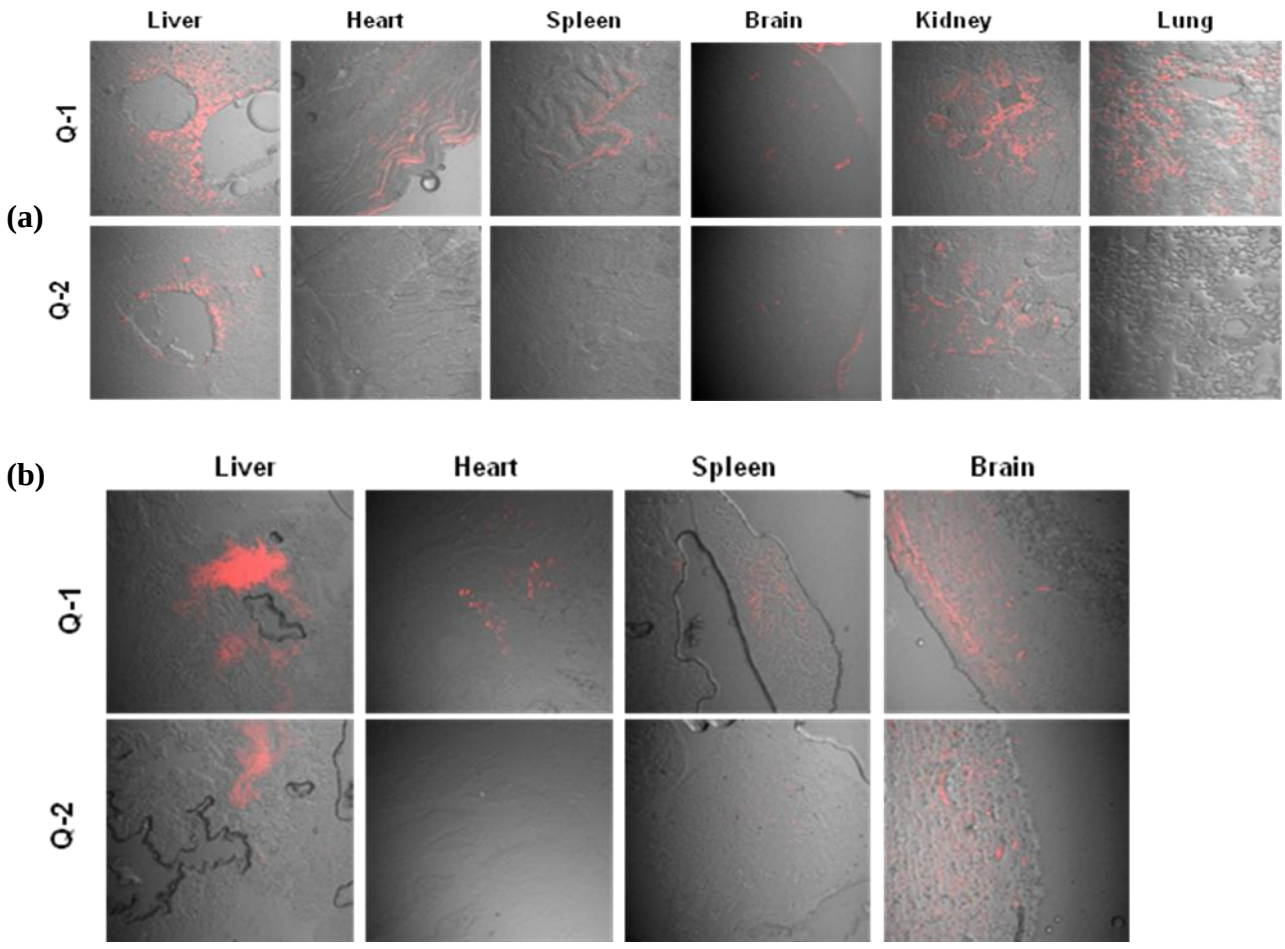

Figure 4. Confocal images of QD sequestration at different organs of (a) mouse and (b) zebrafish model.

After quantitatively analyzing glyco-QDs biodistribution in both models, it was qualitatively supported by confocal images of the tissue sections. We performed paraffin embedded tissue sectioning and QDs sequestration **Q-1** and **Q-2**, as they have distinct biodistribution after 3 h in both the models (fig. 4). The inherent optical property of QDs was used to visualize the sequestration in the tissue section. As seen in fig. 4, the **Q-1** was widely sequestered in the cardiac muscle tissues in the heart, hepatocyte and vacuoles of the liver region, pulmonary fibrosis tissue of lung region, the periarteriolar lymphoid sheath of spleen region, glomerulus structure of kidney region and cortex of brain region respectively. While, **Q-2** sequestration was observed in liver, brain and kidney regions, which further support the ICP-MS data. Further, all

these results clearly support that the zebrafish can be used as an efficient *in vivo* model to study the carbohydrate-mediated interactions.

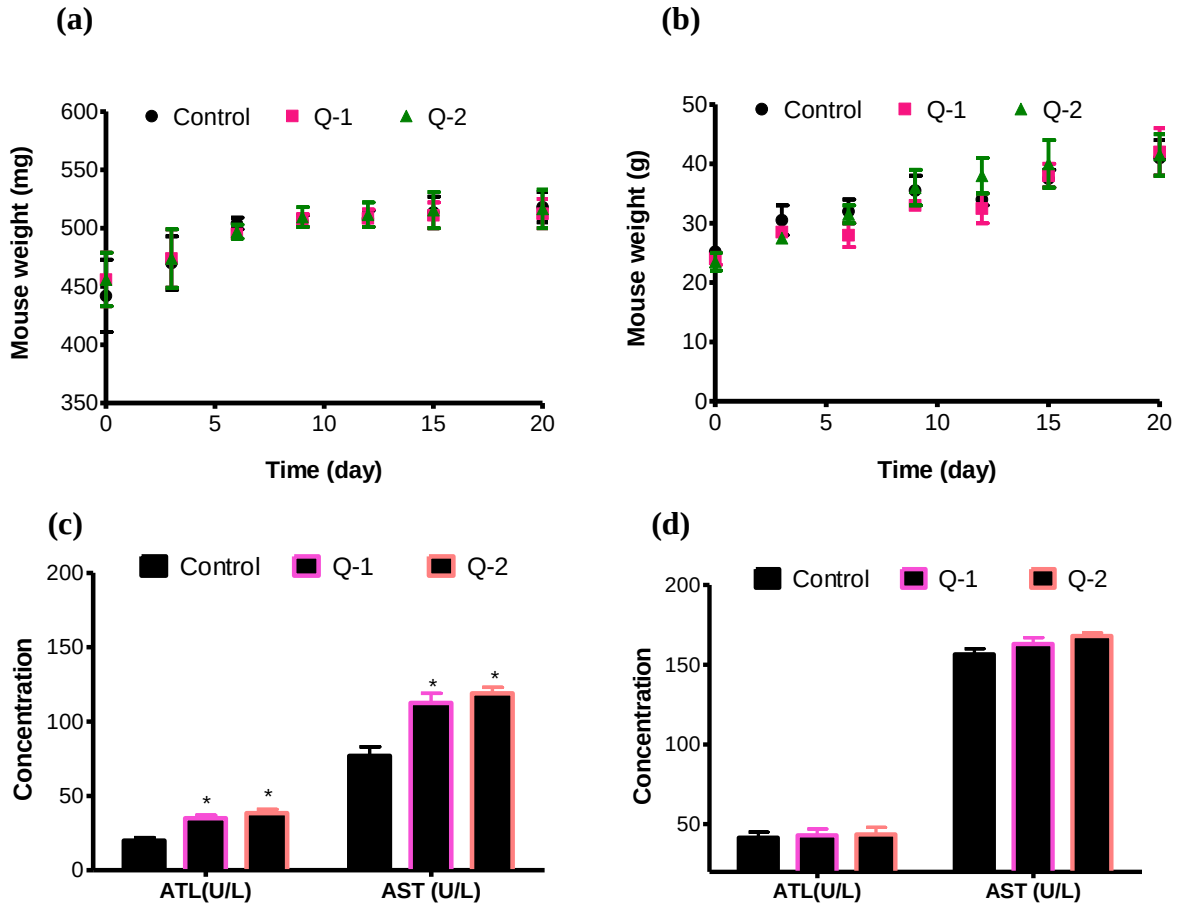

Figure 5. Changes in the body weight of the zebrafish (a) and mice (b) after i.p. administration of Q-1 and Q-2 at 2.5 nmol/kg for 20 days; Serological test results obtained from the zebrafish (c) and mice (d) injected with QDs after 20 days. Results are expressed as mean ±SD (n = 5). *p < 0.05 versus control.

Based on the *in vivo* screening experiments, we examined the long-term toxicity of QDs by measuring the fluctuating body weight in the mice and zebrafish model. QDs (2.5 nmol/kg) were i.p. Injected and the fluctuation in the body weight was monitor over a period of 20 days (fig. 5a & 5b). The body weight of the control and QDs injected mice were approximately identical, illustrating that the QDs had no side effect on the mice model at low concentration. Further, the serological test of kidney function by measuring the alanine aminotransferase (ALT) and aspartate aminotransferase level (AST)[55-56] after 20 days displayed partly variation in the enzymatic activity when compared to the control in zebrafish model, suggesting toxicity of QDs at the lower concentration very high in zebrafish compared to mice (fig. 5c & 5d). Overall, the

comparative studies displayed, the zebrafish as a potential *in vivo* model for glyco-nanotechnology research.

4.6 Conclusion

In this study, for the first time, we have reported the head-to-head comparison of two distinct sialylated-QDs toxicity, biodistribution, and sequestration in mouse and zebrafish model. The serum analysis of the α(2-6) sialic acid-conjugated QD showed long-term blood circulation in both the models compared to other glyco-QDs. Biodistribution results of both the model systems revealed that most of the QDs were sequestered in the liver, with quick clearance was observed in zebrafish compared to that of the mouse model. Furthermore, Q-1 and Q-2 was able to pass the BBB and sequestered in the brain in both the model. These results advocate zebrafish as an ideal simple *in vivo* system for preliminary screening carbohydrate-mediated interactions and thus opening up the immense possibility for the successful application of carbohydrate-based drug delivery and imaging studies in a quick time intervals.

4.70 Materials and methods

4.7.1 Synthesis of Q-1 to **Q-4 :** Glyco-conjugation of QD has been done *via* peptide coupling method, following Thermo Fisher Scientific procedure.[29] In brief, carboxylic acid-quantum dots (0.1 μM) was dissolved in borate buffer (50 mM, pH- 7.4, 0.5 ml). To this solution EDC (10 μM) and N-hydroxyl succinimide (12 μM) was added and stirred at RT for 2 h, followed by the addition of oligosaccharides (1, 49, 55, 56) (10 μM) at RT. The reaction mixture was stirred overnight and quenched with ethanolamine, followed by dialysis of the mixture with 10,000 cut-off membranes in water. Finally, the product was lyophilized and diluted to desired concentration. The concentration of the QDs was established using a previously published procedure.[30] QDs were dissolved in phosphate buffer (50 mM at pH 7.4) and used as such for further biological experiments.

4.7.2 Estimation of the concentration of sialic acid per QDs

Sugar capped QDs (20 nmol) was dissolved in 100 μL of doubled distilled water. To this solution, resorcinol reagent (100 μL) was added and heated to 80 °C on a water bath for 15min.[31]

The reaction mixture was extracted with n-butyl acetate and n-butanol (85:15) mixture. The organic layer separated and the absorbance at 580 nm was measured by UV-spectrometer. The concentration of sugar was determined by plotting a calibration curve of commercial sialic acid-resorcinol derivatives obtained by the same method. The number of sugar molecules per QD was calculated from the ratio of the concentration of sugar and Conc of the QD. **Q-1** to **Q-3** showed 53, 47 and 56 sialic acid residues per each particle respectively. In case of **Q-4**, the concentration of galactose was determined by the phenol-sulfuric acid method.[32] **Q-4** showed 78 galactose residue per each particle.

4.7.3 Characterization of glyco-QDs

UV-visible measurements were performed with Evolution 300 UV-visible spectrophotometer (Thermo Fisher Scientific, USA). Fluorescence spectra were recorded in the FluoroMax-4 spectrofluorometer (Horiba Scientific, U.S.A.).Transmission electron microscopy (TEM) observation was carried out on CM 200, operated voltage 100 kV resolution 2.4 Ao.We used a zeta potential analyzer to measure the surface potential of glyco-QDs. In the measurement, we applied unit field strength (1 Volt per meter) to the QD solution. We measured zeta potential of different sugar conjugated QDs in water.

4.7.4 Mouse model

All animal experiments were performed in accordance with local animal ethical committee regulation. Male and female C57BL mice (3-4 weeks old) were collected from Reliance life science, Bombay. Prior to the experiment, the mice were maintained in the animal house for 48h in 12h/12h light/dark cycle, with proper food and water. The surgical procedures were performed in accordance with Institutional Animal Ethical Committee regulation, set up by CPCSEA, Govt. of India. All experiments were carried out in INTOX quality toxicological services, Pune.

4.7.5 Zebrafish model

Local wild-type zebrafish strain weighing approximately 500-600 mg (2-3 months old) were maintained under standard laboratory conditions at 28ºC under 14:10 h light/dark cycle conductivity of 350 μS of the water maintained at pH 7.2 – 7.4.

4.7.6 Acute toxicity determination

Mice were anesthetized with ketamine and QDs were injected at different concentration via i. p. injection. The number of mice in each experimental and control group was 4 male and 4 female (P = 0.018 compared to control). The highest dose of QDs used was 20 nmol/kg. LD50 value was calculated according to the equation.

$LD_{50} = lg^{-1}\{X_m\text{-}i \times \Sigma p\text{-}0.5\}$ -1

where X_m is the logarithm of the maximal dose, i represents the difference between the logarithm values of two adjacent doses, and P is the mortality of each group.

In case of zebrafish, fishes were anesthetized with 2-phenoxyethanol and QDs were injected. The number of zebrafish in each experimental and control group was 5 male and 5 female (P = 0.0129 compared to control).

4.7.7 Blood sample analysis

Mice were anesthetized with ketamine and received 7 nmol/Kg of quantum dots (**Q-1** to **Q-4**). The number of mice for each experimental and control group was 3 male and 3 female (P = 0.033 compared to control). After 0, 30, 60, 90, 120 and 180 mins. Mice were sacrificed, and 0.5 ml of blood was drawn. Collected blood samples were digested with 500 µl of 70% nitric acid, followed by heating at 90°C for 30 min. Then each digested samples were diluted to 6 ml with Millipore water. The concentration of QDs in the blood samples was determined by ICP-MS (Thermo-Fisher Scientific, Germany) by quantifying the cadmium concentration. Finally, the concentration of cadmium was converted into µg/mg.

Zebrafish were anesthetized with 2-phenoxyethanol and injected 7 nmol/Kg (**Q-1 to Q-4**) *via* intraperitoneal using catheter implantation tubing attached to a cut 22-G needle tip at one end and another end was attached to Hamilton syringe. The number of fish for each experiment was 3 male and 3 female (p = 0.031 compared to control). After 0, 30, 60, 90, 120 and 180 mins zebrafish were sacrificed and its tail was cut to collect the blood sample (~0.1ml). Collected blood samples were digested with 500 µl of 70% nitric acid followed by heating at 90°C for 30 min. Then each digested samples were diluted to 6 ml with Millipore water. The concentration of QDs was determined by ICP-MS (Thermo-Fisher Scientific, Germany) by quantifying the cadmium concentration. Finally, the concentration of cadmium was converted into µg/mg.

4.7.8 Mouse dissection

Mice were received 7 nmol/Kg of quantum dots (**Q-1 to Q-4**) *via* i.p injection. The number of mice for each experiment was 3 male and 3 female (P = 0.021). After 1h, 3h and 24 h mice were sacrificed to the collection of organs. Before dissection, mice were anesthetized using ketamine, followed by pinning down with belly facing up and washed with ethanol. Then dissection was done along the ventral midline starting from the groin up to the chin to expose the organs. Different organs liver, spleen, lung, kidney, heart and brain were collected and washed with PBS buffer (100 mM, pH 7.4) followed by fixation in formalin (5%) solution. These samples were taken as such for further analysis (ICP-MS and confocal imaging).

4.7.9 ICP-MS analysis

Organs were dried and weighed before digesting it in 3 ml of 70% nitric acid and heating the solution at 90 °C for 3 h. The samples were further diluted with 6 milliQ water and filture through the membrane filtered before subjected to ICP-MS analysis.

4.8 Confocal imaging

In case of confocal imaging studies, organs were subjected gradient dehydration with increasing concentration of ethanol (75%, 95%, 100%) for 30 min each. Finally washed with 100% xylene for 1 h and then fixed in paraplast. Blocks are stored in -10 °C for 12 h before proceeding to sections. Sectioning of blocks was done using Leica microtome instrument and sections were collected on PLL-coated glass plates. Before imaging excess paraplast was washed with xylene. Sequestration of glyco-QDs in different organs was analyzed by confocal fluorescence microscopy using a CLSM (Zeiss LSM 710) microscope. The excitation wavelength was 480 nm, emission wavelength was 680 nm. 25X objective was used to image organs.

4.9 Zebrafish dissection

For dissection of organs, zebrafish were anesthetized with 2-phenoxy ethanol in water (1 : 2000). The number of mice for each experiment was 3 male and 3 female (P = 0.018). Both head and tail of the fish were fixed using needles and body wall was cut at the abdomen and cut until the operculum to expose all internal organs. Different organs such as heart, brain, liver and spleen were collected. All organs were washed with Millipore water, dried and weighed before following the above procedure for ICP-MS and confocal slides preparation.

4.9.1 Long-term toxicity evaluation

After i.p. administration of **Q-1** and **Q-2** at 2.5 nmol/kg, the long-term toxicity test was performed based on body weight of the male mice and zebrafish. The number of mice and zebrafish used for each experiment and control is 5. Body weights of the mice and zebrafish weight in both groups were recorded for next 20 days. In a separate experiment, blood samples from control and QDs injected mice and zebrafish and were collected after 20 days and two important hepatic damage indicators, alanine aminotransferase and aspartate aminotransferase level were measured.

4.9.2 Statistical analysis

Statistical comparisons were done using the Student *t* test or one-way ANOVA. The $p < 0.05$ is considered to be statistical significance.

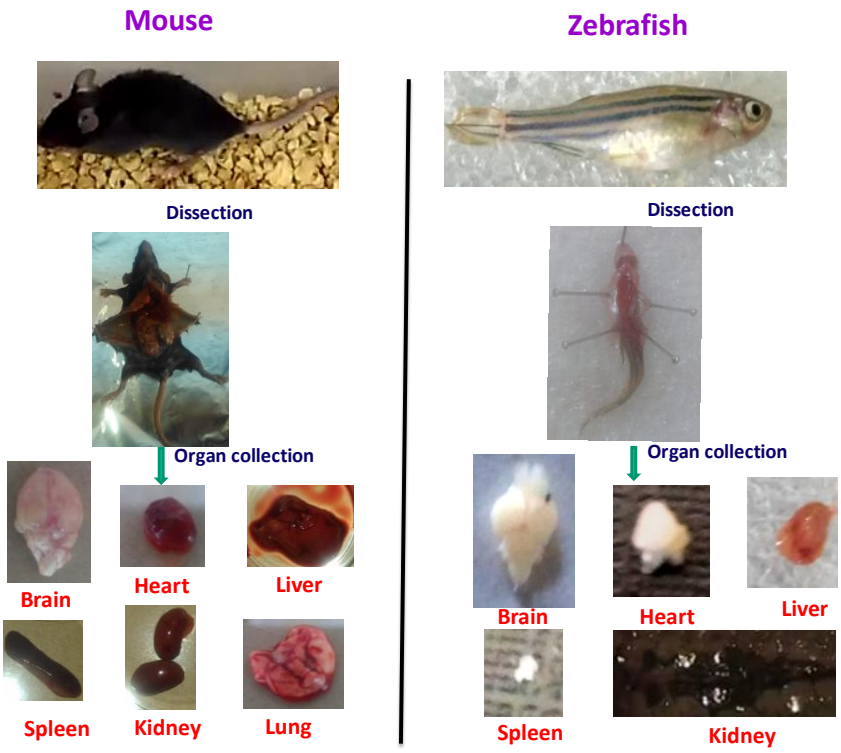

Figure 6. Mouse and zebrafish dissection and collection of different organs.

4.9.3 Synthetic procedure and Spectroscopic details

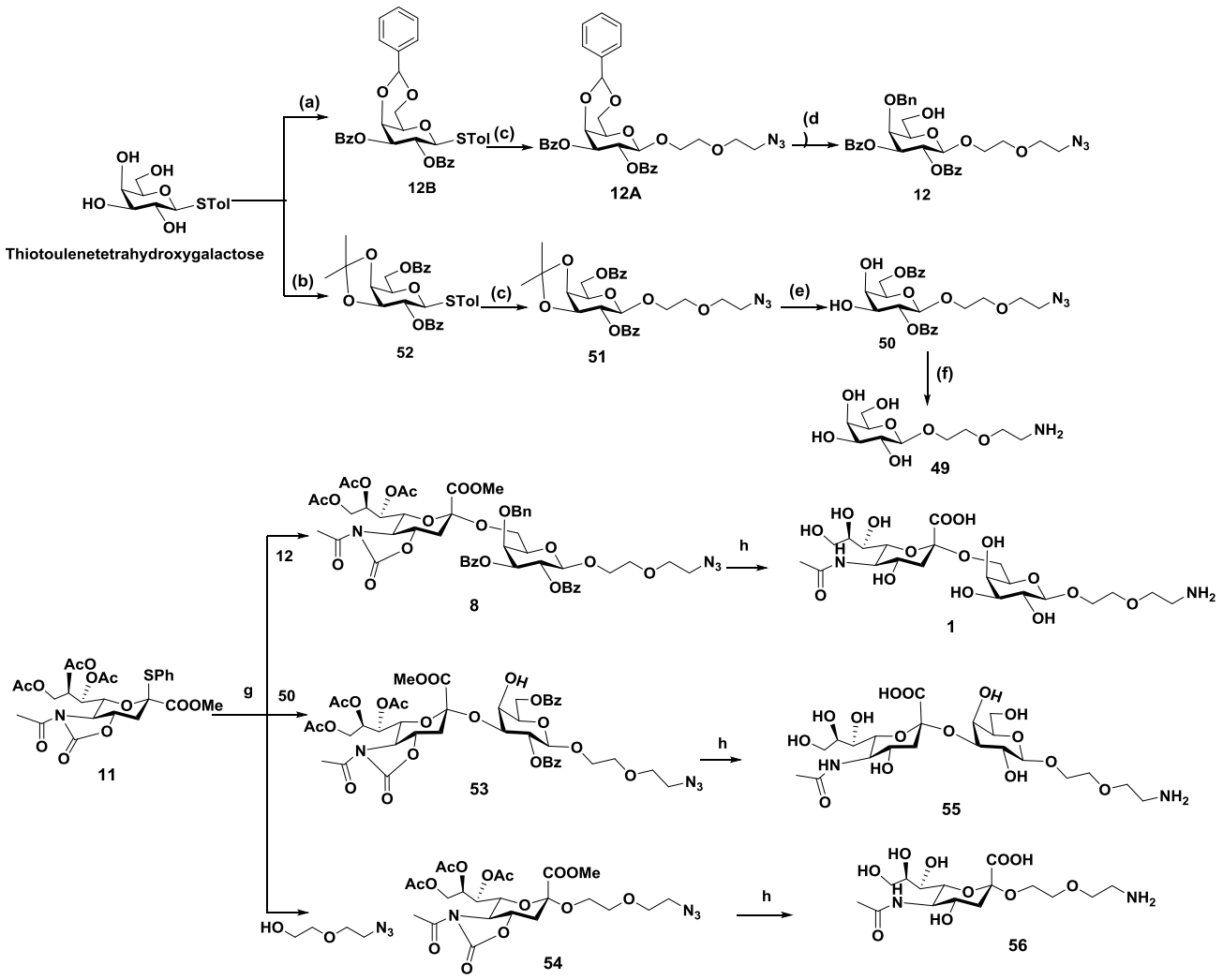

Scheme 2. ***Reagents and conditions*****:** (a) 2,2-dimethoxy benzaldehyde/pTSA/acetonitrile/RT; BzCl/DMAP/pyridine/0°C to RT; (b) 2,2-dimethoxy propane/pTSA/acetone/RT; BzCl/DMAP/Pyridine/0°C to RT; (c) 2-azidoethoxyethanol /NIS/TfOH,-40°C, DCM; (d) $PhBCl_2/Et_3SiH$/-78°C,DCM; (e) $TFA/H_2O/AcOH$, 60 °C; (f) $H_2/Pd(OH)_2$,MeOH:H_2O(1:1),12h; (g) NIS/TfOH, DCM, -40°C; (h) $NaHCO_3/Ac_2O/H_2O$/RT; $H_2/Pd(OH)_2$, MeOH:H_2O(1:1), 12h;

* Synthetic procedure and spectroscopic details of compound **12B, 12A and 12** have provided in **chapter 2**

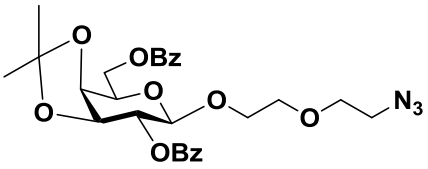

Compound 51: To a solution of **52** (550 mg, 1.02 mmol, 1.0 equiv), azido-ethoxyethanol (1.23 mmol, 1.2 equiv), and activated 4Å powdered molecular sieves (1.5gm) in anhydrous dichloromethane (10 mL), NIS (276mg, 1.23 mmol, 1.2 equiv) and TfOH (9.02 μL, 0.102 mmol, 0.1 equiv) were added at - 40 ^{0}C. The reaction mixture was stirred at - 40^{0}C for 3 h until the disappearance of the donor on TLC, then quenched with triethylamine (80µL, 0.81 mmol, 0.75 equiv) and warmed to room temperature. The reaction mixture was diluted with dichloromethane, filtered through celite, washed with 20% aqueous $Na_2S_2O_3$ solution, dried over anhydrous Na_2SO_4, and concentrated under reduced pressure. The crude product was purified by column chromatography (silica gel, pet ether/ EtOAc 3:1) to afford the compound **51**(400mg, 72%).**^{1}H- NMR** (400 MHz, $CDCl_3$) δ 8.15 – 8.00 (m, 4H), 7.68 – 7.55 (m, 2H), 7.53 – 7.42 (m, 4H), 5.30 (dd, *J* = 8.0, 7.5 Hz, 1H), 4.69 (m, 2H), 4.65 (d, *J*= 8.4 Hz ,1H) , 4.42 (dd, *J* = 7.3, 5.4 Hz, 1H), 4.34 (dd, *J* = 5.4, 2.2 Hz, 1H), 4.24 (ddd, *J* = 7.2, 5.1, 2.2 Hz, 1H), 4.04 – 3.93 (m, 1H), 3.74 (ddd, *J* = 11.2, 7.4, 3.6 Hz, 1H), 3.66 – 3.53 (m, 2H), 3.48-3.45 (m, 2H), 3.17 – 2.98 (m, 2H), 1.66 (s, 3H), 1.39 (s, 3H). **^{13}C-NMR** (400 MHz, $CDCl_3$) δ 166.32, 165.33, 133.20, 133.12, 129.96, 129.91, 129.79, 129.75, 129.76, 129.74, 129.66, 128.46, 128.33, 125.34, 110.90, 100.80, 77.09, 73.70, 73.52, 71.11, 70.46, 70.06, 69.13, 63.75, 50.59, 27.68, 26.34. HRMS m/z calc'd for $C_{27}H_{31}N_3O_9Na$ ($M+Na^+$). 541.2060; found: 541.1957.

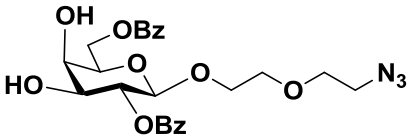

Compound 50: The compound **51** (350mg, 0.646 mmol) was dissolved in chloroform and TFA mixture (10:1; 10ml) at room temperature. After 1 h, the reaction mixture was quenched with triethylamine, evaporated, concentrated and purified on flash column chromatography (silica gel, pet ether/ EtOAc 1:1) to afford compound **50** (280 mg, 86%).**^{1}H NMR** (400 MHz, $CDCl_3$) δ 8.12 – 8.01 (m, 4H), 7.64 – 7.54 (m, 2H), 7.52 – 7.40 (m, 4H), 5.28 (dd, *J* = 9.6, 8.0 Hz, 1H), 4.71(d,J

= 8 Hz, 1H), 4.70-4.57 (m, 2H), 4.08 (d, *J* = 3.1 Hz, 1H), 4.00 (dt, *J* = 11.3, 3.8 Hz, 1H), 3.92 (t, *J* = 6.8 Hz, 1H), 3.88 (dd , *J* = 9.7,3.5 Hz ,1H), 3.78 (ddd, *J* = 10.8, 6.4, 4.2 Hz, 1H), 3.71 (dd, *J* = 5.4, 4.6 Hz, 1H), 3.65 – 3.59 (m, 2H), 3.49 (m, 2H), 3.45 – 3.41 (m, 1H), 3.18 – 3.05 (m, 2H). **^{13}C NMR** (400 MHz, $CDCl_3$) δ 167.05, 166.57, 133.42, 133.35, 129.92, 129.74, 129.70 129.63, 129.62, 129.60, 129.54, 128.49, 128.44, 128.42, 101.17, 74.05, 72.59, 72.34, 70.43, 70.02, 69.13, 68.78, 62.98, 50.58. HRMS m/z calc'd for $C_{24}H_{27}N_3O_9Na$ ($M+Na^+$). 516.1645; found: 516.1642.

General glycosylation procedure A

A solution of donor **11** (200 mg, 0.35 mmol, 1.0 equiv), acceptor (1.2 equiv), and activated 4 Å powdered molecular sieves(216 mg, 2 gm) in anhydrous dichloromethane was stirred at RT overnight and then cooled to -40^{0}C followed by addition of NIS (172 mg, 0.26 mmol, 2.4 equiv) and TfOH (9.5 μL, 0.11 mmol, 1.0 equiv). The reaction mixture was stirred at -40^{0}C for 20 min to 2 h until the disappearance of the donor on TLC, then quenched with triethylamine (22.6 μL, 0.16 mmol, 1.5 equiv) and warmed to room temperature. The mixture was diluted with dichloromethane, filtered through celite, washed with 20% aqueous $Na_2S_2O_3$ solution, dried over anhydrous Na_2SO_4, and concentrated under reduced pressure. The residue was purified by column chromatography (silica gel, Pet ether/ THF 1:1) to afford the sialic acid disachharide.

*** Comp 8** Spectroscopic details have already given in chapter 2.

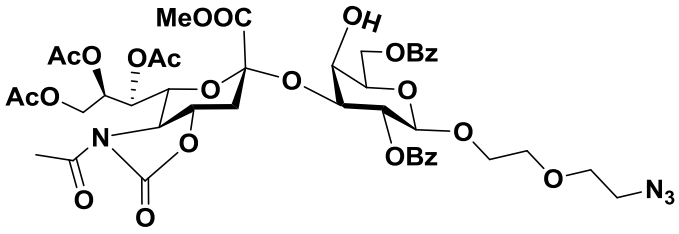

Compound 53: General procedure **A** with donor **11**(200mg, 0.35mmol) and acceptor 50(212mg, 0.422moml) to afford **53**(220mg ,65%) .**^{1}H-NMR** (400 MHz, $CDCl_3$) δ 8.12 (dd, *J* = 39.7, 7.9 Hz, 4H), 7.60 (t, *J* = 7.3 Hz, 2H), 7.48 (m, 4H), 5.56 (m, 1H), 5.52 (t, J = 9.4 Hz, 1H), 5.43(m, 1H), 4.79 (d, *J* = 7.9 Hz, 1H), 4.68 (dd, *J* = 11.3, 6.2 Hz, 1H), 4.57 (m, 3H), 4.44 (dd, *J* = 12.2, 2.0 Hz, 1H), 4.02 – 3.93 (m, 3H), 3.88 – 3.82 (m, 1H), 3.81 – 3.75 (m, 2H), 3.74 (s, 3H), 3.57 (m, 3H), 3.43 (t, *J* = 5.1 Hz, 2H), 3.10 – 2.95 (m, 2H), 2.86 (dd, *J* = 12.0, 3.2 Hz, 1H), 2.77 (s, 1H), 2.45 (s, 3H), 2.14 (dd, *J* = 11.2, 2.0 Hz, 1H), 2.07 (s, 3H), 2.06 (s, 3H), 1.56 (s, 3H). **^{13}C-NMR** (400 MHz, $CDCl_3$) δ 171.77, 170.78, 170.37, 169.96, 168.70, 166.17, 165.27, 153.35, 133.26, 133.24, 130.19, 130.14, 129.98, 129.93, 129.63, 129.60, 128.72, 128.69, 128.51, 128.44,

101.33, 97.36, 75.28, 74.05, 71.67, 71.43, 70.58, 70.24, 69.92, 69.16, 68.26, 66.96, 63.50, 63.07, 58.76, 53.21, 50.50, 36.02, 29.69, 24.55, 21.10, 20.79, 20.22. HRMS m/z calc'd for $C_{43}H_{50}N_4O_{21}$ (M+Na). 981.2859; found 981.2851.

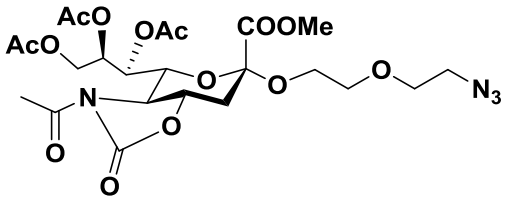

Compound 54: General procedure **A** with donor **11** (200 mg, 0.35 mmol) and 2-azidoethoxyethanol (55 mg, 0.42 mmol) to afford **54** (190 mg , 91%).**^{1}H-NMR** (400 MHz, $CDCl_3$) δ 5.55 (dd, *J* = 8.1, 1.7 Hz, 1H), 5.41 (ddd, *J* = 8.1, 7.2, 2.9 Hz, 1H), 4.60 (dd, *J* = 9.3, 1.7 Hz, 1H), 4.37 (dd, *J* = 12.2, 2.9 Hz, 1H), 4.05 – 4.01 (m, 1H), 4.01 – 3.97 (m, 1H), 3.96 – 3.90 (m, 2H), 3.79 (s, 4H), 3.71 (q, *J* = 2.0 Hz, 1H), 3.66 (m, 2H), 3.47 (ddd, *J* = 10.6, 5.8, 3.6 Hz, 1H), 3.39 – 3.34 (m, 2H), 2.88 (dd, *J* = 12.0, 3.5 Hz, 1H), 2.47 (s, 3H), 2.13 (s, 3H), 2.12 (s, 3H), 2.11 (t, *J* = 12.1, 13.5 Hz, 1H) 2.01 (s, 3H). **^{13}C-NMR** (400 MHz, $CDCl_3$) δ 172.11, 170.77, 170.36, 170.14, 168.75, 153.76, 99.31, 75.58, 75.09, 71.88, 70.12, 70.02, 69.05, 65.08, 63.24, 59.08, 53.11, 50.69, 36.53, 24.79, 21.24, 20.99, 20.85. HRMS m/z calc'd for $C_{23}H_{32}N_4O_{14}$ (M+Na). 611.1813; found:611.1811.

General deprotection procedure B

To a solution of oligosaccharide (1 eq) in ethanol: water mixture (3:1, 5 ml), LiOH (30 eq) was added and stirred at 80^0C for 12h. The reaction mixture was cooled to room temperature and carefully neutralized by IR-120H$^+$ resin to pH-7, diluted with methanol, filtered and concentrated. The crude residue was dissolved in water and $NaHCO_3$ (15eq) mixture and acetic-anhydride (10eq) at 0 ^{0}C. After 3 h, LiOH (10eq) was added and stirred for another 5-6h at RT. Then reaction mixture carefully neutralized by IR-120H$^+$resin to pH-7, diluted concentrated and purified by reverse-phase column chromatography (Bond Elu-C18).The $Pd(OH)_2$ (10 mmole %) was added to the above residue in methanol : water mixture (4 ml, 1:1) and H_2 gas was purged into the reaction mixture. After 12 h, the reaction mixture was filtered and further purified by reverse phase column chromatography (Bond Elu-C18) yielded deprotected sialic acid analogs.

* **Compound 1** spectroscopic details are provided in chapter 2.

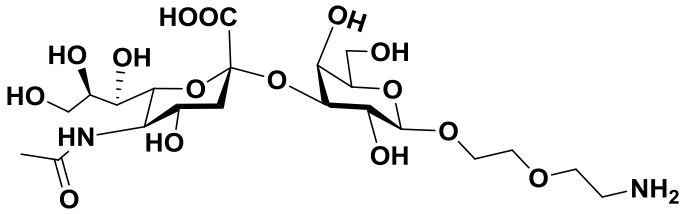

Compound 55: General deprotection procedure **B** of comp **53** yielded 42 mg (42%) of **55**. **^{1}H-NMR** (400 MHz, D_2O) δ 4.41 (d, *J* = 7.9 Hz, 1H), 4.02 – 3.96 (m, 2H), 3.84 (d, *J* = 3.1 Hz, 1H), 3.79 – 3.73 (m, 3H), 3.72 – 3.69 (m, 2H), 3.67 (dd, *J* = 8.9, 4.5 Hz, 2H), 3.64 (d, *J* = 4.0 Hz, 1H), 3.58 (dd, *J* = 4.6, 2.2 Hz, 1H), 3.57 – 3.55 (m, 3H), 3.54 (d, *J* = 1.4 Hz, 2H), 3.51 (m, 2H), 3.49 – 3.46 (m, 3H), 2.66 (q, *J* = 4.4 Hz,1H),1.93(s, 3H), 1.69 (t, *J* = 12.1 Hz, 1H). **^{13}C NMR** (400 MHz, D_2O) δ 175.11, 173.80, 102.56, 102.56, 75.92, 75.03, 72.92, 71.84, 70.20, 69.18, 68.77, 68.31, 67.92, 67.57, 66.38, 62.67, 61.02, 51.75, 39.73, 39.15, 22.08. HRMS m/z calc'd for $C_{21}H_{38}N_2O_{15}$ (M+H). 559.235; found: 559.2352.

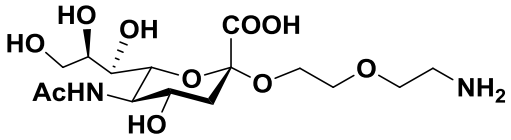

Compound 56: General deprotection procedure **B** of comp **54** yielded comp **56** 60 mg (45%). **^{1}H-NMR** (400 MHz,CD_3OD) δ 3.94 – 3.86 (m, 1H), 3.82 (ddd, *J* = 7.8, 9.4, 2.5 Hz, 2H), 3.69 – 3.52 (m, 9H), 3.47 (dd, *J* = 8.9, 1.7 Hz, 1H), 2.87 – 2.77 (m, 4H), 1.99 (s, 3H), 1.56 (t, *J* = 11.7 Hz, 1H). **^{13}C-NMR** (400 MHz, CD_3OD) δ 174.25, 172.92, 100.50, 73.01, 72.16, 71.66, 70.09, 69.57, 68.99, 68.13, 63.17, 52.89, 50.43, 41.27, 21.28. HRMS m/z calc'd for $C_{15}H_{28}N_2O_{10}$ (M+H). 397.1822; found: 397.1826.

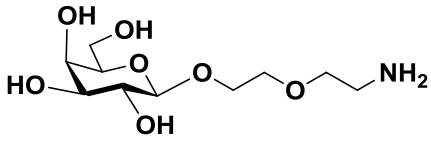

Compound 49: To a solution of compound **50** (250 mg) in dry methanol sodium methoxide 3eq were added and stirred the reaction mixture for 12h at room temperature followed careful neutralization by IR-120H^{+} resin to pH-7. Filtered the solution and then

allowed to hydrogenation in presence of Pd $(OH)_2$ for another 12h . Finally filtered the reaction mixture and concentrated. Purification with reverse phase column yielded **49** as white solid 90mg (65%). **^{1}H NMR (400 MHz, D_2O)** δ 4.29 (d, *J* = 7.9 Hz, 1H), 3.94 (m, 1H), 3.78 (d, *J* = 3.3 Hz, 1H), 3.70 (m, 1H), 3.59 (m, 7H), 3.51 (dd, *J* = 9.9, 3.4 Hz, 1H), 3.39 (dd, *J* = 9.9, 7.9 Hz, 1H), 2.99 (m, 1H), 2.87 (m, 1H). **^{13}C NMR (400 MHz, D_2O)** δ 102.88, 75.20, 72.77, 70.76, 69.63, 68.66, 67.83, 61.01, 47.20, 39.25. HRMS m/z calc'd for $C_{10}H_{21}NO_7$ (M+Na). 290.1216; found: 290.1534.

4.9.4 References

1. A. Varki, *Trends. Mol. Med*., **2008**, 14, 351.
2. R. L. Schanaar, R. Gerardy-Schahn, H. Hidebrandt, *Physiol. Rev*., **2014**, 94, 461.
3. M. K. O'Reilly, B. E. Collins, S. Han, L. Liao, C. Rillahan, P. I. Kitov, *J. Am. Chem. Soc*., **2008**, 130, 7736.
4. M. Hirai, H. Minematsu, N. Kondo, K. Oie, K. Igarashi, N. Yamazaki, *Biochem. Biophys. Res. Commun*., **2007**, 353, 553.
5. R. Zeisig, R. Stahn, K. Wenzel, D. Behrens, I. Fichtner, *Biochim. Biophys. Acta. Biomembr*., **2004**, 1660, 31.
6. F. Yang, Q. Tang, X. Zhong, Y. Bai, T. Chen, Y. Zhang, *Int. J. Nanomed*., **2012**, 7, 835.
7. D. E. Owens, N. A. Peppas, *Int. J. Pharm*., **2006**, 307, 93.
8. T. Ohyanagi, N. Nagahori, K. Shimawaki, H. Hinou, T. Yamashita, A. Sasaki, *J. Am. Chem. Soc*., **2011**, 133, 12507.
9. M. Mora, M. L. Sagrista, D. Trombetta, F. P. Bonina, A. De Pasquale, A. Saija, *Pharm. Res*., **2002**, 19, 1430.
10. M. C. Taira, N. S. Chiaramoni, K. M. Pecuch, S. Alonso-Romanowski, *Drug. Deliv*., **2004**, 11, 123.
11. N. L. Boman, D. Masin, L. D. Mayer, P. R. Cullis, M. B. Bally, *Cancer. Res*., **1994**, 54, 2830.
12. R. A. Bader, A. L. Silvers, N. Zhang, *Biomacromolecules*., **2011**, 12, 314.
13. L. Bondioli, L. Costantino, A. Ballestrazzi, D. Lucchesi, D. Boraschi, F. Pellati, *Biomaterials*., **2010**, 31, 3395.

14. T. M. Allen, C. Hansen, J. Rutledge, *Biochim. Biophys. Acta*. *Biomembr*., **1989**, 981, 27.
15. E. L. Vodovozova, E. V. Moiseeva, G. K. Grechko, G. P. Gayenko, N. E. Nifant'ev and N. V. Bovin, *Eur. J. Cancer*., **2000**, 36, 942.
16. S. H. Bhang, N. Won, T. J. Lee, H. Jin, J. Nam, J. Park, *ACS Nano*., **2009**, 3**,** 1389.
17. S. I. Van Kasteren, S. J. Campbell, S. Serres, D. C. Anthony, N. R. Sibson, B. G. Davis, *Proc. Natl. Acad. Sci U. S. A*., **2009**, 106, 18.
18. P. Padmanabhan, A. Kumar, S. Kumar, R.K. Chaudhary, B. Gulyas, *Acta. Biomater.*, **2016**, 16, 30271.
19. A. H. Lai, J. Hutter, C. W. Hsu, H. Tanaka, S. Varela-Aramburu, L. De Cola, B. Lepenies, P. H. Seeberger, *Nano Lett.*, **2016**, 16, 807.
20. R. Kikkeri, B. Lepenies, A. Adibekian, P. Laurino, P. H. Seeberger, *J. Am. Chem. Soc*., **2009**, 131, 2110.
21. A. Barandov, D. Grunstein, I. Apostolova, R. Buchert, M. Roger, W. Brenner, U. Abram, P. H. Seeberger, *ChemBiochem*., **2014**, 15, 986.
22. T. Ohyanagi, N. Nagahori, K. Shimawaki, H. Hinou, T. Yamashita, A. Sasaki, T. Jin, T. Iwanaga, M. Kinjo, S. Nishimura, *J. Am. Chem. Soc.*, **2011**, 133, 12507.
23. L. Gonzalez-Moragas, A. Roig, A. Laromaine, *Adv. Colloid. Interface. Sci*., **2015**, 219, 10.
24. C. A. MacRae, R. T. Peterson, *Nat. Rev. Drug. Discov*., **2015**, 14, 721.
25. J. W. Lu, Y. J. Ho, Y. J. Yang, H. A. Liao, S. C. Ciou, L. I. Lin, D. L. Ou, *World. J. Gastroenterol*., **2015**, 21, 12042.
26. S. George, T. Xia, R. Rallo, Y. Zhao, Z. Ji, S. Lin, X. Wang, H. Zhang, B. France, D. Schoenfeld, R. Damolseaux, R. Liu, S. Lin, K. A. Brandley, Y. Cohen, A. E. Nel, *ACS Nano.*, **2011**, 5, 1805.
27. M. Newmann, E. Ebrahimie, M. Lardelli, *Front. Genet*., **2014**, 5, 1.
28. A. M, De Rocha, J. R. Ferreira, D. M. Barros, T. C. Pereira, M. R. Bogo, S. Oliveira, V. Geraldo, R. G. Lacerda, A. S. Ferlauto, L. O. Ladeira, M. V. Pinheiro, J. M. Monserrat, *Mol. Integr. Physiol*., **2013**, 165, 460.
29. X. Li, B. Liu, X. L. Li, Y. X. Li, M. Z. Sun, D. Y. Chen, X. Zhano, X. Z. Feng, *Sci. Rep.*, **2014**, 4, 3810.

30. Z. J. Zhu, R. Carboni, M. J. Quercio Jr, B. O. R. Miranda, D. L. Anderton, K. F. Arcaro, V. M. Rotello, R.W. Vachet, *Small.*, **2010**, 18, 2261.
31. J. A. Kovrižnych, R. Soniková, D. Zeljenková, E. Rollerová, E. Szabová and S. Wimmerová, *Interdiscip. Toxicol*., 2013, **6**, 67-73.
32. Z. Wu, G. Li, S. Deng, L. Quyang, L. Li, L. Liu, N. Luo, X. Song, G. He, C. Gong, Y. Wei, *Nanoscale*., **2014**, 6, 11940.
33. J. Li, H. H. Ha, L. Guo, D. Coomber, Y. T. Chang, *Chem. Commun*., **2010**, 46, 2932.
34. S.W. Son, J. H. Kim, S. H. Kum, H. Kum, A. Y. Chung, J. B. Choo, C. H. Oh, H. C. Park, *Skin. Res. Technol*., **2009**, 15, 157.
35. htpps://www.thermofisher.com/order/catalog/product/Q21301MP.
36. C. A. Leatherdale, W. K. Woo, F. V. Mikulec, M. G. Bawendi, *J. Phys. Chem. B*., **2002**, 106, 7619.
37. L. Svennerholm, *Biochim. Biophys. Acta*., **1957**, 24, 604.
38. P. S. Chow and S. N. Landhausser, *Tree. Physiol.,* **2004**, 24, 1129.
39. H. S. Choi, W. H. Liu, P. Misra, E. Tanaka, J. P. Zimmer, B. I. Ipe, M. G. Bawendi, J. V. Frangioni, *Nat. Biotechnol.,* **2007**, 25, 1165.
40. H. S. Choi, W. H. Liu, F. B. Liu, K. Nasr, P. Misra, M. G. Bawendi and J. V. Frangioni, *Nat. Nanotechnol*., **2010**, 5, 42.
41. S. Kim, Y. T. Lim, E. G. Soltesz, A. M. De Grand, J. Lee, A. Nakayama, J. A. Parker, T. Mihaljevi, R. G. Laurence, D. M. Dor, L. H. Cohen, M. G. Bawendi, J. V. Frangioni, *Nat. Biotechnol.,* **2004**, 22, 93.
42. M. K. So, C. J. Xu, A. Loening, S. S. Gambhir and J. H. Rao, *Nat. Biotechnol*., **2006**, 24, 339.
43. A. Verma, O. Uzun, Y. H. Hu, Y. Hu, H. S. Han, N. Watson, S. Chen, D. J. Irvine and F. Stellacci, *Nat. Mater.,* **2008**, 7, 588.
44. N. Lewinski, V. Colvin and R. Drezek, *Small.,* **2008**, 4, 26.
45. T. S. Hauck, A. A. Ghazani and W. C. W. Chan, *Small.,* **2008**, 4, 153.
46. Y. Tang, S. Han, H. Liu, X. Chen, L. Huang, X. Li and J. Zhang, *Biomaterials.,* **2013**, 34, 8741.
47. C. Schulte and R. Nagel, *ATLA.*, **1994**, 22, 12.

48. G. Gregoriadis, A. Fernandes, M. Mital and B. McCormack, *Cell. Mol. Life. Sci*., **2000**, 57, 1964.
49. G. Gregoriadis, B. McCormack, Z. Wang and R. Lifely, *FEBS. Lett*., **1993**, 315, 271.
50. G. Gregoriadis, A. Fernandes, B. McCormack, M. Mital and X. Zhang, *Biotechnol. Genet. Eng. Rev*., **1999**, 16, 203-15.
51. G. Tosi, A. V. Vergoni, B. Ruozi, L. Bondioli, L. Badiali and F. Rivasi, *J. Controlled. Release*., **2010**, 145, 49.
52. L. Bondioli, L. Costantino, A. Ballestrazzi, D. Lucchesi, D. Boraschi and F. Pellati, *Biomaterials*., **2010**, 31, 3395.
53. R. Meng, J. E. Smallshaw, L. M. Pop, M. Yen, X. Liu and L. Le, *Clin. Cancer. Res*., **2004**, 10, 1274.
54. R. –I. Tozawa, S. Ishibashi, J. –I. Osuga, K. Yamamoto, H. Yagyu and K. Ohashi, *J. Biol. Chem*., **2001**, 276, 12624-8.
55. T. D. Farr, C. –H. Lai, D. Grünstein, G. Orts-Gil, C. C. Wang, P. Boehm-Sturm, P. H. Seeberger and C. Harms, *ACS Nano.,* **2014**, 14, 2130.
56. T. Yin, L. Yang, Y. Liu, X. Zhou, J. Sun and J. Liu, *Acta. Biomaterialia.,* **2015**, 25, 172.
57. K. Tanaka, E. R. O. Siwu, K. Minami, K. Hasegawa, S. Nozaki and Y. Kanayama, *Angew. Chem. Int. Ed*., **2010**, 49, 8195.
58. L. Zhang de, S. Y. Liu, J. Zhang, J. K. Zhang, C. X. Hu and Y. D. Liu, *Aquat. Toxicol*., **2016**, 176, 106.
59. W. Liu, Q. Qiao, Y. Chen, K. Wu and X. Zhang, *Aquat. Toxicol.,* **2014**, 155, 360.

4.9.5 ^{1}HNMR and ^{13}CNMR fi

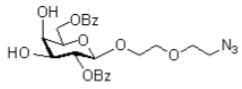
OH
OBz
HO
O
O
O
N3
OBz

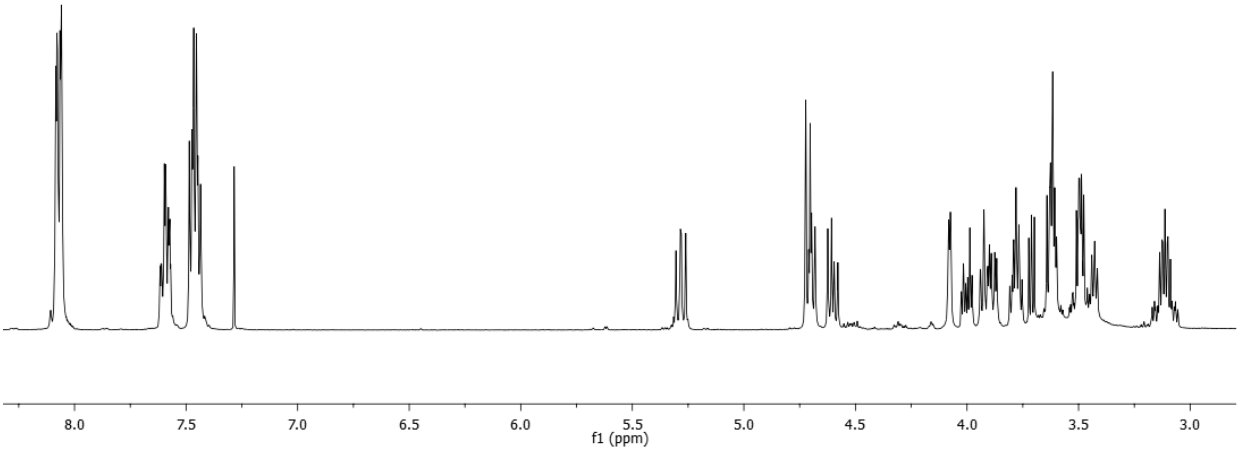
8.0
7.5
7.0
6.5
6.0
5.5
5.0
4.5
4.0
3.5
3.0
f1 (ppm)

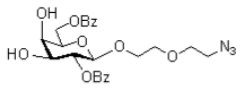
OH
OBz
HO
O
O
O
N3
OBz

165
160
155
150
145
140
135
130
125
120
115
110
105
100
95
90
85
80
75
70
65
60
55
50
45
f1 (ppm)

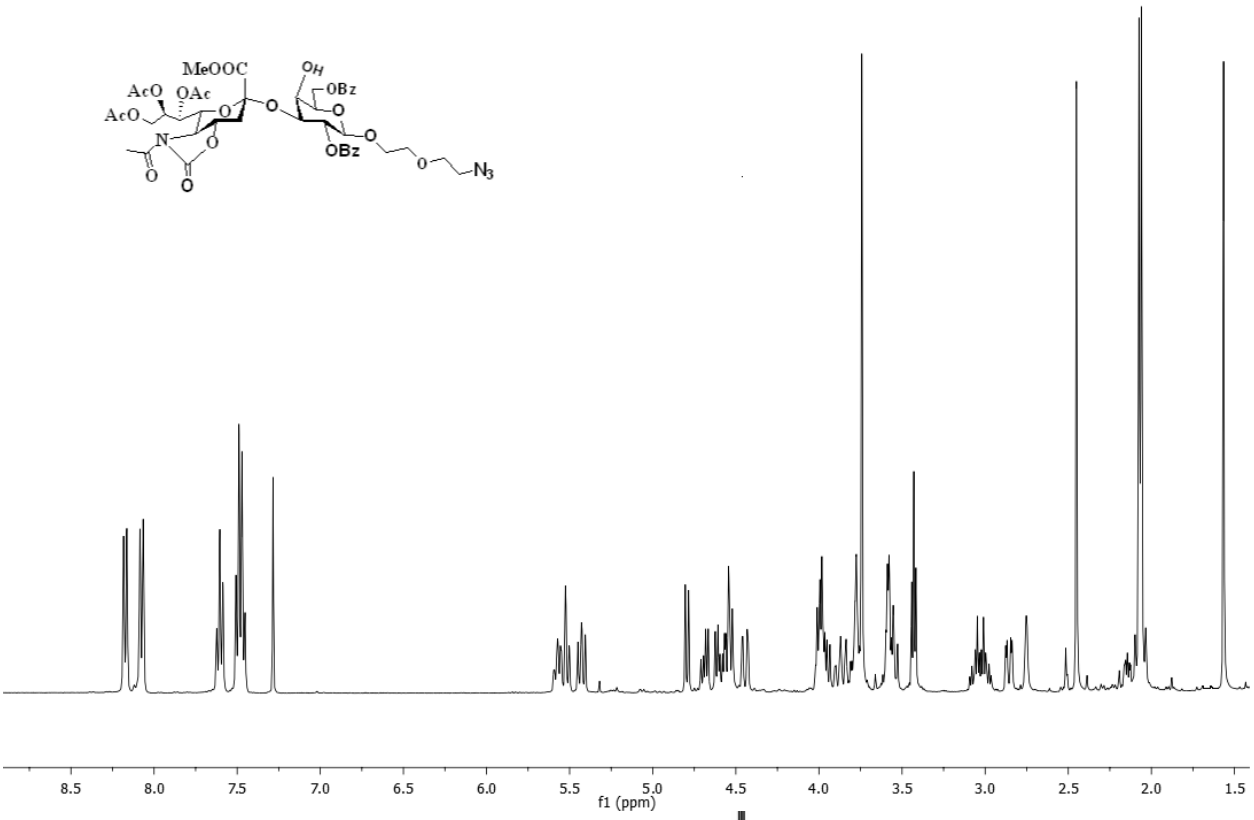
MeOOC
AcO
OAc
AcO
OH
OBz
OBz
N3
8.5
8.0
7.5
7.0
6.5
6.0
5.5
5.0
4.5
4.0
3.5
3.0
2.5
2.0
1.5
f1 (ppm)

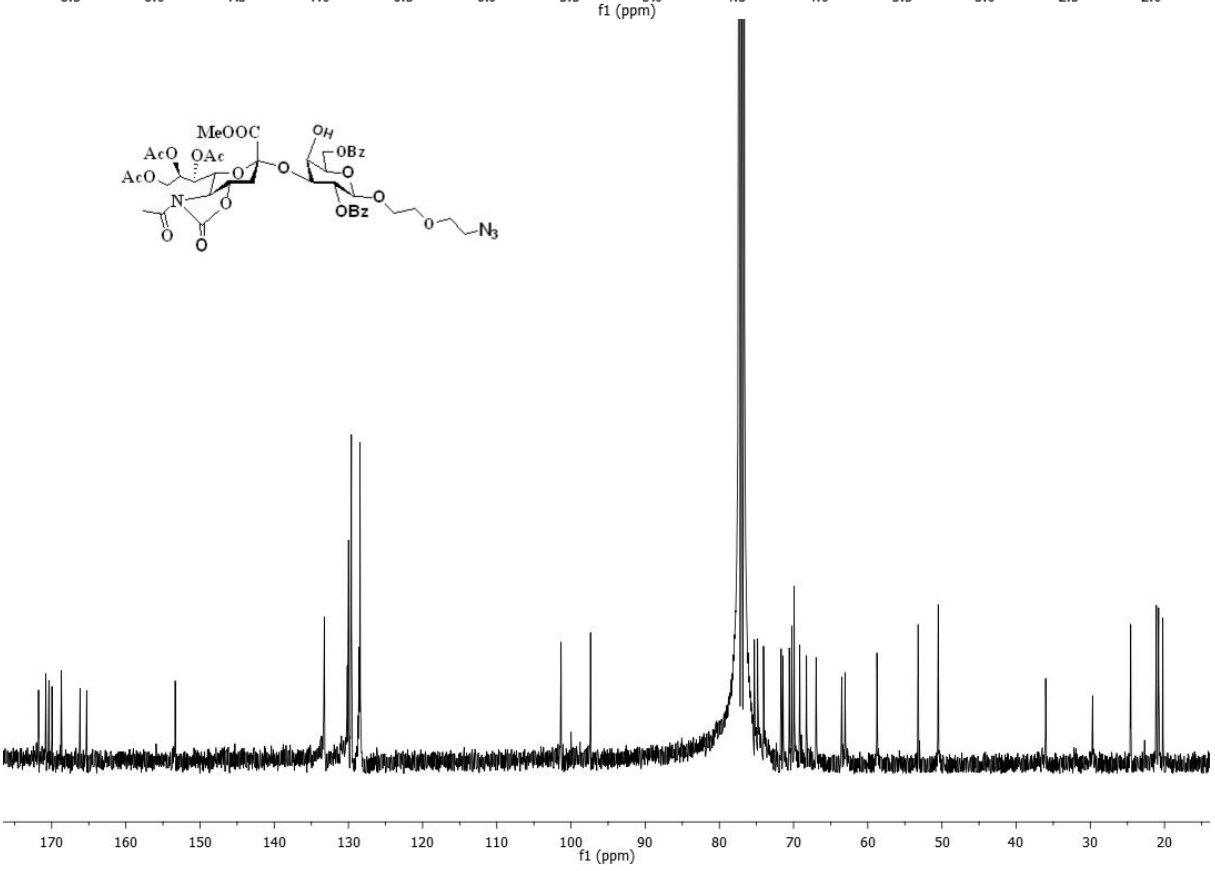
MeOOC
AcO
OAc
AcO
OH
OBz
OBz
N3
170
160
150
140
130
120
110
100
90
80
70
60
50
40
30
20
f1 (ppm)

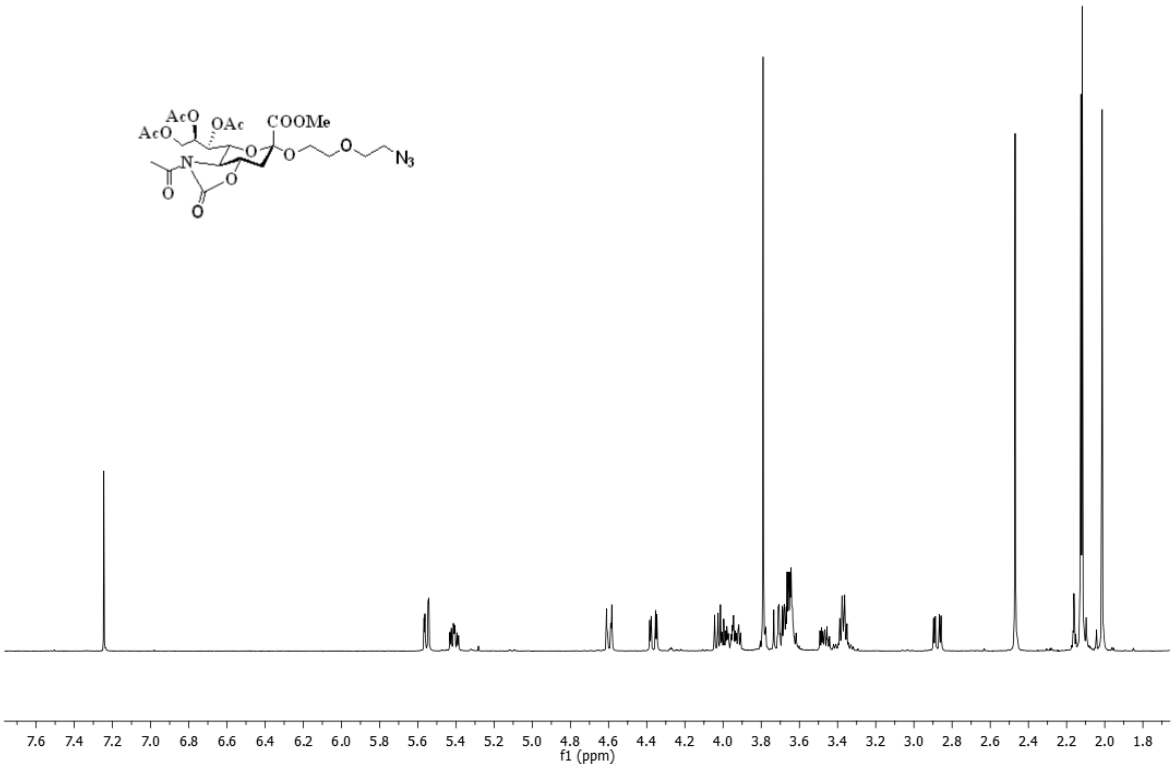
AcO
AcO
OAc
COOMe
O
N
O
O
O
O
O
O
N3
7.6 7.4 7.2 7.0 6.8 6.6 6.4 6.2 6.0 5.8 5.6 5.4 5.2 5.0 4.8 4.6 4.4 4.2 4.0 3.8 3.6 3.4 3.2 3.0 2.8 2.6 2.4 2.2 2.0 1.8
f1 (ppm)

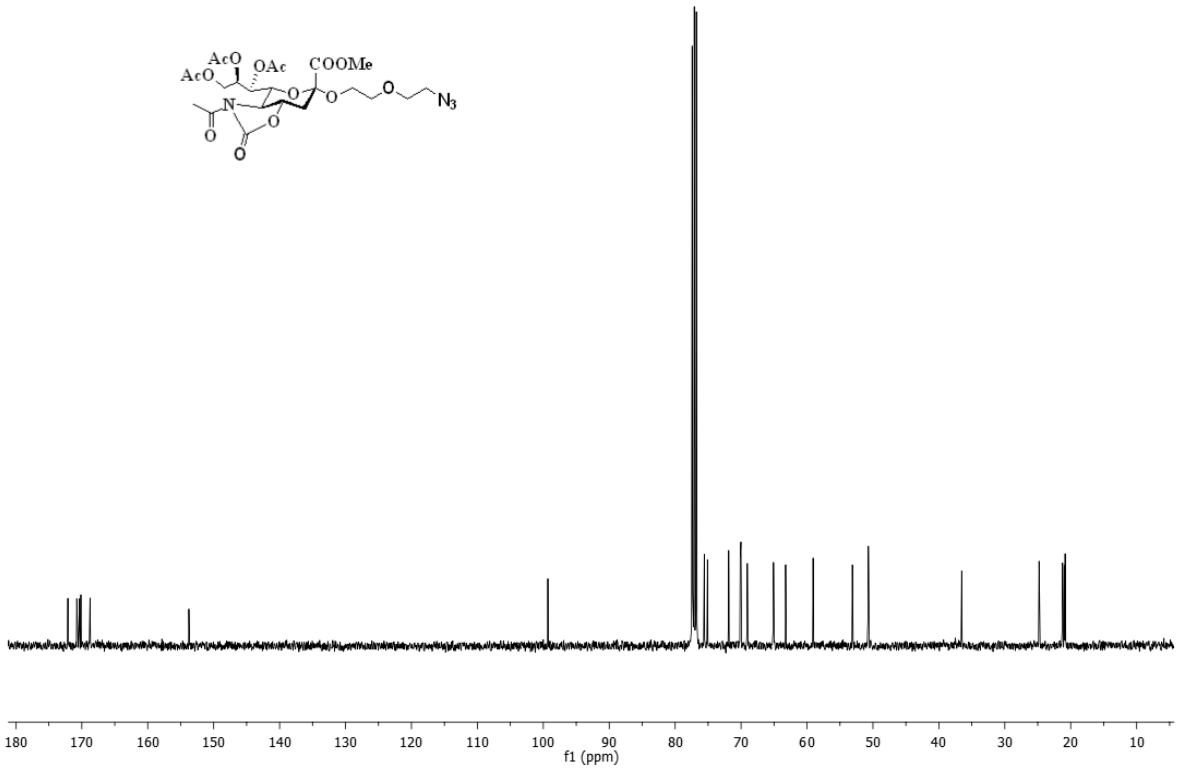
AcO
AcO
OAc
COOMe
O
N
O
O
O
O
O
O
N3
180 170 160 150 140 130 120 110 100 90 80 70 60 50 40 30 20 10
f1 (ppm)

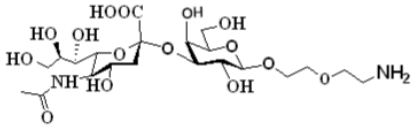
HOOC
OH
OH
HO
OH
HO
O
O
O
NH
HO
O
O
O
NH2
OH

4.6 4.5 4.4 4.3 4.2 4.1 4.0 3.9 3.8 3.7 3.6 3.5 3.4 3.3 3.2 3.1 3.0 2.9 2.8 2.7 2.6 2.5 2.4 2.3 2.2 2.1 2.0 1.9 1.8 1.7 1.6 1.5
f1 (ppm)

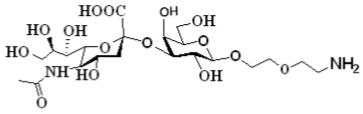
HOOC
OH
OH
HO
OH
HO
O
O
O
NH
HO
O
O
O
NH2
OH

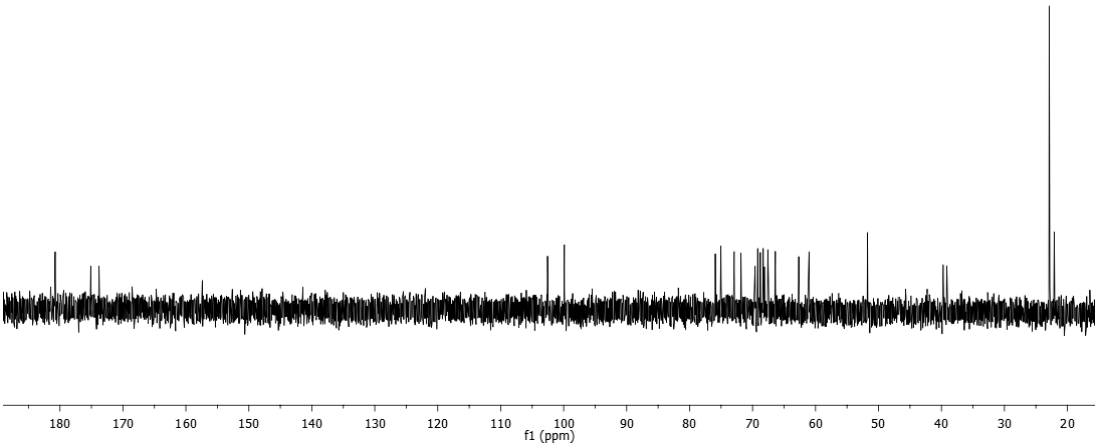
180 170 160 150 140 130 120 110 100 90 80 70 60 50 40 30 20
f1 (ppm)

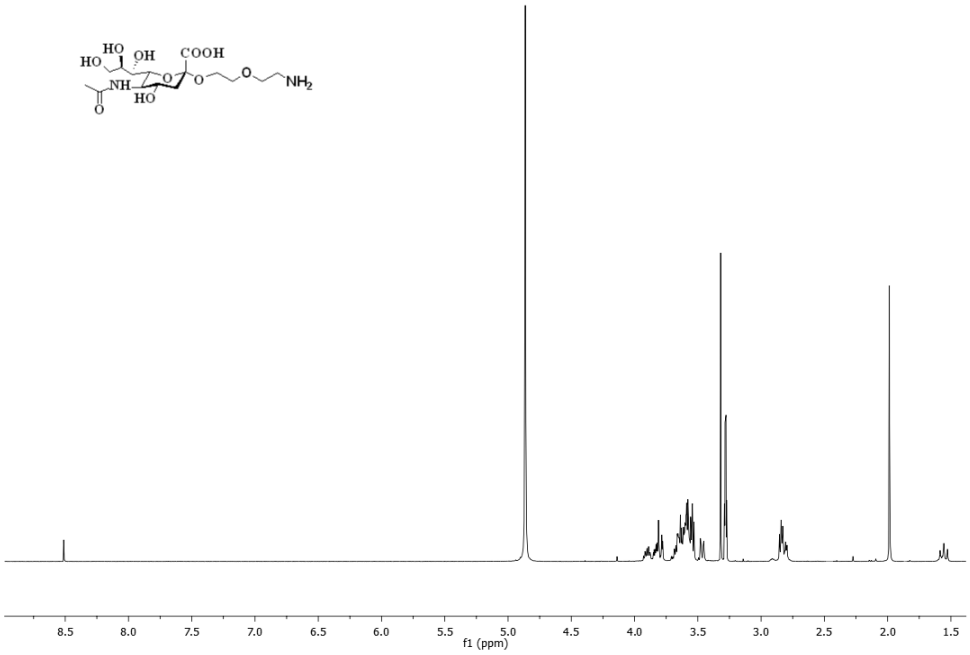
HO
HO
OH
COOH
NH
HO
O
O
O
NH2
8.5
8.0
7.5
7.0
6.5
6.0
5.5
5.0
4.5
4.0
3.5
3.0
2.5
2.0
1.5
f1 (ppm)

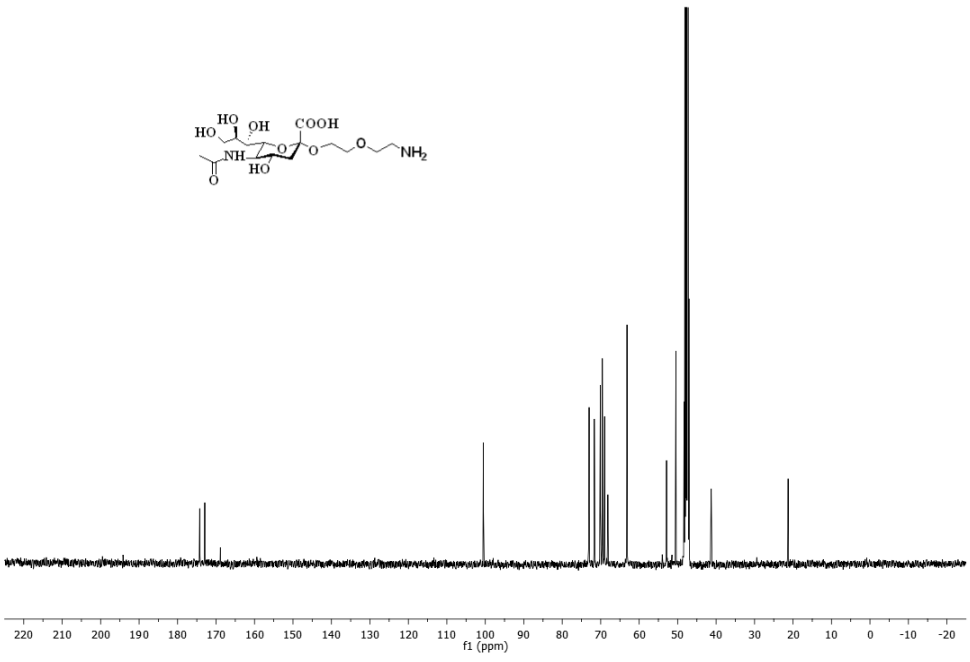
HO
HO
OH
COOH
NH
HO
O
O
O
NH2
220
210
200
190
180
170
160
150
140
130
120
110
100
90
80
70
60
50
40
30
20
10
0
-10
-20
f1 (ppm)